University of Southampton

School of Civil Engineering and the Environment

DEVELOPMENT OF COMPONENT-BASED CONNECTION MODELLING FOR STEEL FRAMED STRUCTURES SUBJECTED TO BLAST OR PROGRESSIVE COLLAPSE

by

Euan Peter Stoddart

Thesis for the degree of Doctor of Philosophy

2012

Project Supervisor: Dr. M.P. Byfield

Abstract

Predicting the behaviour of steel-framed structures subject to unexpected loading conditions is necessary to ensure integrity and prevent collapse during such an event. When analysing a structure of this type it is common to simplify the problem by assuming connections as simple, rigid or semi-rigid (using a rotational spring). Whilst these simplifications are suitable for static and wind loading conditions they are unsatisfactory for explosive and collapse conditions where other factors, such as axial load and strain-rate effects, alter the connection behaviour.

Moment-rotation and direct tension tests have been performed on a range of bare steel semi-rigid connections under static and dynamic loading conditions. Results indicate that when loaded rapidly to failure, in general the connections demonstrate increased rotational stiffness and reduced ductility. These factors could influence the global survivability of a frame structure and therefore need to be explicitly accounted for in problems of a dynamic nature.

Component-based methods are proposed as a technique to include this real connection behaviour in non-linear dynamic structural analysis without having to produce a full three-dimensional FE model of the connection. This method simplifies each deformable joint component as a non-linear spring which, once assembled into a connection model, is able to accurately represent joint behaviour under all conditions. Use of these methods to model the experimental tests indicates good prediction of the overall behaviour and the dynamic effects. These connection models were then incorporated into a series of structural problems to investigate their potential for global analysis of extreme loading events. Results highlighted the importance of including joint performance in problems where ultimate capacity is of interest as connection rotational stiffness and ductility supply can affect the global frame behaviour. Thus prescriptive design measures alone, such as tying force requirements, cannot always guarantee sufficient levels of robustness.

Acknowledgements

My thanks go to my supervisor Dr. Mike Byfield for his technical input, assistance and guidance.

I would also like to express my gratitude to David Goode and all of the staff at DGA Ltd. for allowing me to work with them early on in my research and gain valuable experience of methods used to assess abnormal loadings on structures.

Finally this thesis would not be possible without the dynamic experimental connection tests performed at the University of Sheffield, for which I would like to thank Dr. Andrew Tyas, Dr. Jim Warren and all of the technical staff at the CEDUS laboratory in Buxton.

Declaration

The work presented in this thesis is my own and has been produced by me as a result of my own research. Where the thesis is based on work done by myself jointly with others, I have made clear exactly what was done by others and what I have contributed myself.

No part of it has been submitted to any other University for degree, diploma or other qualification.

E. Stoddart

Contents

List of Figures

Nomenclature

Chapter 2

$F(t)$	Force as a function of time
$I(t)$	Inertia as a function of time
K_e	Elastic stiffness
K_p	Plastic Stiffness
L	Beam span
M_c	Moment capacity of section
M_j	Connection moment
$M_{j,Rd}$	Connection design moment resistance
r_e	Resistance at yield
r_u	Ultimate resistance
S	Shear force
S_j	Rotational stiffness of connection
$S_{j,ini}$	Connection initial stiffness
$V(t)$	Dynamic reaction (shear) force as a function of time
V_{max}	Maximum shear force
y_e	Yield deflection
y_m	Ultimate deflection
y_p	Plastic deflection
$\emptyset$	Connection rotation

Chapter 3

A, B, C, D, E	Diaphragm combinations used to vary the loading rate in the connection tests
DIC	Digital image correlation
FEP	Flexible end-plate connection
FIN	Fin-plate connection
$F_A(t)$	Applied load
$F_C(t)$	Connection reaction force
$F_I(t)$	Inertia force
LDG	Laser displacement gauge
$M_c(t)$	Connection moment
$M_I(t)$	Inertial moment

t	Time
Δt	Change in time or time step duration
WC	Web cleat connection
x_1	Distance from column load end to load cell centreline
x_2	Distance from load cell centreline to column centreline
x_3	Distance from column centreline to connection centreline
x_4	Distance from connection centreline to column free end
x_5	Distance from column load end to LDG1
x_6	Distance from column free end to LDG2
z_{cl}	Displacement of column centreline
$\ddot{z}_{cl}$	Linear acceleration at column centreline
z_1	Displacement from LDG1
z_2	Displacement from LDG2
$\dot{\varepsilon}$	Strain rate
θ	Connection rotation
$\ddot{\theta}$	Connection rotational acceleration

Chapter 4

c	Wave speed
C	Empirical constant for use in Cowper-Symonds strain rate equation
DIF	Dynamic increase factor
FEA	Finite element analysis
f_y	Yield stress
f_u	Ultimate stress
G	Factor of safety to ensure stability in FEA
I	Inertial force
K	Structural stiffness
l	Maximum element length
M	Mass
p	Empirical constant for use in Cowper-Symonds strain rate equation
P	Internal forces in structure
Δt	Change in time or time step duration
$\ddot{u}$	Acceleration

α_y	Factor for dynamic yield stress
α_u	Factor for dynamic ultimate stress
ε_{nom}	Nominal strain
ε_{pl}	Plastic strain
ε_{true}	True strain
$\dot{\varepsilon}$	Strain rate
σ_{dy1}	Dynamic yield stress 1
σ_{dy2}	Dnamic yield stress 2
σ_{nom}	Nominal stress
σ_{true}	True stress
σ_y	Yield stress
ω_n	Natural frequency of mode shape

Chapter 5

A_s	Shear stress area of bolt
d_1	Distance from upper beam flange to connection centreline
d_2	Distance from lower beam flange to connection centreline
d_b	Bolt diameter
$d_{y,br}$	Bearing yield deformation
d_y	End-plate effective segment width
D_{ep}	End-plate depth
DIF	Dynamic increase factor
e_2	Edge distance
E_b	Young's modulus of bolt
E_{ep}	Young's modulus of end-plate
E_p	Young's modulus of plate
f_{ub}	Bolt ultimate stress
f_{up}	Plate ultimate stress
$f_{u,ep}$	End-plate ultimate stress
f_{yb}	Bolt yield stress
f_{yp}	Plate yield stress
$f_{y,ep}$	End-plate yield stress
F_n	Bolt row force defined in text
F_{br}	Bearing force
$F_{br,Rd}$	Plate bearing strength

F_{bty}	Bolt yield load
F_{ep}	Applied end-plate force
$F_{s,Rd}$	Peak friction force
F_{vb}	Bolt shearing force
$F_{vb,Rd}$	Bolt shearing strength
G_b	Shear modulus of bolt
G_p	Shear modulus of plate steel
I_{cf}	Second moment of area of column flange
I_{ep}	Second moment of area of end-plate
$K_{b,br}$	Bending stiffness for bearing model
K_{br}	Bearing stiffness
K_{bt}	Bolt elastic stiffness
K_{cf}	Column flange elastic stiffness
K_{ep}	End-plate elastic stiffness
$K_{i,br}$	Bearing initial stiffness
K_p	Plastic stiffness
K_{sh}	Strain hardening stiffness
K_{vb}	Bolt shear stiffness
$K_{v,br}$	Bearing shear stiffness
L_b	Beam effective length
L_{bt}	Bolt effective length
M_c	Connection moment
$M_{ep,Rd}$	Moment capacity of end-plate
M_o	Beam end moment
n_b	Number of bolts in each bolt row
s	Initial clearance gap between face of beam and column
s_w	Weld thickness
t_{cf}	Thickness of column flange
t_{bh}	Thickness of bolt head
t_{bn}	Thickness of bolt nut
t_{ep}	End-plate thickness
t_p	Plate thickness
t_T	Total combined thickness
t_w	Thickness of washer
t_{web}	Beam web thickness

T_y	Time taken to reach yield
V_{bv}	Bolt shear rate
V_{br}	Bearing rate
V_{ep}	End-plate deformation rate
x_n	Measurement defined in text
Z	Plastic section modulus
ε_{yb}	Bolt yield strain
ε_{yp}	Plate yield strain
$\dot{\varepsilon}$	Strain rate
Δ_{br}	Bearing deformation
Δ_v	Shear deformation
Δ_{sf}	Displacement at zero shear force
Δ_{su}	Displacement at peak shear force
Δ_y	End-plate displacement at yield
$\bar{\Delta}$	Normalised deformation
$\theta_{capacity}$	Connection rotation capacity
μ	Friction slip factor
μ_{sh}	Strain hardening stiffness factor
μ_p	Plastic stiffness factor
υ	Poisson's ratio
γ	Rotational contact factor
Φ_{bv}	Dynamic increase factor for bolt yield strength
Φ_{br}	Dynamic increase factor for bearing yield strength
Φ_{ep}	Dynamic increase factor for end-plate yield strength
Ω_{br}	Dynamic increase factor for bearing ultimate strength
Ω_{ep}	Dynamic increase factor for end-plate ultimate stress

Chapter 6

d_s	Diameter of shear studs
f_n	Natural frequency of structural system
I	Impulse
k	Stiffness of SDOF system
m	Mass of SDOF system
$p_{b,d}$	Bearing strength of the profiled decking

N	Number of shear studs used to connect an edge of profiled sheet on beam normal to sag per metre
SDOF	Single-degree-of-freedom
t_d	Duration of blast load
t_n	Natural period of structural system
T_{deck}	Tensile capacity of steel decking
T_{mesh}	Tensile capacity of reinforcement mesh
u(t)	Central column displacement
ω_n	Rotational frequency of structural system

1 INTRODUCTION

1.1 Scientific background

Structures have always been at risk from natural gas, pressure vessel and dust explosions. Additionally there is the ever-increasing threat from terrorist organisations who, using readily available materials, can build improvised explosive devices (IED's) comparable to many tonnes of TNT. Case studies such as the attacks on the Murrah building in 1995 (Figure 1-1) and the destruction of the Marine HQ in West Beirut in 1983 show the devastating effect these weapons can have on modern structures. It is thus necessary to incorporate structural analysis of extreme events into the design of modern buildings to minimise damage and casualties.

Figure 1-1: Extensive blast damage to the Murrah building, FEMA (1995)

Of interest in this research are the response of the structure to this loading and the prediction of any subsequent collapse. It is hoped that by accurately identifying vulnerable elements and understanding the structure's global behaviour, buildings can be made more robust and less prone to progressive collapse. It is important at this point to specify the two types of loading that occur during such an attack. The first is direct blast from an explosive charge which typically have durations of a few milliseconds. The second is the loading during a progressive collapse which follows the destruction of a structural element such as a column. In this case the time taken for the structure to redistribute its load to adjacent structural members is often between several 10's and several 100's of milliseconds. The aim of this thesis is to investigate the effect these loading rates have on the behaviour of

steel connections and model them in such a way that they can be included in structural analyses.

Current guidance for joint design employs static analyses of the joint to provide checks for the variety of loading conditions expected. Design codes contain assistance for designing connections under a variety of assumptions including simple, rigid or semi-rigid moment-rotation behaviour. The general recommendations are that the joint should be designed on the basis of realistic assumptions regarding the distribution of internal forces and that they should be capable of withstanding the forces and moments applied within acceptable deformation limits and without invalidating the design assumptions. In simple joints the stiffness is low and moment resistance is ignored, whilst in rigid joints full continuity between members is assumed. Anything in between is labeled semi-rigid, and in some cases are modelled using a rotational spring. The behaviour of this spring is defined by predetermined (either experimentally or theoretically) moment-rotation behaviour as shown in Figure 1-2.
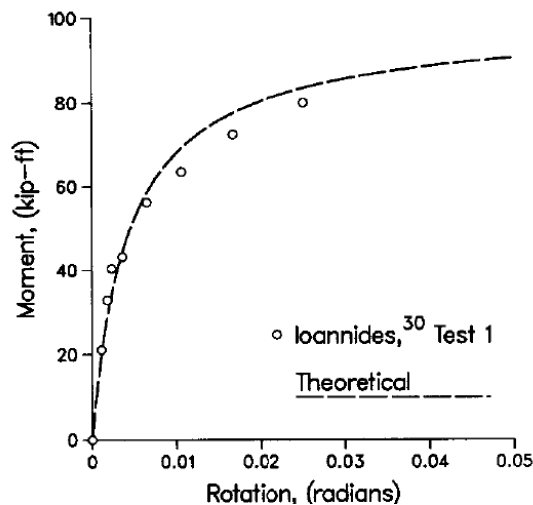
Figure 1-2: Experimental data vs. theoretical moment-rotation curve from Foley and Vinnakota (1995)

One theoretical method used to determine joint moment-rotation behaviour is the component method as employed in BS EN 1993-1-8 (2005) Part 1-8. Each deformable component in the joint is classified as a spring and its behaviour calibrated from either mathematical equations or experimental results. In EN 1993-1-8, all of the components are connected with rigid links and are then grouped as a single rotational spring representing the entire joint, from which the moment-rotation behaviour can be calculated as shown in Figure 1-3.

These rotational stiffness methods are well proven for regular conditions and have been implemented in both seismic and wind moment design [Hensman and Nethercot (2001)]. In these situations, the lateral sway of the structure is partly resisted by the stiffness of the beam-column connections resulting in less bracing requirements and more economical structures.
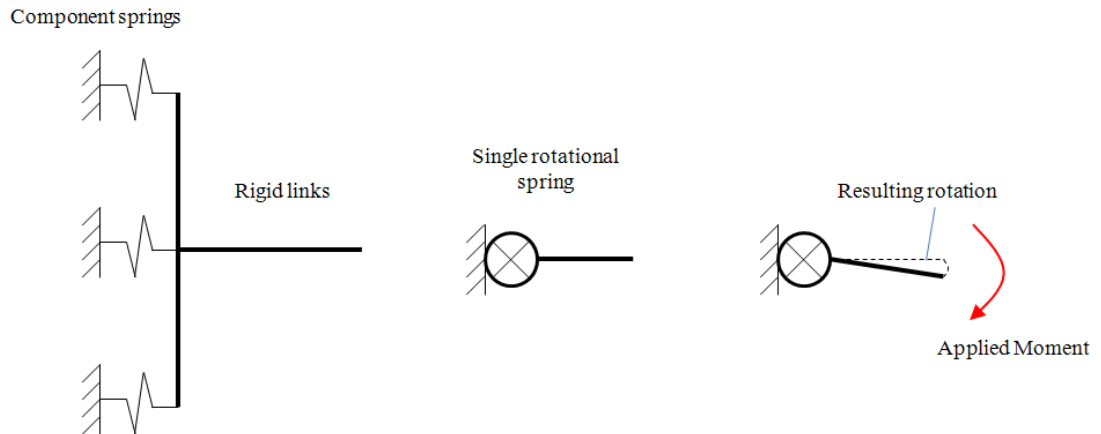
Figure 1-3: Demonstration of component method in Eurocode 3 to calculate moment-rotation

Representing a joint as a single rotational spring is a simple way of including realistic joint performance in design, however the presence of other forces such as shear and axial forces are not possible to include in the behaviour curves. Whilst in most situations these are less important than the applied moment there are occasions when they are critical to the behaviour of the joints.

As Ellingwood et al. (2009) state:

> *"In a collapse event, as deformations become very large and potential catenary action is achieved, the interaction of bending, twisting, and shear combined with axial effects can be potentially significant"*

A scenario in which axial forces play a large part in the global deformation of structures is under elevated temperature conditions. In these cases axial thrust from thermal expansion of the material followed by large sagging deflections are possible due to decreasing material properties at higher temperatures which lead to varying moment-rotation behaviour of the connections. Spyrou (2002), Al-Jabri et al. (2005) and Block et al. (2007) have shown that using the component method for joint modelling is a suitable way of capturing this more complex behaviour. In these cases the component model is used

directly without simplifying to a rotational spring. The advantage of this is that global equilibrium is maintained and thus solution to non-linear problems possible. Additionally failure criterion applied to each element allows complete behaviour to be modelled because the internal forces can be redistributed allowing progressive joint fracture to be captured.
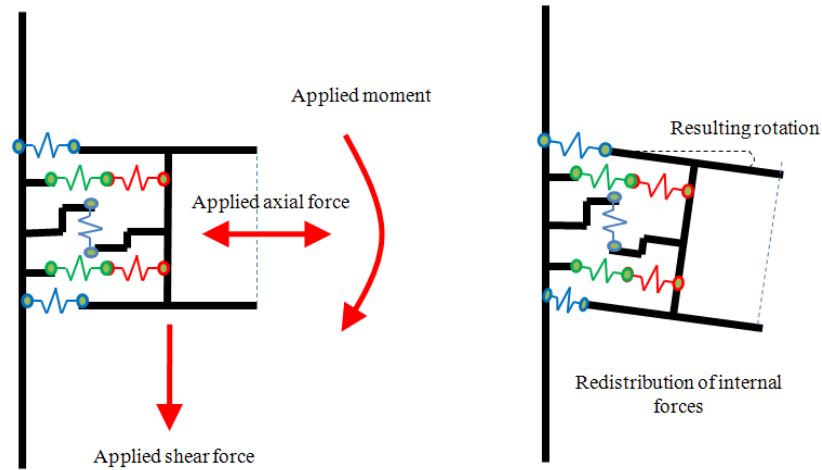
Figure 1-4: Component model subject to combined axial, shear and moment

The component model in Figure 1-4 is similar to that proposed by Block et al. (2007) for an end plate connection and is able to account for deformation due to the end-plate and column flange in bending, bolts in tension and column web in compression as well as the deformation caused by the shear force on the bolts and plate in bearing.

It is this flexibility which has prompted the author to investigate its possible use for joint analysis under dynamic blast and progressive collapse conditions.
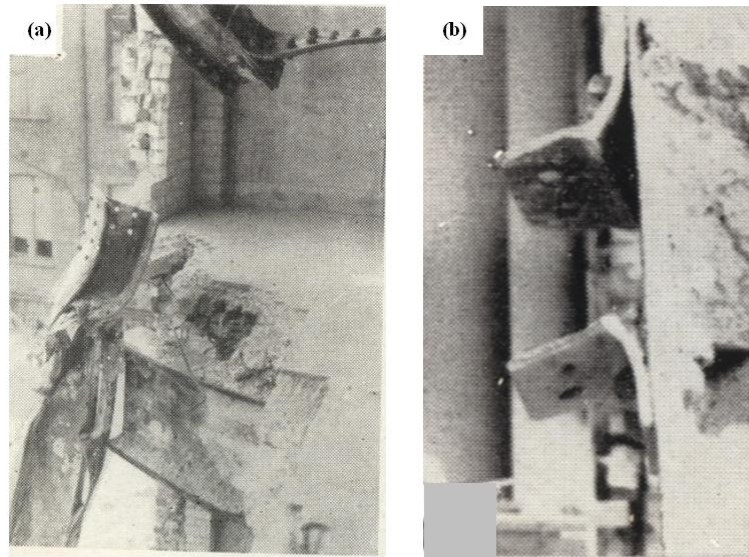
Figure 1-5: (a) Column splice damage and (b) failure of top and bottom cleats from Baker et al. (1948)

Typical models used for progressive collapse analysis of structures [Izzuddin et al. (2007), Fu (2009)] tend to use joint assumptions developed under static conditions. Where high strength rigid connections are used this assumption is usually valid, however where weaker connections are employed the behavior may not be accurately reproduced. Indeed US DoD (2009) guidelines '*Design of buildings to resist progressive collapse*' states that when producing analytical models of progressive collapse:

> *"Model a connection explicitly if the connection is weaker or has less ductility than the connected components"*

The redistribution of loading following blast or progressive collapse is a dynamic event and therefore the connection performance may vary from the static behaviour due to strain-rate effects or inertial restraint leading to premature brittle failure as shown in Figure 1-5. This research project aims to investigate the performance of a range of connection types subject to static and dynamic loading to verify any variance in performance. A joint model which can accurately recreate the true joint behaviour for non-linear dynamic analysis will be developed and compared against experimental test results. Finally, the connection models will be incorporated into global analysis of sub frames for typical column loss and blast scenarios to investigate potential benefits and limitations.

The feasibility of modelling connection behaviour under blast and dynamic loads will be limited to steel frame structures and their sub frames. Beam-column connections will be considered including the fin-plate, flexible end-plate and double-angle web cleat

connection typologies. Previous work is available for these joint classifications under regular conditions and it is thought that this may be adapted for use under dynamic loading.

1.2   Thesis layout

This thesis consists of seven chapters:

Chapter 2 contains a review of current methods of joint modelling and steelwork design including current UK and international codes and standards as well as previous research into joint classification and prediction of behaviour. This also includes a detailed review of methods to analyse structures subject to extreme load conditions such as a blast and/or progressive collapse.

Chapter 3 describes a series of experimental connection tests performed statically and dynamically to investigate behaviour at different rotation rates. Both moment-rotation and direct axial tension tests were conducted on bare steel fin-plate, flexible end-plate and web cleat connections. The loading rate effect, connection behaviour and observed failure modes are discussed for each connection type.

Prior to developing component-based methods for dynamic applications it was necessary to investigate how the connection representation would be incorporated in numerical analysis. The first section of Chapter 4 is concerned with predicting the effect of strain-rate on steel for inclusion in connection models. The second section looks at the use of finite element analysis with emphasis on component-based methods through the use of non-linear, rate dependent springs and how they can be used to represent a complete connection in the finite element software ABAQUS [Simulia (2009)].

In Chapter 5 dynamic component-based methods are developed for fin-plate and flexible end-plate connections which are able to account for the complete range of connection response. The static response is predicted using a simple moment equilibrium method whilst the dynamic response is predicted by incorporating individual component behaviour into ABAQUS, using the methods presented in Chapter 4, and performing a non-linear dynamic time history analysis. Comparisons are made between the predicted behaviour and the experimental results from Chapter 3.

Chapter 6 incorporates the component-based connection models developed in Chapter 5 into a variety of sub-frame models to investigate the influence of connection characteristics on frame behaviour. Scenarios where large connection rotations are experienced in short time durations are of particular interest such as alternate load path analysis following a column loss or response to direct blast loading. Comparisons against existing methods of analysis are presented and the benefits and limitations discussed.

Chapter 7 includes discussion and general conclusions of the research project as well as recommendations for future work.

2 LITERATURE REVIEW

2.1 Introduction

This thesis is principally concerned with the behaviour of steel connections; however there is also a need to understand aspects of blast and explosive engineering. Therefore this literature review will first investigate work conducted on the behaviour of structural steel connections before focusing on the specific use of the component method for joint modelling. Following this the area of blast and progressive collapse will be explored with specific attention paid to structural analysis under these conditions.

2.2 Steel connections

The terms joints and connections are often used interchangeably, in practice however a distinction between the two needs to be made. Faella et al. (2000) define the connection as the part of the joint which physically fastens the beam to the column and is located specifically where this action occurs i.e. the weld or bolts. The joint is the connection plus the surrounding zone of interaction (the panel zone) between the beam and column.

Structural steel frames consist of universal steel beams and columns connected together at various locations in the structure. These joints can be summarised as:

- Beam to beam
- Beam to column
- Column to column
- Column to foundation

This thesis is concerned with beam to column connection types. These are commonly split into two categories; simple and moment connections. Simple connections include partial depth end-plate (Figure 2-1), double angle web cleats (Figure 2-2) and fin-plates (Figure 2-3). These connections have a moment capacity significantly less than the supported member and are assumed to act like a pin support.
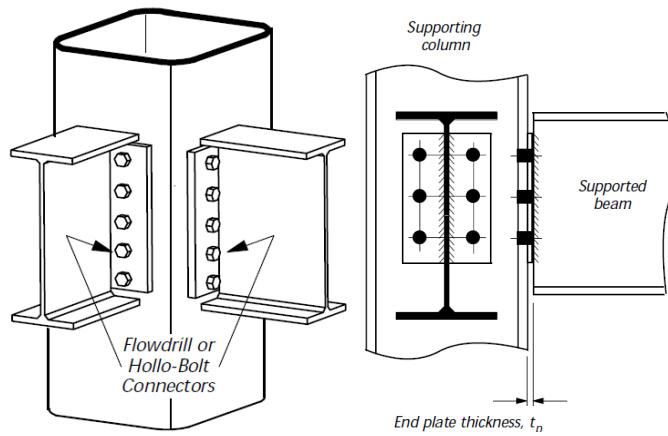
Figure 2-1: Flexible end-plate connection from BCSA/SCI (2002)
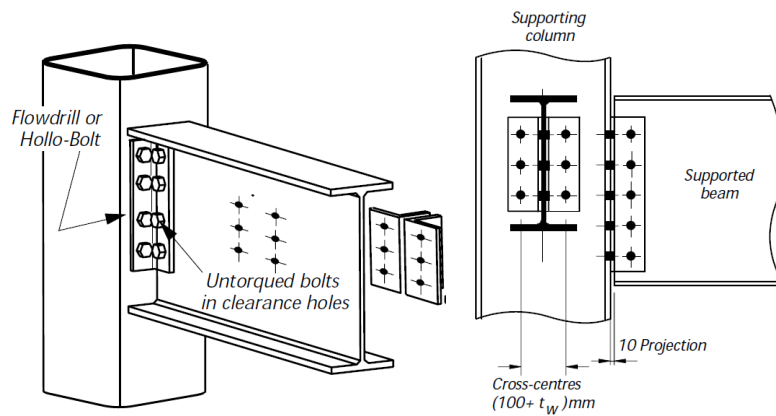
Figure 2-2: Double angle web cleat connection from BCSA/SCI (2002)
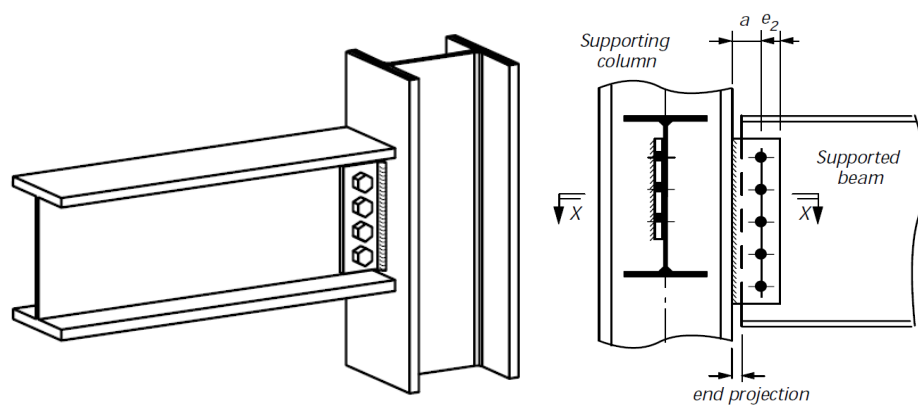
Figure 2-3: Fin plate connection from BCSA/SCI (2002)

Moment connections have a moment capacity greater than the supported member and thus are assumed to act as a rigid support. These can include full length and extended end-plate connections (Figure 2-4) and a variety of welded connections (Figure 2-5).

ZONE	REF	CHECKLIST ITEM	See Procedure
TENSION	a	Bolt tension	STEP 1A
	b	End plate bending	STEP 1A
	c	Column flange bending	STEP 1A
	d	Beam web tension	STEP 1B
	e	Column web tension	STEP 1B
	f	Flange to end plate weld	STEP 7
	g	Web to end plate weld	STEP 7
HORIZONTAL SHEAR	h	Column web panel shear	STEP 3
COMPRESSION	j	Beam flange compression	STEP 2
	k	Beam flange weld	STEP 7
	l	Column web crushing	STEP 2
	m	Column web buckling	STEP 2
VERTICAL SHEAR	n	Web to end plate weld	STEP 7
	p	Bolt shear	STEP 5
	q	Bolt bearing (plate or flange)	STEP 5

Figure 2-4: Extended end plate connection and relevant components from BCSA/SCI (1995)
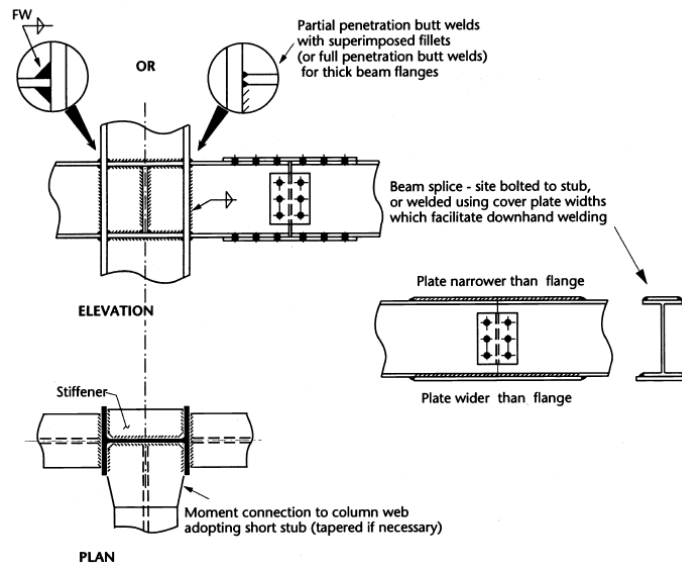
Figure 2-5: Example of a variety of welded connections from BCSA/SCI (1995)

The classification of these joints is now considered.

2.2.1 Joint classification

To simplify the assessment of steel structures connections are often classified according to their stiffness as either "pinned" or "rigid". However, the actual behaviour of many steelwork joints often lies somewhere between these extremes and much recent research has been focused on characterising the stiffness of these "semi-rigid" joints.

Joint classification is usually assessed by defining the behaviour of the joint as a function of the mechanical properties of the connected members. These can be classified according to their stiffness (moment-rotation), strength, rotation capacity or combinations of the three elements.

Stiffness classifications include rigid, simple and semi-rigid and are classified by comparing the joint design stiffness to either fully rigid or pinned behaviour. Strength classifications are made by comparing the joint moment resistance to full-strength and partial-strength boundary conditions.

It was not until the 1930's that the need to understand joint moment-rotation behaviour became apparent [Moore (1988)]. Research was conducted around the globe however it was not until the 1950's that the first attempt at providing design procedures for beam-to-column steel joints was completed by the British Constructional Steel Association. Their series of "Black Books" outlined procedures concentrating on the connections within the joint, i.e. the weld or bolts, and paid little attention to bending of components. Work on modelling joints progressed slowly due to the non-linearity of the moment-rotation behaviour. Since the 1970's, when the use of semi-rigid joints was accepted as a valid form of construction, many efforts have been made to include these for accurate global structural analyses.

Under typical conditions the influence of axial deformation in structural response is not significant and the stiffness of the floors is usually great enough to prevent deformation of the joint in the horizontal plane [Faella et al. (2000)]. It is therefore general practice to assume the joint response can be expressed through the moment rotation relationship [Foley and Vinnakota (1995)]. To include these in design it is often useful to represent the moment-rotation curve analytically as represented in Figure 2-6.
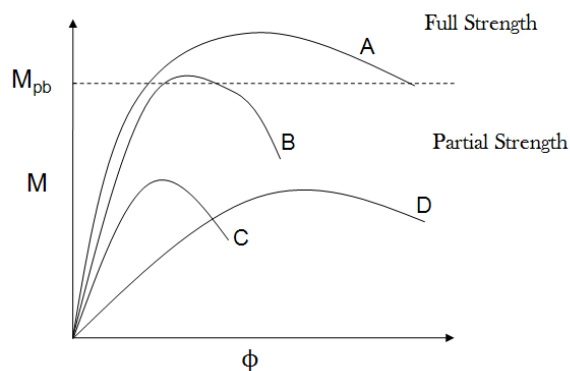
Figure 2-6: Beam-column joint classification according to moment resistance. Faella et al. (2000)

Full strength connections have a design resistance at least equal to the plastic moment resistance of the connected member (Case A) and thus a plastic hinge will form in the connected member. In some cases, however, strain-hardening of the beam could cause

connection yielding (Case B). Partial strength connections have a design resistance less than their connected members (Cases C and D). Here a plastic hinge will form in the connections as long as sufficient rotation capacity can be supplied; hence Case C is unsuitable because its rotation capacity could be exceeded under design loads.

Jones et al. (1983) note that in general it is more accurate to classify all steel frames as semi-rigid construction whilst recognising "simple" and "rigid" construction as theoretical extreme cases. The use of moment-rotation curves allows a prediction of the reduction in beam moment and thus leads to reduced beam sections and cheaper construction. Much work in previous years has gone into producing these connection moment-rotation curves. The most accurate method is achieved using experimental test data but due to the large amount of connection typologies it is unlikely that a designer will have access to reliable data on the exact joint he is studying. Experimental data is therefore often used to validate models which can emulate the actual joint behaviour from input criteria.

2.2.2 Experimental connection testing under static conditions

Although connections in steel frame structures are often assumed as either pinned or fixed, their flexural rigidity plays an important role in the global behaviour of the structure. Therefore most research has focused on the investigation of moment-rotation relationships of these connections to allow designers an understanding of the true behaviour. In addition, studies have been conducted on the tensile capacity of connections to allow the tying capacity to be checked for the purpose of complying with progressive collapse requirements. Accurate experimental data is essential to allow the analysis of realistic behaviour and the development of simplified analytical models.

The Goverdhan (1983) Data Bank includes data collected in the United States between 1950 and 1983. The types of joint studied include end-plate connections, double-cleat connections and several more. Jones et al. (1983) produced a state of the art report including a table of available connection data at the time for a range of popular connections. Further data banks of test data include those developed by Nethercot (1985) which included over 700 individual tests on a variety of connections and the Steel Connection Data Bank (SCDB) formed by Kishi and Chen (1986) which extended the type of connections to include t-stub connections with and without web angles.

The moment-rotation behaviour of bolted end-plate connections was the subject of Aggarwal and Coates (1986) who performed eight tests using gradually increased static loads. Parameters such as end-plate thickness and bolt diameter were varied whilst keeping a constant beam and column cross-section. The need to use a semi-rigid design method to better approximate for actual connection behaviour was noted with the requirement that well-documented moment-rotation curves are available for the connections.

The difference in assumed and actual connection behaviour was the subject of Nethercot et al. (1988) for connections in non-sway frames where simple connection assumptions are assumed. The results of a series of tests of connections types are used to illustrate the difference between the assumed simple behaviour and the actual performance of the connections.

Bernuzzi (1995) conducted a series of tests on beam-column connections under cyclic reversal loading for the purpose of seismic design. The test specimens included top and seat angles, flexible end-plates, flush end-plates and end-plates extended only on one side of the beam. Cyclic moment-rotation curves are presented for each connection type with an analysis of their performance.

In terms of robustness guidelines in the UK, one of the most significant pieces of research was that conducted by Owens and Moore (1992) who investigated the performance and tying capacity of common simple connections. Web-cleat and end-plate connections were both tested under direct tension and it was found that both connection types achieved the design tying capacity which had been recently included in the British Building Regulations. The numerical methods they developed formed the basis of SCI P207 and 212 for the design of simple and moment connections within the UK [BCSA/SCI (1995) and BCSA/SCI (2002)].

Sadek et al. (2011) conducted a series of tests on steel connections designed to represent column loss in a 10 storey building designed as intermediate and special moment frames (IMF and SMF respectively). The sub assembly consisted of 2 beams and 3 columns with the central column loaded until failure. The resulting force displacement profile displayed initial elastic response followed by plastic behaviour to failure with no softening evident. The ultimate beam axial loads recorded were 670kN giving an indication of the expected loads experienced during catenary action.

2.2.3 Experimental connection testing under dynamic conditions

Testing steel connections under dynamic loading is extremely difficult and problematic. The high loads and loading rates required mean that conventional hydraulic actuators are not suitable and drop hammers are not feasible due to their required size to get large loads. Also the required measurements must be recorded at high frequencies to capture the event resulting in expensive equipment requirements.

As a result, although the research of steel connections under static loading is highly developed, the same cannot be said for dynamic conditions and minimal information is available with regard to the dynamic performance of connections. TM5-1300 (1990) contains only a few pages dedicated to connections although it does encourage designers to provide sufficient integrity up to the point of maximum response. Similarly the availability of experimental results categorising the dynamic performance of steel connections is very limited.

One area which has possible links is in seismic design where work has been performed on the performance of connections for seismic applications [Rassati et al. (2004), Khandelwal (2007), Hooper et al. (2008)]. These are generally concerned with moment-resisting connections at relatively low rotations due to horizontal sway. The cyclic behaviour and strength reduction due to this movement is essential for the survivability of the frame however the time duration of each loading cycle is typically above 1 second due to the entire mass of the structure being mobilised. In comparison structural load redistribution following column removal is typically around a hundred milliseconds [Sasani and Sagiroglu (2008)].

FEMA (2000) produced a report, *FEMA-355D: State of the Art Report on Connection Performance*, which summarised the current knowledge of the performance of moment-resisting connections under large inelastic deformation demands with specific emphasis on seismic applications. This includes useful information regarding the non-ductile behaviour of typical connections from which the limiting rotations for these connections can be found. However these do not make up for the lack of data directly related to the dynamic performance of the connections directly loaded by blast.

Munoz-Garcia et al. (2005) showed that the response of simple beam to column steel connections is affected by the rate of loading. The connections considered included

flexible end plate, web cleat, flush and extended end plate types and were modelled using LS-Dyna, an explicit finite element analysis code. Material strain rate sensitivity was accounted for using the Cowper-Symonds formulation. A variety of loading rates were applied in rise times of 1, 10, 100 and 1000 ms. The investigation demonstrated that the shorter the rise time, the less load the connection could sustain, generally making the connection fail in a brittle way despite the fact that the steel model included enhancement factors to account for high strain rates.

There are numerous case studies of steel framed structures collapsing due to accidental or deliberate loading, the most high profile of which were the World Trade Centre 1 and 2 Towers. The collapses were initiated by aircraft impact which caused fires throughout the structures. Severe damage was also experienced by surrounding structures including WTC5, an eight storey steel framed office block. WTC 5 experienced partial progressive collapse due mainly to impact debris from the damaged towers. The impacts caused extensive damage to steel members and caused floor beams to separate from the floor deck and others to separate at the welded connections. A recovered sample from WTC5 is shown in Figure 2-7 which demonstrates a combined shear and tension failure of a connection web plate.

Figure 2-7: Extract from WTC Building Performance Study, FEMA (2002)

This highlights the consequences of dynamically failed connections. Although it is impossible to predict all loading combinations, the ductility and robustness of the connections is paramount in order to minimise risk to building occupants and prevent

collapse. The lack of research in this area must be addressed to find the best performing and most appropriate steel connections under a range of dynamic loads.

2.3   Component-based methods

Mechanical models, also known as spring models or component models, are based on the simulation of the behaviour of the joint using a set of rigid and flexible components. The components are considered as non-linear springs with their own resistance and stiffness, obtained from empirical relationships, and are subjected to a specific loading i.e. column web in compression, beam flange in tension, end-plate in bending. Individual analysis of the components takes place before the components are reassembled to assess the global response of the joint. The behaviour is characterized by stiffness, strength and ductility which can then be used to predict the moment capacity, rotational stiffness and the tying capacity of the joint.

The component method is often incorporated in analysis by using a rotation-controlled method whereby the rotation is increased step-by-step and the force in each bolt row calculated for each step.

Mechanical models have been developed to include most types of common connections. Wales and Rossow (1983) investigated the behaviour of double web angle bolted connections and proposed a model for its simulation subject to bending moment and axial loading (Figure 2-8). The nonlinear behaviour of the bolts was studied and the application of the model to a plane frame demonstrated. This model was developed by Richard et al. (1987) to include the top and seat angles and a simple analytical connection model comprising rigid links and non-linear springs was produced (Figure 2-9). The use of force-deflection data was used to derive the non-linear spring behaviour representing the angle segments and moment-rotation curves generated. The results were then compared against full-scale test data and a close correlation with the experimental data was found. The ability of the model to account for axial forces is significant as these influence the characteristics of the moment-rotation response.
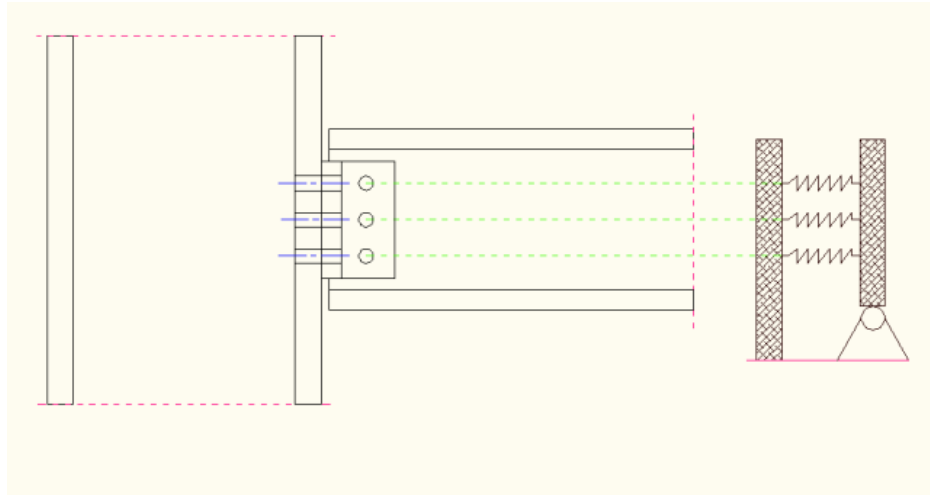
Figure 2-8: Component model for web angle connections from Wales and Rossow (1983)
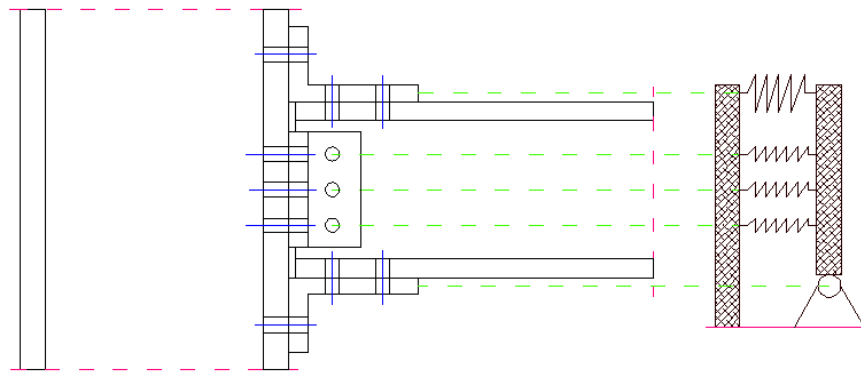
Figure 2-9: Component model extension to include top and seat angle connections

These models cannot accurately predict the behaviour of welded joints because the response is affected by the deformation of the beam and column flanges and the deformation of the panel zone. Tschemmernegg (1987) analysed the behaviour within a welded connection by conducting a series of tests. The results suggest the use of a shear spring in addition to load introduction and connection springs to produce the required elastic-plastic moment-rotation curves.

The components of a joint are the sources of deformation and potential areas of failure. Welds can exhibit brittle failure, and as a result they are not considered a component of the joint and can be modelled by assuming the connection springs are infinitely rigid. However because the weld is not included in the model the potential failure must be closely examined and the weld properly designed. This model remains suitable provided that knowledge of the behaviour of each component of the joint is available.

A large amount of complexity can be included in component models utilising an increasing number of springs. Figure 2-10 shows how these models are assembled with reference to the geometry of the original connection.
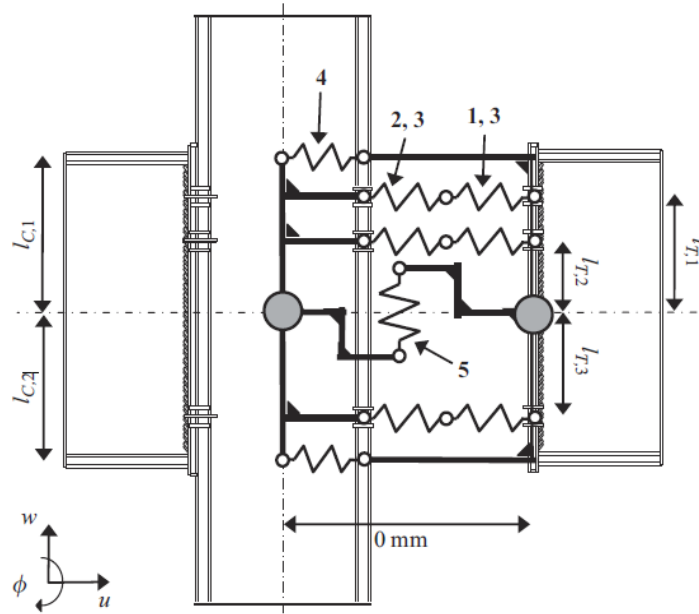
Figure 2-10: Component model of beam-to-column joint from Block et al. (2007)

BS EN 1993-1-1 (2005) Part 1.8 Annex J makes use of the component method for the evaluation of the moment-rotation response of joints. According to this, the component method can be simplified as:

- Evaluating the active components within the joint

- Evaluating the force-displacement relationship for each active component

- Global assembly of all the components to evaluate the moment-rotation curve

The method is capable of dealing with most types of joint by deconstructing them into suitable components. Eurocode 3 includes methods and formulas to define both the resistance and stiffnesses for the joint and also emphasises the importance of correct modelling of the panel zone under shear and compressive forces. The stiffnesses and strengths of the connection springs depend upon the deformation of the panel zone so Eurocode 3 introduces what it calls an interaction parameter (β) which depends upon the moments and shear forces within the zone. Since the forces within the panel zone are not known, the initial value of β must be assumed and the calculations take on an iterative process until convergence on the value is obtained. Different failure mechanisms are

18

identified and the minimum failure load corresponds to the design resistance of the connection. Pucinotti (2001) extends the use of BS EN 1993-1-8 (2005) Annex J to include top-and-seat and web angles.

Eurocode 3 models each component using an equivalent bi-linear spring and these springs are then assembled to form a single nonlinear rotational spring [Bayo et al. (2006)].
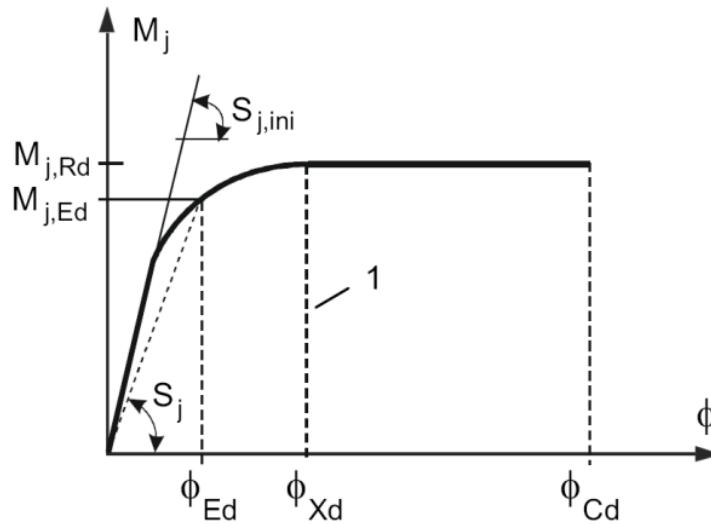
Figure 2-11: Design moment-rotation characteristics; BS EN 1993-1-8 (2005)

This rotational spring, the properties of which are expressed according to the moment-rotation behaviour as shown in Figure 2-11, represents the connection and is attached between the beam and column for global analysis. The behaviour of this spring is characterised by the initial stiffness, $S_{j,ini}$ (from all components) and its moment resistance $M_{j,Rd}$. The method of using rotational springs has been shown by Cabrero and Bayo (2007) as an excellent and versatile analysis tool for joints under normal operating conditions; however problems occur when these conditions are not met. Daniunas and Urbonas (2008) investigated the effect of axial force and concluded that it can indeed have an influence on the rotational stiffness and moment-rotation of the joint. Thus the use of a single rotational spring, with one moment-rotation function, is not suitable for all applications.

A computer program entitled "*CoP - The Connection Program*" [Jaspart and Weynand (1995-2000)] has been produced by the co-authors of Eurocode 3. The software implements the component method outlined above in a user-friendly manner requiring a series of input data. A 2D or 3D representation of the joint is produced and data entered is checked against code limitations and geometrical restrictions.

The software allows a quick <mark>and</mark> easy method to produce economical designs and optimisation of joints.

It must be noted that the revised Annex J of Eurocode 3 does not include formulations for steel joints subjected to an axial force or combinations of axial force and bending moments. Simões da Silva et al. (2000) recognised this and provide values to include these axial forces in calculations. An equivalent elastic model was developed by Simões da Silva and Girão Coelho (2001) to investigate the relationship between these two forces without the need for complex non-linear numerical evaluation.

A development of Part 1.8 has been proposed by Beg et al. (2004) to determine the deformation capacities of the basic components of end-plate connections. The results of the analytical method showed a good agreement with experimental data with 4 different calculations for the strength of the individual components. It was shown that the characteristic values of the measured yield stress should be used in calculating the rotation capacity rather than the design values of the yield stress given in the code.

The advantage of using the component method is that it is able to predict the behaviour of steel joints without having to test the full range of joint combinations and without having to perform costly and time consuming three dimensional finite element simulations.

2.3.1 Flexibility of the component method

The separation of a joint into its individual components allows the method to be applied to a variety of conditions.

Broderick and Thomson (2002) investigated the response of flush end-plate connections under earthquake loading and compared the results against a Eurocode 3 component model. The results were favourable, but underestimated moment resistance whilst overestimating initial stiffness. This is similar to many findings from work done at ambient temperature. An extremely positive outcome of this report was the accurate prediction of failure modes of the joints tested. These results indicate the component method has potential for dynamic conditions.

Another important use of the component method has been in its development under fire and elevated temperatures. These cause large rotations and high axial forces within joints which make it very difficult to predict their behaviour using standard methods.

Spyrou (2002) states, the component-based approach compares very favourably with other methods to predict joint behaviour at elevated temperatures in terms of both economy and the ability to follow the full non-linear response. In his thesis a component model of a balanced, bare steel, two-sided joint is presented. Individual springs are used to simulate the stiffnesses of the individual components and to simplify the situation all tensile forces are grouped as one spring. The ultimate resistance of the joint is calculated using formulae given in EC3: Annex J. The model was then validated against tests performed by Leston-Jones (1997) and Al-Jabri et al. (1998). The model provides good results and was able to accurately predict the failure mode in all cases, thus providing accuracy within acceptable limits for design purposes. The simplicity of this method is emphasised with the ability to modify the arrangement for different temperatures and alternative arrangements.

Spyrou et al. (2004) extended the work looking at steel flush end-plate connections under elevated temperatures using the component method. Their objective was to investigate the tension and compression zones of end-plate connections at elevated temperatures both analytically and experimentally and then assemble a mechanical model to simulate this behaviour. Of importance to the authors was the overall frame response due to the high axial forces created from the restraint to thermal expansion. High temperature tests were completed using image processing techniques to measure deflections. They found that the component method is ideal for this situation, where the large rotations and axial forces can be included in the analysis simply using the stiffnesses of the elements. There was a very close correlation between the analytical model and experimental data produced by Al-Jabri (1999). The advantage of this method is that the moment-rotation-temperature response is generated within the analysis and does not need to be input as data.

Block et al. (2004) further advanced the use of the component method for end-plate connections by considering the behaviour of the column web in compression. This zone is important in fire due to the possible large thermal expansion of beams.

Sarraj (2007) developed a component model for fin plate connections taking account of the deformation of the fin plate, the beam web and the bolt. All three areas of deformation were evaluated at different temperatures using finite element analysis. The resulting load-deformation profiles were curve fitted to provide empirical equations for each region of deformation.

Vlassis et al. (2008) developed a method for progressive collapse assessment of multi-storey buildings based upon the static load deformation behaviour of the structure. In order to calculate the static load deformation behaviour they proposed the use of component-based methods to model the connection demands on a simplified sub assembly. The individual component behaviours were calculated based upon BS EN 1993-1-8 (2005) recommendations for initial stiffness and yield limit, with failure criteria specified based upon previous investigations into the ductility supply of common joints. The method was found to be suitable for such an assessment with the authors noting a need for further investigation in relation to joint response and ductility under combined bending and axial tension.

Sadek et al. (2011) also used component-based methods to study the effect of static column removal in a double spanning sub assembly. The authors called these connection assumptions "*reduced complexity finite element models*". Nonlinear spring elements were used to model the shear behaviour of the bolts and bearing deformation of plate steel. The predicted behaviour showed a very good correlation with the experimental data for both load-displacement and beam axial force development.

2.4   Blast and progressive collapse

In order to assess the suitability of the component method for blast and progressive collapse conditions a review of design methods, expected loading conditions, design criteria and methods of structural analysis under these conditions is presented.

Historically, concern with blast protection has tended to be a reaction to disasters or a particular threat. Much progress has been made over the years in analysing blast phenomena and incorporating this understanding into structural design. With the increase of terrorism throughout the twentieth Century the need for blast resistance has become more and more important.

US design guidelines related to blast such as those by the GSA (2003) and US DoD (2009) dictate the maximum percentage of floor space that can be sacrificed due to the loss of a particular structural element, typically a column. This method assumes that the adjacent structural elements are capable of maintaining their integrity during the redistribution of the loads which can include extremely large connection rotations. Designers and contractors are looking for the most cost-effective solutions to these problems which leads

directly to the purpose of this study: understanding the behaviour of steel beam-to-column joints under blast loading.

2.4.1 Progressive collapse standards and guidance

Investigations into progressive collapse and the ability of a structure to survive unusual loading has resulted in two primary design methods:

- Indirect design, which centres on structural elements having a minimum level of ductility and strength through application of simple design and detailing rules, such as the minimum tying requirement. Also included is the **alternate load path** strategy, where failure of some elements is allowed but the loads are taken up by other load paths.

- Direct Design or the **key element** strategy (specific local resistance method) is where key elements are identified and then designed to resist a specified action. The design is thus resistant against a specific threat.

Both methods have advantages and disadvantages and as a result are rarely used in isolation. The specific local resistance method designs points of high strength in the structure at areas that are thought to be at risk from accidental loading. It requires that these accidental loads be specified and there is therefore no reassurance that the structure will perform adequately for alternative threats. Using the alternate load path approach, the system is designed to allow the redundancy of locally damaged zones. Alternate load paths can be provided by catenary action, arching, vierendeel and out-rigger trusses in floors above and is often favoured as the method is independent of the threat (i.e. column loss may be assumed from either vehicle impact or explosion). This method forces the designer to consider the behaviour of the entire structural system following the occurrence of an abnormal event. However, the analysis skills and computational tools required for this type of design may be outside the practice of many engineers [Ellingwood et al. (2009)]. The use of the key element method is also of particular importance in high risk structures such as government buildings.

In the United Kingdom, buildings are classified into 4 types according to the current UK Building Regulations (2004). Class 1 structures are at a low risk and, assuming they are designed to the appropriate standard, require no additional measures to avoid progressive collapse. Class 2A are required to have the beam/column connections designed sufficiently

to act as horizontal ties and the anchorage of floors to walls is to be ensured. These horizontal ties must have a minimum design capacity of 74kN. There are three methods by which a Class 2B structure can achieve the requirements:

- In addition to horizontal ties, columns and splices are designed as vertical ties for all load supporting members and there are bracing system requirements
- Notional removal of a single column or beam (1 at a time for each storey) should not result in an unstable structure and the loss of floor space should be less than 15% or 70m^2 (100m^2 for BS EN1991-1-7) and should not extend to adjacent bays.
- Where removal of the above elements exceeds the damage criteria, these elements are to be designed as key elements.

Class 3 must satisfy all of the above and a significant risk assessment into all normal and abnormal loads must take place.

The principal documents in the Eurocodes relating to structural robustness are BS EN 1990 (2002) which defines the ultimate limit states and combinations of actions and BS EN 1991-1-7 (2006) which describes how the requirements should be met. Way (2011) outlines adoption of these Eurocodes in the United Kingdom. Two generic strategies are adopted for designing structures against accidental loading based on whether the accidental action is identified (Section 3.3) or unidentified (Section 3.4). These strategies include:

- Preventing the action occurring
- Key element design
- Designing structural members for sufficient ductility and capable of absorbing significant strain energy before rupture
- Incorporating redundancy in the structure through alternate load paths
- Prescriptive design and detailing rules

As Way (2011) states it is important to consider that the measures provided are
"…designed to strike a balance between cost and safety and which experience suggests produces structures that perform adequately in extreme circumstances."

IStructE (1995) provides the following recommendations for the design of new buildings to obtain a level of robustness for specific blast designs:

- Continuous top steel in reinforcing slabs

- Effective connections between beams and slabs

- Lateral restraint to the bottom flange of steel beams

- Additional ties or bolts between beams and perimeter columns

- Moment resisting connections between beams and columns

Guidelines in the United States are more explicit about designing to prevent progressive collapse. GSA (2003) produced a document entitled *"Progressive collapse analysis and design guidance"* which includes a chapter devoted to steel frame building analysis and design. The minimum criteria is that floor girders and beams are capable of spanning two full spans essentially providing alternate load paths in the case of column loss. This is achieved by considering both the behaviour of the supporting column and beams and also the structural continuity provided by the connections. This structural continuity is described as "fundamental" to mitigating progressive collapse in steel frame structures. The selection of beam-column connections is achieved by considering:

- Beam-to-beam continuity

- Connection resilience

- Connection redundancy

- Connection rotational capacity

- Connection strength demands

In addition only connections which have been qualified by full-scale testing to ensure they have the required properties may be used in new builds. Attention is paid to the use of moment connections where a plastic hinge is formed in the beam and the connection is assessed to ensure it has the satisfactory strength, rotational capacity and ductility to withstand the redistributed loads.

The guidelines advise the use of three dimensional analytical models subject to a linear elastic, static analysis procedure. Two dimensional models may also be used. The potential for progressive collapse is assessed for the case of instantaneous column loss at a variety of floor levels for both interior and exterior columns. Once the column is removed the survivability of the individual elements is assessed using demand capacity ratios (DCRs). If the DCR for any member or connection is exceeded, based upon shear force, the element is considered to have failed and is removed from the analysis and all related loads are

redistributed to other members in adjacent bays. If a DCR is exceeded, based upon moment capacity, a hinge is inserted at the centre of yielding for the connection or member. This process is applied to all structural elements and then the entire process repeated with the modified frame model. If moments are redistributed throughout the structure but there remain DCRs exceeded outside of the allowable collapse region, then the structure is considered to have a high potential for progressive collapse.

Although not required for the static analysis, the removal time of the column can have an influence on the response of the structure during a dynamic analysis and the guidelines take account of this by limiting the removal time to 1/10 of the time period of the removed element. Structures found to have a high potential for progressive collapse are to be redesigned.

An additional guide for preventing progressive collapse is the United States US DoD (2009) Unified Facilities Criteria (UFC) 4-023-03 *"Progressive collapse analysis and design guidelines for new federal office buildings and major modernization projects"*. The document closely follows the approach of FEMA (1997) 273 and 264 by incorporating flow charts to check if the structure requires progressive collapse design, the level of which is related to the occupancy category (OC) of the structure. If it is found necessary to design for progressive collapse then procedures are outlined which employ tying forces, alternate load paths, enhanced local resistance or a combination of all three. In general these methods use the load and resistance factor design approach (LRFD) with factors obtained from ASCE/SEI (2010). Three analysis procedures are employed; linear static (LSP), non-linear static (NSP) and non-linear dynamic (NDP). Demand capacity ratios are used, similar to GSA, to assess the capability of each structural element. Analytical models used to perform alternate load path analysis are discussed in the following section.

Both the DoD and GSA guidelines use similar scenario-based methods to aid designers in avoiding progressive collapse however the DoD guidance also provides a tie force procedure to allow large deformations through catenary action [Ellingwood et al. (2009)].

Use of the tying approach assumes that the connections have sufficient ductility, rotational capacity and axial capacity to allow structural members to span over lost vertical support as shown in Figure 2-12. It has been used in the UK Building Regulations since the

progressive collapse witnessed at Ronan Point, however the mechanics behind this approach are not well defined [Marchand and Alfawakhiri (2004)].
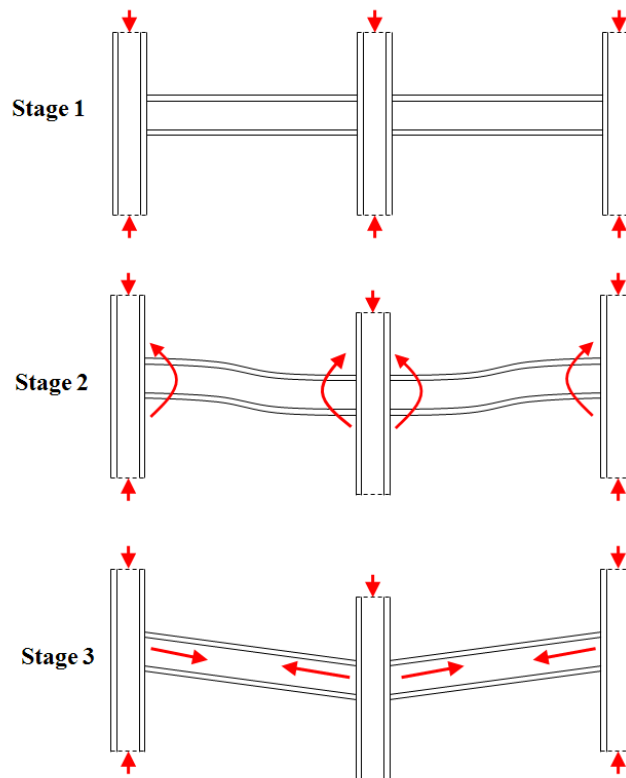
Figure 2-12: Tying force development in a steel frame with semi-rigid connections as a result of loss of column

In order to form the catenary described above, the connections must be able to provide the tensile capacity following the flexural response and allow load redistribution. Deflection at the lost column of 10 percent of the double span is permissible within the guidelines however there is concern that the majority of connections are not able to sustain such large rotations. Following the LRFD approach, the design tie strength is taken as the product of a strength reduction factor and nominal tie strength calculated in accordance with the relevant material codes.

Currently the ASCE Structural Engineering Institute's Progressive Collapse Committee is developing new guidelines to aid all those involved to understand the risks and methodologies with an emphasis on mitigating progressive collapse reliably in the future.

Byfield and Paramasivam (2007) developed a method to predict catenary action for steel framed structures with semi-rigid connections. The method is based upon a static analysis and uses dynamic amplification factors to account for the dynamic nature of a column loss scenario. Factors of safety against collapse were presented as the ratio of connection tensile

capacity against the required tensile load. A case study was conducted for a typical multi-storey office block using fin plate connections with results indicating that following a column loss major structural collapse was likely.

2.4.1.1 Alternate load path procedures

Whilst indirect methods (providing tying forces between structural elements) and specific local resistance methods (design key elements to withstand abnormal loads) exist to reduce potential for progressive collapse, this section is concerned with the use of alternate load paths and how structures can be analysed to predict load redistribution in the event of the loss of a key member. This requires the engineer to consider the most suitable analytical procedure, model complexity and design assumptions within the constraints of expense, computing power and time. Cormie et al. (2009) define five analytical procedures used to perform such an analysis:

      i.   Linear static using dynamic load factors
      ii.   Non-linear static using dynamic load factors
     iii.   Non-linear static pushover (energy balance procedure)
     iv.   Linear dynamic
      v.   Non-linear dynamic

Linear methods require the material response to remain in the elastic range and second order (P-delta) effects and instabilities to be ignored. This limits their use to small-displacements and often leads to very conservative design in order to prevent invalidating the assumptions. Non-linear methods include material plasticity and are able to account for second order effects allowing alternative load path mechanisms such as catenary, membrane and arching action to develop.

All of the methods are required to account for the dynamic inertial effects of the collapse. The earliest and simplest methods use dynamic load factors (DLF) to modify the dead and live loads in a static analysis. The DLF is the ratio of the dynamic to static load required to produce the equivalent static peak displacement and can normally range in value from 2 for an elastic system subject to instantaneous column loss to 1 for fire scenarios where failure occurs relatively slowly. In methods incorporating material non-linearity, calculation of the DLF is complicated by energy dissipation during the ductility phase where members achieve significant plastic rotations and deformations. In these cases a dynamic multiplier

of 2 has been found to be conservative [Tsai and Lin (2009), Marchand and Alfawakhiri (2004)] and a factor of 1.5 has been recommended by Ruth et al. (2006) to provide a more realistic approximation and results in more economical designs. Use of these methods requires engineering judgement to select a realistic DLF.

A non-linear static pushover procedure has been recently developed by Izzuddin et al. (2008) which does not require an estimation of load factors to predict the dynamic response. This technique is based upon energy balance of the system where the potential energy released by the column removal is compared against the energy absorption capability of the frame. The method allows analysis at various levels of structural idealisation from a double span beam scenario to an entire bay of a multi-storey structure. The non-linear static response of the damaged system is calculated by gradually applying the gravitational loads in a static analysis. The static model can be created using either detailed or simplified models taking account of material nonlinearity and nonlinear connection response. The resulting non-linear load vs. peak displacement curve accounts for both elastic and plastic phases before either hardening (from catenary action) or softening (due to local element failure).
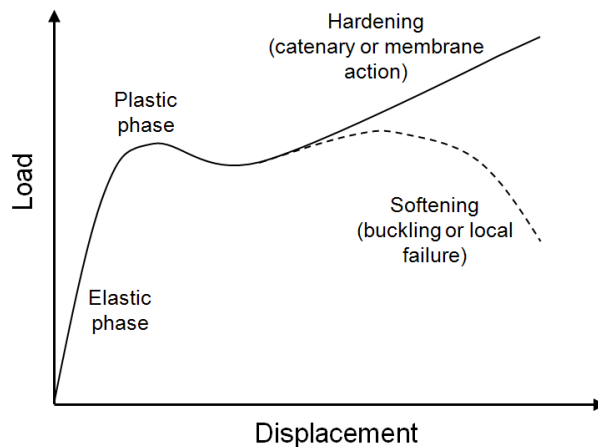
Figure 2-13: Typical nonlinear static response curve

Once the nonlinear static response is established a simplified dynamic assessment is conducted by assuming the response is dominated by a single deformation mode as originally described by Biggs (1964). This assessment procedure is used to transform the nonlinear static response into the maximum dynamic response by considering the energy balance between the work done by the load and the internal energy stored within the structure. As such, at the time of column removal the resistance is less than the applied gravity load and the structure accelerates. The difference between the work done and the

internal strain energy is the resulting kinetic energy. At the point where the resistance becomes greater than the applied load more strain energy is generated than the work being performed and the kinetic energy is reduced eventually bringing the structure back to rest. The value of displacement is calculated such that the strain energy and work done are equal giving the maximum dynamic displacement. If there is insufficient area under the nonlinear static curve to balance the work done then the structure has not reduced the kinetic energy to zero and thus collapse is likely. Assuming equivalence is achieved, the final stage is to perform a ductility assessment to ensure it remains within the limit state.

In a dynamic analysis the equations of motion are solved over discrete time steps which allow the complete time history response of the structure to be calculated. Because the dynamic effects are explicitly accounted for there is no requirement to define a dynamic load factor or calculate a pseudo-static response first. It is uncommon to perform linear dynamic analysis because the benefits of capturing the true behaviour of the structure are outweighed by its inability to account for geometric nonlinearity and the requirement to stay in the elastic regime. In general non-linear dynamic procedures are preferable as these are able to account for dynamic effects and load redistribution through the structure. US DoD (2009) guidance on producing analytical models to analyse and evaluate a structure's response is very precise. Where connections are weaker or less ductile than adjacent structural members, the connection must be modelled explicitly.

A full three dimensional computer model of a structure including the connections which incorporated accurate material properties (including strain-rate effects) and exact loading conditions would precisely replicate the real response. This has been attempted for high priority structures such as the collapse of the World Trade Center Towers as detailed in the final NIST report NIST (2005). A model of the entire structure was created and analysed in stages using a variety of finite element packages. These included details such as the behaviour of furnishing materials under impact debris and the effect of strain-rate and temperature on structural elements. Also modelled was the aircraft impact itself in order to calculate the initial structural damage from which the subsequent fire and collapse were analysed. One advantage the investigative team had was the large archive of photographic and video evidence, the technical documents describing the structures and the experimental data of the material properties that were obtained following the event. This data allowed

the team to compare the test results against the real behaviour and verify each stage of the analysis.
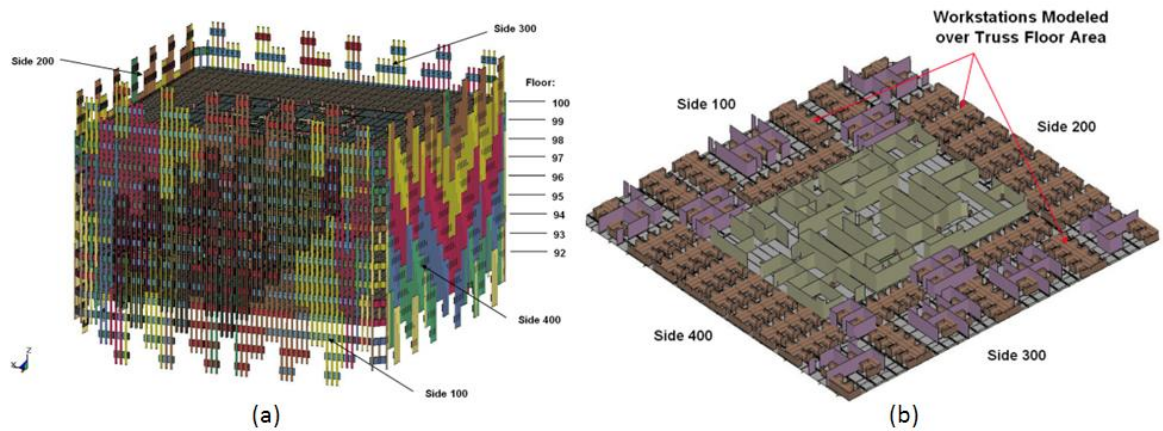
Figure 2-14: (a) Multiple floor structural model of WTC1 (b) Structural model of interior contents and partitions NIST (2005)

The complexity of creating a realistic numerical model coupled with the difficulty of verifying any results means that full representations of structures are rarely attempted. Instead assumptions are often used to reduce the model and computational time. If these assumptions are valid, the method is able to account for large deformations, nonlinear material properties at variable strain rate and allows the development of alternative load paths through catenary action. This provides the most realistic results and the most efficient designs for the prescribed load scenarios.

All of the analysis methods outlined above have their advantages and disadvantages as summarised in Table 2-1. In general the simpler procedures produce conservative designs but are easily verified. Conversely the more complicated methods allow a greater understanding of the real behaviour and more economical designs but require significant expertise to execute. Thus designing for progressive collapse is a balance of cost of resources against cost of construction. A typical structure will require static and stability analyses prior to commission and therefore these may be adapted using a dynamic load factor to provide an initial estimation of progressive collapse performance. Depending upon the level of robustness required these initial estimations can be followed by subsequent increasingly complex methods until sufficient performance is obtained. This *progressive analysis method* Marjanishvili (2004) allows the results for each step to be compared against the previous whilst ensuring the correct level of complexity is achieved.

The most complete analysis guidelines to date include those published by the United States General Services Administration GSA (2003) and the United States Department of Defense US DoD (2009) both of which identify methods of analyses which can be used for the alternate load path analysis. In comparison UK Building Regulations (2004) and Eurocode BS EN 1991-1-7 (2006) provide requirements and acceptance criteria but do not recommend specific computational methods.

	Linear Static DLF	Non-linear Static DLF	Non-linear Static Pushover	Linear Dynamic	Non-linear Dynamic
Include material plasticity	✘	✔	✔	✘	✔
Account for strain hardening	✘	✔	✔	✘	✔
Include second order (P-delta) effects	✘	✔	✔	✘	✔
Negates the use of dynamic load factor	✘	✘	✔	✔	✔
Explicitly account for strain-rate material effects	✘	✘	✘	✘	✔
Account for damping	✘	✘	✘	✘	✔
Allowable in GSA GSA (2003)	✔	✔	See note[1]	✔	✔
Allowable in DoD US DoD (2009)	✔	✔	See note[1]	✘	✔

Table 2-1: Comparison of progressive collapse procedure capabilities

2.4.2 Structural response to blast loading

A structure can respond in several ways depending upon the blast characteristics and in particular the loading duration. Often this duration is a small percentage of the natural period of the whole structure and so has little impact on the lateral force resistance of the

---

[1] The non-linear static pushover method has been developed since DoD and GSA guidance were published and at the time of writing is not currently included. This may change as new versions of the guidance are produced.

building, however the higher frequencies of individual elements are often in this range and thus are liable to severe local damage [Marchand and Alfawakhiri (2004)]. The failure of individual elements can lead to subsequent failures culminating in a progressive collapse.

Current methods of predicting response to this blast loading are usually limited to the US Military's TM5-1300 (1990) *"Structures to resist the effects of accidental explosions"*. This provides a comprehensive method for the design of structures to resist blast loading. The method is based upon early work by Biggs (1964) and uses single-degree-of-freedom system based charts to predict structural behaviour.

The manual establishes design procedures and construction techniques to limit blast damage and explosion propagation. Design charts have been developed from experimental data and the fundamental theory to allow simple flexural elements to be designed for pressure-time loading.

The method uses conservation of energy, internal strain energy and virtual work to create an equivalent lumped mass-spring system which is produced specifically to provide maximum deflections of the element. This provides a quick approximation of the deflection that can be expected under a specified load, however the deflection-time history remains unknown and different design charts are needed depending upon the details of the element and the assumed shape of the load. The deflected shape is then assumed on the basis of end support conditions. Baker et al. (1983) state that *"the fundamental mode and the static-deformed shape give very similar results for a uniform loading"* when applied to displacements.

The SDOF method can incorporate elastic-plastic and plastic behaviour by modifying the spring stiffness during analysis. Under the action of external loads, the structural element is deformed and internal forces develop. The sum of these internal forces trying to restore the element to its static position is defined as the resistance. It is convenient to consider the resistance of an element as a force in the opposite direction to the applied load. The variation of resistance and deflection can be expressed graphically by a resistance-deflection function as shown in Figure 2-15.

The level of resistance is linear until a plastic hinge occurs within the element. Assuming the load still acts, deformation continues but the resistance has a new value based upon this elastic-plastic range until another plastic hinge occurs. This continues until a failure

mechanism is achieved at which point, the element's ultimate resistance, r_u, is achieved. The number of elastic-plastic ranges required before the ultimate resistance is achieved depends upon the element type and end support conditions. An investigation into the use of SDOF procedures to calculate the response of one way spanning elements is presented in Appendix B.
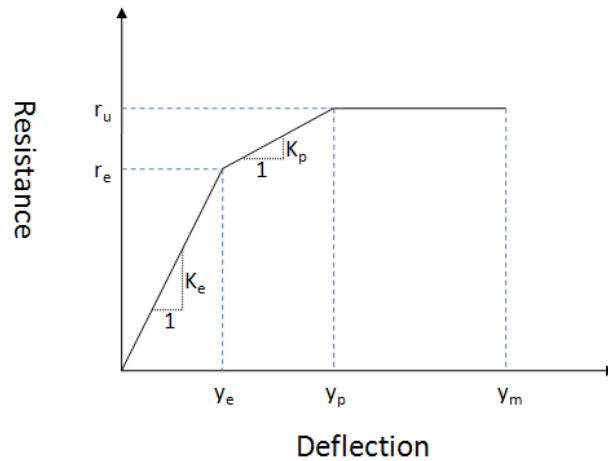
Figure 2-15: Tri-linear resistance function for a structural element

Naito and Wheaton (2006) used equivalent SDOF system modelling to assess the performance of structural elements subjected to explosive loading. A static, elastic pushover analysis of a shear wall was conducted to identify the failure location. This portion of the wall was then modelled as a lumped mass-spring system to approximate the dynamic response under blast. Nonlinear resistance behaviour was considered and resulting maximum displacements were found. The SDOF model was found to closely follow the results of the experimental data with regards to displacement, the possibility of shear failure was not considered. The authors state the importance of investigating shear forces, particularly under high impulse blast loads, but give no guidance on how to use the SDOF model to predict them.

One alternative to SDOF systems is the multi-degree-of-freedom method. Here every mass particle moves dependent on the loading and other particles and thus each has its own equation of motion. This problem can be solved in two ways, using either the lumped mass method or the distributed mass method. In the lumped mass method, the system is discretized into a finite number of nodes. Each node then has its own equation of motion and these are all assembled and solved. Accuracy of this method depends upon the number of dynamic degrees of freedom. The distributed mass method uses an infinite number of

degrees of freedom and the partial differential equations for the system are developed from force equilibrium. The standard derivation is available in many textbooks including Chopra (2000) and Biggs (1964).

Paramasivam (2008) used this theory to investigate the behaviour of columns under blast load. He concluded that when t_d/t_n is less than 0.1, an SDOF analysis will tend to underestimate the shear forces at the supports by as much as 50%. This is because the SDOF systems were established to provide accurate values of deflection and thus take account of the first mode of vibration because the higher modes have a negligible effect. However, under impulsive blast loading the higher modes can have a significant effect on the shear force thus leading to a significant underestimation. Simplified end conditions are assumed and thus inaccuracies arise when looking at other aspects of the response.
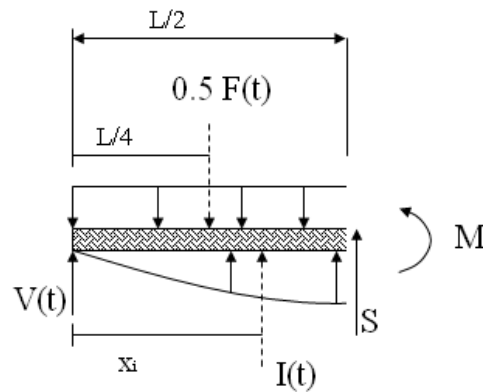
Figure 2-16: Determination of dynamic reactions including inertia effects

The distribution of the inertia force acting on the beam, *I(t)*, is identical to the deflected shape due to the motion being harmonic. The dynamic reactions acting at the supports, *V(t)*, depend upon both the load, *F(t)*, and the inertia force. These factors are used in the computer software WBiggs v4.4 produced by Baker Engineering and Risk Consultants Inc (2002) which is used by blast consultants to estimate response and reactions to blast loading. In comparison TM5-1300 (1990) only provides method to calculate maximum support shear using:

$$V_{max} = \frac{r_u L}{2} \tag{1.1}$$

Where r_u is the maximum resistance of the element.

35

For both single and multi-degree of freedom analyses the support conditions must be defined at the start as either perfectly simple or rigid. Therefore they take no account of semi-rigid connection behaviour or the effect of axial force or large rotations.

Thus there are methods available to calculate response to blast loading. However there are at present few studies which analyse the interaction of blast loads with the structural components in depth rather than looking at the effect on the building as a whole. The approach in TM5-1300 (1990) does not provide guidance or performance criteria for the steel connections, and effectiveness must be judged based on the performance of the steel frame.

Sabuwala (2005) examined the behaviour of steel connections under blast using finite element analysis and showed that the criteria in TM5-1300 (1990) used to judge the capability of a steel frame based purely upon rotation of structural members is inadequate. This leads directly to one of the aims of this study; to incorporate connection models which can represent the full range of actual connection behaviour into simple substructures and analyse their response to blast loading.

2.4.3 WW2 reports relating to frame performance

A bank of knowledge exists in the structural investigation of accidental and intentional explosions particularly those studies conducted during the Second World War. During this period much engineering work was conducted which, due to the intense pressure of warfare, was of considerable novelty and ingenuity. Although much of this work was not published at the time due to national security the Institution of Civil Engineers realised that this wealth of information would be lost and thus took steps to ensure the information would be published at an appropriate opportunity. The result was *The Civil Engineer in War - A symposium of papers on war-time engineering problems: Volumes 1-3*. Volume 1 [ICE (1948)] considered transportation issues such as bridges and airfields. Volume 2 ICE (1948)] investigated naval aspects of civil structures such as docks and harbours. And of most interest to this thesis, Volume 3 [ICE (1948)] looked at the properties of materials and structures. The effect of explosions on a variety of structures is covered in these volumes but of particular interest are the papers which examine the effect of explosions on framed structures.

Thomas (1946) notes the importance of reverse loading in vulnerable structures. This occurred when an aerial bomb penetrated the structure and then using a delayed fuse subsequently detonated between floors. The lower floor is subject to downward loading whilst the upper floor is subject to an upward loading that it is not designed for.

Baker et al. (1948) investigated over 50 cases of high-explosive bomb attack on multi-storey steel-framed buildings. The investigations showed the resilience of such structures as stated by the authors:

> *"a fully steel-framed building designed and constructed in accordance with good modern practice has considerable ductility and continuity, and is therefore highly resistant to damage by explosion"*

The behaviour of steel connections is of considerable interest. Flange cleats and web cleats were common methods of joining steelwork where the cleats were attached to the supported member using rivets (in place of the welds commonly used today) and then bolted to the supporting member.

Of interest is the observation that there is often considerable axial force within the supported beam which is then transferred to the connection causing tearing of the cleats or tensile failure of the bolts. The requirements of the connections are then a combination of axial loading and bending moment. The tendency of connections to fail in shear was noted although a number of tension failures were also recorded. The influence of the bending of the beam is recorded and failures occur not simply due to pure shear.

There have been many similar reports produced since the Second World War detailing structural damage as a result of explosions. These range from accidental gas explosions as made by Moore (1983) to analysis of terrorist bomb damage such as Mlakar (1998). Whilst these show the effects of such explosions the very nature of a post-event analysis means detailed monitoring of the behaviour before and during the event cannot be done.

2.4.4   Incorporating connection performance

For steel structures, it is widely accepted that connections are the most vulnerable elements within the structural system, Marchand (2004). Careful consideration must be paid to their design to ensure a suitable level of ductility and robustness. The importance of connection

performance is demonstrated by the analysis of bomb damaged multi-storey structures following the Second World War Baker et al. (1948) which led to the authors to conclude:

"Most structural failures in steel-framed buildings can be traced to weakness in the connexions."

Test data for all connection typologies is not available resulting in the use of simplified joint assumptions to predict frame response. These connection assumptions are rigid, simple or semi-rigid. Rigid joints are assumed to have an infinitely high rotational stiffness whilst simple joints provide no moment resistance. In reality every joint will exhibit behaviour somewhere in between these two extremes and can therefore be termed semi-rigid.
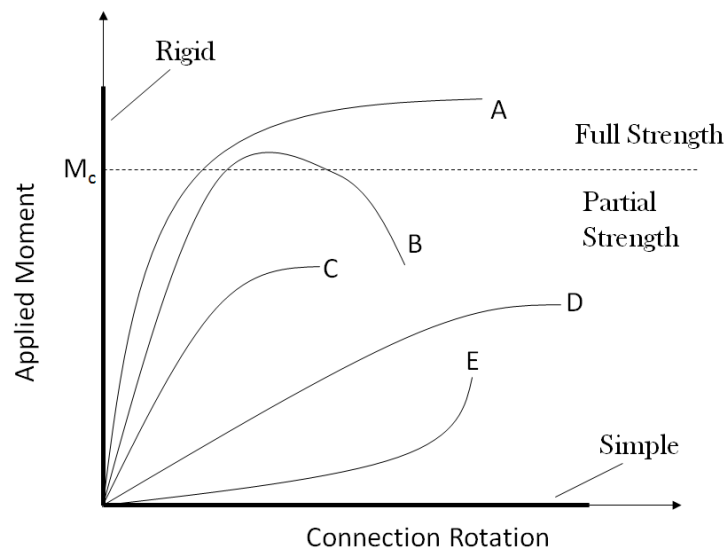
Figure 2-17: Beam-column joint classification according to moment resistance

Semi-rigid connections can be further classified according to the moment capacity (M_c) of the weakest supported member as shown in Figure 2-17. Full strength connections have a design resistance at least equal to the plastic moment resistance of the supported member (Case A) and thus a plastic hinge will form outside the connection region. In some cases however strain hardening of the member could cause early connection yielding (Case B). Partial strength connections have a design resistance less than their connected members (Cases C, D and E). In these cases the supported member remains elastic and all rotation demand is supplied by the joint, thus the rotation capacity is of primary importance. Where large rotations are a possibility, partial strength connections with limited rotational capacity (Case C) are to be avoided. The effect of prying action, where the beam flange

contacts the column (Figure 2-18), must be included as this can influence the stiffness of the connection and lead to premature failure (Case E).

Rotation about centre of connection · Rotation about lower beam flange · Failure
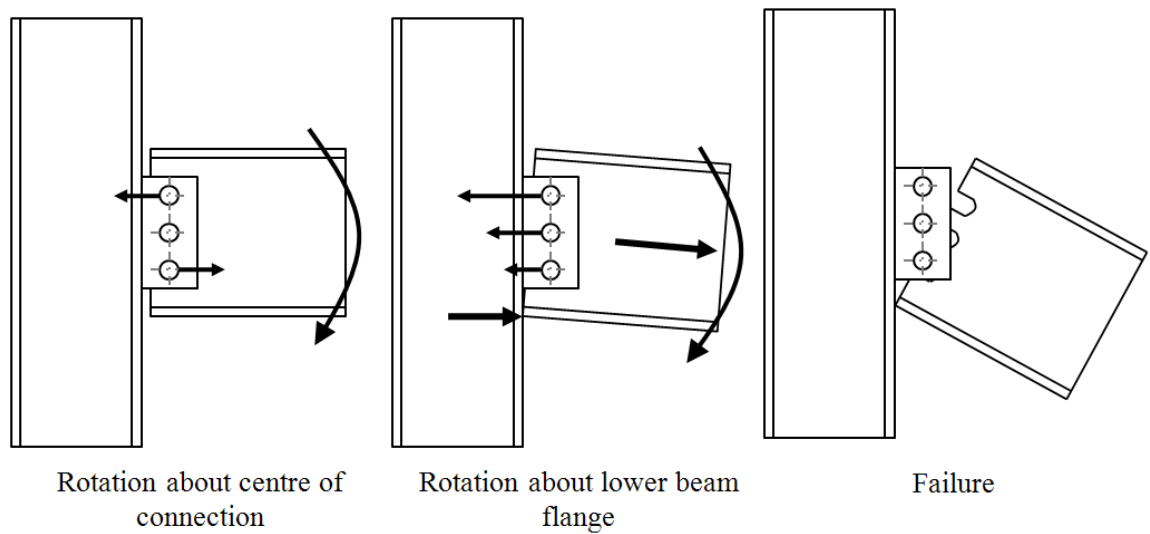
Figure 2-18: Development of prying action in "simple" connection

Incorporating semi-rigid behaviour into global structural analysis is necessary in order to capture the true rotational and tensile capacities, as these may influence the ultimate strength of structural members and the global survivability of the frame. The most complete way of achieving this is to use experimental data from connection tests, however the large number of connection types and variations mean that it is unlikely data exists for every design situation [Marchand (2004) and Izzuddin (2010)]. Advanced finite element models of connections have the ability to simulate accurate joint behaviour but require high levels of technical skill and computational expense. A simple alternative is the use of rotational hinges to account for nonlinear moment-rotation behaviour Liu et al. (2010). Typical parameters include elastic/plastic moment-rotation stiffness, yield/ultimate strength and ultimate rotation, however reliable formulae for quantifying this performance for the vast number of connection typologies and configurations are not always available, BCSA (2005).

For progressive collapse modelling, behaviour is further complicated by the presence of high axial loads and dynamic strain-rate effects. Tyas et al. (2011) have shown the rate of rotation has a significant effect on connection performance. The connection axial load capacity is commonly obtained from direct tension tests [Owens and Moore (1992)] which does not include connection rotation and subsequent prying action meaning that the predicted axial capacity may be significantly greater than in reality. This problem has been

the subject of recent investigations [Byfield and Paramasivam (2007)] where results indicated that many simple connections possess insufficient ductility to accommodate the large rotations that occur during catenary action. For these scenarios a single rotational hinge, or yield element, assumption which does not take account of axial loads is usually deemed unsuitable. Ellingwood (2005) notes that knowledge of connection behaviour before, during and after extreme events is essential for accurate prediction of alternate load path development.

The solution may be through the incorporation of component-based methods where the 'spring' elements are incorporated directly into the structural model and each active component makes its contribution to the overall behaviour independently through its structural properties. This will allow the prediction of the load distribution and failure mechanisms within the connection and account for all loading conditions including axial forces whilst modelling global equilibrium of the system.

2.5   Conclusions

This section has reviewed the literature relating to steel connections with close attention paid to the development of the component method. Dynamic loading on structures is a complex scenario and whilst connection simplifications can be made to facilitate analysis, the implication of these simplifications is not ideal. Progressive collapse analyses employing simple joint assumptions are a case in point where the dynamic strength, rotational stiffness and capacity of the connections are effectively unknown due to the unique combinations of axial, shear and bending moment. These limitations may be solved by using suitable component connection models which are able to take account of all loading conditions.

The method used in this thesis is to develop component models of bare steel connections which are able to account for dynamic factors such as material strength and inertial forces. These refined dynamic models will then be verified against experimental testing before being included in nonlinear dynamic structural analysis of steel frames and sub frames.

3 DYNAMIC MOMENT-ROTATION AND DIRECT TENSION TESTS ON SEMI-RIGID STEEL CONNECTIONS

3.1 Introduction

A number of tests have been conducted to establish the behaviour of common semi-rigid steel connections under dynamic loading conditions. The present work extends the scope to investigate problem areas in connection behaviour, in particular when connections are loaded rapidly to failure. Fin-plate (shear tab), flexible end plate and web cleat connections were studied.

The test arrangement, connection specification, instrumentation, testing procedure and results are described. The behaviour during the tests is detailed and the failure mechanism and analysis are discussed.

The test facility itself was designed and constructed by academic and technical staff of the University of Sheffield. The connection tests and subsequent analysis were conducted by the author.

3.2 Methodology

A purpose built dynamic connection test rig was constructed at the University of Sheffield's CEDUS laboratory. The rig was capable of providing loads in excess of 200 kN with a variable rise time from less than 5 ms up to static equivalent loading rates. This load was used to accelerate a column section away from a rigidly fixed beam. The column decelerates at a rate dependent on the stiffness of the connection and the inertial moment. The test rig allows tensile and moment loads or combinations thereof and is therefore suitable for the investigation of behaviour of progressive collapse due to column loss where large tensile loads and rotations are necessary to allow catenary action.

The rig layout allows for full-scale joint configurations to be tested under dynamic loading. There are 2 loading arrangements (Figure 3-1);

      a) Single loading ram with the free end unrestrained

      b) Dual loading rams for direct tension testing
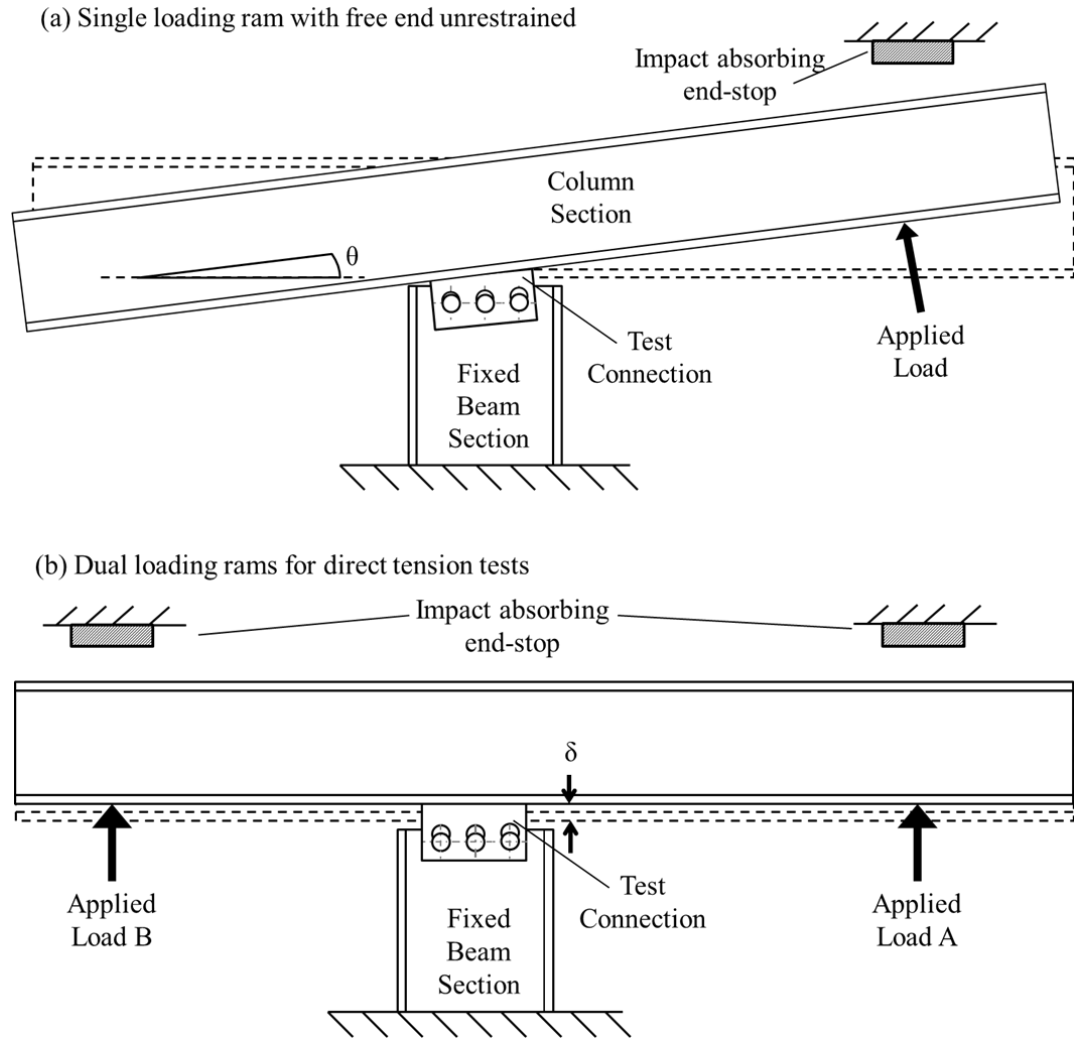
Figure 3-1: Plan of loading arrangements

The test rig itself consists of a cylindrical gas receiver which is charged using a compressor. The gas receiver was 1170mm long and had an external circumference of 153mm and a wall thickness of 16mm giving a total volume of $13.23*10^6$ mm^3. The pressure is released by the bursting of a calibrated diaphragm and the load applied to the test column using either one or two rams depending on test requirements. The test column is a 2m long 254x254x167 UKC section with 250x20mm thick stiffeners welded between the flanges at 500mm centres. The column is mounted on roller bearings to allow it to move freely under the applied load. Instrumentation allows calculation of the moment of inertia which is then used to find the actual force and moment applied to the connection. The test beam is fixed in location during each test but can be moved in relation to the load position to vary the moment.

3.2.1   Instrumentation

The instrumentation system used in the tests was designed to capture all of the necessary data (rotation, velocity, acceleration and applied loads) to determine the behaviour of the connections under dynamic loading. This includes laser displacement gauges, accelerometers and load cells. These were controlled using TiePie engineering oscilloscopes. All recording inputs were duplicated into an older LeCroy oscilloscope as a backup. In addition a digital 3D image correlation system developed in collaboration with the University of Bradford and Dantec Dynamics was used. This not only provided the displacement of the viewable region of the connections but the full-field measurement delivers accurate information about local and global strain distribution as well as crack growth which enabled an investigation into the failure mode for applicable tests and allowed a comparison between static and dynamic behaviour.

Custom built load cells were constructed from short lengths of steel hollow section using semi-conductor strain gauges wired to eliminate bending effects in the output strain. These were calibrated in a UKAS accredited test machine and demonstrated an accuracy of +/- 1kN in the range of 0 to 250 kN..

Linear voltage displacement transducers (LVDT) are commonly used to measure displacement. These use a central core rod which moves through a coil inducing a voltage which is calibrated. LVDTs are a highly reliable, however due to their mechanical nature they are not ideal for dynamic problems. In this case a more suitable alternative is a laser displacement gauge. These use the principle of triangulation (Figure 3-2) to determine object displacement. The sensor head projects a laser beam to the object and the diffuse-related light from the object's surface is received as a spot image. This spot image moves within the position sensitive device (PSD) and the optical triangle is used to compute the exact distance between the sensor and the object. The main benefits of using laser displacement gauges are high accuracy (+/-0.5mm) and extremely fast reaction time (frequency rate in excess of 40kHz).
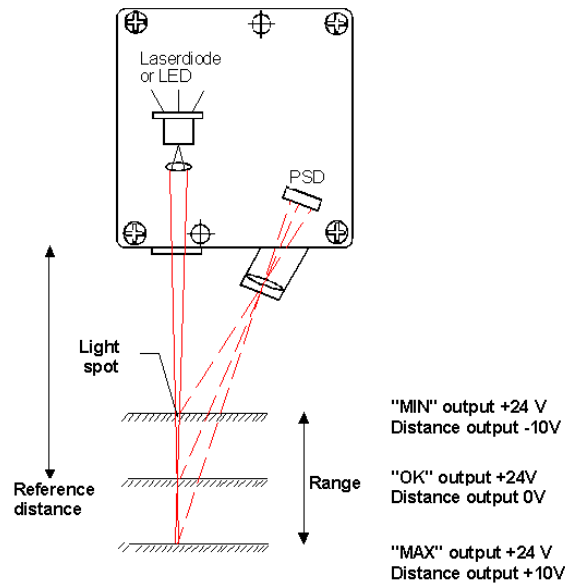
Figure 3-2: Use of laser displacement gauge from NFM (2011)

Two laser displacement gauges manufactured by MEL Microelektronik GMBH were located at 100mm from either end of the column section. From these the rotation, rotational velocity and rotational acceleration can be calculated. The main requirement for using these gauges is to ensure the body is mounted in a fixed position perpendicular to the target surface. To protect the gauges they were mounted on the fixed side of the rig behind the loading ram, thus if anything went wrong they would not be damaged. In some tests a third displacement gauge was used to provide additional information when required.

Two accelerometers manufactured by PCB Piezotronics Ltd were used to record the acceleration of the column section and used to verify the laser displacement gauge data. These accelerometers had a range of +/-500 and +/-50g. A single accelerometer was used for each test and was located at the position of the load ram.

Rapid deceleration caused by the column being brought to rest could cause severe damage to the sensitive equipment. The solution was to increase the time duration of the deceleration by placing deformable material between the column and end stop. The associated cabling was suspended from the roof to allow the accelerometer to move unimpeded.

The calibrated compression load cells were used to measure the loads applied to the column section throughout the tests. The load cells were mounted at a fixed distance from the end of the column section and a hemispherical steel bearing ensured they measured the applied load perpendicular to the column flange (Figure 3-3).
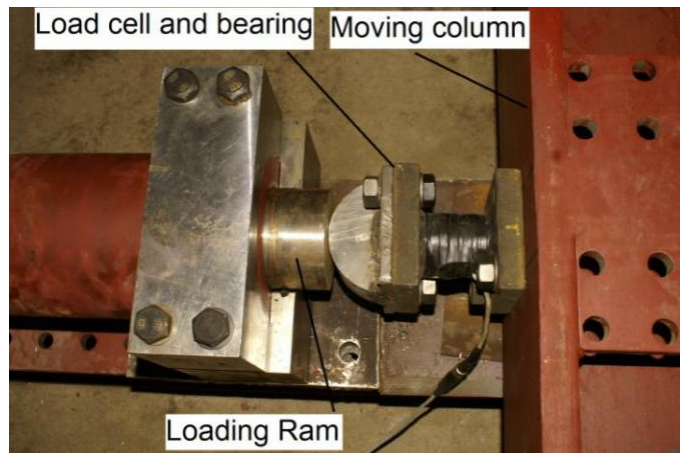
Figure 3-3: Load cell arrangement

The loads were applied by the pneumatic ram using a variety of loading conditions dictated by the diaphragm installed in the pressure receiver. A series of bursting trials were carried out in order to predict the load-time history for a variety of diaphragm arrangements. The diaphragms were made from either 0.51mm (thin) or 0.9mm (thick) brass and bolted into a specially constructed cassette with a 27mm aperture (Figure 3-4).
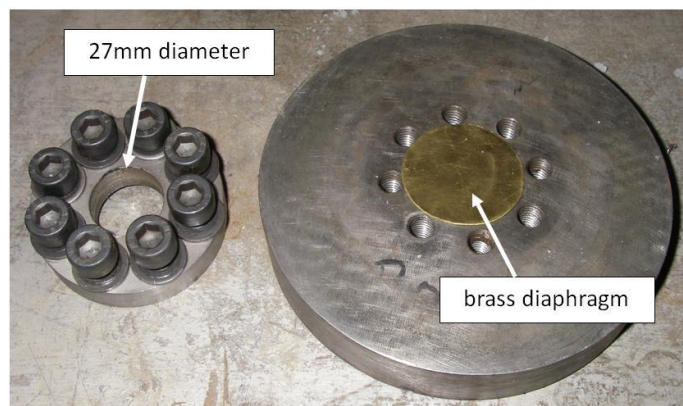
Figure 3-4: Diaphragm and cassette system

Figure 3-5 shows the results from these trials which all demonstrate a rise time of approximately 40ms showing that this is governed mainly by the aperture size and not by the forcing pressure.
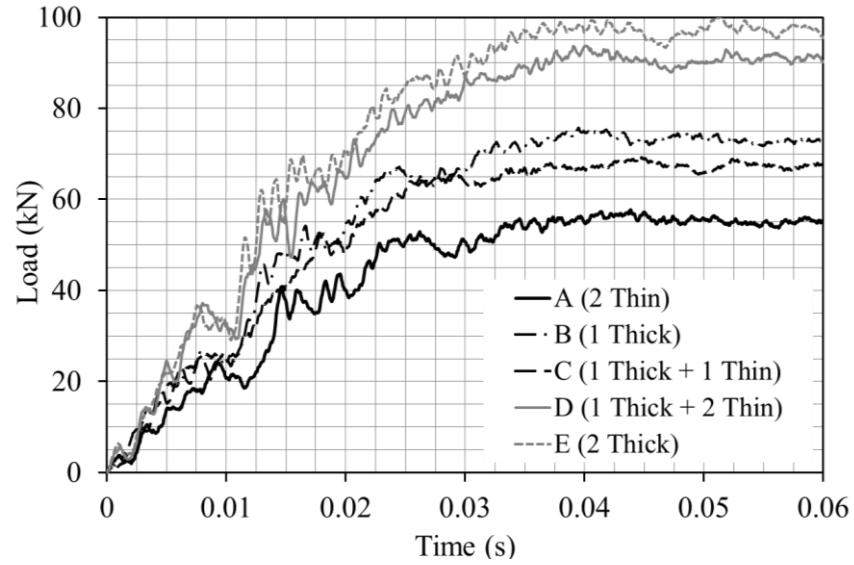
Figure 3-5: Diaphragm bursting trials

For convenience each diaphragm combination is given a unique identification letter.

A – 2 thin diaphragms

B – 1 thick

C – 1 thick and 1 thin

D – 1 thick and 2 thin

E – 2 thick

A fixing for a pressure transducer is located in the main receiver to monitor the pressure in the system at all times. However a working transducer was not available. As an alternative a dial pressure gauge was installed in the control room to monitor pressure. It was not necessary to record the pressure during the test because the load applied to the column was recorded.
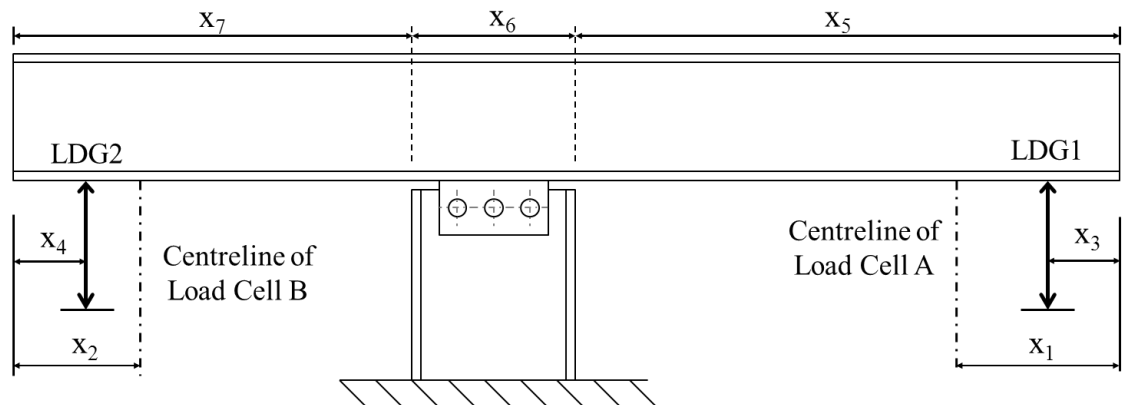
Figure 3-6: Position of test measurements and dimensions

Prior to each test, all measurement and monitoring devices were checked to ensure they were functioning correctly and giving reliable readings. All settings including test measurements (Figure 3-6) were recorded in the trial log.

3.2.2   Calculation of connection moment

Where one load ram was used, the inertial moment of resistance (M_I) was calculated by assuming it behaved as a homogenous infinitely stiff rod rotating about a variable pivot point.
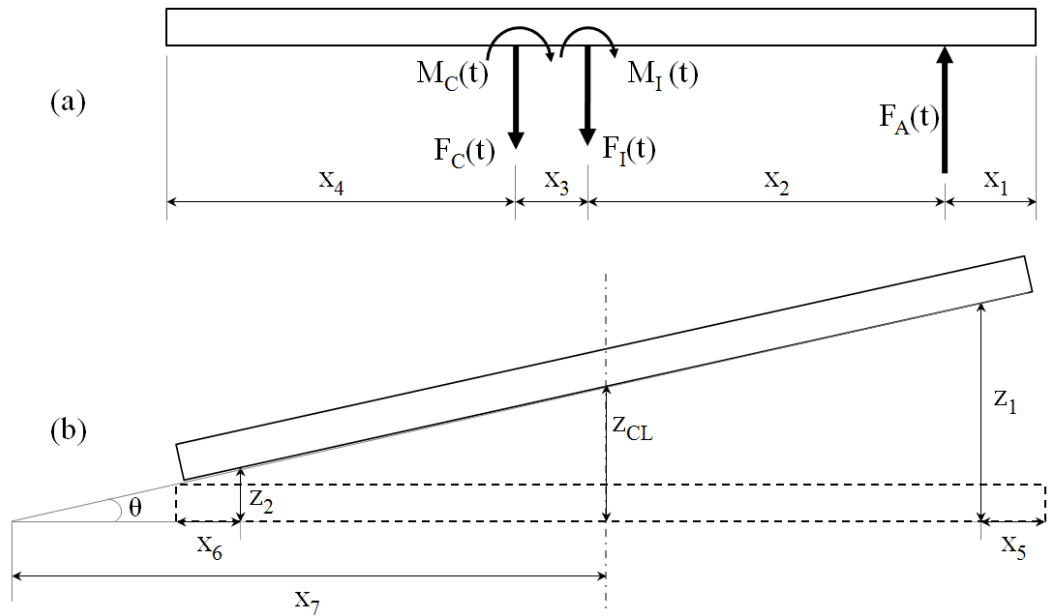
Figure 3-7: (a) Free body force diagram of column (b) Position of laser displacement gauges

From dynamic force equilibrium:

$$F_C(t) = F_A(t)cos\theta(t) - F_I(t) \tag{3.1}$$

From dynamic moment equilibrium about the centerline of the connection:

$$M_C(t) = F_A(t) * (x_2 + x_3) - M_I(t) - F_I(t) * x_3 \cos \theta(t) \tag{3.2}$$

At each time step the rotation was calculated from the laser displacement gauge data:

$$\theta(t) = tan^{-1}\left[\frac{z_1(t) - z_2(t)}{L - (x_5 + x_6)}\right]$$

(3.3)

The rotational acceleration ($\ddot{\theta}$) was calculated by double differentiation of the laser displacement gauge data (LDG) and verified against the accelerometer readings (an example of which is shown in Figure 3-8) which were used to calculate the inertial moment of resistance.
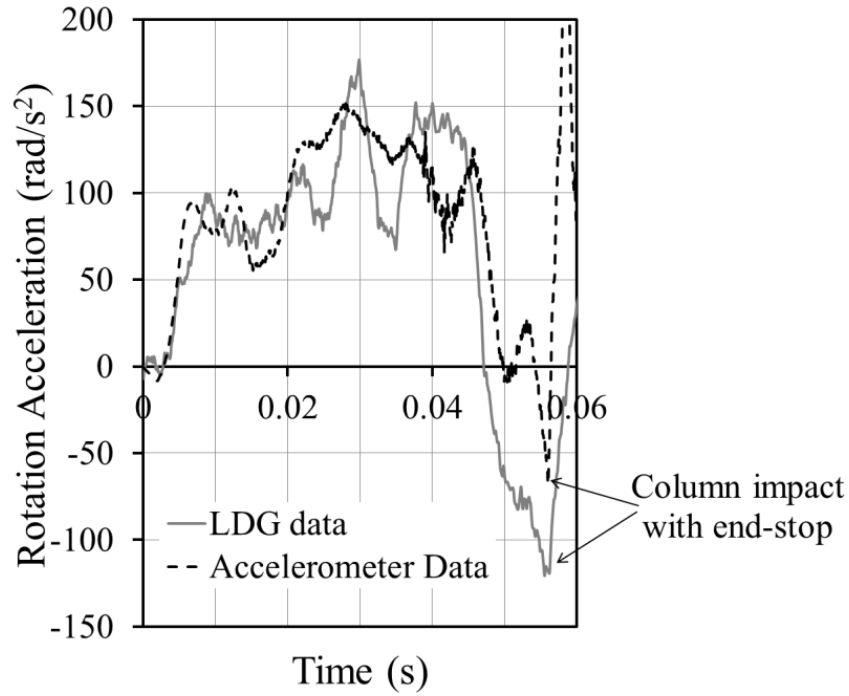
Figure 3-8: Comparison of accelerometer and laser displacement gauge data for test FEP17

$$M_I(t) = \ddot{\theta}(t)I$$

(3.4)

$$F_I(t) = \ddot{z}_{cl}(t)M$$

(3.5)

An illustration of calculating the connection moment is shown in Figure 3-9. In tests conducted in the absence of a connection, this allowed the moment of inertia of the column section to be experimentally determined which should correspond with the applied moment (Figure 3-9a). Although the inertial moment was very noisy (as a result of the column having no resistance) the average value shows a good prediction of zero connection moment. It was noted that the accelerometer gave very good readings of rotational

acceleration up to 1 degree of rotation and then diverged from the values calculated from the displacement data, due to it being accelerated in more than one plane. Therefore the accelerometer was used to check the calculated acceleration up to 1 degree of rotation for all of the connection tests.
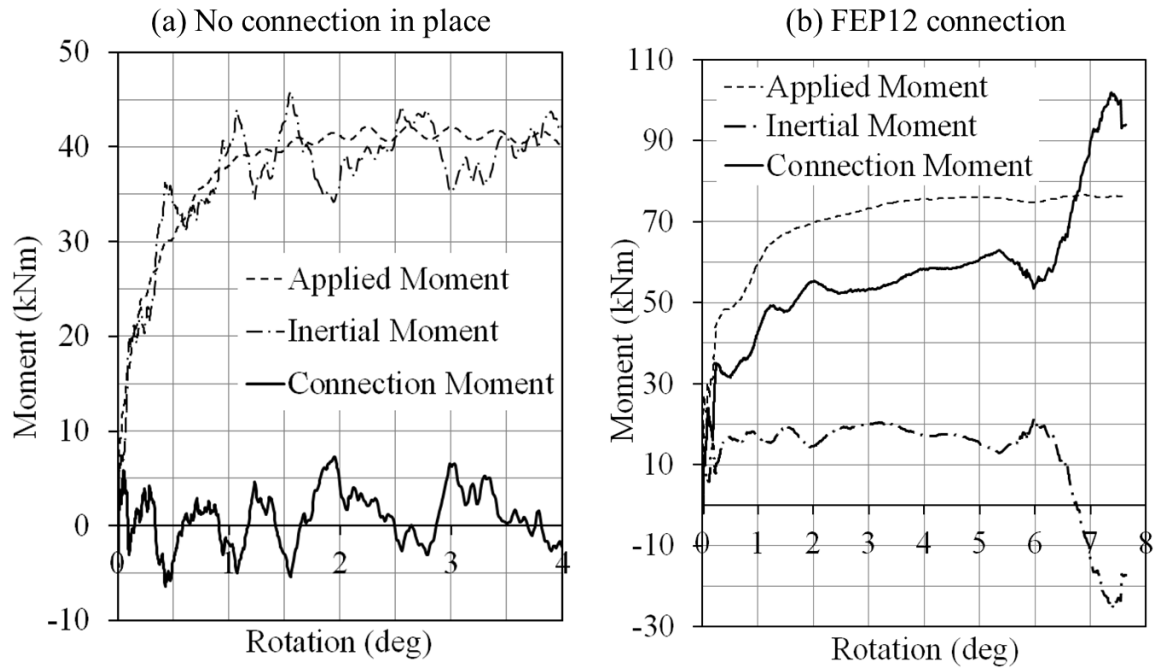
Figure 3-9: Calculation of connection moment

The connection test FEP12 in Figure 3-9b demonstrates the reduction of inertial moment when a connection is in place (because the column is rotating slower) and thus the calculation of the connection moment. In this case after approximately 6 degrees of rotation the flying column begins to decelerate which is resisted by the connection and thus the connection moment increases above the applied moment.

3.2.3   3d image correlation

The image correlation system consisted of two high speed cameras fixed on an aluminium bar installed on a tripod as shown in Figure 3-10. These were controlled using a dedicated personal computer and all data recorded directly to an external hard drive (Figure 3-12).
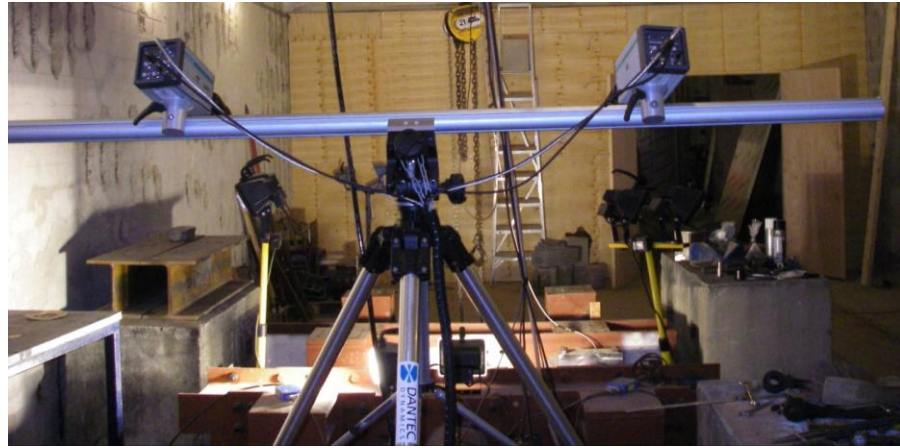
Figure 3-10: Reverse of image correlation system

The SYNC OUT from the timing hub was connected to the SYNC IN of both cameras to allow remote synchronization and triggering.

Figure 3-11: Reverse of Q450 camera system
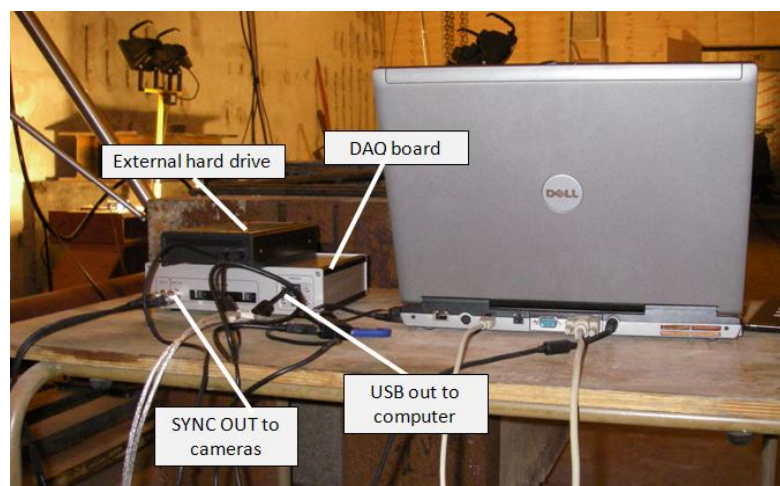
Figure 3-12: Camera control setup

A full displacement field of the connection is measured using the system. The test connection was painted with a random speckle pattern and images taken of the joint using

two high speed video cameras. The cameras employ a CMOS sensor and have a maximum 512×512 pixel resolution and a peak framing rate of 10 kHz at full frame resolution.

The cameras were set up so that they viewed the painted area of the joint at fixed oblique angles with a minimum angle between them of 30 degrees. This arrangement allowed the location of any point on the joint to be located in a three dimensional space using standard stereoscopic analysis techniques. An area of approximately 300mm×200mm was viewed and images were collected at a frame rate of 5000fps. The collected images were processed so that the 3D position of the pattern was determined based on the location and optical characteristics of the cameras and their lens.

The revised images were then spilt into "facets", small areas (12×12 pixels) and then the speckle pattern in these small areas was correlated with the changed speckle pattern at the same location observed in subsequent images. This provided information on the 3D displacement of the material at this location between images. Facet based correlation algorithms work by optimising the best combination of mappings between identified particles in order to represent translation, shearing and rotation. This can obtain a good accuracy in three dimensions for materials subject to translations, rotations and shearing [Considine et al. (2005) and Siebert and Becker (2005)]. The accuracy of the data is dependent on the resolution of the cameras and the calibration co-efficients used to combine the data from the two images into three dimensional data. Images were collected, processed and the correlation undertaken using Istra4D software v4.2.1 [Becker et al. (2006)]. Time series of several tenths of a second were captured so that the entire time history of the joint movement could be obtained.

The strain rate was calculated using the following equation from Pierron et al. (2010):

$$\dot{\varepsilon}_\alpha \left(t + \frac{\Delta t}{2} \right) = \frac{\varepsilon_\alpha(t + \Delta t) - \varepsilon_\alpha(t)}{\Delta t}$$

(3.6)

Where α is in the *x*, *y* or *z* directions and Δt is the inter frame time.

The camera data was also used to verify the laser displacement data with good results.

3.2.4   Defining and capturing failure

After initial trials it became clear that the load controlled nature of the testing meant that the static tests provided a clear failure point, however determining the point of failure for the dynamic tests was difficult. This was because the dynamic nature of the problem meant the column section was always in motion and the connection failed at some point before it was brought to rest upon impact with the end stop. In addition failure could either be defined as the complete separation of the connection, a single component failing (such as a bolt), or somewhere in between.

In this thesis, failure is defined as the point at which the connection no longer behaves as it was designed i.e. a single part of the connection has reached its ultimate value and failed. Although in theory the connection may still have reserve strength and ductility from other components this was chosen to allow a direct comparison between the static and dynamic test data. This failure point was found by either identifying large fluctuations in the data sets or from high speed video.

3.2.5   Problems and modifications to test procedure

A major problem with regard to the image correlation system was the effect of spalling paint from the surface of the connection. Because the system works by tracking points on the surface, as soon as the paint cracks off the system fails.
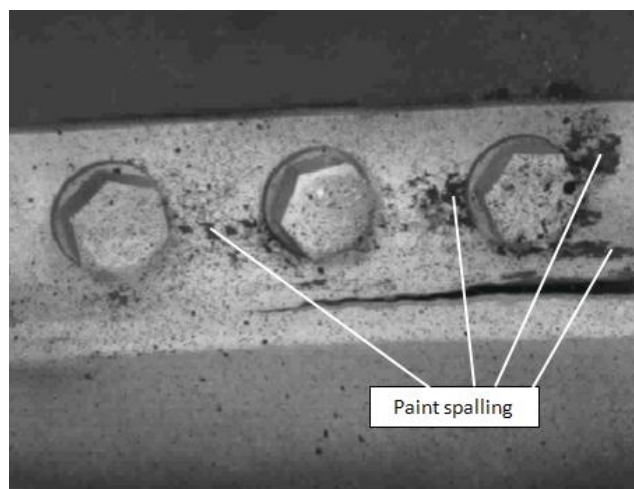
Figure 3-13: Paint spalling on connection during dynamic test

To solve this problem the connections were carefully prepared by removing all rust and imperfections using an angle grinder (Figure 3-14). Following this a self-etching primer

was applied to form a chemical bond with the steel before applying the speckled effect with aerosol based paint.
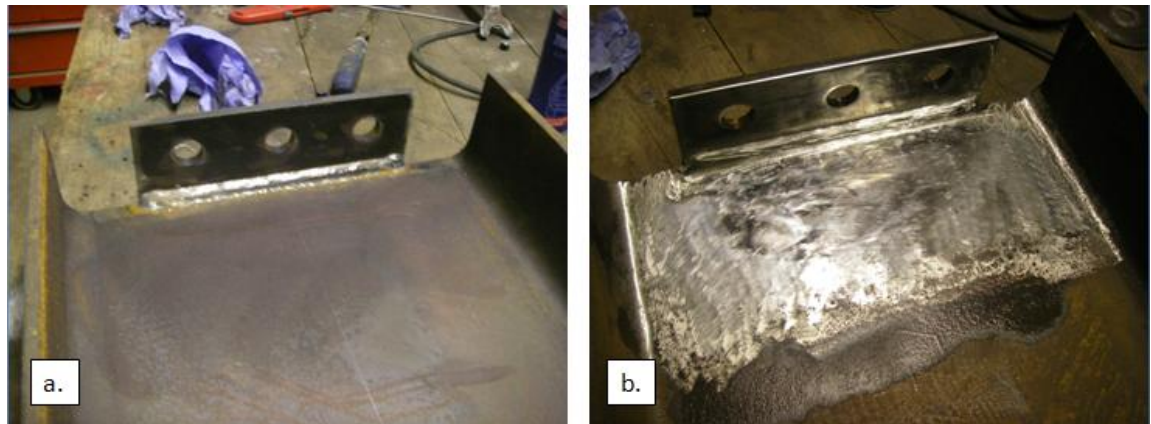
Figure 3-14: (a) Initial connection (b) Prepared connection prior to painting

This method worked well and very little, if any, paint spalling was present in the experimental tests.

Another problem encountered was how to synchronise the recorded data to the camera images to find when failure initiates. The solution was to use a micro-switch to trigger the camera system from the motion of the column and record this signal on the data logger. The time bases could then be offset to overlap the trigger signal.

3.3 Moment-Rotation Testing

This subsection describes tests performed upon semi-rigid connections using a single loading ram where the opposite end of the column was allowed to rotate freely. In all cases the load ram was located 440mm from the end of the column and the connection installed at a centerline of 1100mm from the same end giving a moment lever arm of 660mm. The principal aim of these tests was to investigate the connection moment vs. rotation behaviour at different loading rates. Results are shown for the three different connection types tested and a comparison of their relative performance presented. Analysis of each connection test is included in Appendix A.

3.3.1 Fin-plate (shear tab) connections

3.3.1.1 Specification

The testing of fin-plate connections posed a unique challenge as welding directly onto the column section was unsuitable as multiple tests were required. The solution was to weld

the fins onto 20mm thick steel plate which was then bolted to the column. Figure 3-15 shows the connection detail. All steel was specified to grade S275 and M20 grade 8.8 bolts in 2mm clearance holes were used. 11 M20 bolts are used at the non-connection end of the beam stub to secure it to the test rig.
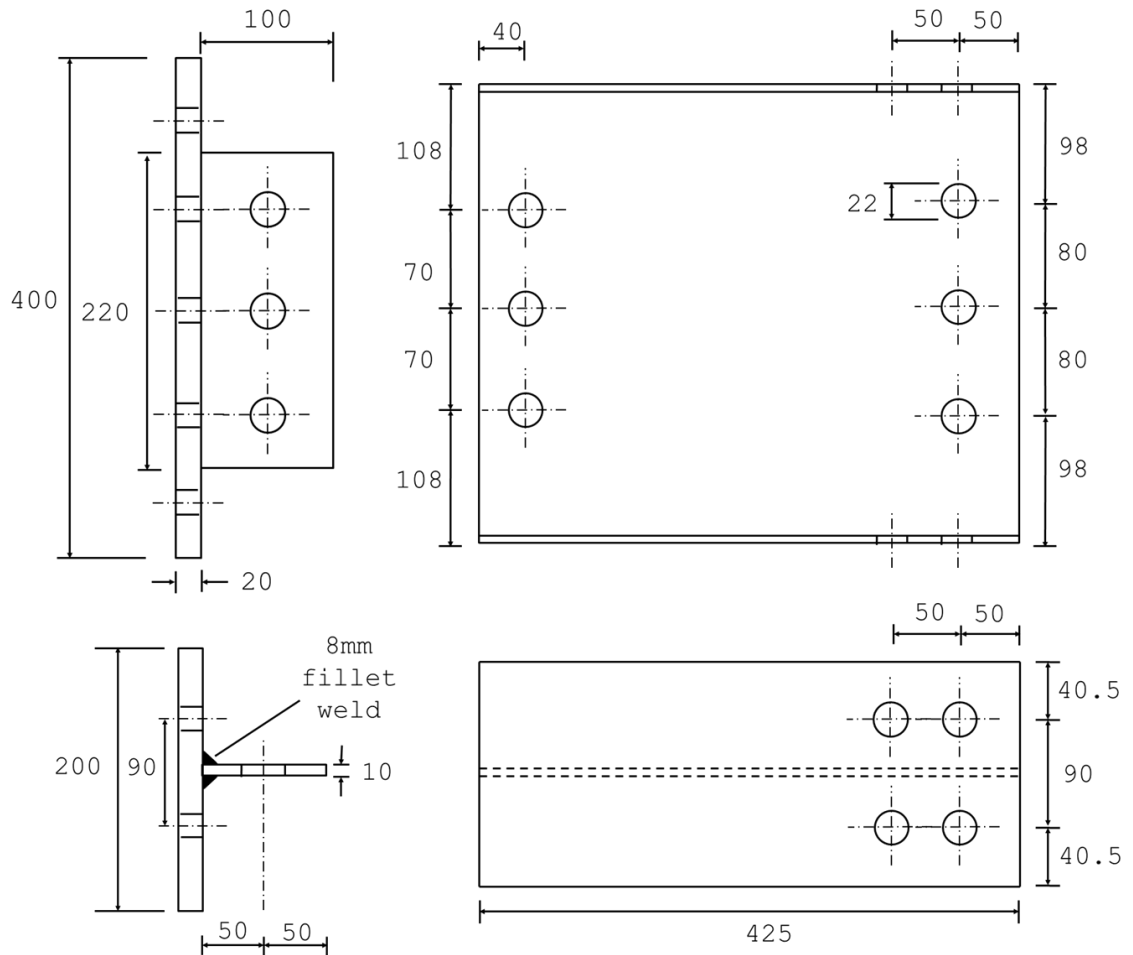
Figure 3-15: Fin-plate connection detail

The design guidelines predict a tying capacity of 193kN with the critical check being 12ii *Structural integrity of supported beam – bearing capacity of beam web*.

3.3.1.2 Results

The dominant failure mode of all the fin-plate connections was bolt shear in contrast to the design guidelines which suggest that the beam web is the critical check. 2-3 millimeters of deformation in the beam web were also recorded, with even less deformation of the fin as expected due to the thicker plate.

Test Number	Loading Type	Failure Moment (kNm)	Failure Rotation (deg)	Peak Loading Time (ms)	Peak connection axial load (kN)	Factor of Safety (Axial Load)	Failure Type
FIN1	Dyn (C)	61.7	4.8	34	82.6	0.43	Bolt shear
FIN2	Static	50.4	5.9	-	60.1	0.31	Bolt shear
FIN5	Dyn (A)	52.7	5.1	34	60.4	0.31	Bolt shear

Table 3-1: Table of results for fin-plate connections

Figure 3-16: Test connection FIN1

Figure 3-17: Typical deformation of fin plate

Figure 3-18: Typical deformation of beam web

3.3.1.3 Observations and analysis

The fin-plate connections showed evidence of strain-rate sensitive behaviour. FIN5 experiences a higher loading rate than FIN1 (Figure 3-19a) and fails at a lower rotation (Figure 3-19b).
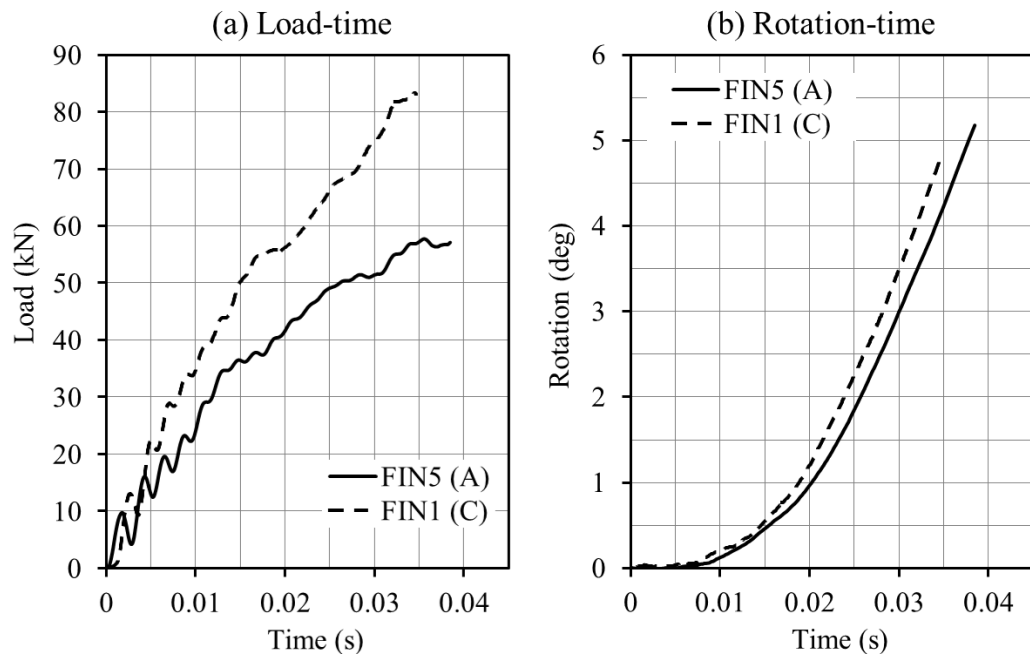
Figure 3-19: Dynamic testing (a) Load-time (b) Rotation-time

The applied load versus rotation (Figure 3-20a) indicates the column inertia has a large effect on column rotation. A comparison of static and dynamic connection moment-rotation behaviour is presented in Figure 3-20b. The principal differences are an increased stiffness throughout the entire response and an increased moment capacity.
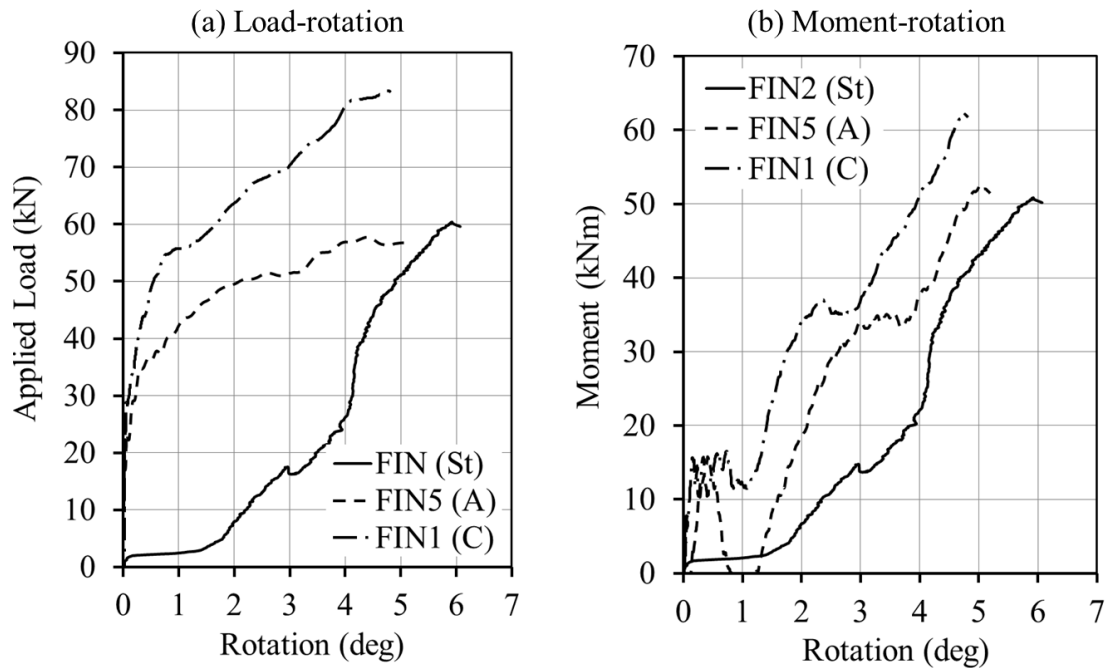
Figure 3-20: Test results for fin-plate connections

The dynamic tests demonstrate an increased stiffness at low rotations up until approximately 1.5 degrees. It is thought that this is due to the nature of the loading where a high axial load is applied and the whole column moves in the same direction due to the inertia which causes the clearance holes in all of the bolts to be taken up. Any rotation therefore causes contact with the beam web rather than move into the initial clearance hole. This contrasts with the static tests where the connection can rotate from the start of the loading about the central bolt with the clearance holes taken up by this initial rotation.

An important feature of these semi-rigid connection tests is the point at which the column makes contact with the lower beam flange and thus introduces a different point of rotation. This also has the effect of introducing prying action. From trigonometry and assuming the connection rotates about the central bolt hole this would occur at a rotation of 3.2 degrees. The experimental tests support this as an increased stiffness is shown in all tests between 3 and 4 degrees. This increased stiffness is a direct result of the changing of the point of rotation, introducing a longer lever arm between each bolt row.

The dynamic loading conditions have caused failure at reduced rotation but higher moment capacity likely due to strain-rate effects on the individual regions of the connection.

3.3.2 Flexible end-plate connections

3.3.2.1 Specification

The detail for the flexible end-plate connections is shown in Figure 3-21, all steel specified to grade S275 and M20 grade 8.8 bolts in 2mm clearance holes. The standard end-plate dimensions for a 356x171x45 UB section from the SCI Green Book (BCSA/SCI (2002)) were used which specified an 8mm thick end-plate, however 6 connections were also tested with a 10mm thick end-plate to compare the effect of this stiffer component.
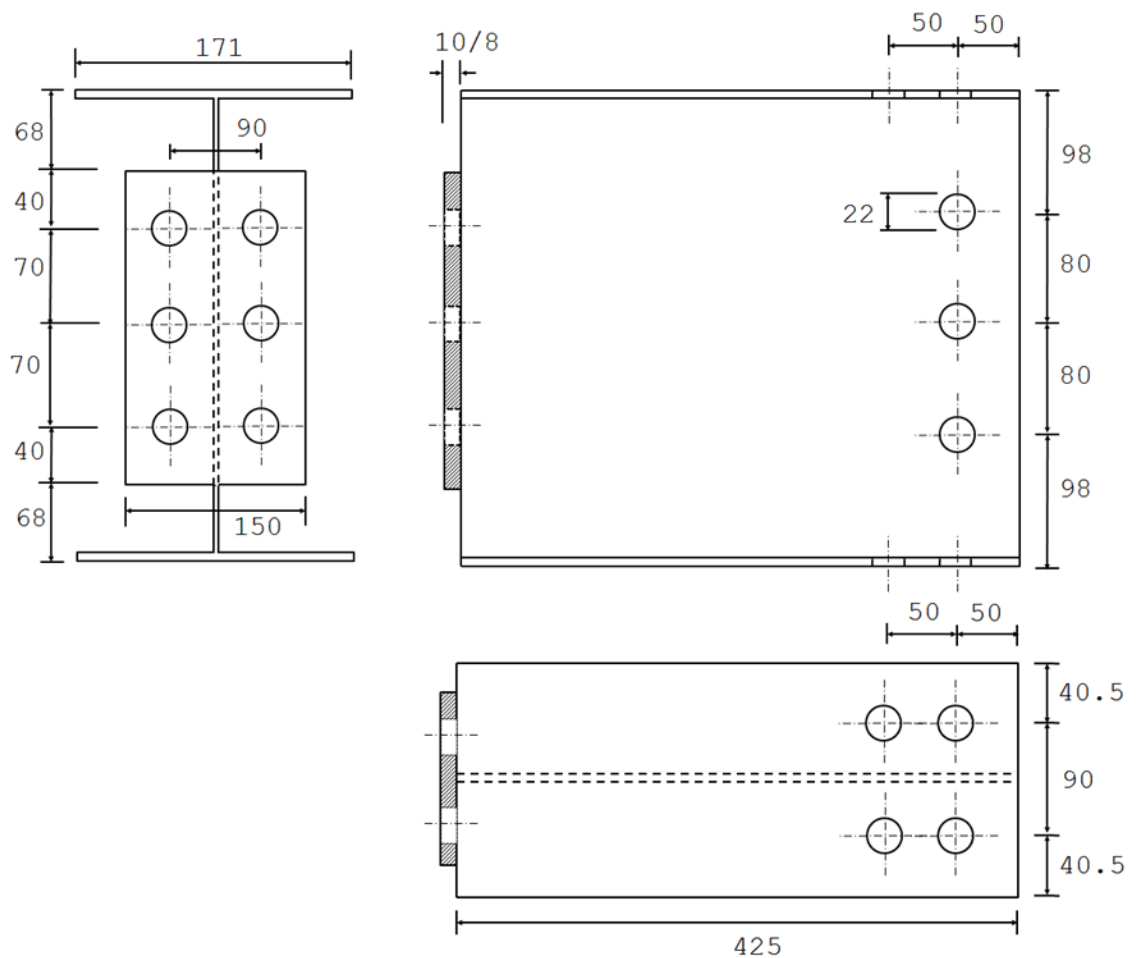
Figure 3-21: Flexible end-plate connection detail

For the 8mm thick end-plates the design guidelines give a tying capacity of 171 kN with the critical check being Check 11 *Structural integrity - tension capacity of the end-plate*.

3.3.2.2 Results

The results for the 8mm thick end-plate connections are shown in Table 3-2.

Test Number	Loading Type	Failure Moment (kNm)	Failure Rotation (deg)	Peak Loading Time (ms)	Failure axial load (kN)	FoS (Axial Load)	Failure Type
FEP1	Static	50.2	6.2	-	58.8	0.34	End-plate fracture
FEP2	Dyn (E)	75	5.8	40	97.7	0.57	End-plate fracture
FEP3	Dyn (A)	60.1	6.3	39	52.3		No
FEP4	Dyn (B)	63.4	5.8	40	65.7	0.38	End-plate fracture
FEP5	Static	48.3	6.7	-	56.8	0.33	End-plate fracture
FEP6	Dyn (E)	73.1	7.0	47	84.2	0.49	End-plate fracture
FEP9	Dyn (A)	54.8	-	40	47.4		No Failure
FEP9 (cont)	Static	45.7	7.4	-	54.2	0.32	End-plate fracture
FEP14	Dyn (A)	57.7	5.6	37	45.0	0.26	End-plate fracture
FEP16 (data logger failed to trigger)	Dyn (A)	-	-	-	-		Yes (end-plate)

Table 3-2: Single ram test results for 8mm flexible end-plate connections

The results for the 10mm thick end-plates are presented below in Table 3-3.

Test Number	Loading Type	Failure Moment (kNm)	Failure Rotation (deg)	Peak Loading Time (ms)	Failure axial load (kN)	FoS (Axial Load)	Failure Type
FEP7	Dyn (B)	86.77	6.2	45	69.2		No Failure
FEP7 (cont)	Static	82.2	9.6	-	92.8	0.54	Fracture of end-plate, beam web tearing and weld-end-plate interface
FEP8	Static	98	13.2	-	116.7	0.68	End-plate fracture
FEP10	Dyn (B)	79.8	7.9	40	71.4		No
FEP10 (cont)	Static	76.6	11.5	-	89.5	0.52	End-plate fracture, bolt
FEP11	Dyn (E)	113.5	6.2	39	113.0	0.66	End-plate fracture, bolt, weld-end-plate interface
FEP12	Dyn (C)	100.4	9.8	40	90.7	0.53	End-plate fracture, bolt
FEP13	Static	74.7	10.1	-	89.1	0.52	Weld-end-plate interface
FEP15	Static	81.5	9.6	-	97.4	0.57	Weld-end-plate interface
FEP17	Dyn (A)	91.4	7.1	40	87.1	0.51	End-plate fracture, weld-end-plate interface

Table 3-3: Single ram test results for 10mm flexible end-plate connections

3.3.2.3 Observations and analysis

All 8mm thick end-plate connections failed due to tearing through the end-plate at the root of the fillet weld (end-plate fracture) as shown in Figure 3-22. Upon examination this was in the heat affected zone of the end-plate which is a result of the weld process.
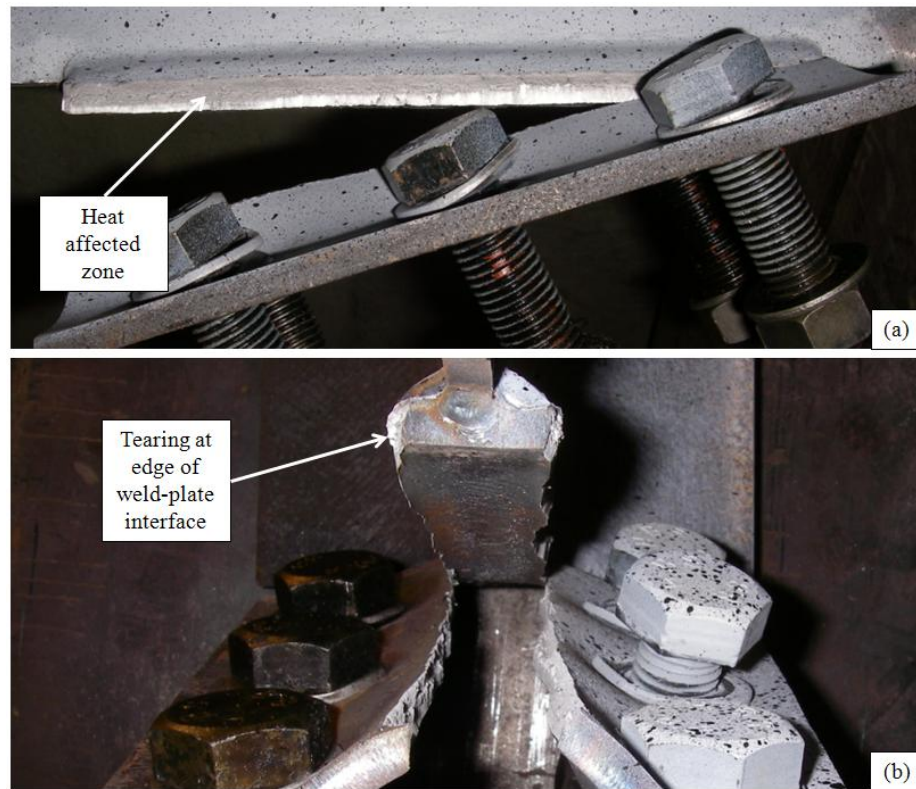
Figure 3-22: Typical 8mm end-plate failure showing tearing at root of weld

Figure 3-23: Complete failure of FEP20 showing rotation of beam web

In all cases a clear tear was observed as shown in Figure 3-22b and in some tests the entire end-plate was severed. The rotation of the beam web following end-plate failure (Figure

3-23a) indicates that both sides did not fail at precisely the same time. This could be due to a variety of factors including how symmetrical the end-plate was welded or whether there was eccentricity in the applied load.

When the thickness of the end-plate was increased to 10mm the rotation capacity of the connection was increased. It would appear that by preventing the early premature failure of the end-plate the strength reserve of the other components could be utilised and thus provide additional capacity. A variety of failure mechanisms were observed for the 10mm thick end-plates including tear out of the beam web as shown in Figure 3-24.
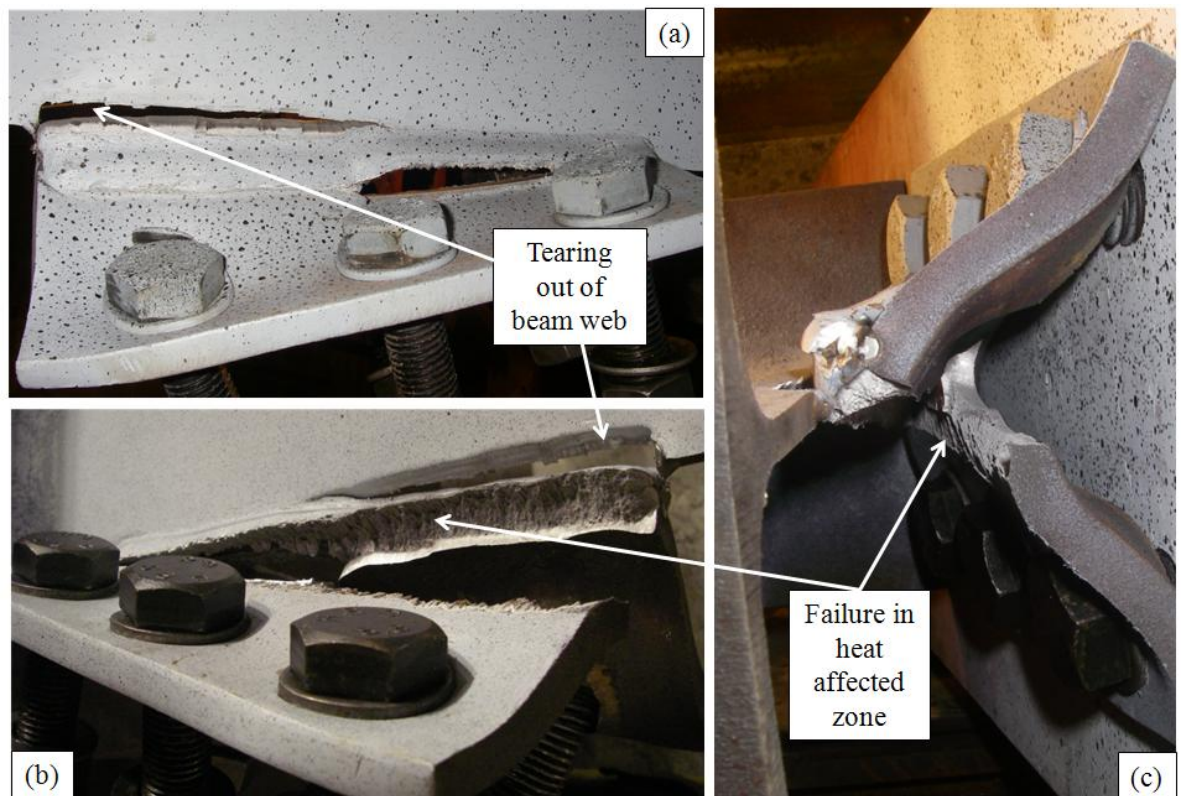
Figure 3-24: FEP7 failure showing beam web tear out and end-plate failure

Fracture of the end-plate was also observed but in most cases failure occurred along the centreline of the end-plate rather than at the edge of the fillet welds as shown in Figure 3-25b. In addition, the increased strength and failure load caused some of the bolts in the connection to fail (Figure 3-26). The location of the bolt in relation to the point of rotation appears to dictate the type of bolt failure. The bolt furthest away from the point of rotation, Bolt 1 in this case, appears to be a shear failure whilst Bolt 2 appears to have failed due to axial tension, although evidence of shearing to the upper threads is also visible.
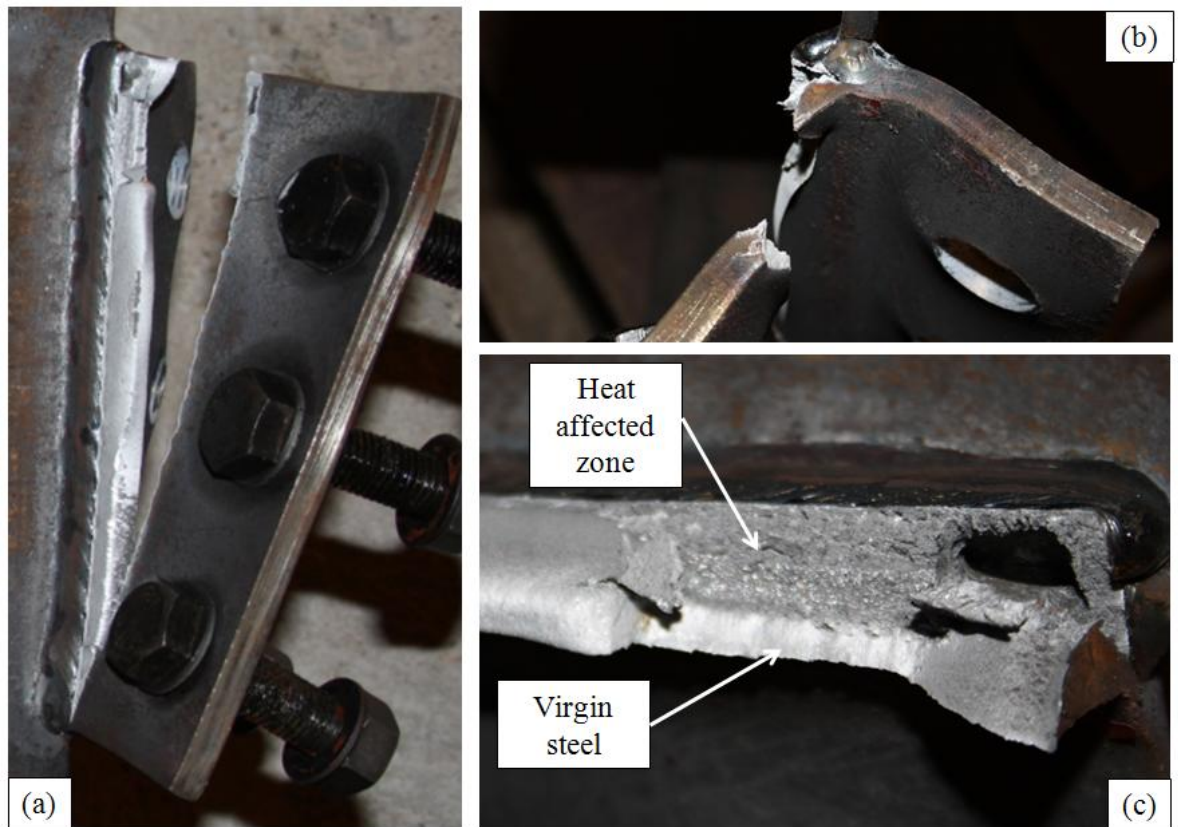
Figure 3-25: FEP11 failure
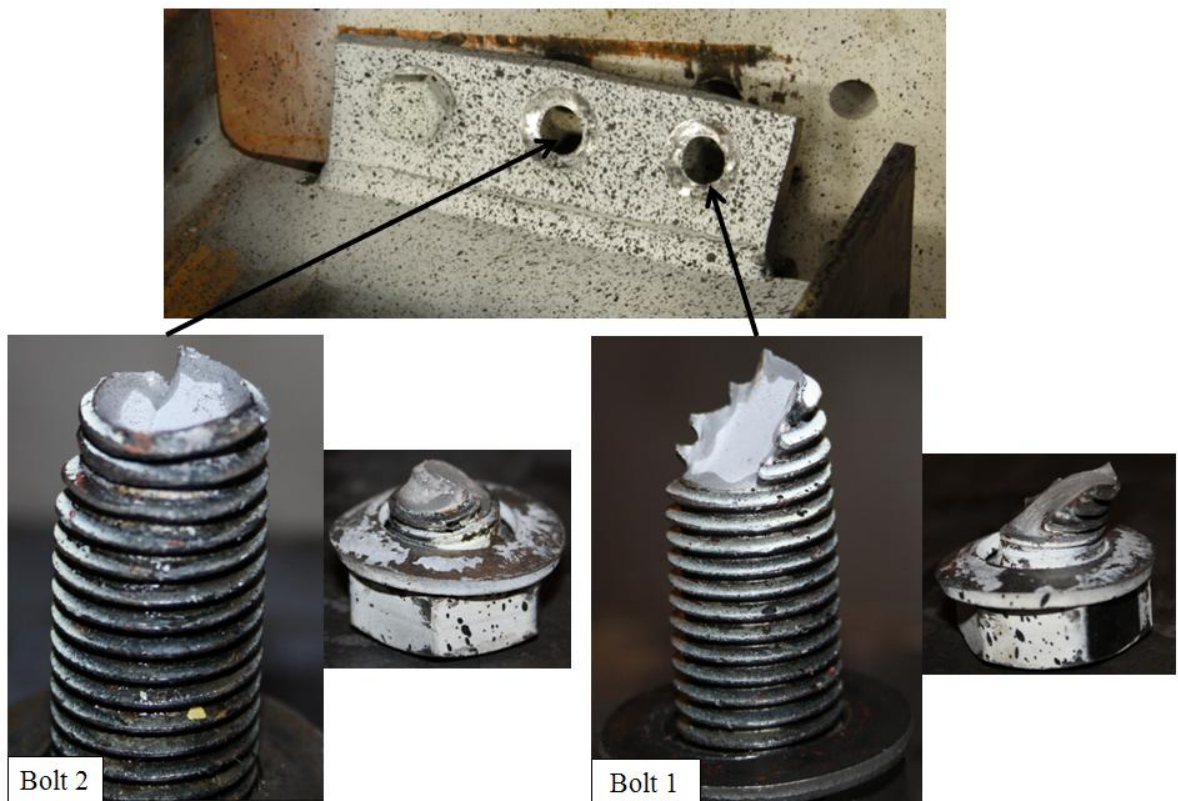
Figure 3-26: Bolt failures in FEP11

The final failure mechanism observed for the 10mm thick end-plates was where the end-plate remained intact and was torn away from the face of the weld (Figure 3-27). In this case no bolt failure was observed but there was a large amount of deformation to the end-plate itself.
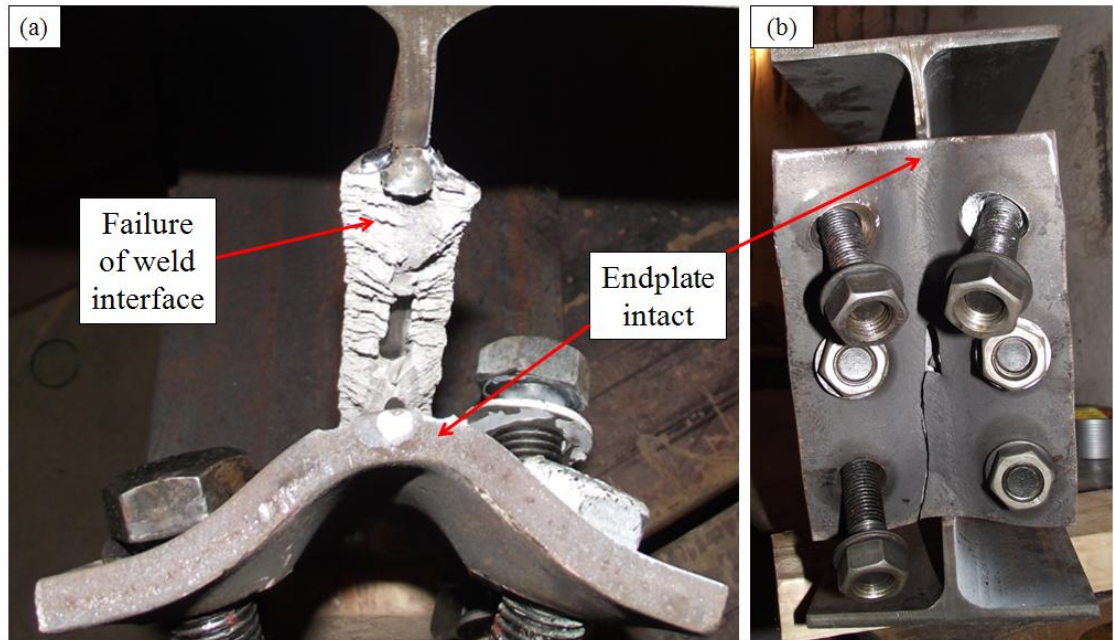
Figure 3-27: FEP15 failure showing the face of the end-plate torn away from the weld

The results from select 8mm flexible end-plate experimental tests are shown in Figure 3-28.
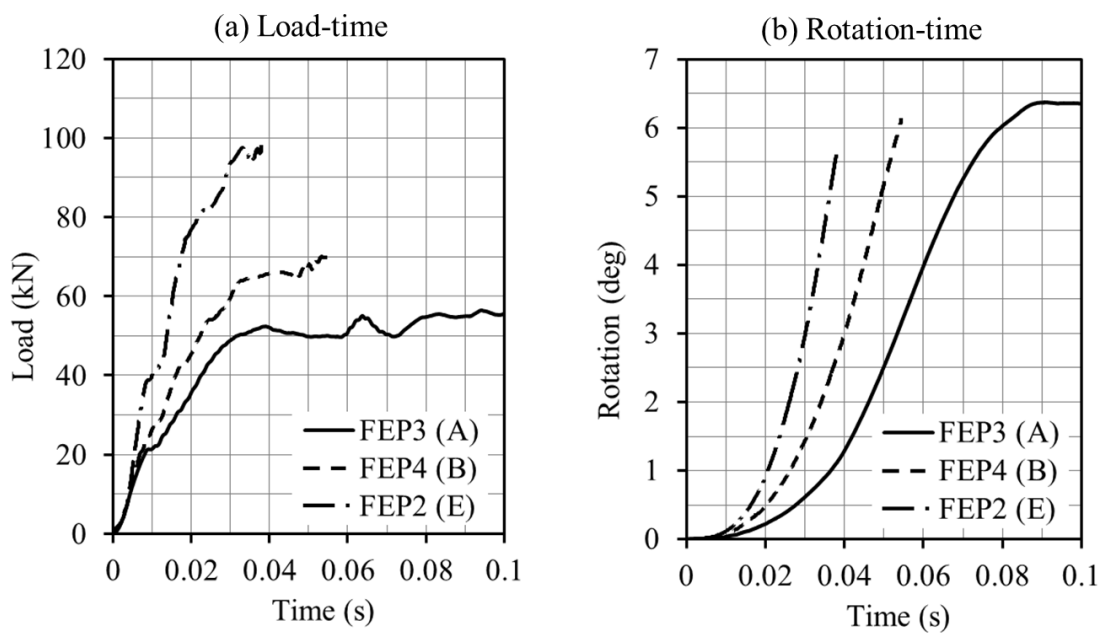
Figure 3-28: 8mm end-plate data

The peak load applied to FEP3 was 57kN which was not sufficient to cause failure. However the peak rotation was 6.4 degrees, greater than the rotation achieved in either of the higher load rate tests (FEP2 and FEP4). These results indicate that the lower the loading rate, the greater ductility supply of the connection. From the load-time history (Figure 3-29a) the loading rate for FEP2 was approximately twice that of FEP3. The resulting moment-rotation graph for the 8mm thick end-plate connections (Figure 3-29b) indicated that there was a dynamic effect on the yield moment of the end-plate which was increased by approximately 30%. The initial elastic stiffness appears to have increased however the post yield stiffness was very similar to that of the static test. Failure occurred between 5.5 and 6.5 degrees of rotation.
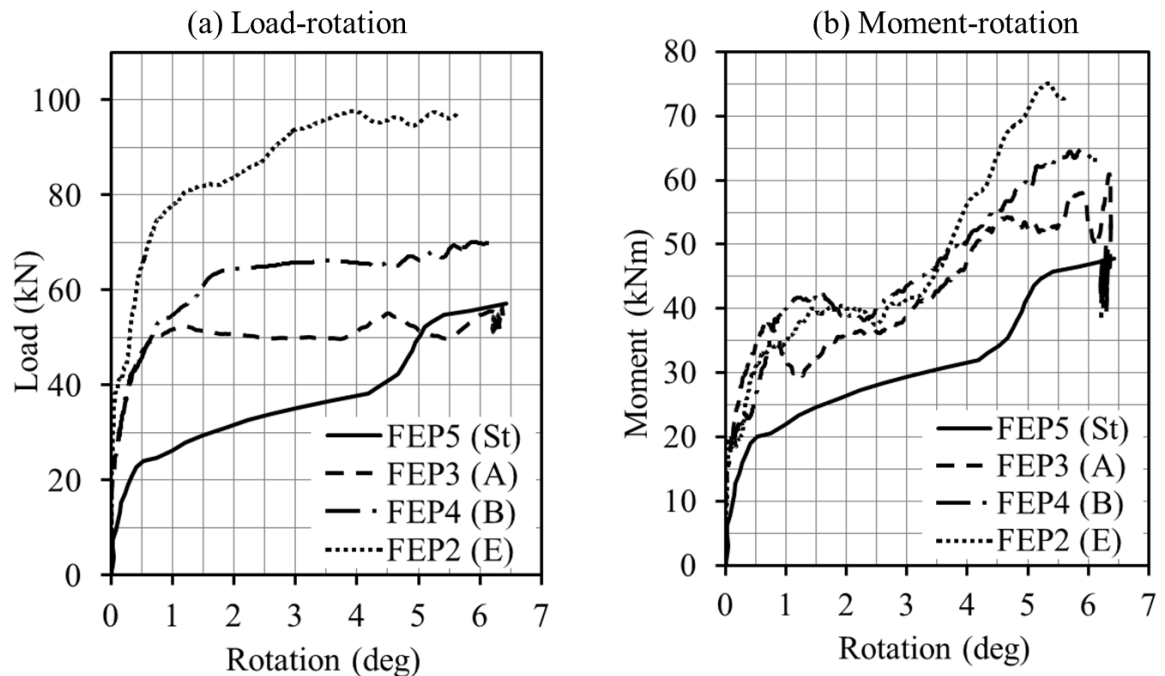
Figure 3-29: 8mm flexible end-plate behaviour

The 10mm end-plate data are shown in Figure 3-30. Although similar diaphragms are used as the 8mm flexible end-plate tests, the applied dynamic loads are considerably higher at similar rotations (Figure 3-30a). This is explained by the fact that the thicker end-plate provides greater resistance and because the load ram is driven by compressed air the reduced swept volume creates a higher pressure. It is noted that FEP10 used a thicker diaphragm combination (B) than FEP10 (A) and yet had a lower peak load. This is attributed to premature failure of the diaphragm arrangement but does not affect the results as only the load output is required for analysis.
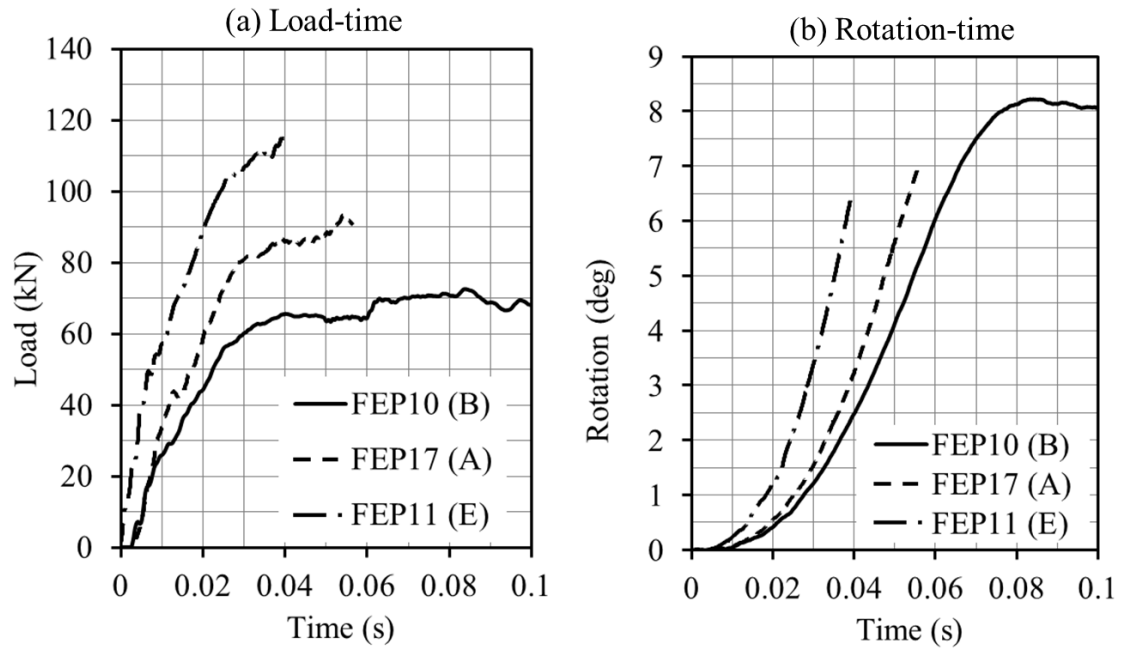
Figure 3-30: 10mm end-plate data

In comparison with the 8mm thick end-plate connections, the 10mm thick end-plates appear to show considerable lack of ductility when loaded dynamically with failure reduced from just over 10 degrees down to just over 6 degrees. This reduction is assumed to be due to changing the failure mechanism as a result of higher rates of loading where rather than being able to redistribute the loading throughout the connection the load becomes concentrated at certain locations such as the bolts.
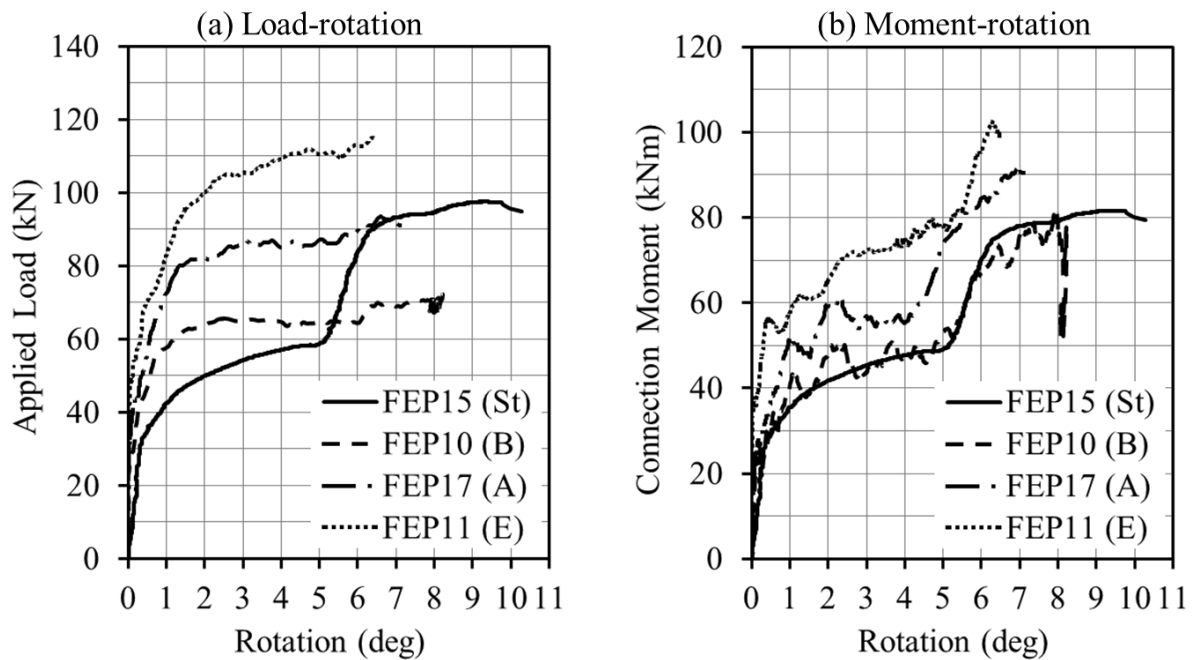
Figure 3-31: 10mm flexible end-plate behaviour

The increase in stiffness at approximately 5.3 degrees is a result of prying action. This is greater than the equivalent rotation for the 8mm end-plate due to the thicker end-plate where contact occurs at about 4.3 degrees. From geometry this shows that for both end-plate thicknesses rotation occurs approximately about the lowest line of bolts suggesting there must be some deformation of either the end-plate itself or the beam web.

The average loading rate is calculated by dividing the load by the time at 20ms and can be used to compare the overall behaviour. The general trend (Figure 3-32a) indicates that the failure rotation is related to the loading rate. The effect seems to be greater for the thicker 10mm connection.
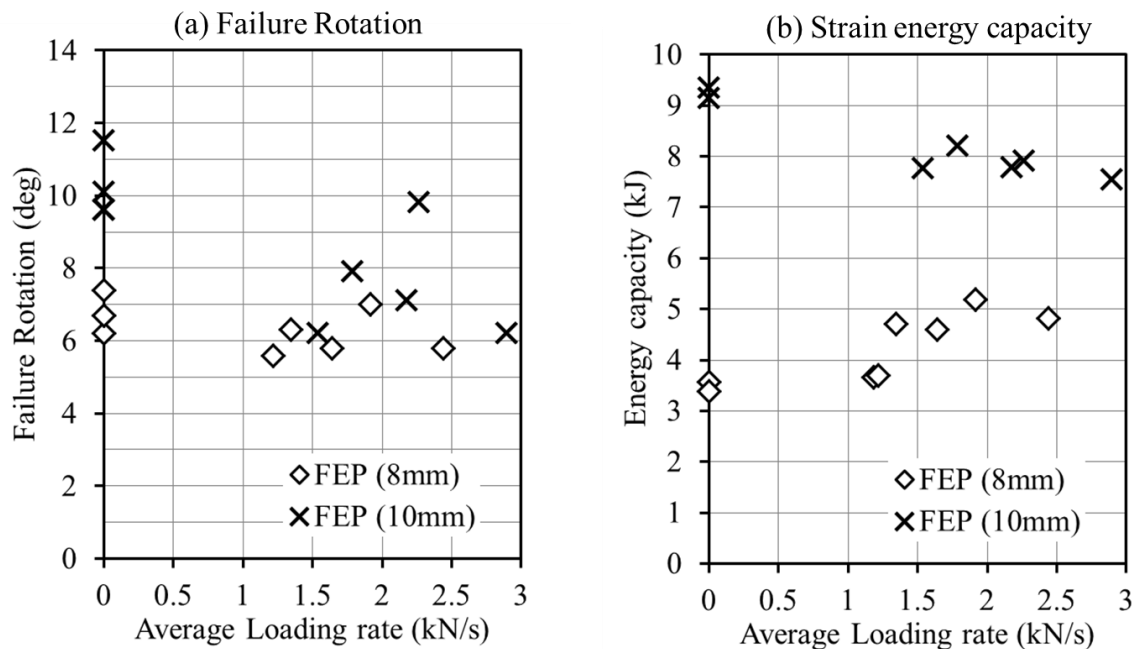
Figure 3-32: Effect of loading rate

Moment-rotation curves can be used to predict the amount of energy absorbed by the connection before failure by integration of the curve. These are plotted against the average loading rate in Figure 3-32b. For the more flexible 8mm end-plate connection, the strain-rate effect is to increase the energy capacity of the connection whilst in comparison the stiffer 10mm plate's energy capacity is reduced. It is thought that this is due to the reduced failure rotation at higher loading rates caused by the stiffer plate creating local areas of high strain and resulting in premature failure. This offsets the increased ultimate moment capacity. In comparison the 8mm flexible end-plate connection failure rotation was not reduced by such a large percentage and thus the connections demonstrated an increased capacity.

3.3.2.4 Digital image correlation (DIC)

The digital image correlation (DIC) system proved particularly useful for the flexible end-plate connections where the behaviour of the plate could be studied by looking at the strain distribution across the plate and comparing them against the static results at similar rotations. In addition by plotting the strain against time the strain-rate could be calculated. In order to ensure accurate readings, results were compared against the laser displacement gauges (LDG) for both dynamic and static test. In Figure 3-33a the midspan of the column was assessed during a dynamic test and in Figure 3-33b the displacement at two points was tracked and then used to calculate the rotation of the column. These showed good correlations and gave confidence in the strain readings of the system.
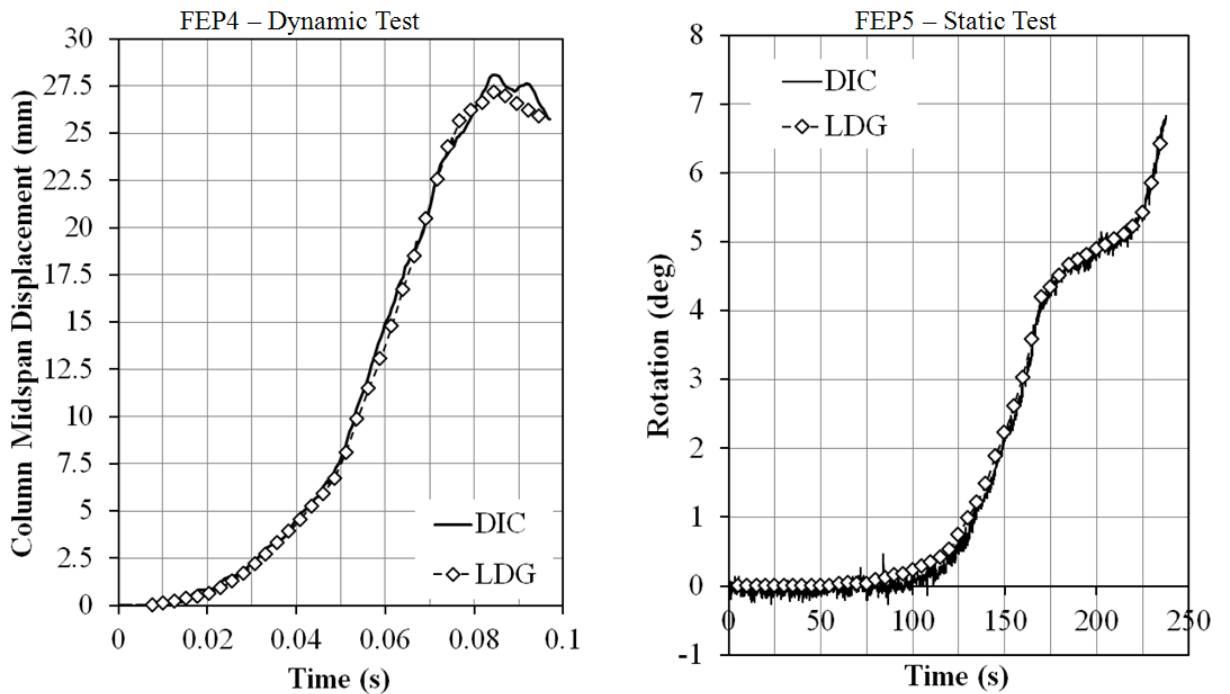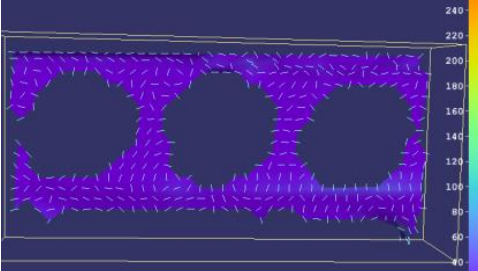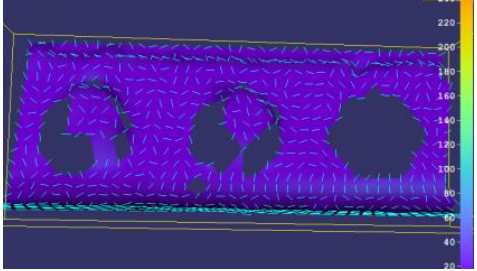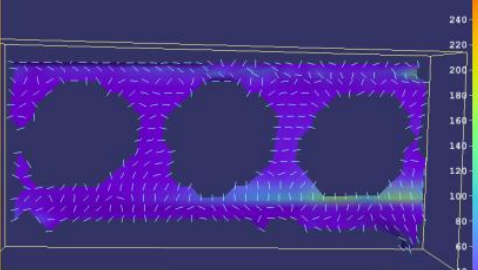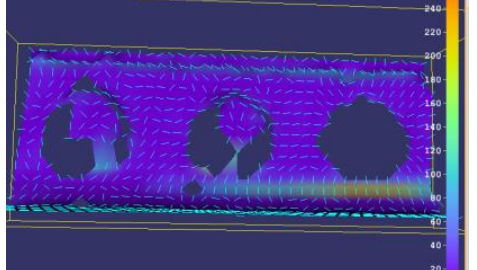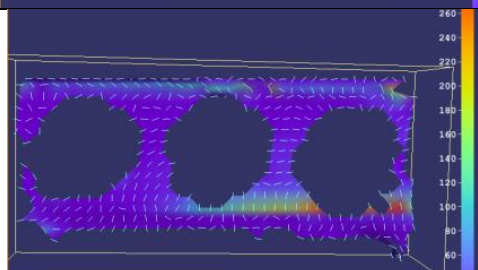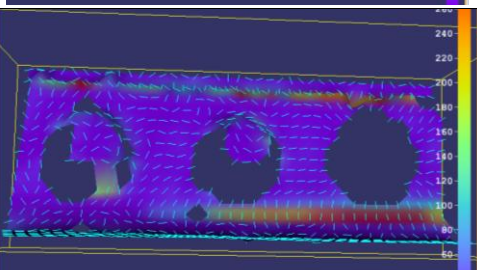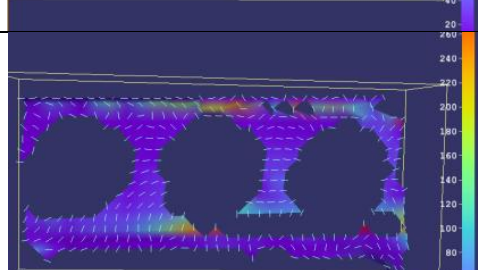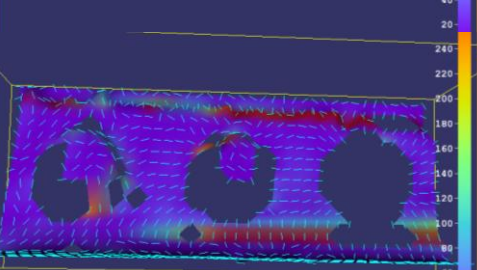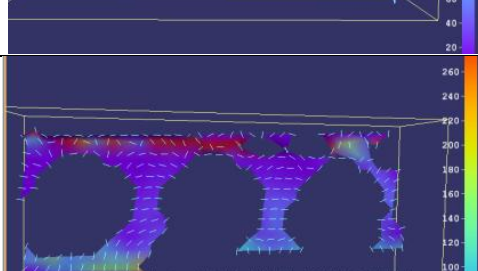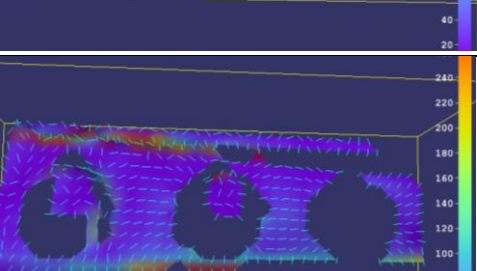
Figure 3-33: Comparison of DIC techniques and laser displacement gauges

A comparison of static and dynamic strain distribution is presented in

Table 3-4. This shows that the dynamic tests experience higher strains at similar rotations which would enforce the theory that the connection is behaving stiffer due to the higher rate of loading. There is also a wider distribution of strain across the face of the connection.

Table 3-4: Comparison of static and dynamic stress distribution for 10mm thick end-plate connections

Rotation (degrees)	Static test - FEP15 (Stress shown in MPa)	Dynamic test - FEP11 (Stress shown in MPa)
1		
3		
5		
7		
9		

The DIC technique indicates that the peak strain/stress is located at the base of the right hand bolt hole and that this is where failure initiates. This agrees with connection tests

where failure was not achieved but significant rotation was experienced and cracking was observed along the line of weld (Figure 3-34).
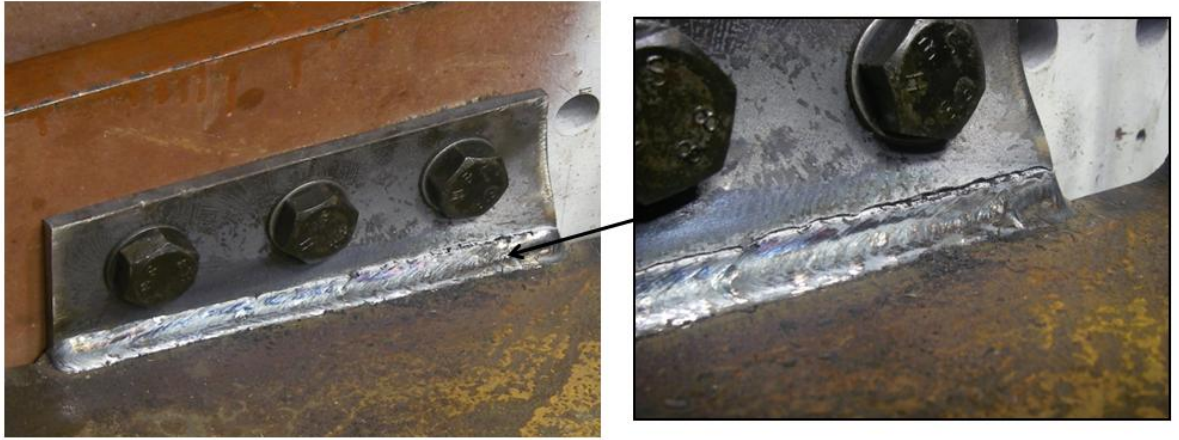
Figure 3-34: Cracking in end-plate connection (FEP3)

The strain-rate of the end-plate in the region below the right-hand side bolt was investigated using the DIC technique for a variety of loading rates. It was shown that strain rates of between 2 and 8 strain/second were experienced which equated to rotational velocities of 3-7 radians per second.
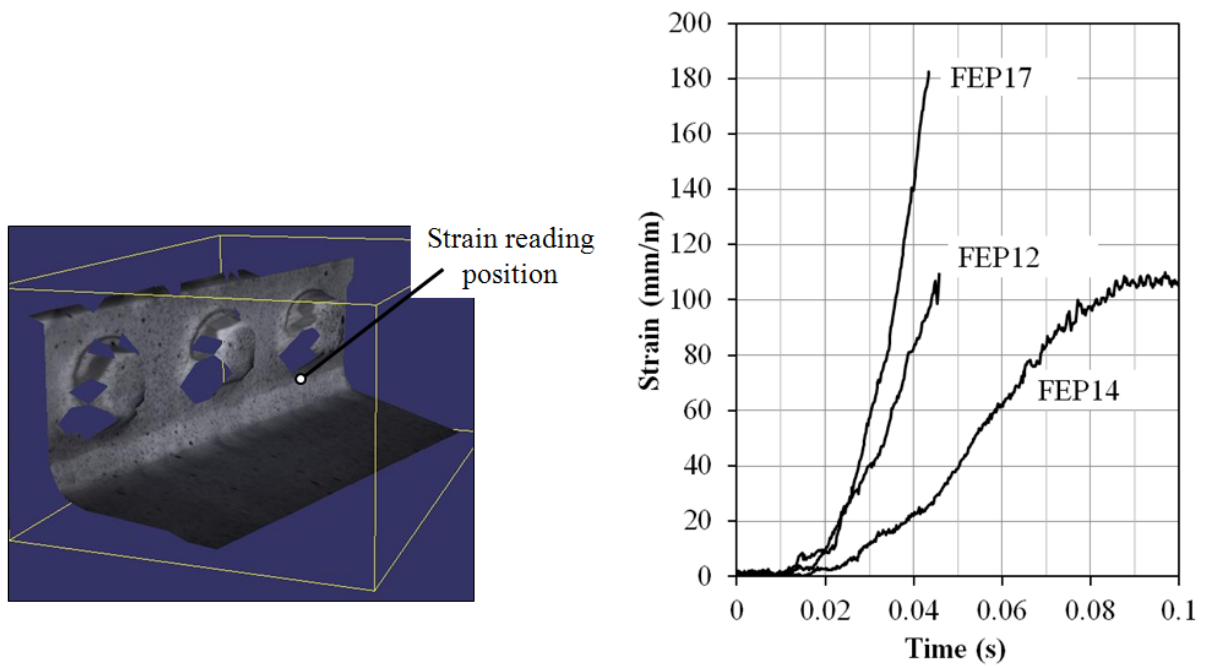
Figure 3-35: Strain readings using DIC techniques

3.3.1   Double angle web cleat connections

3.3.1.1 Specification

This series of tests investigates double angle web cleat connections. The beam stub is a 356x171x45UKB made from grade S275 steel with standard 90x90 angle web cleats of both 8 and 10mm thickness as shown in Figure 3-36. The bolts used are standard M20 grade 8.8 in 22mm diameter clearance holes. The standard detail is for 10mm thick angles but as a comparison 8mm thick angles were also tested.
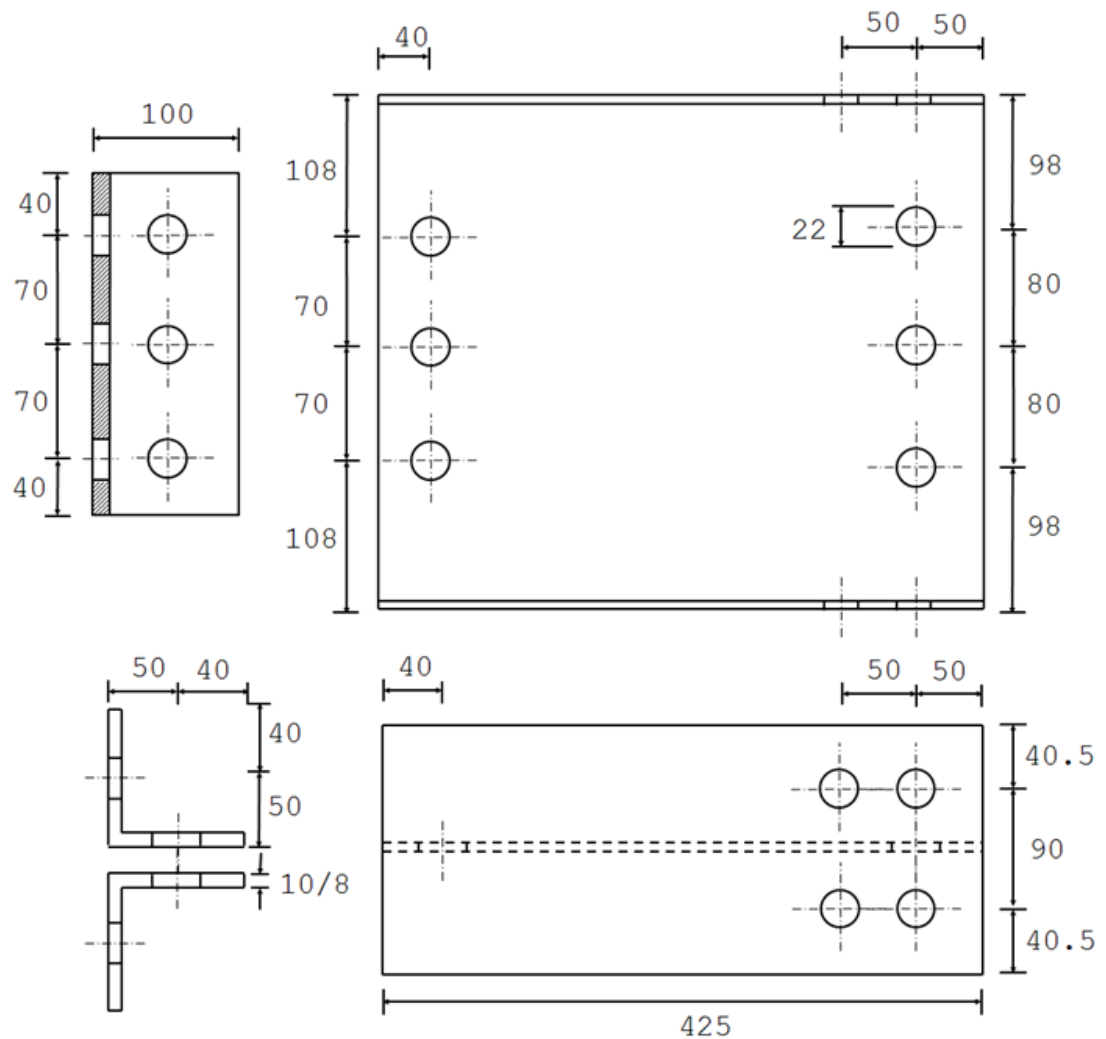
Figure 3-36: Web cleat connection details

According to the design guidelines from BCSA/SCI (2002), the standard 10mm thick angle connection has a tying capacity of 193 kN with the critical check being 12ii *Structural integrity of supported beam – bearing capacity of beam web*.

The test matrix involves 4 loading conditions (1 static and 3 dynamic) and 2 cleat thicknesses (8mm and 10mm).

Figure 3-37 shows a web cleat connection prepared for testing.

Figure 3-37: Web cleat connection in test rig prior to testing

3.3.1.2 Results

Test Number	Angle Thickness (mm)	Loading Type	Peak Moment (kNm)	Failure Rotation (deg)	Peak Loading Time (ms)	Peak applied axial load (kN)	Failure
WC1	8	Static	45.2	13.8	-	94	Beam web block shear
WC2	8	Dyn (C)	-	-	-	-	Beam web block shear
WC3	8	Dyn (C)	-	-	-	-	Beam web block shear
WC4	8	Dyn (E)	53.3	10.1	35	133.8	Beam web block shear
WC5	8	Dyn (A)	46.0	12.0	32	51.0	Beam web block shear

Table 3-5: Single ram test results for 8mm thick web cleat connections

Test Number	Angle Thickness (mm)	Loading Type	Peak Moment (kNm)	Failure Rotation (deg)	Peak Loading Time (ms)	Peak applied axial load (kN)	Failure
WC6	10	Static	48.3	11.6	-	64.9	Beam web block shear
WC7	10	Dyn (E)	62	6.0	28	95.0	Beam web block shear
WC8	10	Dyn (A)	49.2	-	37	45.1	No failure but large bearing deformation
WC9	10	Static	48.1	-	-	68.2	Test stopped early
WC10	10	Dyn (E)	63.2	5.3	30	75.8	Beam web block shear

Table 3-6: Single ram test results for 8mm thick web cleat connections

3.3.1.1 Observations and analysis

All tests consistently showed beam web block shear as the main failure mechanism which is in agreement with the design manual. However the design tying capacity of 193 kN for the 10mm cleats was never reached. This is probably due to the combined moment and tension which caused the beam web to fail prematurely. Deformations of the beam web are shown in Figure 3-38. The bolts themselves show relatively little signs of deformation. The angle at which the shear block is torn from the beam web was similar for all load cases. All tests showed evidence that the lower bolt hole had experienced bearing in both directions. This is consistent with the assumption that initially the column would rotate about the central bolt hole until the beam flange made contact with the column, after this it would rotate about the lower beam flange
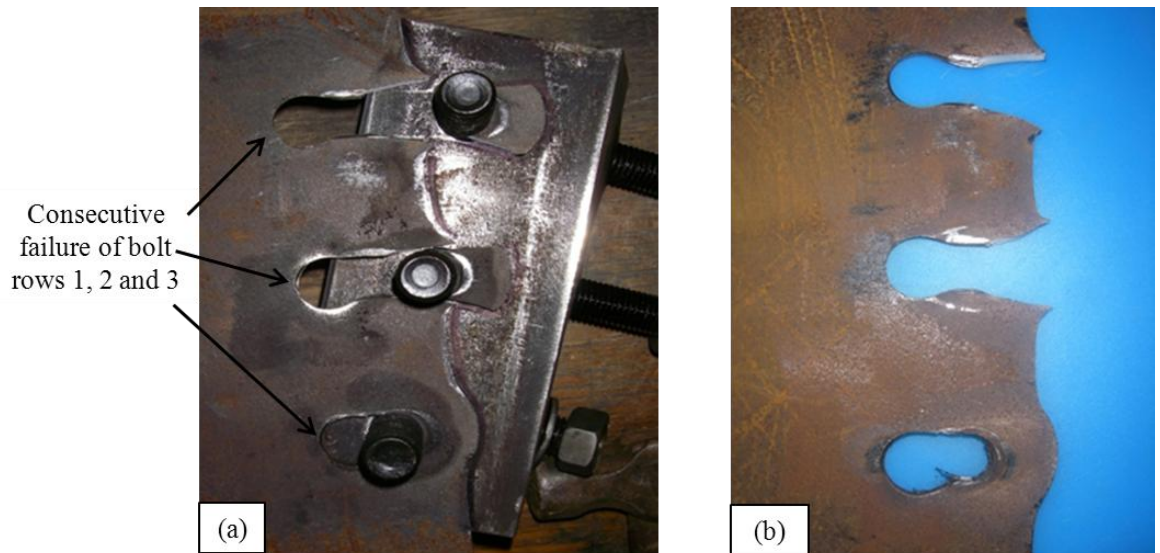
Figure 3-38: Typical beam web deformation and block shear

Deformations of the web cleats themselves are shown in Figure 3-39 showing a comparison for dynamic load case between 8mm and 10mm cleats. The 8mm cleats show a larger failure deformation (Δ_F) and it is interesting to note that the corners of both sets of cleats have made contact at the centre, having bent around the beam web. It may be that this contact limits the deformation in the web cleat region.
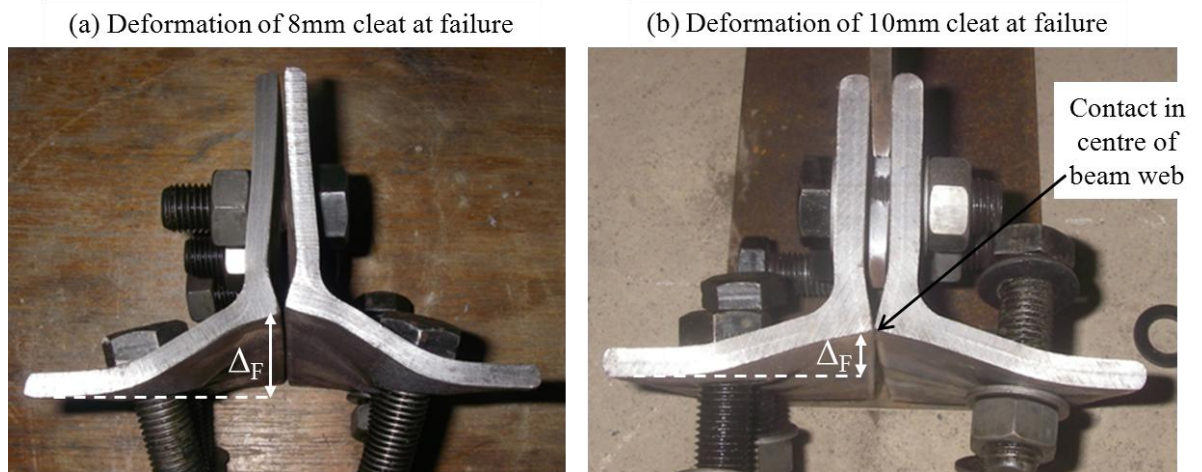
Figure 3-39: Typical web cleat deformation after dynamic failure (a) 8mm angles (b) 10mm angles

The load and rotation time history for a selection of the 8mm thick cleat connections is shown in Figure 3-40. This indicates that WC4 experienced approximately twice the applied loading rate compared with WC5 and subsequently failed at a reduced rotation.
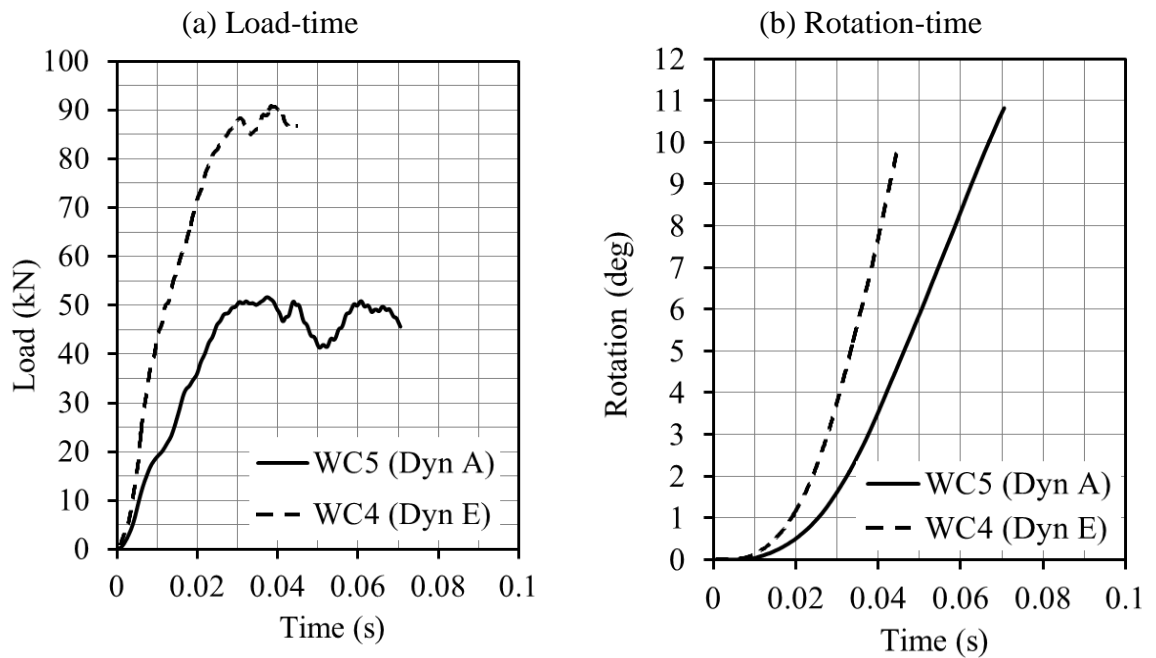
Figure 3-40: 8mm web cleat connection data (a) Load-time (b) Rotation -time

Comparison of the load-rotation in Figure 3-41a indicates that the inertia of the column increases the load at low rotations, as seen in all previous tests. An increase in stiffness is demonstrated in the first degree of rotation similar to that demonstrated in the fin-plate connections which is thought to be due to the same reasons; in the dynamic tests the inertia of the column causes the entire body to move away from the connection taking up the clearance holes in the connection. Any rotation therefore requires the top bolt to bear against the beam web. This was backed up by the DIC data which indicated that the entire column initially moved away from the applied load before rotation could occur. In the static tests, the column can simply rotate about the point with least resistance meaning the clearance in the top and bottom bolt holes can be taken up. The connections also demonstrate a drop in moment at approximately 5 degrees which was much more noticeable in the dynamic tests. It is thought that this is due to the load being localised at the top bolt row in the dynamic tests with a sudden drop in capacity indicating plastic behaviour until the next bolt hole begins to take up load as a result of prying action.
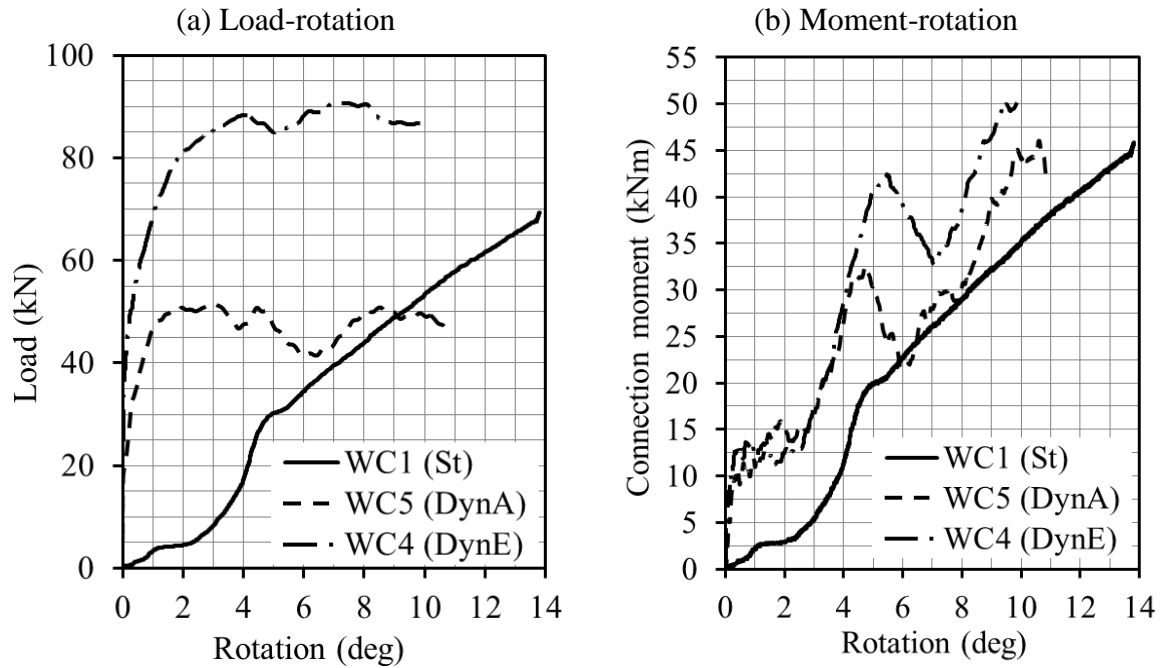
Figure 3-41: 8mm web cleat behaviour (a) Load-rotation (b) Moment-rotation

Recorded test data and results for 10mm thick cleated connections are presented in Figure 3-42 and Figure 3-43 respectively. In general the trends are similar to the thinner cleats although the failure rotation when loaded dynamically is reduced by a greater amount, thus sensitivity to dynamic load appears to be increased.
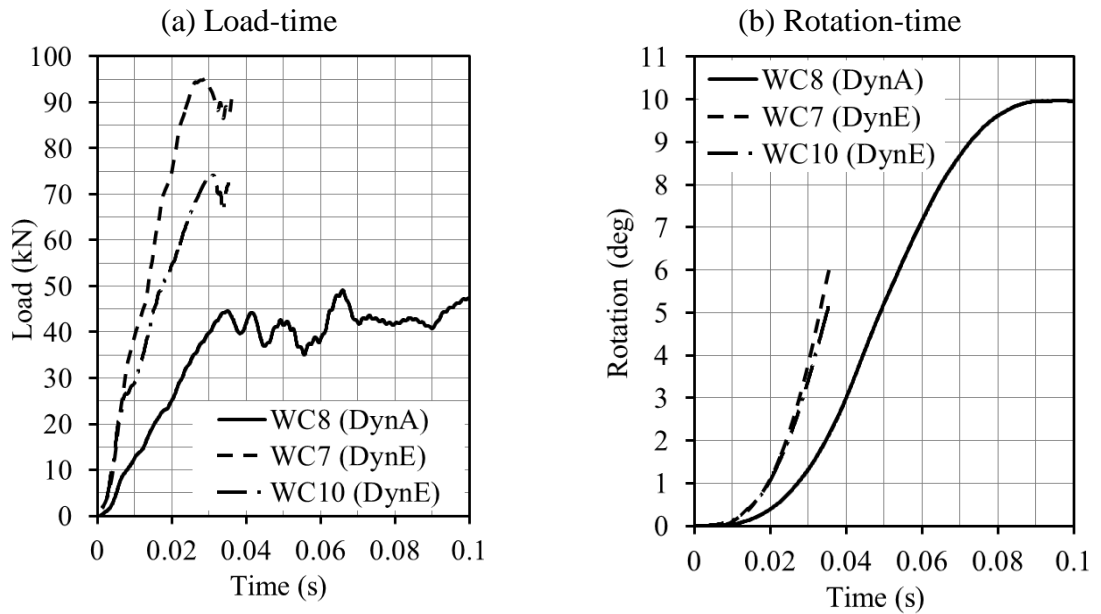
Figure 3-42: 10mm web cleat connection data (a) Load-time (b) Rotation-time
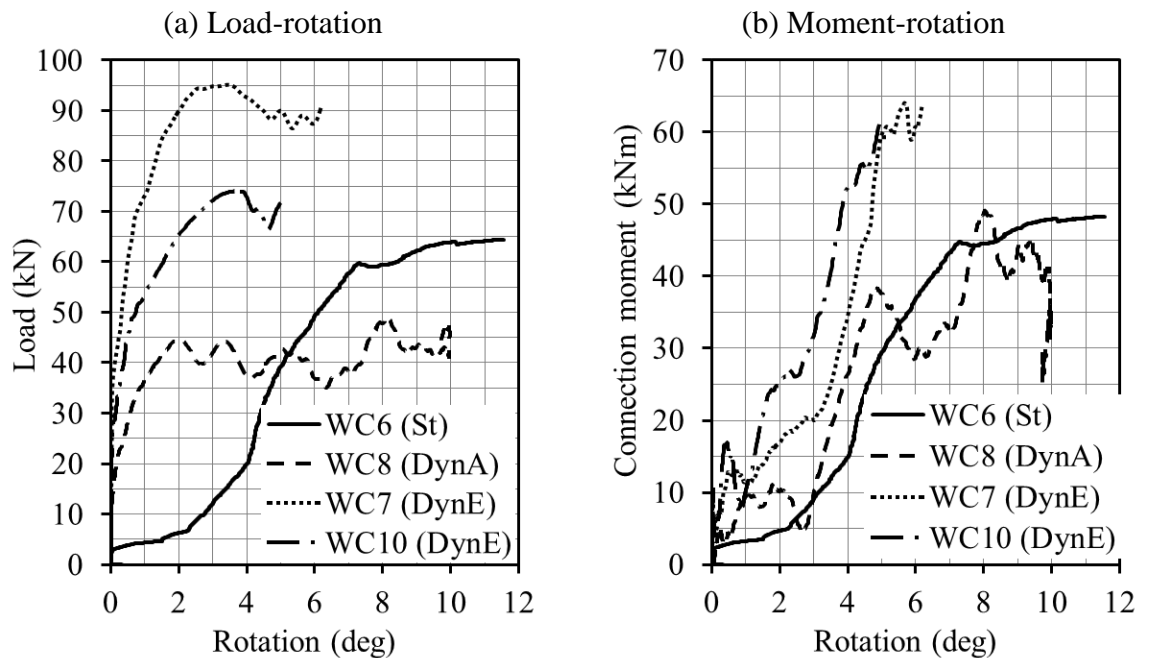
Figure 3-43: 10mm web cleat behaviour (a) Load-rotation (b) Moment-rotation

The use of 8mm thick angles is preferable to the 10mm angles because their greater ductility allows larger rotations before failure whilst maintaining a similar moment capacity. The stiffer 10mm angles also appear to make the connection more sensitive to dynamic loading as shown in Figure 3-43b where the failure rotation is in some cases reduced by up to 50%. It is thought that this is due to the cleat behaving stiffer and thus providing less ductility meaning the load has to be directed through the bolt in shear and into the beam web resulting in failure at lower rotations.

3.4   Direct Tension Testing

In order to allow a direct comparison against previous research into the tying capacity of connections a number of tests were conducted using two loading rams to provide a direct tensile force. No web cleat connections were tested in direct tension as after the initial tests it was apparent that the rig could not provide enough dynamic load to fail the weaker fin-plate and end-plate connections.

Table 3-7: Table of results for direct tension tests

Test Number	Plate Thickness (mm)	Loading Type	Peak Loading Time (ms)	Peak applied axial load (kN)	Failure	Factor of Safety (Axial Load)
FEP18	8	Static Tension	-	260.6	End-plate fracture	1.52
FEP19	8	Dyn (E) Tension	48	218.3	No Failure	
FEP19 (cont)	8	Static Tension	-	281.1	End-plate fracture	1.64
FEP20	8	Dyn (E) Tension	53.2	157.7	No Failure	
FEP20 (cont)	8	Static Tension	-	280.5	End-plate Fracture	1.64
FIN3	-	Static Tension	-	318.4	Bolt shear	1.66
FIN4	-	Dyn (E) Tension	41	192.0	No failure (approx 2mm extension)	
FIN4 (cont)	-	Static Tension	43	307.9	No Failure (leak in system, additional 4mm extension)	1.60

It was not possible to fail either the 8mm end-plate or fin-plate connections dynamically due to the added stiffness provided by the symmetrical loading conditions. The average factor of safety against design values for the tying capacity of end-plate connections was 1.61. Similarly the average fin-plate failure load gave a factor of safety of 1.63.

The results of the direct tension tests were included with the moment-rotation testing results to compare the applied loads at failure. The resulting plot (Figure 3-44) shows the reduced strength of the connections once rotations are included. The direct tension tests (indicated by failure at zero degrees rotation) all failed at an axial load at least 1.5 times that of the design capacity, whilst the moment-rotation tests all failed at substantially less than the design capacity.
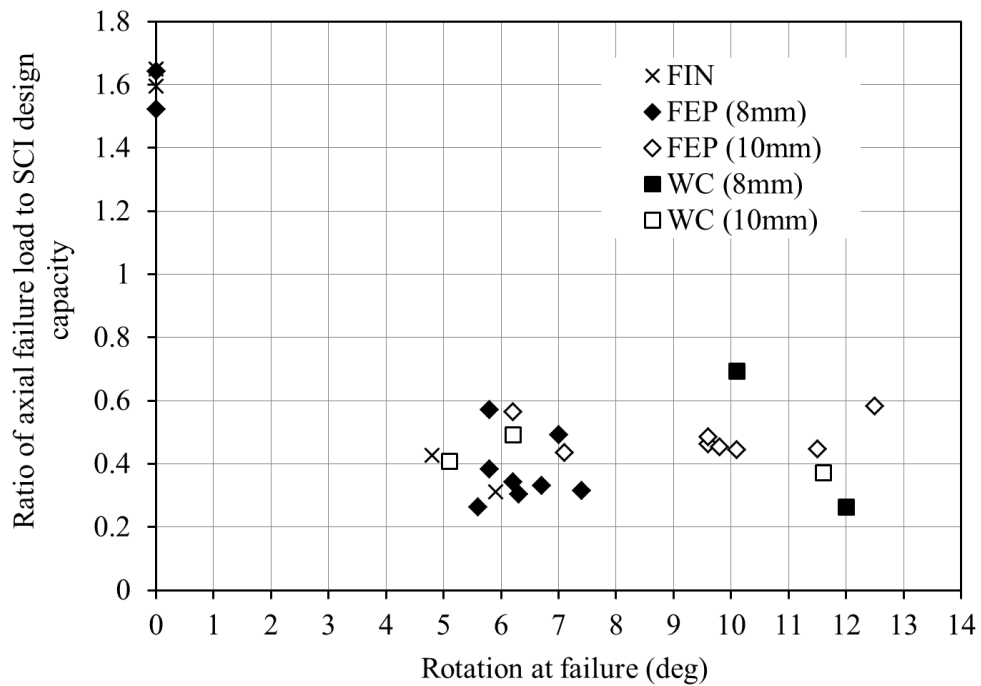
Figure 3-44: Comparison of failure loads for all test results

It is these results which the author believes demonstrates the importance of including connection behaviour in progressive collapse models. For catenary action to be provided in a steel frame the connections must rotate and once they do the assumption that they can provide the full tying capacity of the connection does not appear to hold true.

3.5 Conclusions

All of the tested connections demonstrated dynamically sensitive moment-rotation behaviour. In general when loaded dynamically the connections were less ductile with a reduced failure rotation, but demonstrated an increased ultimate moment capacity. The response of web cleat and flexible end-plate connections to dynamic loading is superior to the fin-plate connections due to their greater ductility, which increases the energy that can be absorbed before failure. However for all tested connections the rotation capacity was reduced when loaded dynamically.

The direct tension tests proved that both flexible end-plates and fin-plates are capable of achieving their design axial load capacities (171 and 193 kN) by at least a factor of safety of 1.5, including when loaded dynamically. The single ram tests however demonstrated that this capacity is greatly reduced following connection rotation and thus there is a need to account for this in scenarios where large rotations are likely.
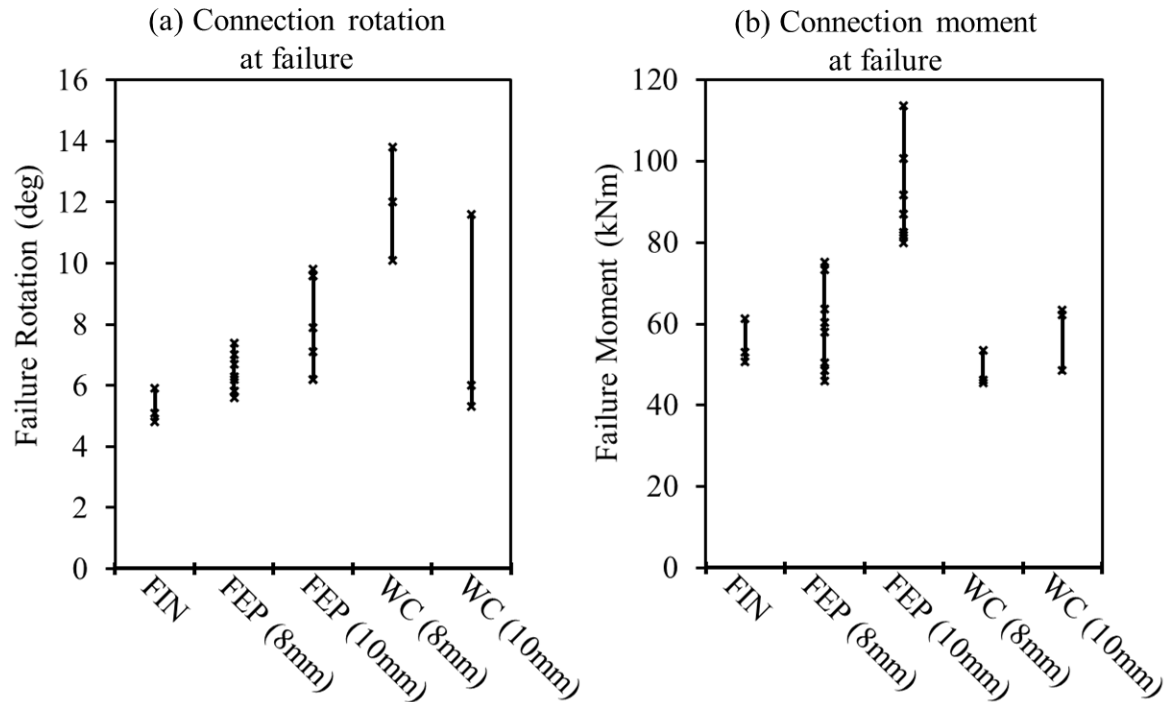
Figure 3-45: Range of experimental results

Figure 3-45a and b shows the range of failure rotations and moments for all tested connections at both static and dynamic loading rates. The length of the line indicates the range of values between static and dynamic behaviour hence a smaller line indicates a reduced sensitivity to dynamic effects. It is useful to remember that all of these connections are classified as "simple" and therefore ideally should have a large failure rotation and exhibit very little moment. The best connection in this sense is the 8mm thick web cleat connection whose minimum failure rotation was approximately 10 degrees when loaded dynamically. In comparison, the 10mm thick web cleat connection performed well under static loading but failure rotation was reduced by approximately 50% when loaded dynamically. The BCSA/SCI (2002) connection guidelines specify a 10mm thick angle for this specific beam section however it has been shown that 8mm thick angles provide greater ductility whilst maintaining a similar load and capacity. In this sense, the robustness of structures could be improved by using weaker, more ductile connections.

The failure moment for both thicknesses of web cleat was very similar as failure was dictated by block shear of the beam web. In comparison the 8mm and 10mm thick flexible end-plate connections demonstrated substantial differences in failure moment as failure was dictated by tearing of the end-plate itself. The fin-plate connections performed badly in terms of failure rotation with no test exceeding 6 degrees of rotation. This is attributed to the lack of deformable regions within the joint and thus an overall lack of connection

ductility. The 10mm end-plate connection exhibited considerable moment before failure which could invalidate "simple" design assumptions.

In conclusion all tested connections demonstrate variable behaviour and thus accurate connection representation is essential to predict premature failure in load cases where large connection rotation or dynamic loading is experienced.

4   MATERIAL PROPERTIES, FINITE ELEMENT ANALYSIS AND CONNECTION REPRESENTATION

4.1   Introduction

This chapter investigates procedures required to develop dynamic component-based models. Prediction of dynamic material properties and procedures to incorporate non-linear springs in numerical analysis were explored. In combination, these then allow dynamic component-based connection models to be analysed.

4.2   Material properties and strain-rate effects

Material properties were tested according to the relevant standards. S275 steel was specified for all beam sections and plate elements. All bolts used were high strength Grade 8.8. Nominal material properties are presented in Table 4-1.

Material	S275 Steel	Grade 8.8 Bolt
Nominal Yield Stress (N/mm^2)	275	640
Nominal Ultimate Stress (N/mm^2)	430	800

Table 4-1: Material properties from BS EN 1993-1-1 (2005) Table 3.1 and BS EN 1993-1-8 (2005) Table 3.1

Standard material coupon tests have been conducted on the parent metal to obtain their stress-strain behaviour (Sarraj, 2007). These are shown in Figure 4-1 and Figure 4-2.
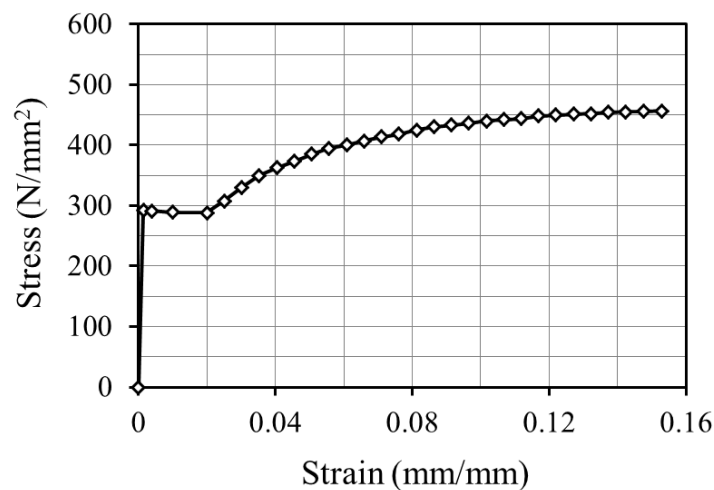
Figure 4-1: Stress-strain curve for nominal S275 steel
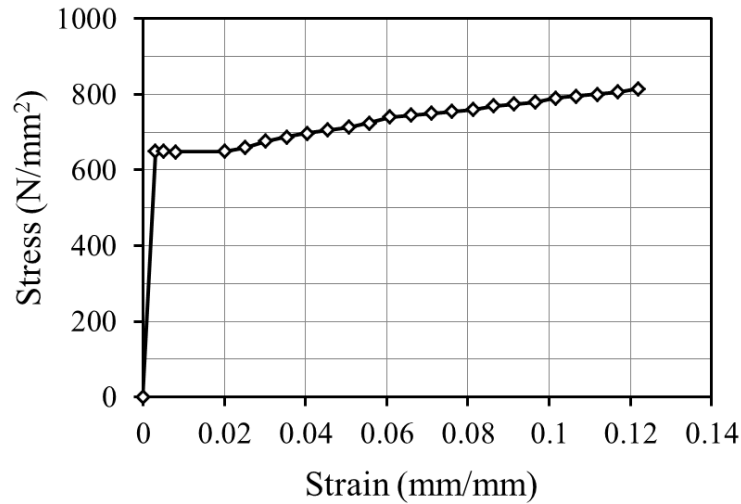
Figure 4-2: Stress-strain curve for 8.8 high strength bolts

The material tests of S275 indicate a yield stress of 292MPa and an ultimate stress of 462MPa. The grade 8.8 tests indicate a yield stress of 651MPa and ultimate stress of 817MPa. The material tests indicate a slight enhancement of the nominal values as expected. The properties obtained from the material tests will be used for the remainder of this thesis to allow accurate prediction of the individual component behaviour.

The material properties of steel are affected by strain rate. Unlike deformation at low strain-rates, which can be characterised by a number of simple mechanisms and is relatively linear, high strain-rate deformation is a more complicated phenomenon. Deformation of materials at atomic level involves dislocation or slip of groups of elements within the crystal lattice. In simple terms, at slow loading rates the slip occurs over the longest lengths of microstructure because it has time to find the weakest part of the lattice. At higher loading rates, the loading does not have time to find the weakest part of the microstructure and instead tries to slip along more direct planes. This can result in a strength increase.

A good example of this behaviour is observed when looking at concrete. At low loading rates, cracks tend to propagate through the cement matrix surrounding the aggregate; whereas at higher loading rates the cracks may be driven through the aggregate (Figure 4-3). The fracture of this aggregate requires more energy and thus a strength increase is observed.

low loading rate   high loading rate
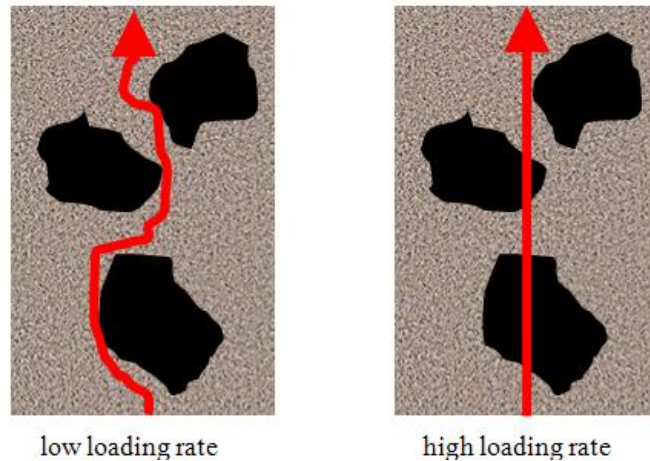
Figure 4-3: Crack propagation in concrete subject to different loading rates

In steel high strain-rate behaviour is characterised by extremely localized areas of high strain along narrow bands, known as adiabatic shear bands (ASBs). According to Odeshi et al. (2005) this term applies only when the strain-rate exceeds 10^2 s^{-1}. Adiabatic shearing causes damage to the material and reduces its load carrying capacity.

This damage is primarily a result of two simultaneous processes; strain hardening and thermal softening [Odeshi et al. (2005)]. At the start of the deformation, strain hardening dominates the behaviour. Following this, large localized strains, along the adiabatic shear bands, cause an increase in temperature leading to thermal softening and a weakening of the material.

When performing a numerical analysis under blast loading the high strain-rate effect must be taken into consideration in order to accurately capture real behaviour of the material. Nabil Bassim and Panic (1999) have shown that when the strain rate is very high this dynamic yield strength can, in some cases, increase beyond the ultimate strength of the steel as shown in Figure 4-4. The ultimate tensile strength also increases slightly however the elastic modulus is generally not affected by strain-rate.
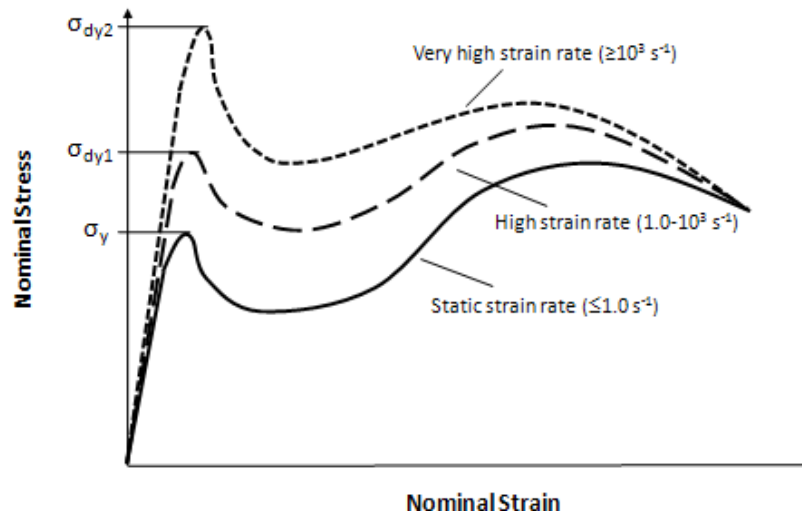
Figure 4-4: General stress-strain relationship of steel under various strain-rates. Liew (2008).

A variety of methods are employed to test dynamic material properties. For low loading rates (up to approximately 10 strain per second), conventional static testing equipment can be adapted by simply applying the load quicker than equivalent static testing. Alternatively, a drop hammer can be used to apply loads up to 100 strain per second depending on drop velocity and material resistance.

However the standard method to assess material strength under high strain-rate loading is to use a Split Hopkinson Pressure Bar (SHPB) where strain rates of up to 1000 strain per second are possible. A thin sample of material is placed between two instrumented steel bars and then a dynamic load applied to one end. A stress pulse is generated which travels along the length of the first bar into the specimen and through to the second bar. Strain gauge measurements along both bars allow measurement of the incident, reflected and transmitted pulses. Analysis of these pulses allows calculation of the dynamic stress, strain and strain rate experienced by the sample. It is possible to test materials in both compression and tension using the SHPB.

The effect of strain rate is commonly presented as a ratio between the static and dynamic strength in the form of a dynamic increase factor (DIF). Cowper and Symonds (1957) developed a rate dependent plasticity model in order to calculate the dynamic yield strength from the equivalent plastic strain rate:

$$\sigma_y(dynamic) = \left[1 + \left(\frac{\dot{\varepsilon}}{C}\right)^{\frac{1}{p}}\right] \sigma_y(static) \qquad (4.1)$$

Where *C* and *p* are empirically determined constants (*p*≈5 and *C*≈40-40000/s depending on steel grade). The importance of including strain-rate effects, even for relatively low strain-rates, can be shown using Cowper-Symonds equation. By varying the strain rate from 0 to 10 s^{-1} the yield strength is increased by a factor of 1.75 for S275 steel (C=40). This may prove critical for connections using angles or end-plates where the rotation capacity of the connection is provided by the deformation of these components.

Accurate prediction of failure requires the ultimate stress as well as the yield stress of the steel to be used. A study of dynamic increase factors for both yield and ultimate stresses was conducted by Malvar and Crawford (1998). The study included a detailed literature review of the effects of high strain rate. Results indicated that there was a greater dynamic effect on the yield stress than that of ultimate stress, and in agreement with Cowper and Symonds the higher strength steels were less affected. Equations to calculate the DIF (for both yield and ultimate stress) from the strain rate and static yield stress were proposed:

$$DIF = \left[\frac{\dot{\varepsilon}}{1 * 10^{-4}}\right]^{\alpha} \qquad (4.2)$$

Where:

For dynamic
yield stress

$$\alpha_y = 0.074 - 0.040\frac{f_y}{414} \qquad (4.3)$$

For dynamic
ultimate stress

$$\alpha_u = 0.019 - 0.009\frac{f_y}{414} \qquad (4.4)$$

A comparison of Cowper-Symonds and Malvar-Crawford's methods for expected strain rates is presented in Figure 4-5 which shows a maximum difference of 0.05 for S275 steel at a strain rate of 10/s.
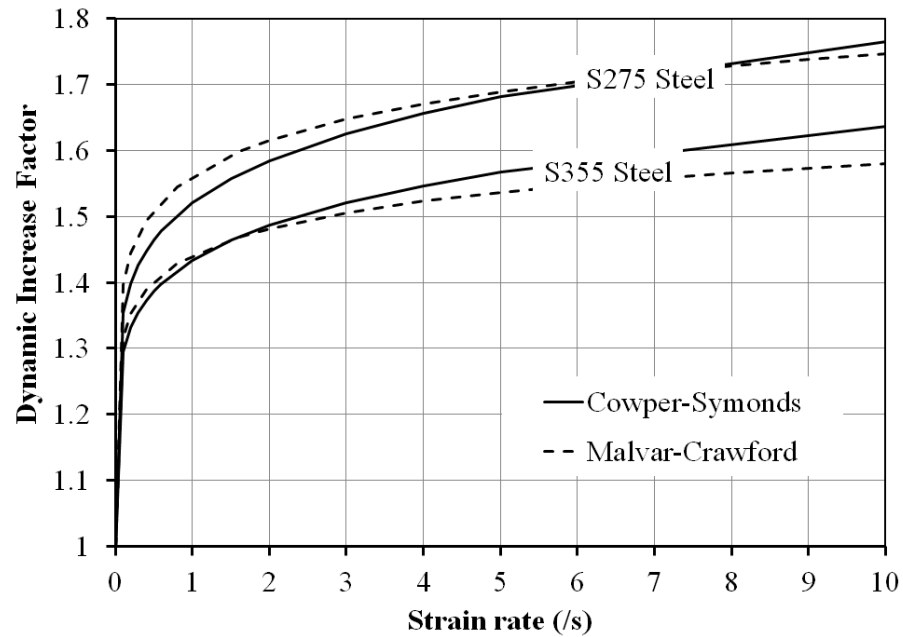
Figure 4-5: Dynamic increase factor for yield strength of mild steels

The dynamic material properties in the component-based connection models will be calculated using the Malvar-Crawford equations. This will allow a prediction of the dynamic enhancement of both the yield strength and the ultimate strength for individual components.

4.3   Finite element analysis

The finite element method is an analytical tool that can be applied very effectively to the analysis of many of the problems facing engineers. Put simply, the goal is to develop a mathematical model based on realistic assumptions which can be used to accurately predict the behaviour of the physical model. The finite element method developed into the form we know today in the 1960's and since then has been used in virtually all fields of engineering.

The power of finite element methods lies within its versatility. For example a multitude of loading, geometric and support conditions can be examined using any number of elements of different shapes, sizes and material properties all contained within one piece of computer software. User-prepared input data defines the problem and thus an understanding of these parameters is essential to be able to obtain results with accuracy and confidence.

4.3.1 Procedure

An analysis using FEA consists of three stages: pre-processing, simulation and post processing.

ABAQUS/CAE was used exclusively in the preprocessing stage to create the required input files. This input file contains a complete description of the numerical model and includes a minimum of geometry, element section properties, material data, loads and boundary conditions, analysis type and output requests. The simulation phase can be performed using either ABAQUS/Standard or ABAQUS/Explicit. The differences between these two modules will be discussed later.

Formulation is the method used to determine the element's behaviour. Stress analysis in ABAQUS is based upon the Langrangian description of behaviour. Integration is used to evaluate material response at each integration point in an element. The accuracy of a model depends upon the mesh resolution and time step value, particularly when dealing with fast spatial and temporal transients i.e. a rapid change in pressure and velocity when a blast wave interacts with a solid surface.

For explicit applications, the time step must be small enough that the stress wave does not propagate from one element to another within this time. The maximum time step is therefore determined by:

Time step
$$\Delta t = \frac{l}{c} G$$
(4.5)

Where *l* is the element length, *c* is the wave speed in the material and *G* is a reduction factor to keep the time step below the critical value (typically between 0.8 and 0.9).

From above it is seen that doubling the mesh resolution in a three dimensional model effectively increases the time for the analysis by a factor of 16. This is because there will be 8 times the number of physical elements in the model and the length of these elements will be halved thus Δt will be halved meaning the same problem will require double the amount of steps.

4.3.2 Dynamic analysis

Essential to this thesis is the analysis of non-linear dynamic problems using finite element analysis. The major difference between static and dynamic analysis is the inclusion of inertia forces in the equation of equilibrium. Another difference is found in the definition of the internal forces. In a static analysis, the internal forces are derived from the deformation of the structure. A dynamic problem also has inertia forces contributed by the motion of the structure.

Equation of motion for dynamic problem

$$M\ddot{u} + I - P = 0$$

(4.6)

Where M and $\ddot{u}$ are the mass and acceleration of the problem and I and P are the internal forces of the structure and applied external forces respectively.

A detailed explanation of methods to solve the dynamic equations of motion is presented by Cook et al. (1989). What follows is a brief explanation of the variety of methods available in ABAQUS to solve the dynamic equations of motion.

4.3.2.1 Modal superposition

The first in ABAQUS/Standard uses a frequency extraction step followed by modal dynamics. Real structures have a large number of natural frequencies and different modes. These individual frequencies are calculated by considering the response of the unloaded structure. In this case the equation of motion is:

$$M\ddot{u} + Ku = 0$$

(4.7)

The solution to this ordinary differential equation is of the form [Simulia (2007)]:

$$u = \phi e^{i,\omega t}$$

(4.8)

Substituting this yields what is known as the eigenvalue problem:

$$K\phi = \lambda M\phi$$

Where $\qquad\qquad\qquad\qquad\qquad\qquad\qquad\qquad\qquad$ (4.9)

$$\lambda = \omega^2$$

The system developed has *n* number of eigenvalues which is the same number of degrees of freedom of the system. Making λ_n the *n*th eigenvalue, its square root, ω_n, is the natural frequency of the *nth* mode of the structure. The corresponding value of $\emptyset_n$ is known as the eigenvector or mode shape.

The natural frequencies and mode shapes of a structure can be used to describe its dynamic response to loading. This is achieved using the modal superposition technique where each shape is multiplied by a scale factor. The deformation of the structure can be calculated from a combination of these mode shapes. This method reduces the large set of global equilibrium equations to a relatively small number of uncoupled second order differential equations and thus results in significantly reduced computational time. However this technique is valid only for problems with linear elastic materials, small displacements and no contact conditions and therefore unsuitable for most progressive collapse analyses.

4.3.2.2 *Implicit dynamic solutions*

If nonlinearities are present in the simulation then the natural frequencies may change during analysis and the modal superposition technique cannot be used. When nonlinear dynamic response is needed, the equation of motion must be integrated directly. The most general solution method is an incremental method in which the equilibrium equations are solved at *t*, *t+Δt*, *t+2Δt* etc. The nonlinear dynamic procedure available in ABAQUS/Standard uses implicit time integration. Implicit methods solve the equilibrium equations for the dynamic quantities at *t+Δt* based on these values at *t* and *t+Δt*. Due to the implicit nature of the problem, the non-linear equations must be solved and the global matrix must be transposed. Thus a global set of equilibrium equations must be solved and the structural stiffness matrix inverted for each time increment in order to maintain equilibrium between internal structural forces and applied loads. These iterative methods are necessary to achieve a solution within an acceptable tolerance.

Although these methods can be used for certain dynamic scenarios, they are generally not suitable for highly dynamic problems like blast or impact. This is due to the highly non-linear nature of the problem which causes stability and convergence problems.

4.3.2.3 Explicit dynamic solutions

An alternative method to solve nonlinear dynamic problems is to use explicit methods. These obtain values for dynamic quantities at $t+\Delta t$ based entirely on the available values at time t. The benefit of this is that the governing equilibrium equation can be solved directly without the need to transpose the stiffness matrix at each increment. The drawback is that this method requires very small time steps to maintain its stability during dynamic analysis of structural members as otherwise the solution can easily drift from the exact solution. These explicit solutions can model discontinuous nonlinearities such as contact and failure more easily than implicit solutions. The explicit algorithm propagates the solution as a stress wave through the model element by element thus making it suitable for problems where stress wave effects are important.

Sun et al. (2000) performed a comparison of implicit and explicit finite element methods using ABAQUS. Several dynamic problems were modelled and the performance of these two direct integration solution methods was compared. The problems were categorised as fast and slow contact and the advantage of explicit for fast and implicit for slow cases was demonstrated. Thus the preferred use of the explicit method for short transient problems and the implicit method for longer duration problems was verified. Another comparison of explicit and implicit methods has been reported by Rebelo et al. (1992) with similar conclusions. They also concluded that difficulties in three dimensional modelling will be encountered when using the implicit method due to local instabilities making force equilibrium difficult to achieve.

4.3.3 Spring modelling

Use of the component method requires rate-dependent, non-linear force-displacement behaviour. This is achieved through the use of springs of which there are numerous options available within ABAQUS.

Initially spring elements were used to connect two nodes and an initial stiffness assigned. In principle this method worked for both static and dynamic problems however the spring is limited to linear-elastic behaviour and no failure criteria can be applied. An alternative

solution was sought which could replicate the non-linear behaviour. The method the author has found most suitable for this is to use axial connector sections.

These are described in detail in Simulia (2009) and are able to model non-linear behaviour with specified failure criteria (defined by either extension or force).

The connector sections can be assigned to any node or geometry sets within ABAQUS element definitions and thus permits the use of rigid and deformable bodies within the model. Its properties are governed by the behaviour options which include rate dependent plasticity.

It is important to specify the correct output to understand what is going on within the components. The important properties of this connection type are the failure status (CFAILST1), total force component (CTF1) and the relative position or displacement component (CP1). From these properties the behaviour of the spring can be determined throughout the analysis. This allows beam and shell elements within a frame model to be connected using rigid elements and axial connector sections.

4.3.4 Materials

ABAQUS contains a large material library which allows most engineering materials to be modelled. A metal deforming plastically under tension may experience extension and thinning of the material. This process is called necking and is of importance in numerical modelling. The engineering stress (force per unit of deformed area) is known as the nominal stress and is lower than the material's ultimate strength. This is caused by the cross sectional area of the test specimen reducing as it is stretched.

In order to account for this behaviour when defining plasticity data in ABAQUS, the true stress and true strain must be used. Hibbitt et al. (2007) provide expressions to convert test data (usually given in terms of nominal stresses and strains) to the true stress/strain values for use in ABAQUS.

The true strain (ε_{true}) is found using:

$$\varepsilon_{true} = \ln(1 + \varepsilon_{nom})$$

(4.10)

The true stress (σ_{true}) is then calculated.

$$\sigma_{true} = \sigma_{nom} * (1 + \varepsilon_{nom})$$

(4.11)

Finally the total strains are decomposed into elastic and plastic components and the plastic strain (ε_{pl}) calculated.

$$\varepsilon_{pl} = \varepsilon_{true} - \left(\frac{\sigma_{true}}{E}\right)$$

(4.12)

ABAQUS interpolates between an unlimited number of input data points allowing very accurate material properties to be captured.

4.4   Connection representation

The geometrical properties of each connection are used to develop a component-based connection model in ABAQUS/CAE. The behaviour of each deformable joint component is captured using an axial connector section with the non-linear force-displacement behaviour defined in Chapter 5 for both fin-plate and flexible end-plate connections. Connector sections are joined with discrete rigid elements to represent the face of the beam which in turn is connected to one dimensional beam elements through which the loading is applied.
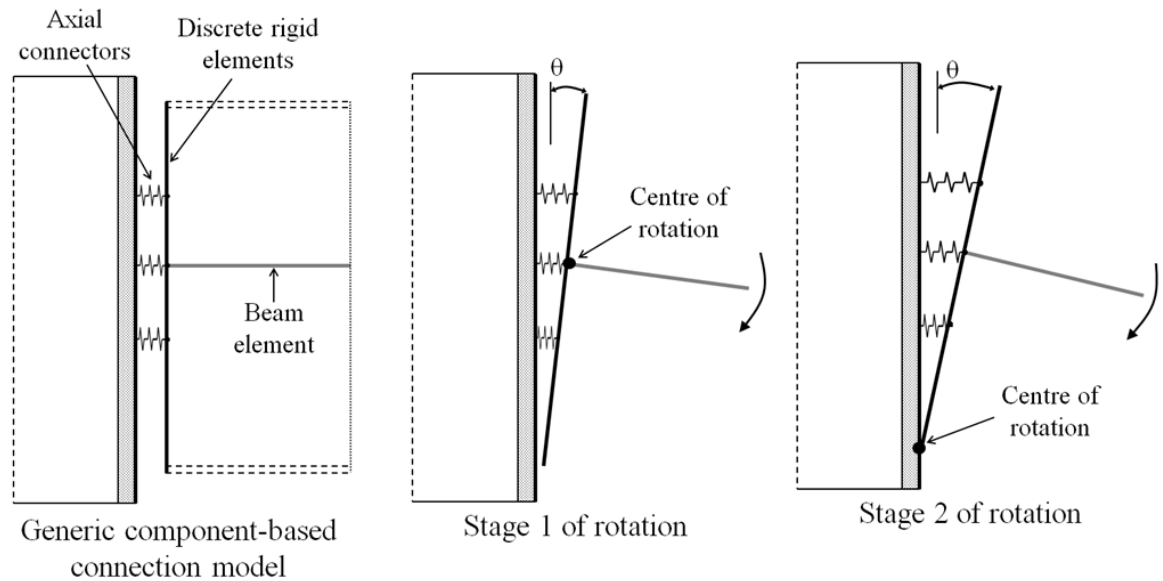
Figure 4-6: Connection representation

A 'hard' surface-to-surface contact definition is applied to the two rigid elements representing the column and face of the beam. This allows the connection to change its centre of rotation when the beam lower flange contacts the column (Stage 2 in Figure 4-6).

This assembly allows a two-dimensional representation of the connection which can account for prying action and the resulting increase in connection stiffness when the lower beam flange contacts the column. Because the system is always in dynamic equilibrium effects of load reversal and axial load can also be included.

4.5 Conclusions

Dynamic behaviour of individual components will be included by modifying the material yield and ultimate strength according to the approximate strain-rate using Equations 4.2 – 4.4. The component-based connection models will be assembled in finite element software using rigid and axial connector sections and solved using a non-linear explicit solver to allow calculation of the entire range of connection behaviour. The effect of prying action can be accounted for by defining contact between the rigid elements representing the face of the beam and the column flange. This technique allows the inclusion of beam and column elements for investigating behaviour of structural sub frames.

5 DEVELOPMENT OF COMPONENT-BASED METHODS FOR DYNAMIC LOADING CONDITIONS

5.1 Introduction and background

The connections within a steel framed structure are the most vulnerable elements within the system and as such require correct detailing to achieve the necessary ductility and robustness [Marchand and Alfawakhiri (2004)]. The component method is one of a variety of methods used for joint modelling. It is attractive in that simple joint components can be investigated individually before being assembled into a joint arrangement which can then predict the non-linearity of the whole joint.

A reasonable amount of work has been completed on the behaviour of individual components and it is this work that will be developed for use under blast and progressive collapse conditions. The majority of this work was conducted to classify the behaviour of components at elevated temperatures for the purpose of fire engineering. In the methods developed herein the ambient temperature behaviour is used and the influence of the dynamic nature of the loading included. This is achieved by including the inertia effects and modifying the material properties to account for the varying strain-rate. These dynamic factors tend to increase the stiffness but reduce the ductility of components and therefore can influence the behaviour of the joint.

The following section collates information on components within common steel connection types. Of most interest is the force-displacement relationship for each component which can then be included in numerical analysis.

The following assumptions are made for all component models:

1. Geometric properties are taken directly from the layout of the joint
2. Material properties are strain-rate dependent
3. Individual component characteristics are taken either from current models, mathematical formulation or experimental testing
4. Component characteristics include elastic stiffness, yield strength, plastic stiffness, failure load and failure displacement

This research seeks to establish whether a component connection model similar to those normally proposed under ambient conditions can provide an acceptable representation of the dynamic connection behaviour. The individual components are assembled into a global connection model which can be compared against the experimental data from Chapter 3.

In the component models developed herein, dynamic increase factors (DIF) are used to account for the variable material properties at different loading rates using the work by Malvar and Crawford (1998) presented in Chapter 4. As stated previously, the DIF for yield strength (Φ) is given by:

$$\Phi = \left[\frac{\dot{\varepsilon}}{1*10^{-4}}\right]^{0.074-0.040\frac{f_y}{414}} \tag{5.1}$$

The DIF for ultimate strength (Ω) is found using:

$$\Omega = \left[\frac{\dot{\varepsilon}}{1*10^{-4}}\right]^{0.019-0.009\frac{f_y}{414}} \tag{5.2}$$

5.2 A dynamic component-based model for fin plate connections

Fin plate connections, or shear tab connections as they are sometimes called, consist of a length of plate welded to the supporting member and then bolted to the supported member on site. Their rotational capacity is derived from hole distortions in the plate due to bearing, out of plane bending of the plate or shear deformation of the bolts. Their advantages are the speed and ease of erection and the ability to overcome the problem of shared bolts in two-sided connections. A study of these connection types is presented in Astaneh-Asl et al. (2002) and full design guidelines and capacities for fin plate connections in the UK are found in *Joints in Steel Construction: Simple Connections* produced by BCSA/SCI (2002). These guidelines aim to prevent bolt fracture by limiting the ratio of the plate thickness to the bolt diameter and thus provide checks for bearing resistance only. This method aims to make the critical failure mechanism bolt bearing rather than bolt shear to prevent premature failure and provide a greater rotation capacity. However, experimental work by Yu et al. (2007) found that failure from bolt shear is still a possibility.

Following the 1994 Northridge earthquake in the United States detailed analysis of the behaviour of steel structures was undertaken, many of which were connected with fin plate connections. The results suggested these connections exhibited a rotational strength and stiffness which was previously thought to be negligible. Liu and Astaneh-Asl (2004) conducted a study on the moment-rotation behaviour of fin plate connections in composite structures for application in seismic design. Simple guidelines for estimating the moment and rotation capacity are presented based on the trends witnessed in a series of test data.
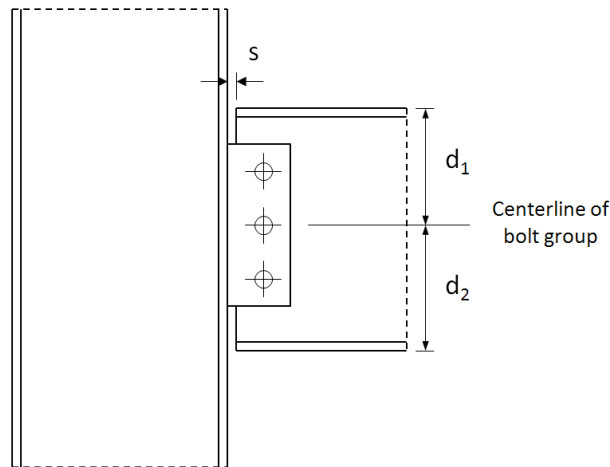
Figure 5-1: Arrangement of fin plate connection

The method assumes beam rotation about the centerline of the bolt group as shown in Figure 5-1 with the rotation capacity limited to contact between the bottom beam flange and the column.

Rotation capacity from Liu and Astaneh-Asl (2004)	$$\theta_{capacity} = \frac{d_{max}}{s}$$ Where d_{max} is the greater of d_1 or d_2	(5.3)

The moment capacity is calculated by assuming the shear force is taken by the top bolts depending upon their shear capacity. The remaining bolts and slab in compression are then used to resist the bending moment. Contact between the bottom beam flange and column does not cause instant failure, therefore the method developed by Liu (2004) is conservative for progressive collapse modelling.

Guravich and Dawe (2006) conducted tests on a variety of common joint typologies including fin plate connections under a combination of shear and tension. The findings

98

indicated that the connections are capable of maintaining significant tensile loads up to the joint shear capacities. Ductility was obtained by bearing in the bolt holes. Similar results were obtained by Selamet and Garlock (2009) who used FE methods to investigate their behaviour under fire loading where high tensile loads often occur.

These provide a simple method to calculate basic joint properties but in order for a component model to be created the individual component behaviour must be calculated. Sarraj (2007) developed a component-based model for fin plate connections in fire. This model treated each bolt row individually as a group of springs in series representing the bearing of the fin plate, the bearing of the beam web, the shear of the bolt and a final spring representing the surface friction. A detailed parametric study was conducted on all of the models using finite element analysis with good results. This model was later improved by Yu et al. (2009) who included a further spring to represent the bottoming out of the beam flange on the column. The required components for a fin plate model are thus:

- Plate in bearing
- Bolt in single shear
- Friction
- Beam and column contact

5.2.1   Plate in bearing

Rex and Easterling (2003) realised that one of the fundamental components of a steel connection is the load-deformation behaviour of bolts bearing on steel plates. As a result they conducted a detailed experimental and analytical study of a single bolt bearing against a single plate. The parameters that were investigated included end distance ($e2$), plate thickness (t_p) and bolt diameter (d_b). The plate width was not included due to previous observations leading to the conclusion that it would have little effect on the behaviour of a real connection. Normalised load-deformation behaviour was used to represent the behaviour and was curve fitted to the experimental data. No friction was included in the model because the bolt was not fully tightened because there was a gap between the cover plates as shown in Figure 5-2.
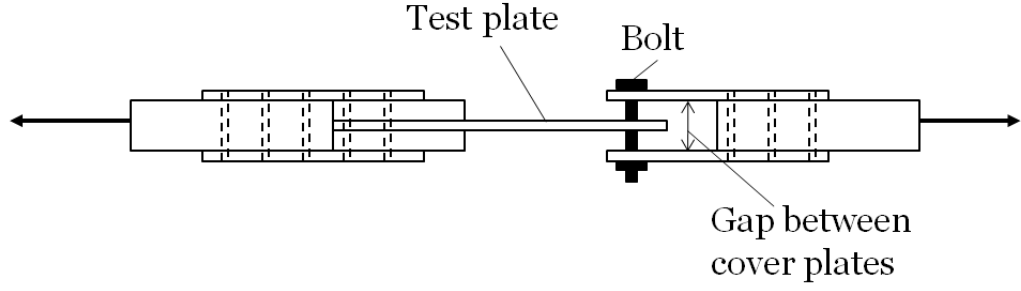
Figure 5-2: Diagram of Rex (2003) test setup

The relationship used to approximate the relationship between normalized deformation ($\bar{\Delta}$) and the bearing force (F_{br}) is given as follows:

$$\frac{F_{br}}{F_{br,Rd}} = \frac{2.1\bar{\Delta}}{(1 + \bar{\Delta}^{0.5})^2} - 0.012\bar{\Delta} \qquad (5.4)$$

The normalised deformation is related to the hole elongation (Δ_{br}) by:

$$\bar{\Delta} = \Delta_{br}\frac{K_{i,br}}{F_{br,Rd}} \qquad (5.5)$$

$F_{b,Rd}$ is the nominal plate bearing strength calculated using the following equation from AISC (1993):

LFRD design
specification AISC
(1993)

$$F_{br,Rd} = e2\Omega_{br}f_{up}t_p \qquad (5.6)$$

The initial stiffness ($K_{i,br}$) is extremely important in characterising the load-deformation behaviour and is dependent upon three parameters of the plate, namely the bearing stiffness (K_{br}), bending stiffness ($K_{b,br}$) and shearing stiffness ($K_{v,br}$). The final stiffness is found by assuming these three parameters work in series using the Young's modulus (E_p) and shear modulus (G_p) of the plate steel.

$$K_i = \cfrac{1}{\cfrac{1}{K_{br}} + \cfrac{1}{K_{b,br}} + \cfrac{1}{K_{v,br}}} \tag{5.7}$$

The bearing stiffness model is calculated by assuming a two dimensional problem and assuming the steel in contact with the bolt is at yield stress.

$$K_{br} = 145 t_p \Phi_{br} f_{yp} \left[\frac{d_b}{25.4} \right]^{0.8} \tag{5.8}$$

Bending Stiffness:

$$K_b = 32 E_p t_p \left[\frac{e2}{d_b} - 0.5 \right]^3 \tag{5.9}$$

Shear Stiffness:

$$K_v = 6.67 G_p t_p \left[\frac{e2}{d_b} - 0.5 \right] \tag{5.10}$$

The effect of strain rate is included by considering an infinitely stiff bolt moving at a constant bearing rate (V_{br}). The time taken to reach the yield bearing deformation ($d_{y,br}$) is used to predict the strain rate as follows:

$$\dot{\varepsilon} = \frac{\varepsilon_{yp}}{T_y} \tag{5.11}$$

$$T_y = \frac{d_{y,br}}{V_{br}}$$

where

$$\varepsilon_{yp} = \frac{f_{yp}}{E_p} \tag{5.12}$$

$$\dot{\varepsilon} = \frac{V_{br}f_{yp}}{E_p d_{y,br}} \tag{5.13}$$

Combining with Equations 5.1 and 5.2 gives the following:

$$\Phi_{br} = \left[\frac{V_{br}f_{yp}}{E_p d_{br} * 1 * 10^5}\right]^{0.074 - 0.040\frac{f_{yp}}{414}} \tag{5.14}$$

$$\Omega_{br} = \left[\frac{V_{br}f_{yp}}{E_p d_{br} 1 * 10^{-4}}\right]^{0.019 - 0.009\frac{f_y}{414}} \tag{5.15}$$

Rex and Easterling (2003) determined a typical yield bearing deformation (d_{br}) of 0.102mm which is used for both the fin-plate and beam web and allows the DIF to be plotted as a function of the bearing rate (Figure 5-3).
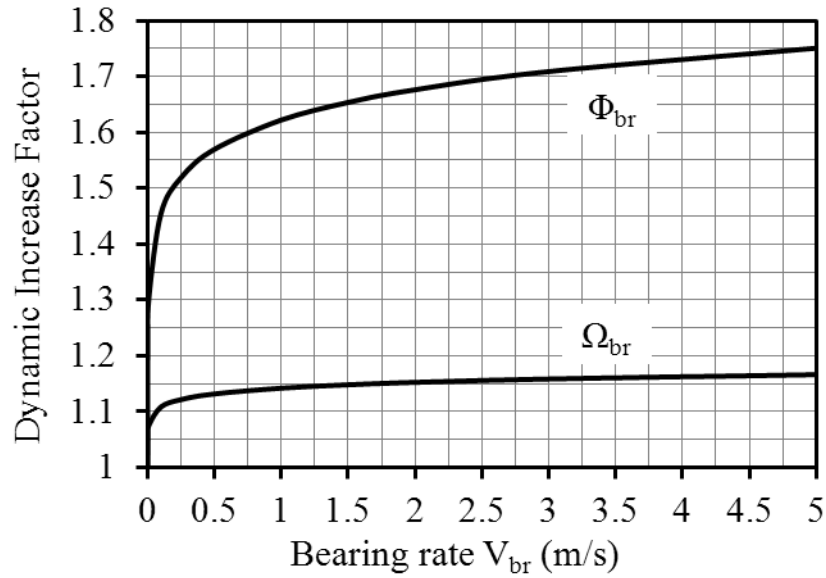
Figure 5-3: Effect of bearing rate on DIF for 7mm thick plate of S275 steel

5.2.2 Bolt in single shear

Owens and Cheal (1989) carried out work on bolts subject to shear under static conditions for typical 20mm diameter bolts. The position of the thread was varied to alter the position of the shear plane. The results from these tests indicate that where the shear plane is in the

shank, the shear capacity can be increased by up to 50% with similar increases seen in the deformation capacity. The fin plate connection utilizes bolts subject to single shear and therefore an analytical model to predict this force-displacement relationship is required.

The bolt shear deformation model is developed from previous work by Sarraj (2007) who conducted a parametric study of finite element models to investigate the single shear behaviour of Grade 8.8 bolts.

The shear deformation (Δ_v) is related to the applied shear force (F_{vb}) using the following equation.

$$\Delta_v = \frac{F_{vb}}{K_{vb}} + 2.5\left(\frac{F_{vb}}{F_{vb,Rd}}\right)^6 \tag{5.16}$$

The bolt shear stiffness (K_{vb}) is dependent upon the bolt shear modulus (G_b), shear stress area (A_s) and bolt diameter (d_b) and calculated using:

$$K_{vb} = \frac{0.15 G_b A_s}{d_b} \tag{5.17}$$

The value of 0.15 is a correction factor to account for the cross-sectional shape and material properties which Sarraj (2007) gives as appropriate for the bolt shearing analysis.

The proposed bolt shearing strength ($F_{v,Rd}$) is adapted from BCSA/SCI (2002) to make full use of the ultimate bolt strength:

BCSA/SCI (2002)
$$F_{vb,Rd} = 0.6 f_{yb} A_s \tag{5.18}$$

For grade 8.8 bolts
$$\frac{f_{ub}}{f_{yb}} = 1.25 \tag{5.19}$$

$$F_{v,Rd} = 0.6 * 1.25 * f_{yb}A_s$$

$$= 0.75\Phi_{bv}f_{yb}A_s$$

(5.20)

Very little work exists on classifying the performance of bolts subject to a dynamic shearing force. Kim et al. (2009) investigated the shear behaviour of high strength M30 bolts with grooves cut into them to create a shearing plane of 20mm diameter. Results indicated that at a shear rate of 9.5m/s the shear strength was increased by 20.8%. From previous studies of bolts by Owens and Cheal (1989) the yield stress is achieved over an initial deformation of 1/40 of the bolt diameter. It is therefore proposed to use this value to approximate the strain rate by dividing the yield strain by the time taken to reach the yield strain for a set shear rate (V_{bv}).

$$\dot{\varepsilon} = \frac{\varepsilon_{yb}}{T_y}$$

(5.21)

where:

$$T_y = \frac{d_b}{40V_{bv}}$$

(5.22)

$$\varepsilon_{yb} = \frac{f_{yb}}{E_b}$$

providing:

$$\dot{\varepsilon} = \frac{40V_{bv}f_{yb}}{d_bE_b}$$

(5.23)

The shear rate is therefore directly proportional to the strain rate which is then used to calculate the dynamic increase factor for the bolt in shear from Equation 5.1:

$$\Phi_{bv} = \left[\frac{4 * 10^5 V_b f_{yb}}{d_b E_b}\right]^{0.074 - 0.040\frac{f_{yb}}{414}}$$

(5.24)

The DIF can then be plotted as a function of shear rate as shown in Figure 5-4. This indicates a shear strength increase of 17.5% at a shear rate of 10m/s.

104
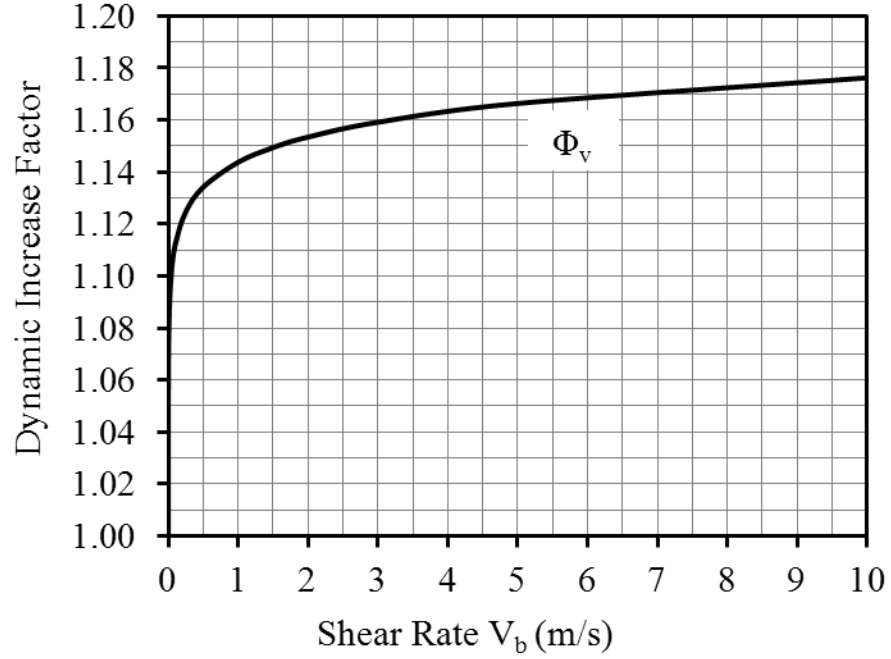
M20 bolts are usually installed in 22mm diameter clearance holes therefore, assuming the bolts are installed centrally, there is 1mm of movement in either direction. This is accounted for by offsetting the stiffness curve for each bolt. Experimental data of bolts tested at 20°C indicates that once the bolt ultimate shear strength is achieved the bolt fractures immediately.

5.2.3   Friction

A triangular relationship is used to model the friction between the fin plate and beam web from Yu et al. (2009). The peak friction force ($F_{s,Rd}$) includes a slip factor (μ) and is given by:

$$F_{s,Rd} = 0.28 \mu f_{ub} A_s \tag{5.25}$$

Where A_s is the stressed area of the bolt. BS EN 1993-1-2 (2005) suggests a slip factor value of between 0.2 and 0.5 depending upon the friction classification. Yu et al. (2009) used a value of 0.2 which is also adopted here.

The displacements at the peak shear force (Δ_{su}) and zero resistance (Δ_{sf}) are:

$$\Delta_{su} = 0.18d_b \qquad (5.26)$$

$$t_T < 20 \ then \ \Delta_{sf} = 16$$

$$20 \leq t_T \leq 38 \ then \ \Delta_{sf} = 16 - 0.3(t_T - 0.5) \qquad (5.27)$$

$$38 < t_T \ then \ \Delta_{sf} = 4$$

Where t_T is the combined thickness of the two plates.

Dynamic friction is not accounted for at this stage but could be included following future investigations.

5.2.4 Beam-flange contact spring

During loading, it is possible that the bottom of the beam flange will contact the column and cause the centre of rotation to shift. In component-based modelling, this contact is often included through the use of an additional spring whose stiffness is zero until the initial clearance is taken up at which point it becomes infinitely stiff. This method is a simple approximation which allows prying action to be included but cannot account for any relative slip between the beam lower flange and column. Whilst this is often inconsequential for connection tests it was thought that in the case of progressive collapse this slip could alter the rotation point and thus the overall behaviour. Therefore a contact definition was made between the rigid elements representing the face of the beam and column flange.

5.2.5 Verification of proposed model

A single bolt row consists of fin-plate in bearing, beam web in bearing and bolt in shear in series and these were incorporated into a complete connection model as shown in Figure 5-5b.
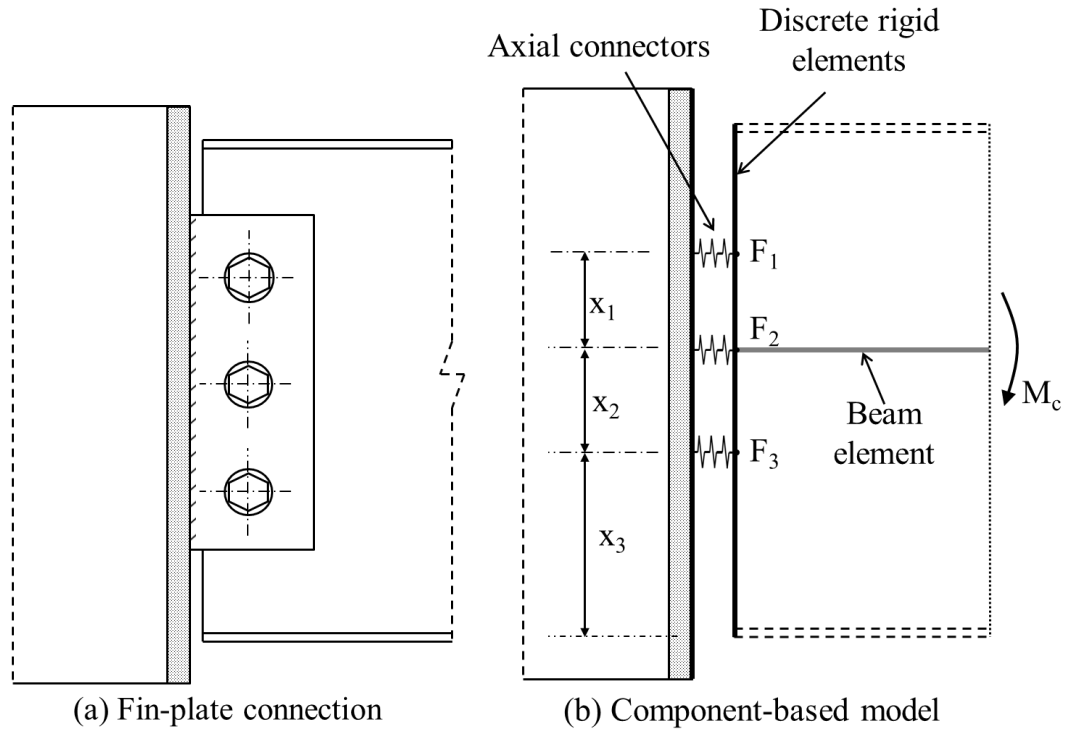
Figure 5-5: Fin-plate connection and component-based model (without shear spring)

Before a dynamic analysis was undertaken the static behaviour of the component model was assessed using a rotation controlled analysis where an incremental rotation was applied and the resulting forces in each bolt row calculated from static equilibrium.
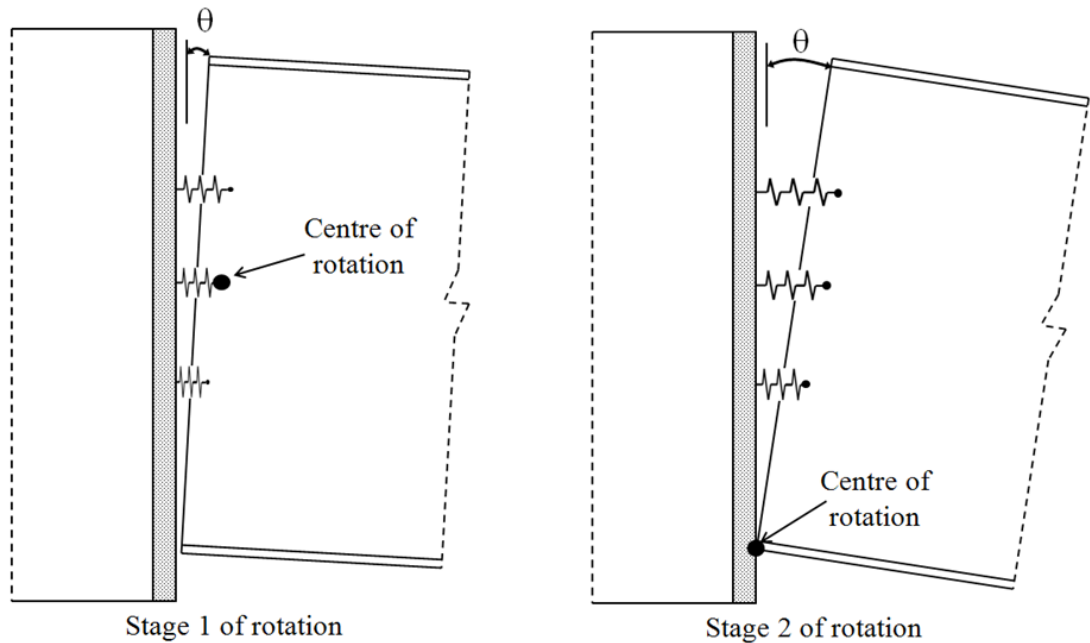
Figure 5-6: Stages of rotation for fin-plate connection

Calculation of the static behaviour subject to pure moment requires the point of rotation to be defined. Initially rotation is assumed to occur about the central bolt hole (Figure 5-6a) and the connection moment is calculated using:

$$F_1 x_1 = M_c + F_3 x_2 \tag{5.28}$$

Where:
$$F_1 = F_3 \tag{5.29}$$

$$F_1 = \frac{M_c}{x_1 + x_2} \tag{5.30}$$

Where F_n and $\varDelta_n$ are the forces and extensions in bolt row n respectively. The displacement of each bolt row is calculated according to the stiffnesses of the combined bolt row and the rotation found by:

$$\theta = tan^{-1} \left[\frac{\Delta_1 + \Delta_3}{x_1 + x_2} \right] \tag{5.31}$$

until
$$\theta = \theta_{contact} = tan^{-1} \left[\frac{0.01}{x_2 + x_3} \right] \tag{5.32}$$

After this rotation the beam contacts the column and rotation is assumed to occur about the beam lower flange (Figure 5-6b. Taking moments about the contact point gives:

$$M_c = F_1(x_1 + x_2 + x_3) + F_2(x_2 + x_3) + F_3(x_3) \tag{5.33}$$

The spring stiffnesses for a variety of extension rates are calculated from the previous equations and presented in Figure 5-7.
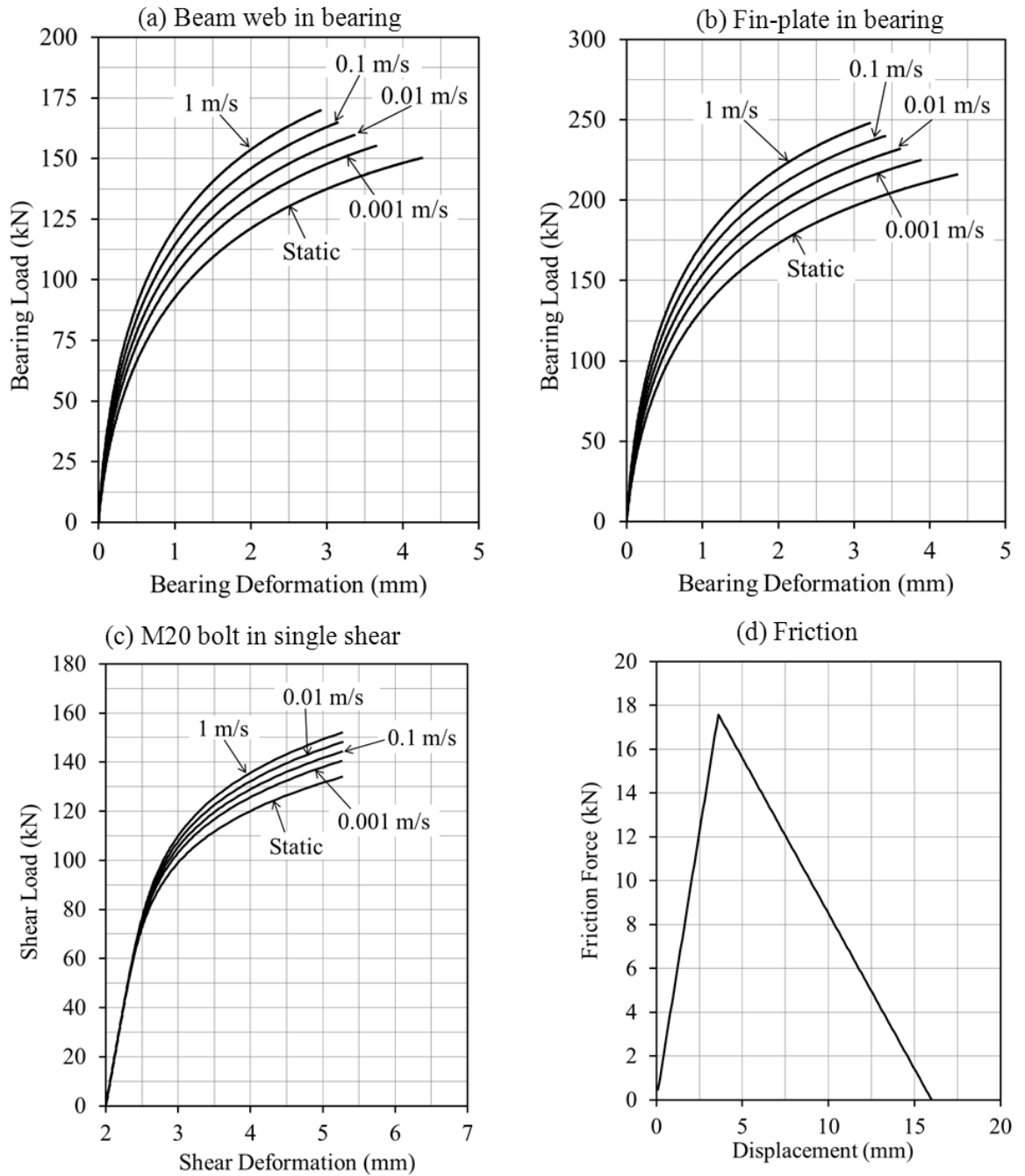
Figure 5-7: Spring stiffnesses for tested fin-plate connection at dynamic deformation rates

The predicted static behaviour is shown in Figure 5-8a, which shows a reasonable comparison with the experimental data. The initial stiffness and yield moment is predicted well, however the model appears to predict a stiffer response in the strain hardening or plastic phase. This may be attributable to over estimating the material strength at this loading rate or the fact that the connection model does not account for web buckling or crushing of the lower flange which would allow further rotation at the respective moment. The predicted method assumes a sudden increase in stiffness due to the change in point of rotation which is not seen in the experimental data. The second increase in stiffness at

approximately 4 degrees rotation is the point at which the middle bolt begins to bear against the fin-plate and beam web and is seen in both the predicted and experimental results. The ultimate rotation is lower than witnessed in the experimental tests.

The prediction method was also used for the connection subject to direct tension and compared against the experimental result using dual loading rams (Figure 5-8b). The final predicted displacement is less than the experimental result because during the experimental test, the load in each ram was not exactly equal meaning a small amount of rotation was experienced which affected the centre of mass displacement reading.
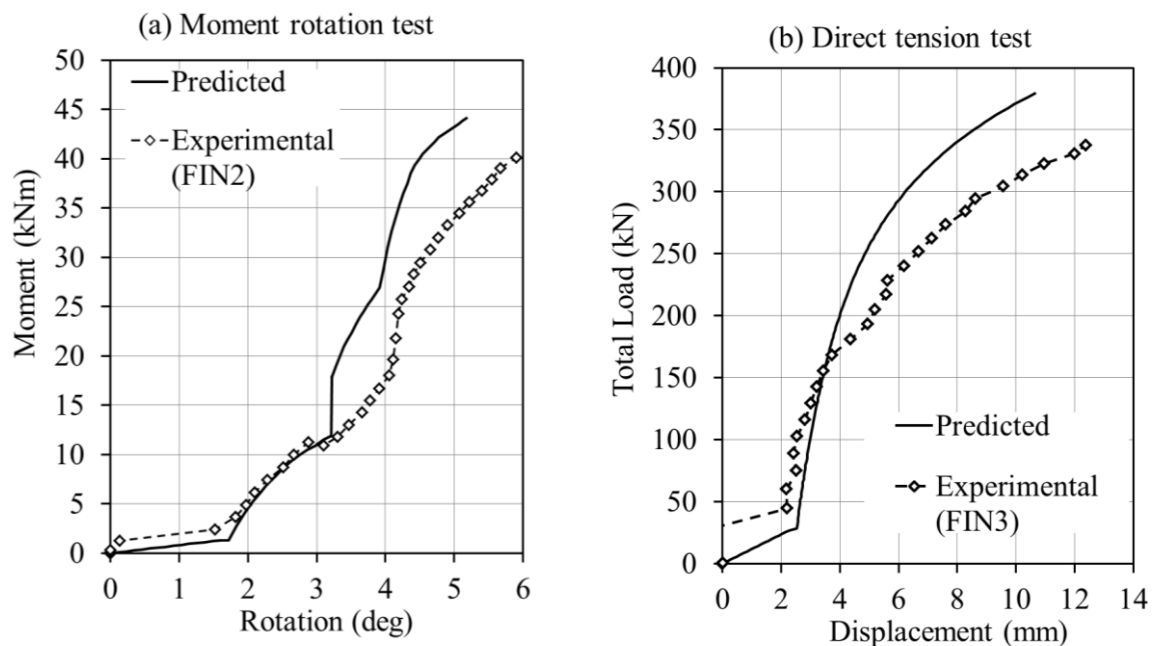
Figure 5-8: Static behaviour comparison for fin-plate connections

For a dynamic analysis, the column was modelled using rigid elements (R2D2) from the explicit element library with point masses distributed along its length totalling the mass of the actual section. A node set was created at the point of loading and also at the two ends in order to calculate the displacement during the analysis. The load recorded during each experimental connection test was used as input for its corresponding component-based model and applied at the same position.

When the column is loaded it is forced to rotate and the rate of rotation causes the bolt row components to extend at different velocities. As a result the individual forces are different for dynamic and static loading leading to an increased moment at lower rotations. The resistance gradually increases with rotation until the lower beam flange contact occurs at which point an increase in stiffness is observed. The ultimate connection load is dictated

by the failure of the upper bolt row which in all cases was predicted to be by bolt shear; in agreement with the experimental data. This initial failure allowed further rotation and led to consecutive failures of the other bolt rows.

The load-time history from each test was used as input for the dynamic component-based model with a complete set of data available in Appendix A. The loading from FIN1 is shown in Figure 5-9 with results for the analysis shown in Figure 5-10 and Figure 5-11.
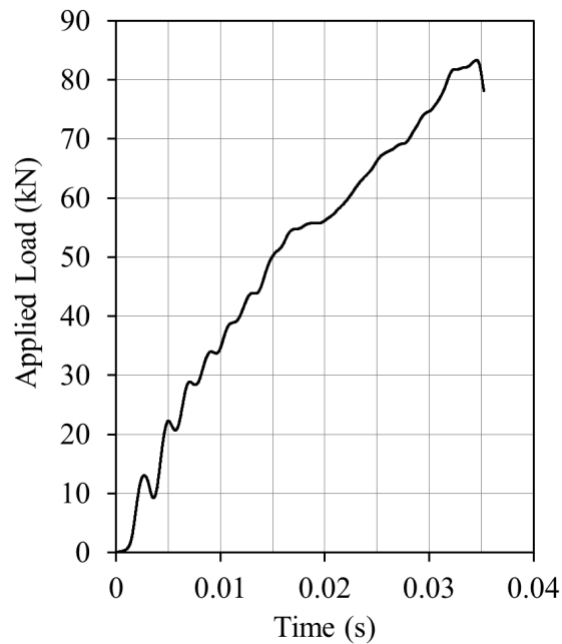
Figure 5-9: Load-time history for FIN1

The physical dynamic behaviour of the column shows good correlation against experimental test results. The rotation-time history is excellent until 16ms when the experimental test falls off slightly. The centre of mass displacement does not show an exact match, possibly due to a slight change of the position of the rotational pivot through the experiment.
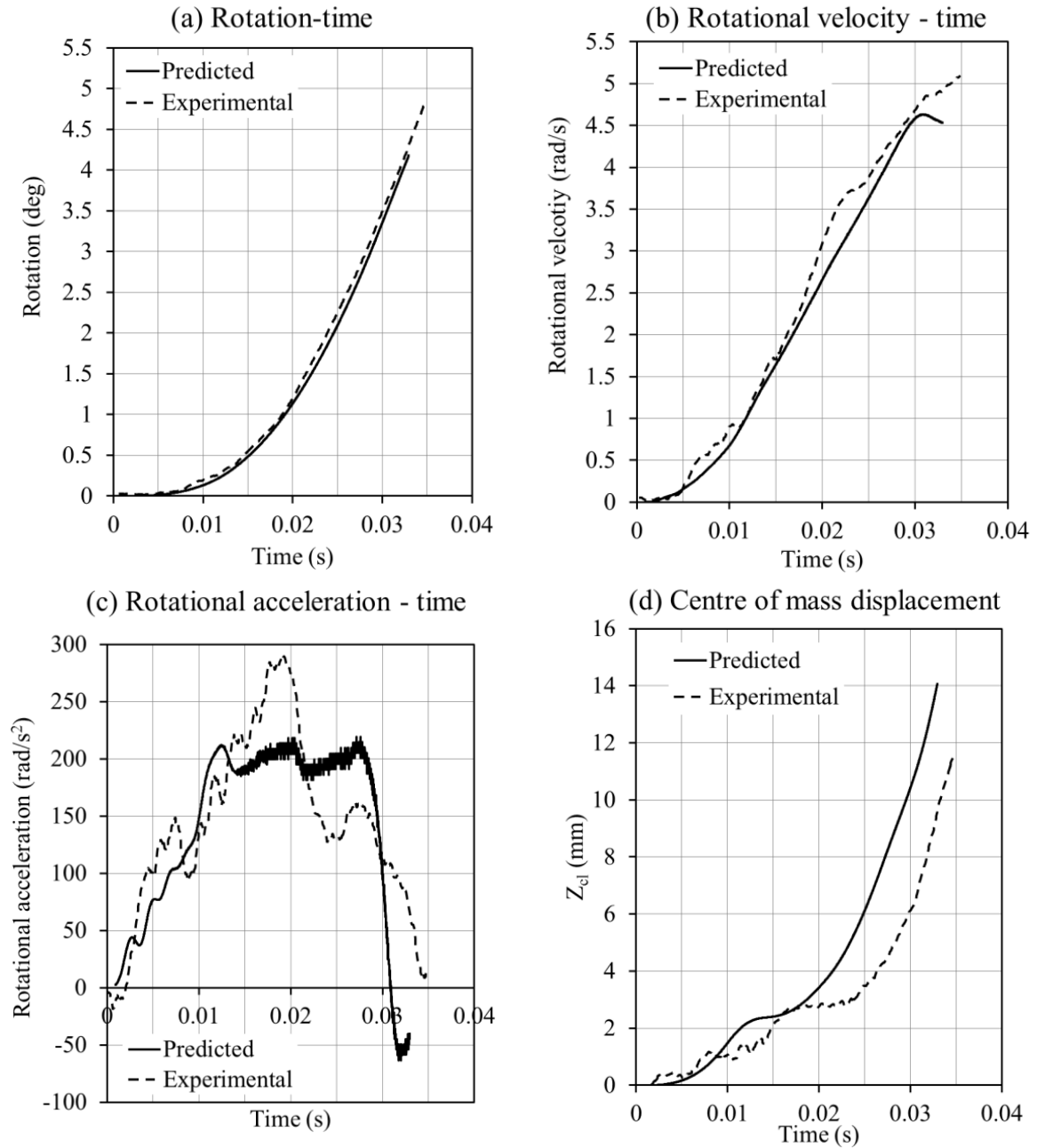
Figure 5-10: Comparison of the physical behaviour of flying column (FIN1)

The failure mode predicted by the component-based model is bolt shear in agreement with experimental data. This failure occurred at a very similar rotation and time.
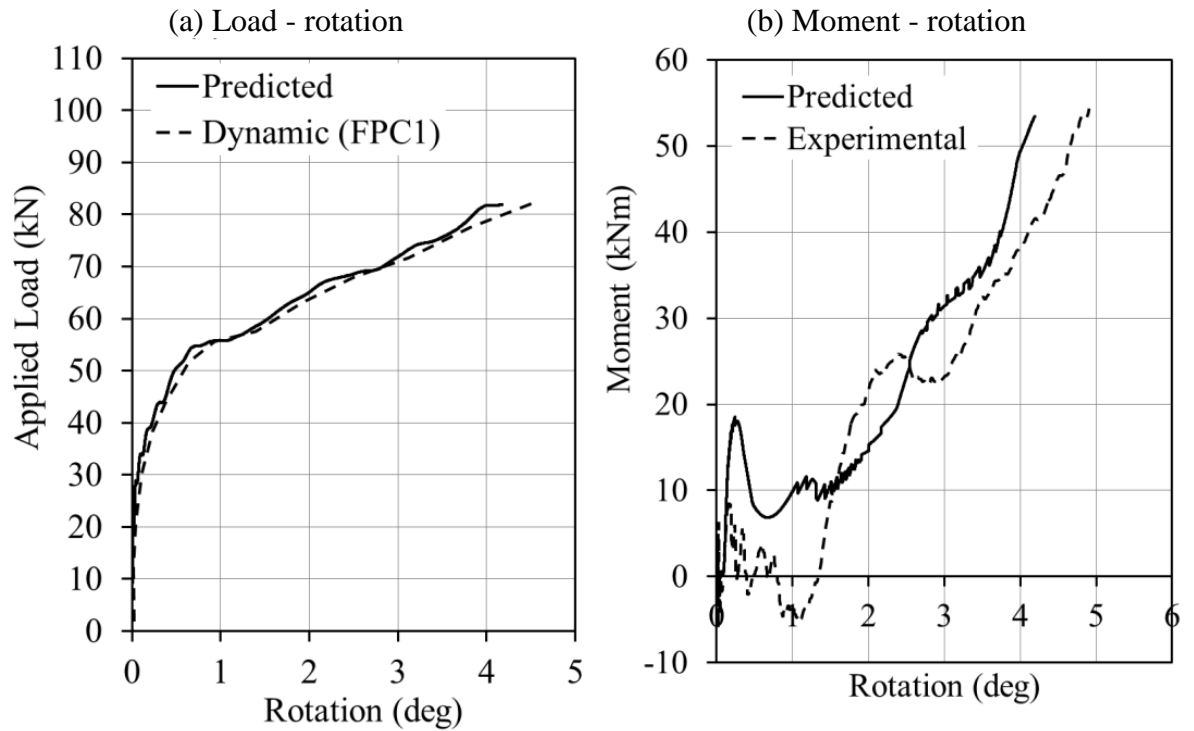
Figure 5-11: Comparison of test results (FIN1)

The applied load-rotation (Figure 5-11a) shows a good trend against the experimental data. From observation of the moment-rotation curves (Figure 5-11b), the initial stiffness and yield moment is predicted with good accuracy, however the model appears to predict a stiffer response in the strain hardening or plastic phase. This may be attributable to over estimation of the material strength at this loading rate or the fact that the connection model does not account for web buckling or crushing of the lower flange which would allow further rotation at the respective moment.

The component-based model was able to predict dynamic connection behaviour, for the rates of loading experienced during the experimental testing, with reasonable accuracy. In comparison to the static behaviour, the model predicted increased yield moment and plastic behaviour combined with reduced failure rotation. The method in general allows the inclusion of second-order geometric effects, caused by changing geometry, such as prying action at large rotations. Alternative configurations, such as additional bolt rows, would require further validation before they could be implemented with a similar level of confidence.

5.3 A dynamic component-based model for flexible end-plate connections

Flexible (or partial-depth) end-plate connections consist of a length of drilled plate welded onto the web of the beam section which is then bolted to the supporting member on site.

They differ from flush or full depth end-plate connections in that the end-plate length is less than the depth of the beam section and therefore does not require welding to the beam flanges. In general they are assumed to have significant flexibility and rotational capacity which is derived from the ductility of the end-plate. They are classed as a "pinned" connection and are widely used in the construction of braced multi-storey steel framed buildings in the UK due to their ease of fabrication and speed of erection with full design guidelines and capacities found in *Joints in Steel Construction: Simple Connections* produced by BCSA/SCI (2002). Although the "pinned" assumption simplifies analysis, in practice the actual joint behaviour exhibits some rotational stiffness and an ultimate rotational capacity. Because of their popularity a significant amount of work has been carried out on this joint type which has resulted in a wealth of knowledge on their behaviour with most research concentrated on the moment-rotation characteristics as demonstrated by Aggarwal and Coates (1986). Work has also been completed to characterise individual component behaviour. The principal components of a bare steel flexible end-plate connection are:

- End-plate in bending
- Bolts in tension
- Column flange in bending
- Column web in compression

These components are incorporated directly into a connection model based upon the geometry of the real connection. Increase in yield and ultimate strength of individual components at higher rates of strain is taken into account and the model is capable of predicting the extension rate of each element in a given bolt row.

5.3.1   End-plate in bending

Previous investigations have attempted to predict the behaviour of the end-plate in bending [Al-Jabri (1999), Spyrou et al. (2004), Heidarpour and Bradford (2008), Block et al. (2007) etc]. In the model presented below it is assumed that the end-plate behaves as an idealized T-stub subject to an applied load, F_{ep}. The number of tension springs, n, used to model the end-plate determines the effective segment width d_y according to the overall depth, D_{ep}. The end-plate is restrained against rotation at the beam web by the weld and at the bolt locations.

Effective
segment
width

$$d_y = \frac{D_{ep}}{n}$$

(5.34)

Figure 5-12 shows the idealization of the end-plate subject to a tension force. The initial elastic behaviour is calculated from beam-deflection theory assuming the end-plate behaves as two fixed-fixed beams each of length L_b.
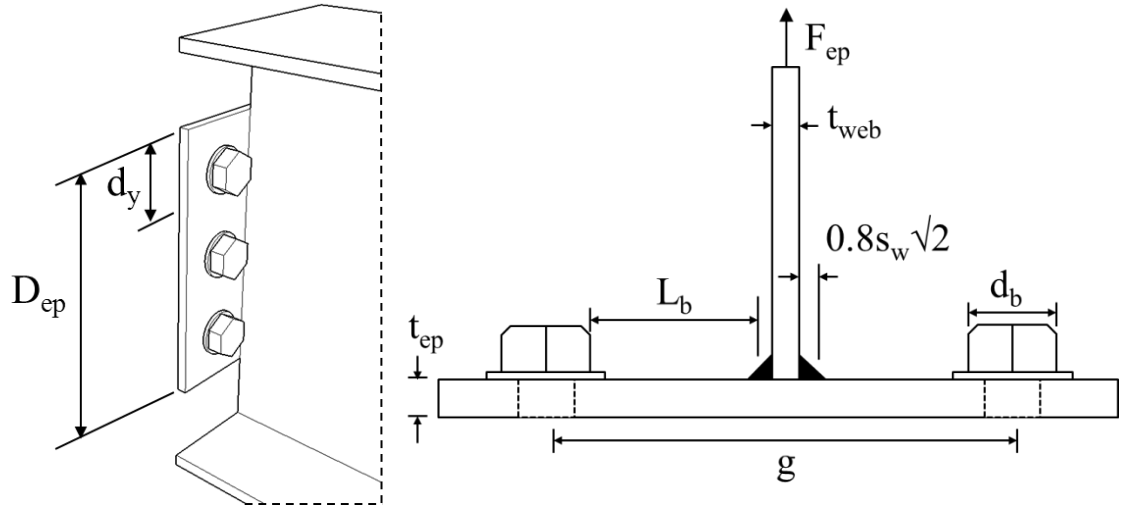
Figure 5-12: End-plate idealization

The length of beam, L_b, is calculated from the geometric properties:

$$L_b = \frac{g - d_b - t_{web}}{2} - 0.8s_w\sqrt{2}$$

(5.35)

Where s_w is the weld thickness at the beam web to end-plate interface as defined by Spyrou et al. (2004).

The free-body diagram of a single side of the end-plate is shown in Figure 5-13.
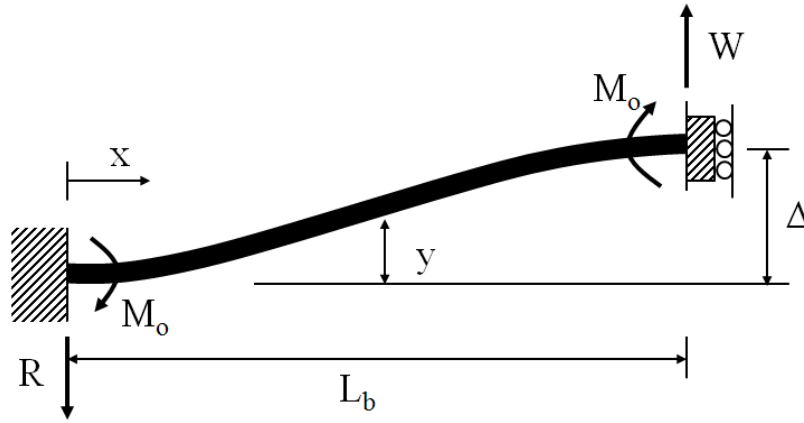
Figure 5-13: Free-body diagram of fixed-fixed beam

For a length x of beam, the bending moment is:

$$M = Rx - M_o \tag{5.36}$$

Using the second order differential of the deflection curve:

$$EI\frac{\delta^2 y}{\delta x^2} = -M = M_o - Rx \tag{5.37}$$

Integrating both sides with respect to x:

$$EI\frac{\delta y}{\delta x} = M_o x - \frac{Rx^2}{2} + C_1 \tag{5.38}$$

$$EIy = \frac{M_o x^2}{2} - \frac{Rx^3}{6} + C_1 x + C_2 \tag{5.39}$$

From the boundary conditions at the left hand support where the curvature and deflection is zero both constants of integration, C_1 and C_2, are found to be zero.

$$M_o = \frac{WL_b}{2}$$

(5.40)

$$R = W$$

At the right hand support, the maximum deflection (Δ) is found by substituting L_b for x:

$$\Delta = \frac{1}{EI}\left(\frac{WL_b{}^3}{4} - \frac{WL_b{}^3}{6}\right) = \frac{WL_b{}^3}{12EI_{ep}}$$

(5.41)

This gives an initial elastic stiffness for one half of the end-plate of:

Elastic Stiffness for one half of end-plate

$$K_e = \frac{W}{\Delta} = \frac{12EI_{ep}}{L_b{}^3}$$

(5.42)

where

$$I_{ep} = \frac{d_y t_{ep}{}^3}{12}$$

(5.43)

For both sides of the end-plate

$$K_{ep} = 2K_e = \frac{2Ed_y t_{ep}{}^3}{L_b{}^3}$$

(5.44)

The stiffness is assumed to remain elastic until the formation of plastic hinges at $x = 0$ and L_b. The yield moment ($M_{ep,Rd}$) of the end-plate at a given strain rate is calculated from the plastic section modulus.

$$M_{ep,Rd} = Z\Phi f_{yep}$$

(5.45)

Where f_{yep} is the end plate yield strength at a given strain rate and the plastic section modulus is given by:

Plastic section modulus

$$Z = \frac{bd^2}{4} = \frac{d_y t_{ep}{}^2}{4}$$

(5.46)

Calculating the yield moment in terms of the applied load:

$$M_{ep,Rd} = \frac{W_{ep,Rd}L_b}{2}$$

(5.47)

The overall load which causes yielding of the end-plate ($W_{ep,Rd}$) is expressed as:

$$\frac{W_{ep,Rd}L_b}{2} = 2\left[\frac{d_y t_{ep}{}^2}{4}\right]\Phi_{ep}f_{yep}$$

(5.48)

$$W_{ep,Rd} = \frac{d_y t_{ep}{}^2 \Phi_{ep}f_{yep}}{L_b}$$

In terms of the overall T-Stub force F_{ep}:

$$W = \frac{F_{ep}}{2}$$

(5.49)

Therefore T-Stub yield force

$$F_{epy} = \frac{2d_y t_{ep}{}^2 \Phi_{ep}f_{yep}}{L_b}$$

(5.50)

The plastic response of the end-plate is calculated based upon recommendations by Al-Jabri et al. (2005) who proposed a tri-linear force-displacement relationship. In this relationship the initial elastic phase is followed by a strain-hardening phase before becoming fully plastic. The strain-hardening and plastic stiffnesses are calculated as a ratio of the elastic stiffness.
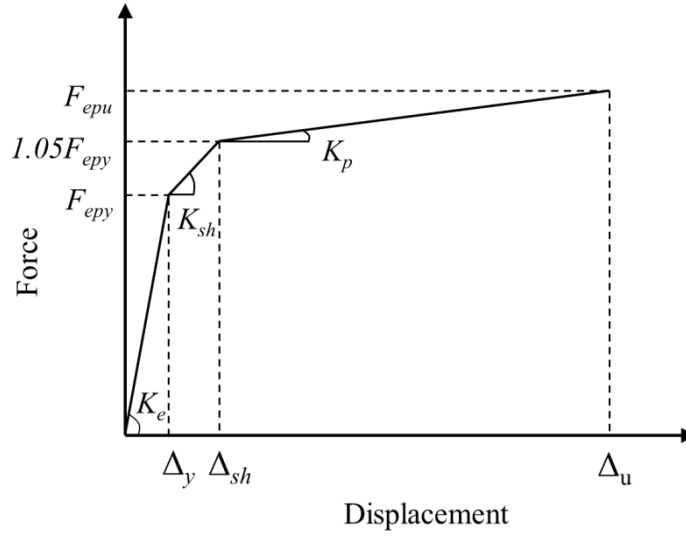
Figure 5-14: Force-displacement behaviour of end-plate

$$K_{sh} = \mu_{sh} K_e \tag{5.51}$$

$$K_p = \mu_p K_e \tag{5.52}$$

In the current model values for μ_{sh} and μ_p are 0.08 and 0.03 respectively. The ultimate capacity of the end-plate is found in a similar way to the yield strength:

$$F_{epu} = \frac{2 d_y t_{ep}{}^2 \Omega_{ep} f_{uep}}{L_b} \tag{5.53}$$

The strain-rate effect is calculated by assuming an end-plate deformation rate (V_{ep}) at the beam web during the elastic region. The strain at the surface of the plate is calculated and then converted to an approximate strain-rate by dividing by the time it would take to reach the yield deformation (T_y).

Yield end-plate strain

$$\varepsilon_{y,ep} = \frac{f_{y,ep}}{E_{ep}} \tag{5.54}$$

The yield displacement Δ_y is calculated from Equations 5.41, 5.49 and 5.50

119

Yield displacement

$$\Delta_y = \frac{W_{ep,Rd}{L_b}^3}{12EI_{ep}} = \frac{2f_{y,ep}{L_b}^2}{Et_{ep}}$$

(5.55)

The time to yield (T_y) is calculated:

Yield time

$$T_y = \frac{\Delta_y}{V_{ep}}$$

(5.56)

The strain rate is then found by dividing the peak strain by the time taken to reach this strain using Equations 5.54 and 5.56.

Strain-rate

$$\dot{\varepsilon} = \frac{\varepsilon_{y,ep}}{T_y} = \frac{f_{y,ep}V_{ep}}{E_{ep}\Delta_y} = \frac{2V_{ep}t_{ep}}{{L_b}^2}$$

(5.57)

Substituting for the strain rate and combining with Equations 5.1 and 5.2 allows a prediction of the material dynamic increase factor as a function of the end-plate deformation rate and geometry:

$$\Phi_{ep} = \left[\frac{2V_{ep}t_{ep}}{{L_b}^2}\right]^{0.074-0.040\frac{f_{y,ep}}{414}}$$

(5.58)

$$\Omega_{ep} = \left[\frac{2V_{ep}t_{ep}}{{L_b}^2}\right]^{0.019-0.009\frac{f_{y,ep}}{414}}$$

(5.59)

This allows the dynamic increase factor for both the yield and ultimate strength to be calculated from Equations 4.2 – 4.4 and tabulated for different deformation rates as shown in Figure 5-15.
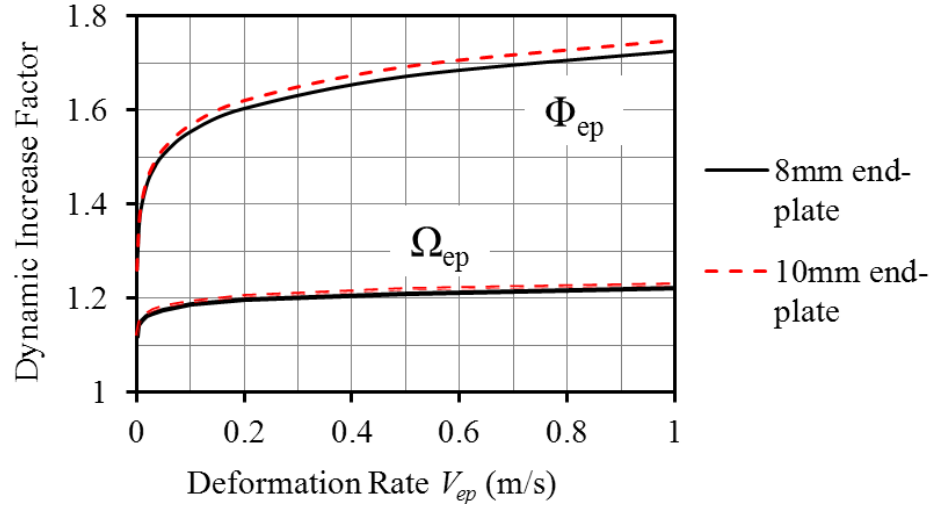
Figure 5-15: Effect of deformation rate on DIF for end-plate component

5.3.2 Bolt in tension

The behaviour of threaded assemblies has been the subject of previous work. Initial studies looked to examine the load distribution within the threaded regions. Goodier (1940) measured the extension of bolt and nut combinations and from these calculated the approximate load distribution. Whilst there was considerable load concentration at low loads, a more uniform distribution was achieved at higher loads. Sopwith (1947) developed a theoretical model to predict the load distribution by considering bending and deformation of the individual threads including the yield phase of the connector. Results showed good agreement with experimental data. Following this work, Alexander (1977) produced a method to predict the ultimate load based upon the thread engagement length which also allowed a prediction of the failure mechanism. These have led to standards for fasteners subject to direct tension such as ASTM (2011) F606-11 and BS EN 1993-1-8 (2005).

The behaviour of a threaded assembly at higher rates of loading and strain has received less attention. Mouritz (1994) conducted one of the first dynamic investigations for strain rates ranging from 10^{-5} to 10^2 s^{-1}. Three methods were used to apply the loads; tensile testing, drop hammer impact and underwater explosive shock testing. Multiple conclusions were drawn from these tests. Firstly, the threads were shown to be significantly weaker than the shank suggesting the need to consider the failure load of the threads in design. Microscopic investigation of damage to the threads indicated that the failure mechanism is not influenced by strain-rate. The overall elongation of the fasteners at failure was approximately 30% for the 3 testing techniques indicating that the plastic deformation behaviour of the shank is not influenced by strain rates up to 10^2 s^{-1}.

More recent tensile tests have been conducted by Fransplass et al. (2011) on threaded assemblies at strain rates up to $1.9*10^3 \text{ s}^{-1}$. Conclusions indicated that thread engagement, grip length and high strain rate had varying effects on the strength and ductility of the assembly. A modification to the Alexander (1977) method was proposed to predict the failure load and mechanism at elevated strain rates.

The tensile bolt behaviour is predicted using a similar model to Al-Jabri et al. (2005) assuming it is subject to a direct tensile force evenly distributed over the bolt tensile area A_s. The effective bolt length, L_{bt}, is predicted using:

$$L_{bt} = \frac{t_{bh} + t_{bn}}{2} + 2t_w + t_{ep} + t_{cf} \qquad (5.60)$$
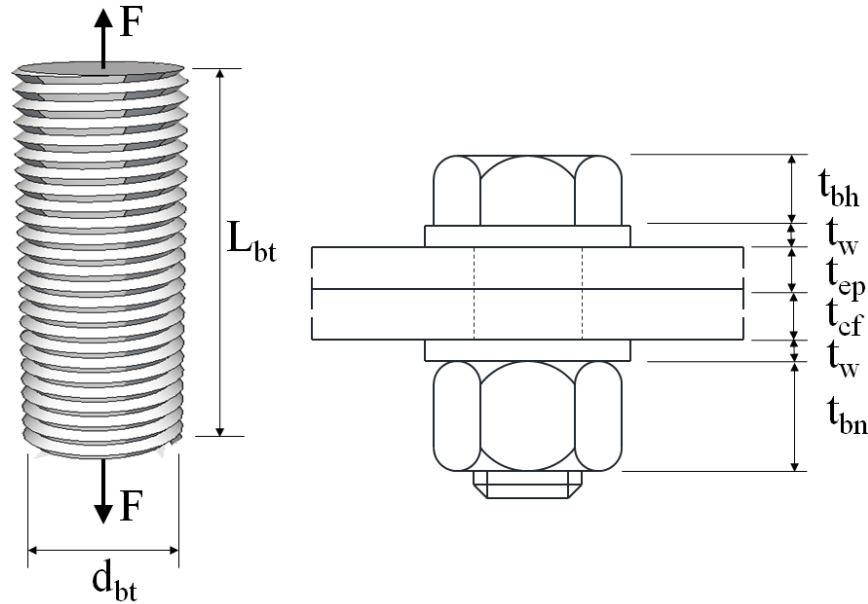
Figure 5-16: Bolt dimensions

The initial elastic behaviour is calculated using Hooke's law:

$$\sigma = E_b \varepsilon \qquad (5.61)$$

The stress in the bolt is equal to the applied force divided by the bolt tensile area and the strain is equal to the deformation length divided by the original length.

$$\frac{F}{A_s} = E_b \frac{\Delta}{L_{bt}}$$

(5.62)

Giving an initial elastic stiffness, K_{bt}, of:

$$K_{bt} = \frac{E_b A_s}{L_{bt}}$$

(5.63)

The tensile yield load, F_{bty}, is given by:

$$F_{bty} = f_{yb} A_s n_b$$

(5.64)

Where n_b is the number of bolts considered in each tensile zone.

Dynamic testing of bolts in tension was conducted by Munoz-Garcia et al. (2005). Their observations indicated that very little ductility is observed following the onset of yielding regardless of the strength of the bolt or nut. Therefore once the yield load is achieved it is assumed the bolt has failed. Their findings also noted that there was no apparent dynamic effect on the bolt behaviour and therefore no dynamic enhancement was included in the above model.

5.3.3 Column flange in bending

For connections where the end-plate is bolted to the flanges of a column the deformation of the flanges is required. Al-Jabri et al. (2005) adopted an earlier method by Jaramillo (1950).
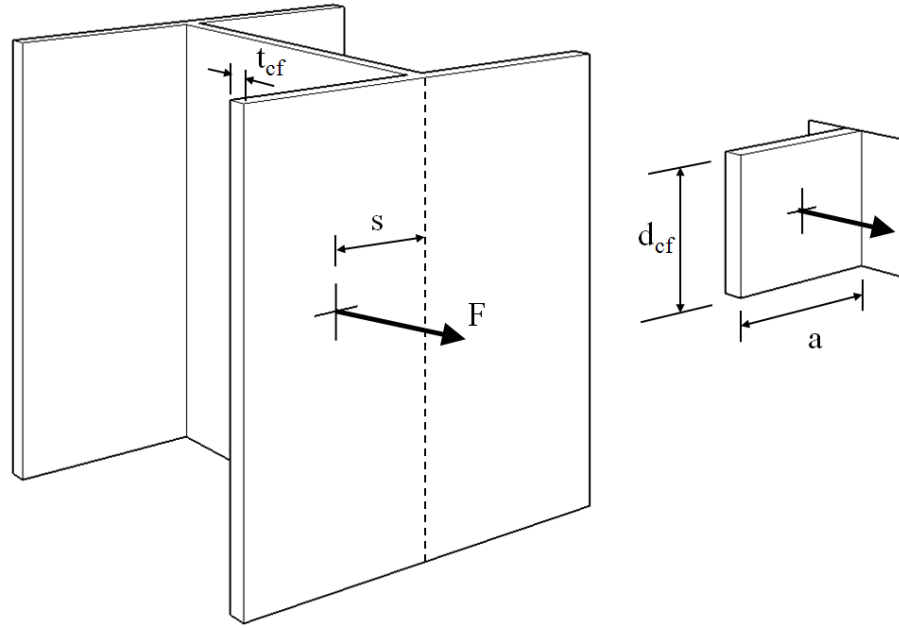
Figure 5-17: Column flange idealization

The flexural rigidity of the flange, I_{cf}, is calculated using:

$$I_{cf} = \frac{E t_{cf}^2}{12(1 - v^2)}$$

(5.65)

Where v is the Poisson's ratio for steel. The initial stiffness of the column flange, K_{cf}, is then found from:

$$K_{cf} = \frac{\pi I_{cf}}{\beta a^2}$$

(5.66)

Where β is a dimensionless function of the distance from the centre of the flange to the bolt location, found using Eqn 5.53 or Figure 5-18.

$$\beta = -0.0542 + 0.416 \frac{s}{a} - 0.7584 \left(\frac{s}{a}\right)^2 + 0.9216 \left(\frac{s}{a}\right)^3$$

(5.67)

124
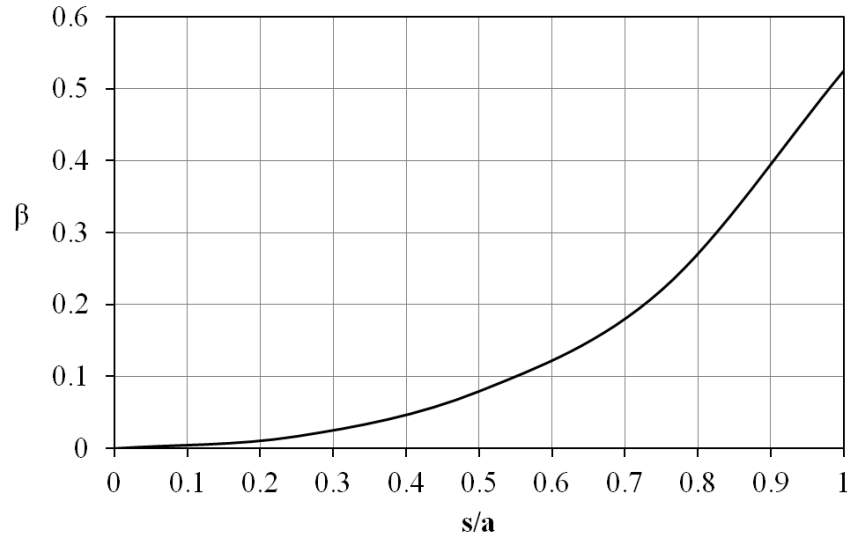
Figure 5-18: Calculating β from Eqn 5.53

The yield force of the column flange is calculated using the following formula from Al-Jabri et al. (2005), after which the column flange is assumed to have lost integrity and failed.

Column flange
yield force

$$F_{cfy} = \frac{f_y t_{cf}^2 d_{cf}}{m}$$

(5.68)

Where m is the distance from the centre of the bolt to 20% into the column root radius. The tested column section was stiffened by welding 20mm thick plates between its flanges. Therefore bending of the column flanges was not considered in the connection model for the experimental tests.

5.3.4 Column web in compression

The column section used in the connection tests was a 254x254x167UC which has 32mm thick flanges. In addition 20mm thick stiffeners were welded between the flange and web to make it as rigid as possible. Therefore the column web in compression is not considered in the current component model.

5.3.5 Verification of proposed model

At each bolt row the end-plate in bending and bolt in tension were incorporated into a complete connection model as shown in Figure 5-19b.

(a) Flexible endplate connection   (b) Component-based connection model
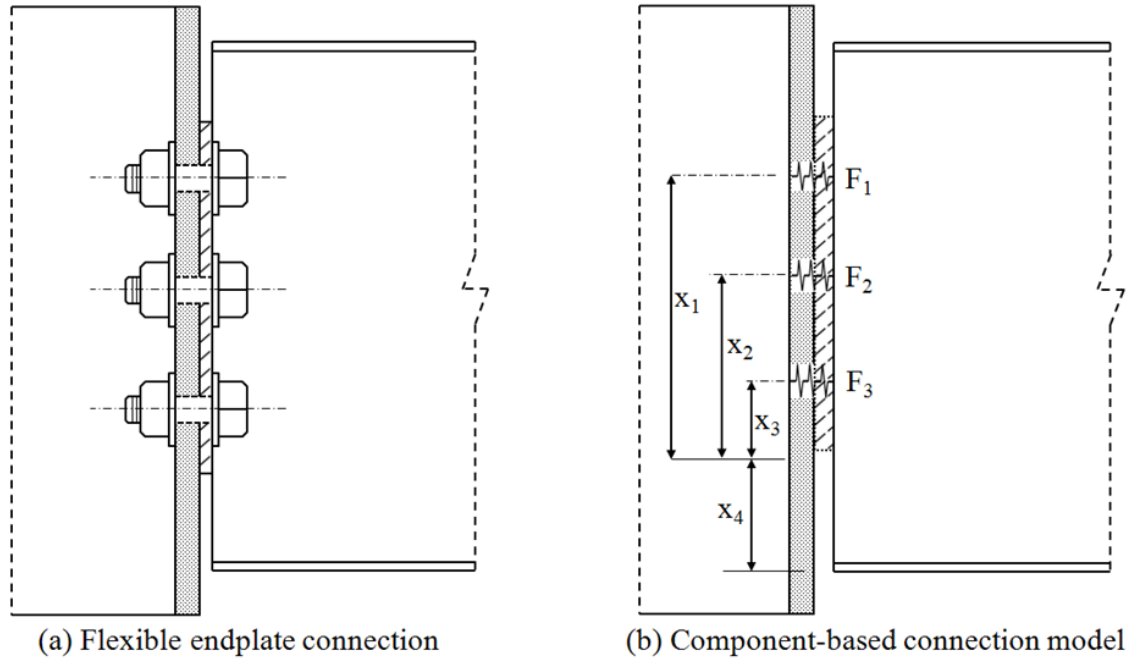
Figure 5-19: End-plate connection and component-based model (without shear spring)

Prior to the analysis of the dynamic enhancement of the connections, a rotation controlled analysis was performed to predict the static behaviour of the component-based connection model.

Stage 1 of rotation   Stage 2 of rotation
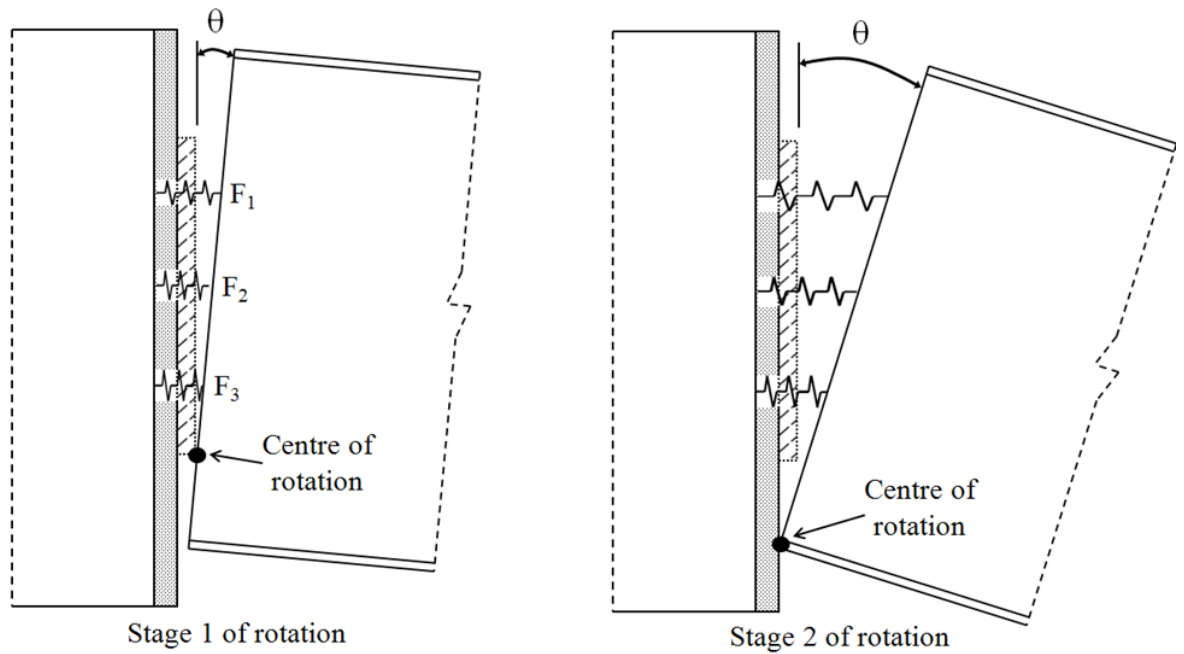
Figure 5-20: Stages of rotation for flexible end-plate connection

In stage 1 of the rotation (Figure 5-20a) moments were taken about the theoretical edge of the end-plate giving:

$$M = F_1 x_1 + F_2 x_2 + F_3 x_3 \qquad (5.69)$$

Stage 1 ends when the beam lower flange contacts the column. The experimental results indicated that the rotation at which this occurs is less than expected, likely due to crushing of the end-plate and beam web. In order to take this into account a reduction factor (γ) is applied to the endplate thickness in order to reduce the rotation at which contact occurs:

$$\theta_{contact} = tan^{-1}\left[\frac{\gamma t_{ep}}{x_4}\right] \qquad (5.70)$$

where $\gamma = 0.65$

The experimental tests also indicated that the moment does not instantaneously increase once contact occurs. Instead the pivot position gradually transfers from the corner of the end-plate to the beam lower flange. This behaviour is predicted by assuming a linear movement of the pivot position to the lower beam flange over a rotation of one degree. Once this occurs moments are simply taken about the beam lower flange.

$$M = F_1(x_1 + x_4) + F_2(x_2 + x_4) + F_3(x_3 + x_4) \qquad (5.71)$$

The individual component behaviours are calculated for the geometrical properties of the experimental tests in Chapter 3 and are shown in Figure 5-21.

(a) 8mm end-plate in bending

(b) 10mm end-plate in bending

(c) Bolts in axial tension

(d) Column flange in bending
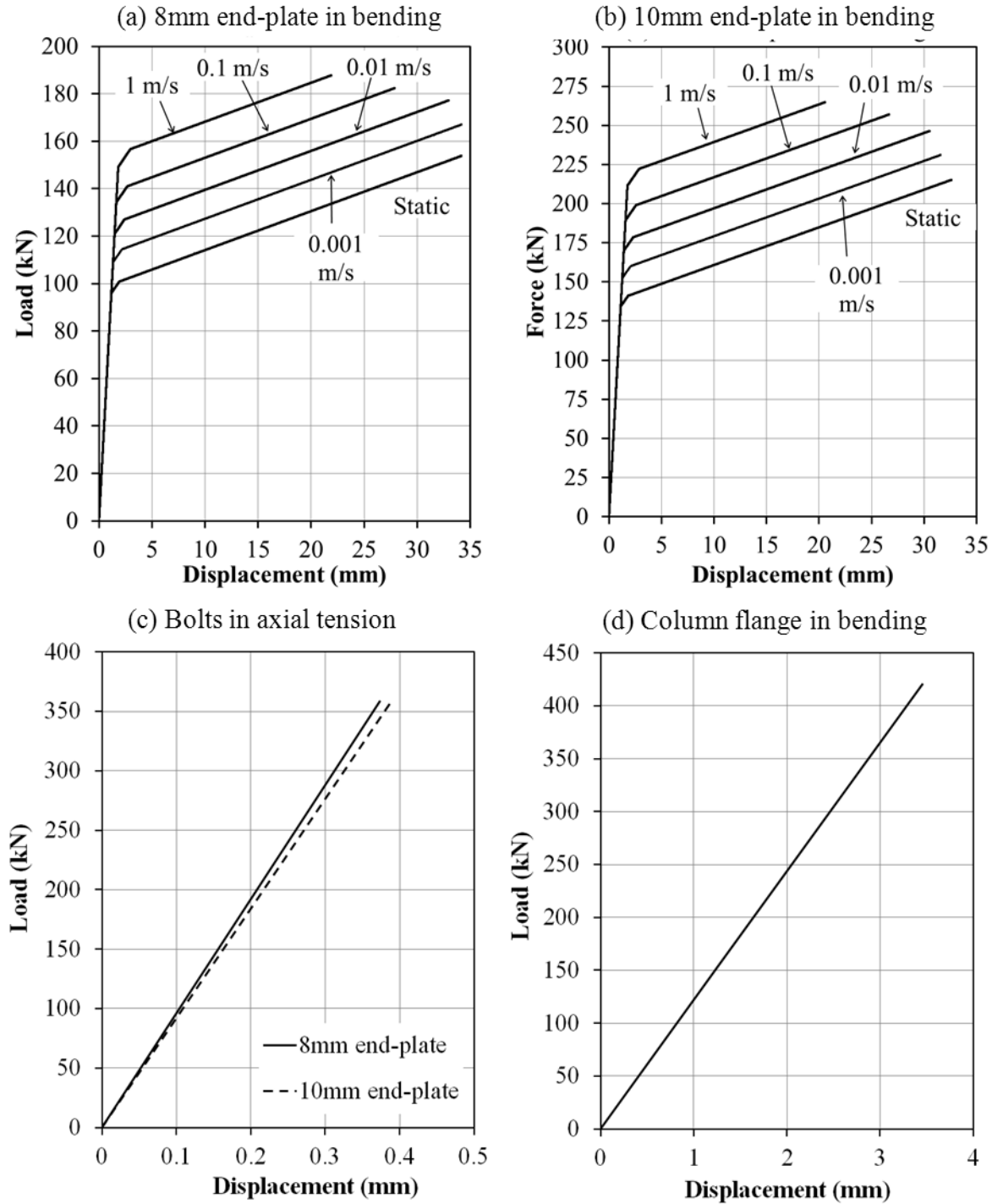
Figure 5-21: End-plate connection component behaviours

The static rotation capacity is calculated based upon the weakest component, which in all cases is the end-plate. For the 8mm end-plate the failure load is 154kN corresponding to a total displacement at the upper bolt row of 24.8mm and a connection rotation of 5.93 degrees. The 10mm end-plate failure load is 215.1kN corresponding to a total displacement of 34.6 mm and a failure rotation of 8.29 degrees.

Comparisons of the static behaviour for both an 8mm and 10mm thick end-plate are shown in Figure 5-22. The initial stiffness and initial yield load is predicted well by the proposed model for both 8mm and 10mm end-plate connections. The plastic stiffness in stage 1 of the rotation appears to be show a reasonable correlation with the experimental data. Contact between the beam and column occurs earlier in the rotation than the prediction model. After contact has occurred the pivot position moves linearly to the lower beam flange thus increasing the lever arm and the moment. This has allowed the full range of behaviour to be captured for both thicknesses of end-plate. For the 8mm end-plate the ultimate rotation capacity is slightly underestimated compared with the connection tests whilst for the 10mm thick end-plate FEP8 exhibits a higher ultimate moment capacity.
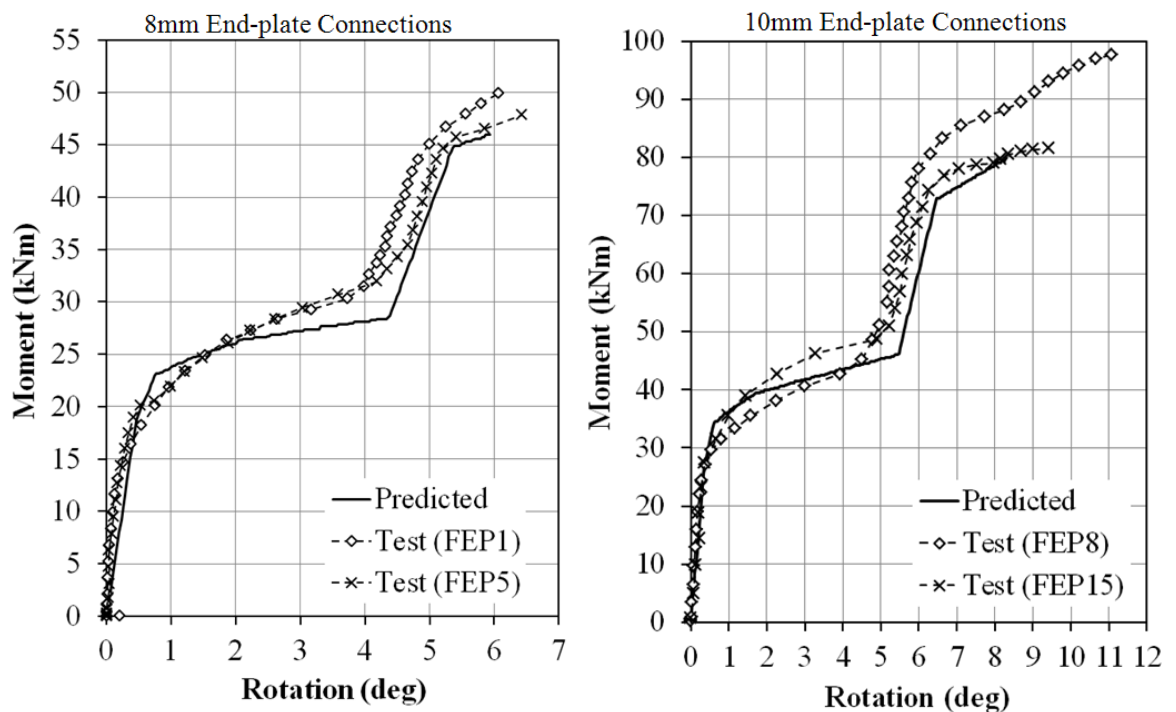
Figure 5-22: Comparison of predicted static response with test results

A comparison of the physical behaviour for a dynamic test of an 8mm end-plate connection (FEP2) is presented in Figure 5-23. The rotation-time history indicates a high accuracy up to t=0.026s and after this the prediction begins to diverge from the experimental data. The general trends for the physical behaviour are reasonable across the entire loading duration. The predicted failure mode was tearing of the end-plate, in agreement with the data. The experimental failure rotation was 5.9 degrees compared to the prediction of 7.1 degrees which suggests an overestimation of the failure load of the end-plate.
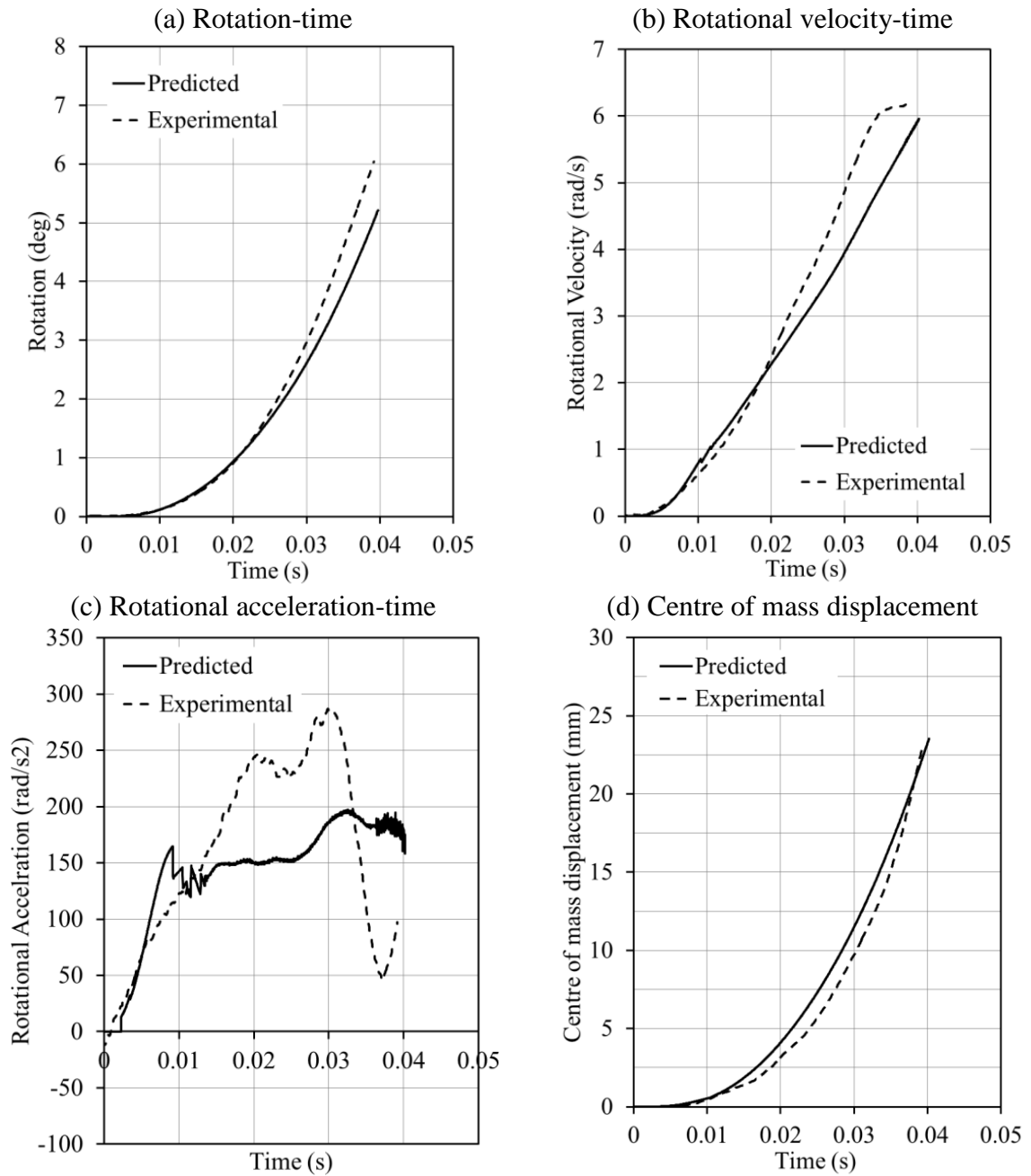
Figure 5-23: Comparison of 8mm end-plate physical behaviour (FEP2)

A similar comparison for a 10mm end-plate connection (FEP11) is shown in Figure 5-24. In general the trends are very similar for the 8mm connection in that there is a good correlation for the first 20ms of the behaviour and after this the prediction model demonstrates a reduced rotational velocity. The experimental test shows a failure rotation of approximately 6.4 degrees at a time of 39ms which compares to a prediction of 7.3 degrees at 47ms. The predicted centre of mass displacement is always lower than the experimental results indicating that the rotation point has moved from the lower beam flange. This may indicate crushing of the beam web or an alternative region of deformation.
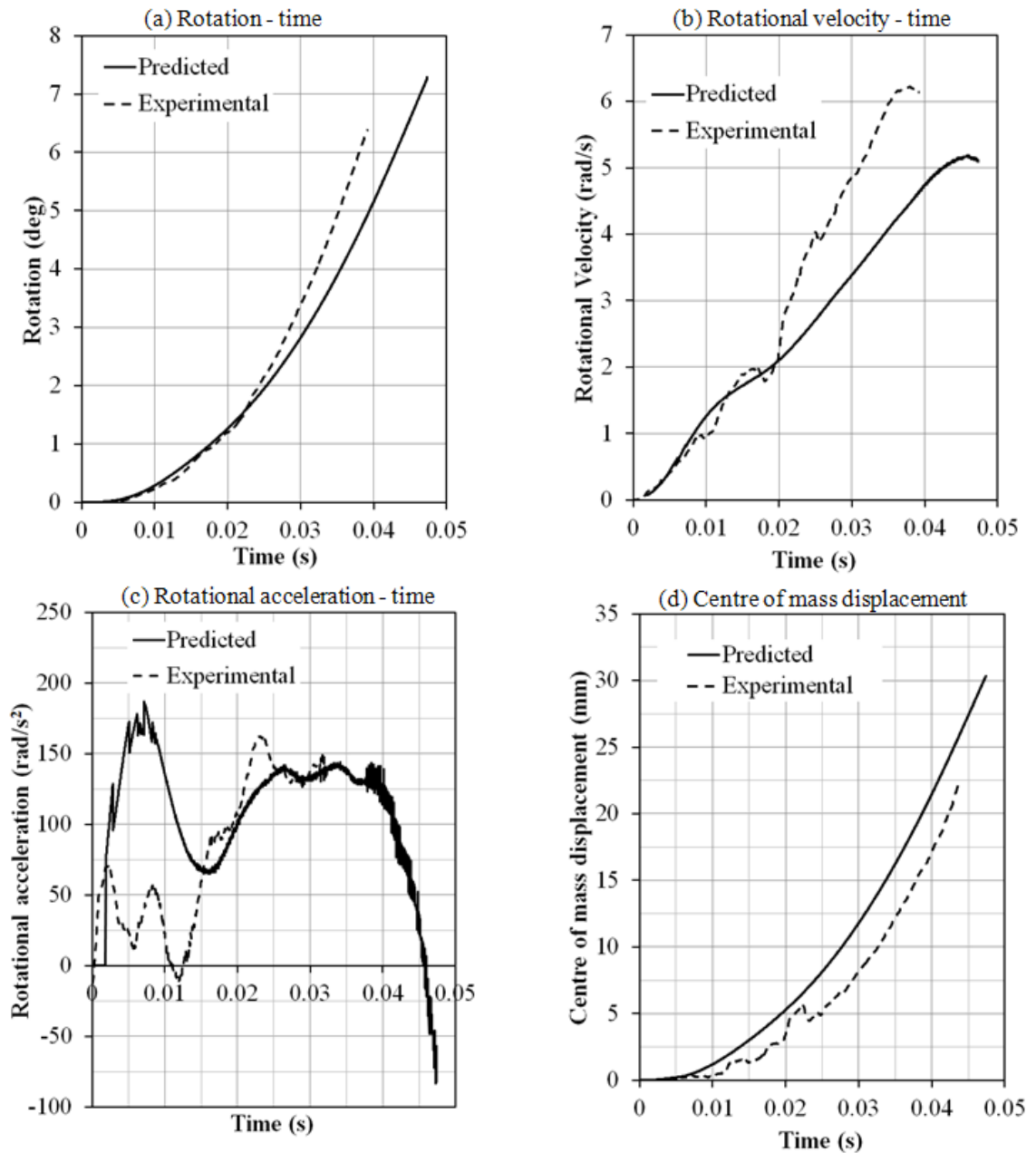
Figure 5-24: Comparison of 10mm end-plate physical behaviour (FEP11)

For the dynamic testing the moment of inertia was removed using the rotational acceleration of the column to give an indication of the actual moment at the connection. In the prediction method the moment is calculated by summing the moment provided by all bolt rows for each time step.

For selected tests the digital image correlation system was used to monitor the strain across the face end-plate. This allowed a comparison against the predicted strain-rate obtained from the component-based connection model as shown in Figure 5-25 for a 10mm end-plate.
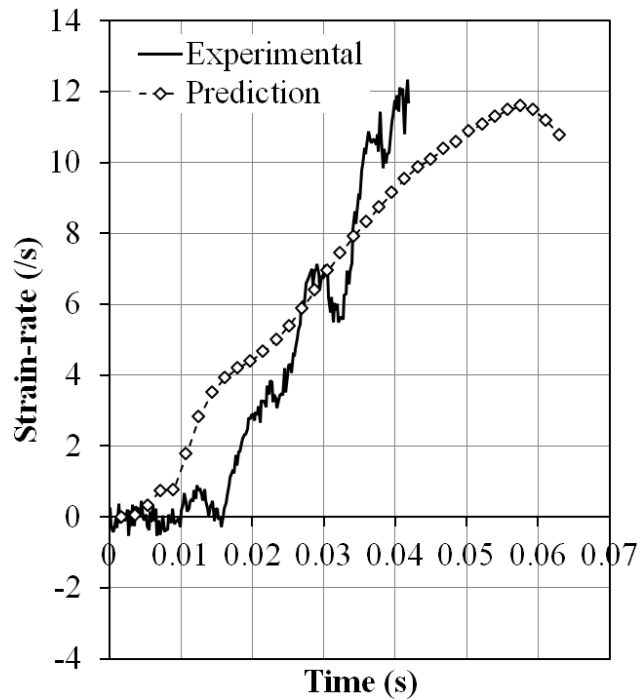
Figure 5-25: Comparison of predicted and recorded strain-rate for FEP17

A comparison of moment-rotation curves under static and dynamic loading is shown in Figure 5-26. This indicates that there is a dynamic enhancement of yield moment and failure capacity for both 8mm and 10mm thick end-plate connections which the component-based method can predict with reasonable accuracy for these loading rates. Experimental results of the 10mm end-plate indicate there is an increase in initial elastic stiffness when loaded dynamically which the proposed method cannot account for as only the plastic behaviour varies with load rate. The dynamic tests FEP2 and FEP11 had peak rotational velocities of 6.3 and 5.1 rad/s respectively which corresponded to peak extension rates in the components of approximately 0.008 and 0.007 m/s.
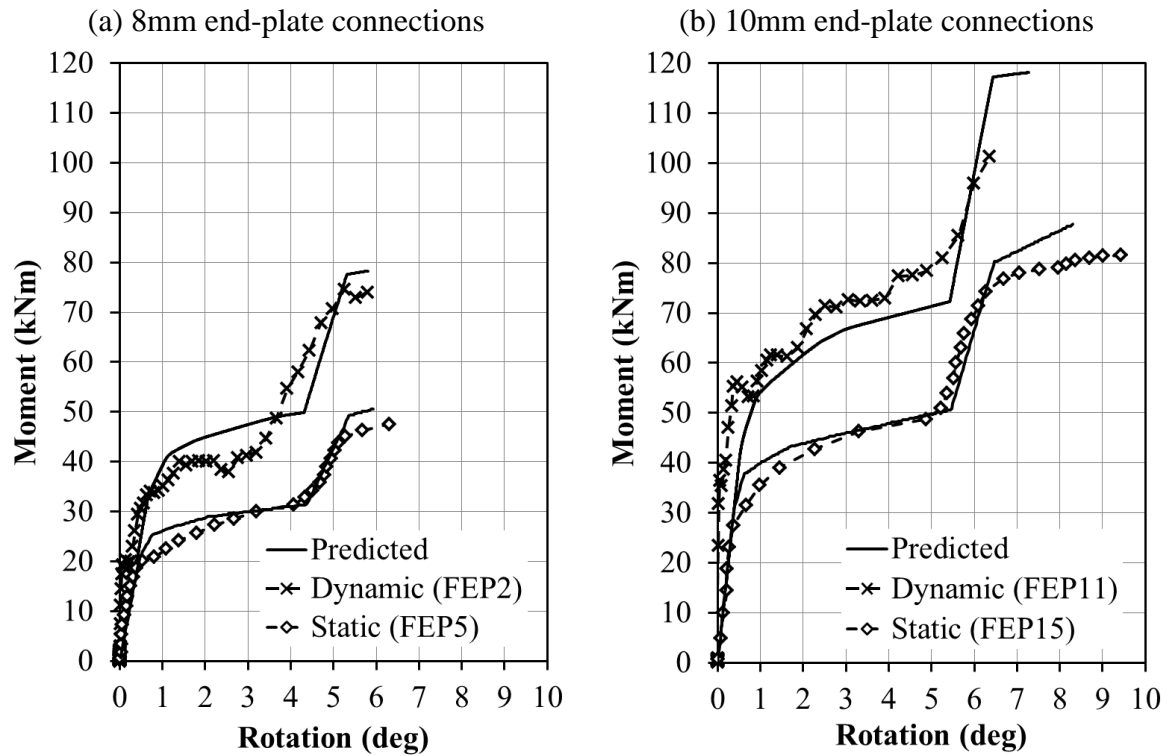
Figure 5-26: Dynamic enhancement of moment-rotation behaviour for connections taken to failure

The test results were plotted against the loading rate. The 8mm end-plate model shows a reasonable prediction of yield moment enhancement for the load rates tested (Figure 5-27a) but in all cases the failure rotation was below the predicted value (Figure 5-27b).
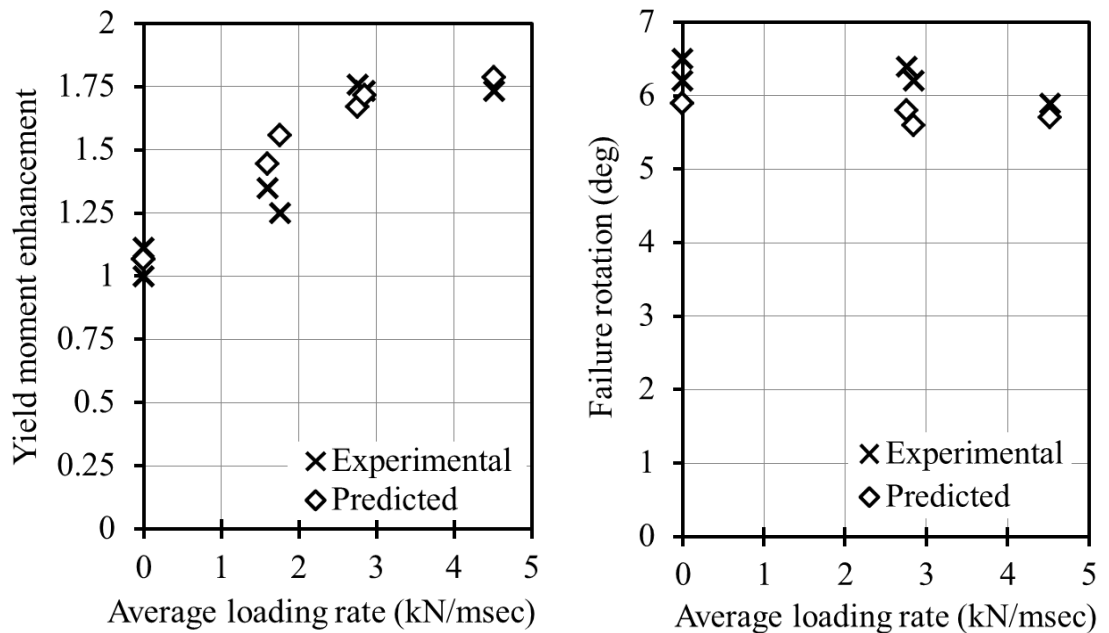
Figure 5-27: Experimental and predicted dynamic load effects for 8mm end-plate connections

The 10mm end-plate model is able to predict the yield moment with reasonable accuracy for all load rates (Figure 5-28a). The component-based model shows a reasonably linear

reduction in failure rotation at elevated loading rates (<mark>Figure 5-28</mark>b) which corresponds well with the experimental data if the static anomaly of 11.2 degrees is disregarded.
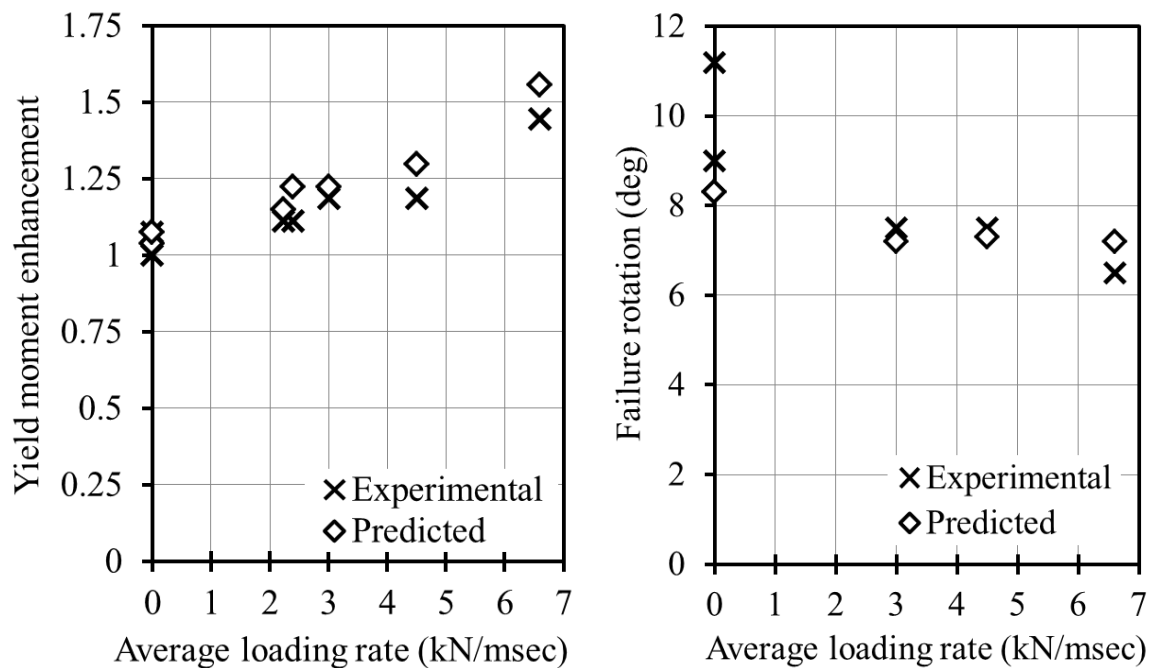
<mark>Figure 5-28: Experimental and predicted dynamic load effects for 10mm end-plate connections</mark>

5.4 Summary

Component based models for fin-plate and end-plate connections at varying loading rates have been developed. These were formulated by adapting common methods developed for Eurocode 3 and fire engineering using simple prediction of strain-rate within the vulnerable components. This allows the large wealth of knowledge available in this field to be exploited fully before conducting expensive testing on specific components.

The recorded loading from each experimental test was used as input for the component-based numerical analysis which allowed a direct comparison of the complete physical behaviour of the system as well as the connection response. Observation of the rotation-time history of the column showed that the method was capable of accurately predicting the connection response.

Good correlation was observed against the experimental data at both dynamic and quasi-static loading rates for both connection types. A closer match against the experimental data was found for the flexible end-plate model compared to the fin-plate model. One reason for this is that the end-plate connection has defined points of rotation throughout the analysis whereas the fin-plate can rotate about any point between the outer bolts until contact

occurs with the column flange. This causes oscillations in the connection model when loaded dynamically which make it difficult to accurately calculate the true inertia without capturing a large amount of noise.

In general the component-based models allowed a good prediction of the connection behaviour throughout the loading cycle and were able to account for dynamic effects woth reasonable accuracy.

6 COMPONENT-BASED CONNECTION MODELS IN BLAST AND PROGRESSIVE COLLAPSE ANALYSIS

6.1 Introduction

In order to investigate the performance of the connections under dynamic conditions, the component-based joint models were incorporated into finite element analysis of subframe arrangements. Burgess (2007) calls this combination of mechanical models and finite element principles *macro-element* models and notes their suitability for frame analysis where high axial beam forces are encountered. In this method the dynamic, non-linear spring behaviour is defined at the start of the analysis and the dynamic solution is calculated in incremental time steps.

6.2 Studies of sub-frame arrangements

To study the effect of joint behaviour on adjacent structural members it is necessary to conduct systematic studies in which various parameters influencing the behaviour of the structural system are analysed. The analysis of sub-frames reduces the computational effort whilst still producing results that are comparable to complete structural frame response.

6.2.1 Blast analysis of "simply supported" beam

This section looks at the use of component-based connection models for predicting the reaction of a structural beam to theoretical blast loading. A parametric study was conducted for a range of t_d/t_n values. The sub-frame considered is an 8.5m long 356x171x45UB beam with a distributed load. The problem is analysed for 5 different conditions:

- Single-degree-of-freedom analysis assuming simple support conditions
- ABAQUS beam with simple support conditions
- ABAQUS beam with component connection model representing fin-plate connections from Chapter 5
- ABAQUS beam with component connection model representing 8mm end-plate connections from Chapter 5
- ABAQUS beam with component connection model representing 10mm end-plate connections from Chapter 5

For each load case a triangular force-time history (Figure 6-1a) is assumed of duration t_d and equivalent peak total load F. This force is assumed to be uniformly distributed across the face of the beam. In all cases the applied impulse (I) was kept constant at 2.5kN-sec. Thus the load duration is varied and the resulting peak load calculated using:

Peak load
$$F = \frac{2I}{t_d}$$
(5.72)

Peak equivalent
distributed load
$$f = \frac{F}{L}$$
(5.73)

The load series is shown in Table 6-1.

t_d (s)	t_d/t_n	Peak Load, F (N)	Peak Equivalent Distributed Load, f (N/m)
0.0065	0.1055	769231	90497
0.007	0.1136	714286	84033
0.008	0.1298	625000	73529
0.009	0.1460	555556	65359
0.01	0.1622	500000	58823
0.012	0.1947	416667	49020
0.015	0.2433	333333	39216
0.02	0.3245	250000	29412
0.025	0.4056	200000	23529
0.03	0.4867	166667	19608
0.035	0.5678	142857	16807
0.04	0.6489	125000	14706
0.05	0.8112	100000	117645
0.06	0.9734	83333	9804

Table 6-1: Loading parameters for single beam

The use of fin-plate and flexible end-plate connections was investigated using component-based methods. The component-based connection models were incorporated into the finite element software ABAQUS using axial connector sections and discrete rigid elements in the same way as demonstrated in Chapter 5. In addition a shear spring was added at the centre-line of the connection to transfer the shear load from the beam to the supports. This

spring is assumed to be rigid at present as defined by Block et al. (2007) but could be developed further in future to include slip and shear failure of the bolts. Beam elements were then used to represent the beam itself and the time history solved using ABAQUS/Explicit.
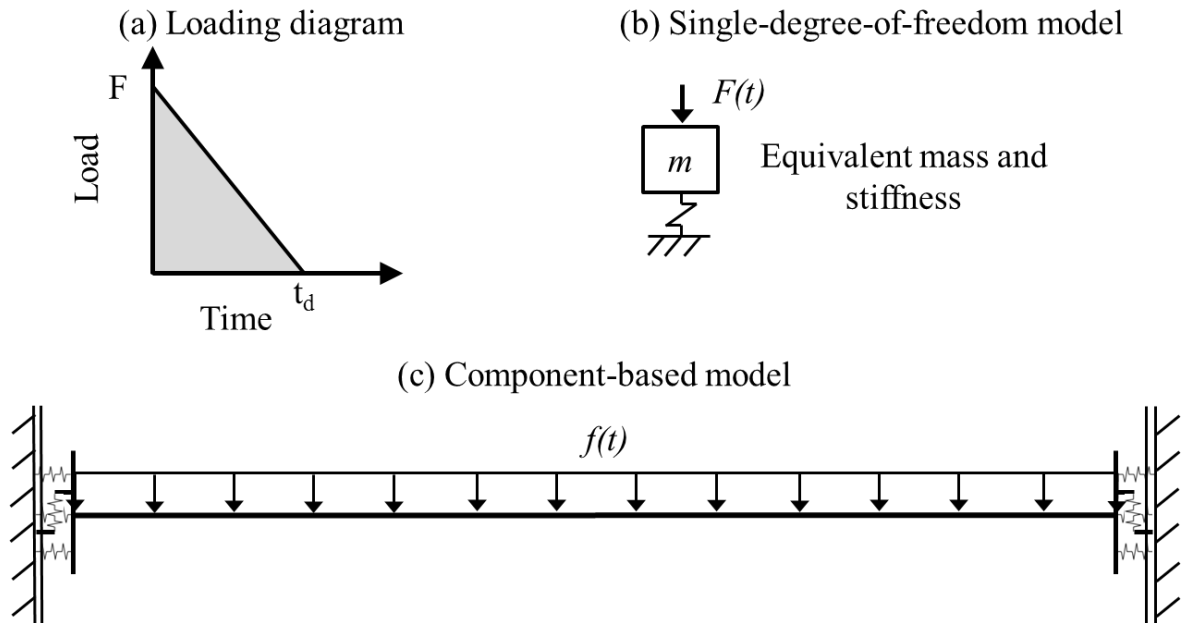
Figure 6-1: (a) Load diagram (b) SDOF model (c) Component-based model

The response was compared against the use of equivalent single-degree of freedom (SDOF) methods. A detailed investigation into the use of SDOF methods is presented in Appendix B. This is a standard method for predicting the response of structural elements to blast loading where the mass, resistance and loading of the original system are replaced with equivalent values for a lumped-mass spring system based upon energy equivalence. This is achieved through the use of shape functions derived from the expected deflected shape of the real system. Different deflected shapes can be used throughout the analysis based upon the various deformation stages of the structure from initial elastic conditions through to fully plastic behaviour. Both fin-plate and flexible end-plate connections are classed as nominally pinned; therefore the response is calculated based upon a simply supported one-way spanning element. The US Department of Defense [DoD (2008)] provides the most recent guidelines for performing such an analysis (superseding the previous standard TM5-1300 (1990)) and this procedure was used to calculate the SDOF parameters summarised in Table 6-2.

Stage	Stiffness, k (N/m)	Load-mass factor	Ultimate Resistance (kNm)	Total Mass, M (kg)	Dynamic reactions
Elastic	$3.10*10^6$	0.78	275.1	382.5	0.39R+0.11F
Plastic	0	0.66	387.5	382.5	0.38R+0.12F

Table 6-2: Equivalent SDOF parameters

The equivalent lumped system was analysed by solving the equation of motion numerically using WBiggs 4.4 developed by Baker Engineering and Risk Consultants Inc (2002).

The natural period of the system (t_n) is calculated using:

Rotational frequency

$$\omega_n = \sqrt{\frac{k}{m}}$$ (5.74)

Natural frequency of the system

$$f_n = \frac{\omega_n}{2\pi}$$ (5.75)

$$t_n = \frac{1}{f_n}$$ (5.76)

The SDOF results were compared against the use of component-based methods for both the fin-plate and end-plate connection models developed in Chapter 3. The midspan displacement plotted in Figure 6-2a shows that the results for the beam with fin-plate connections matched almost exactly the SDOF prediction for all tested values of t_d. In contrast the beam with end-plate connections showed reduced deflection in all cases which, whilst conservative for limiting peak deflection, demonstrates the importance of including the real connection behaviour. The peak dynamic reaction forces are presented in Figure 6-2b which predict that as t_d/t_n approaches 0.1 the SDOF method can under predict the shear by as much as 40% where fin-plate connections are used or worse for end-plate connections. This agrees with work by Paramasivam (2008) who investigated the use of multi-degree of freedom systems (MDOF) for similar analysis.
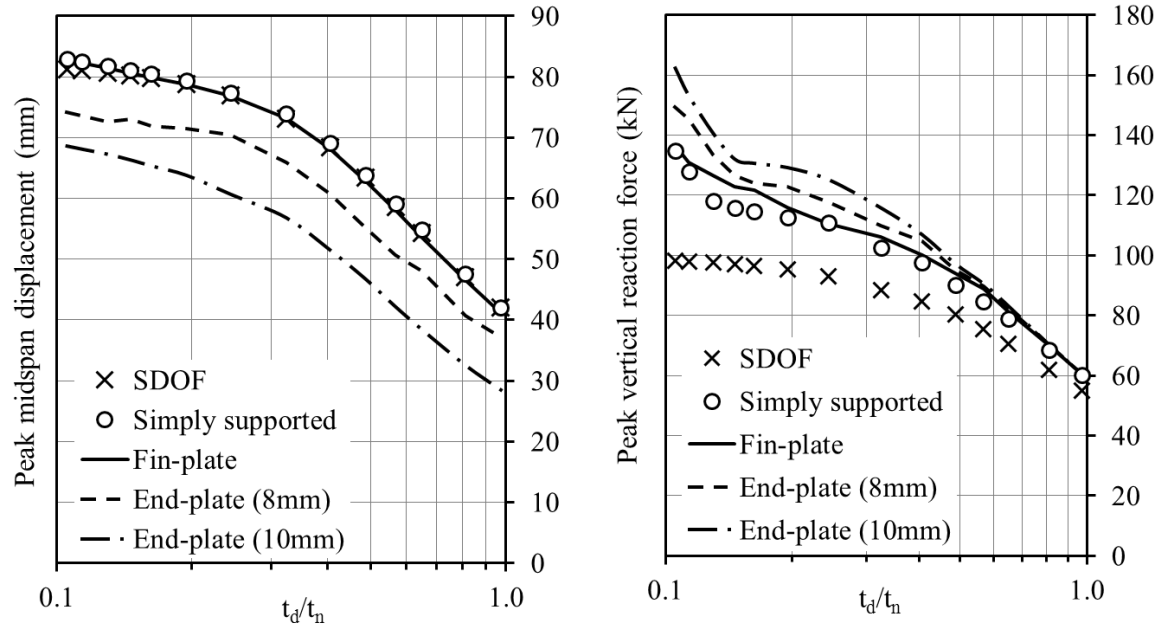
Figure 6-2: Beam response (a) Midspan displacement (b) Vertical reaction force

The reason for this difference is due to the fact that the SDOF method predicts the dynamic reaction force based upon the applied force and resistance of the element. As there is only a single degree of freedom, the resistance can only have a single mode of vibration which is based on the first mode of vibration of the structural element. In reality the element has multiple modes of vibration which have proven to drastically affect the dynamic reaction forces. This behaviour is in agreement with Paramasivam (2008) whose work showed that the deflection response is dominated by the first mode of vibration however the dynamic shear reactions are often dominated by the 3rd and 5th modes of vibration. This difference is further enhanced by the tray shaped deflection profiles typically seen in blast loading which SDOF methods cannot account for and causes additional shear at the beam ends. The peak displacement was typically achieved in a few milliseconds at rotation rates of between 0.5 and 1.5 rad/s.

The fin-plate connections demonstrate a very close approximation to the simple support assumption for both displacement and shear force however the end-plate connection demonstrates reduced displacement and increased shear force. These results indicate that connection restraint must be included in analysis as it can affect the performance of the frame and failure criteria and cause additional shear loading at the member ends.
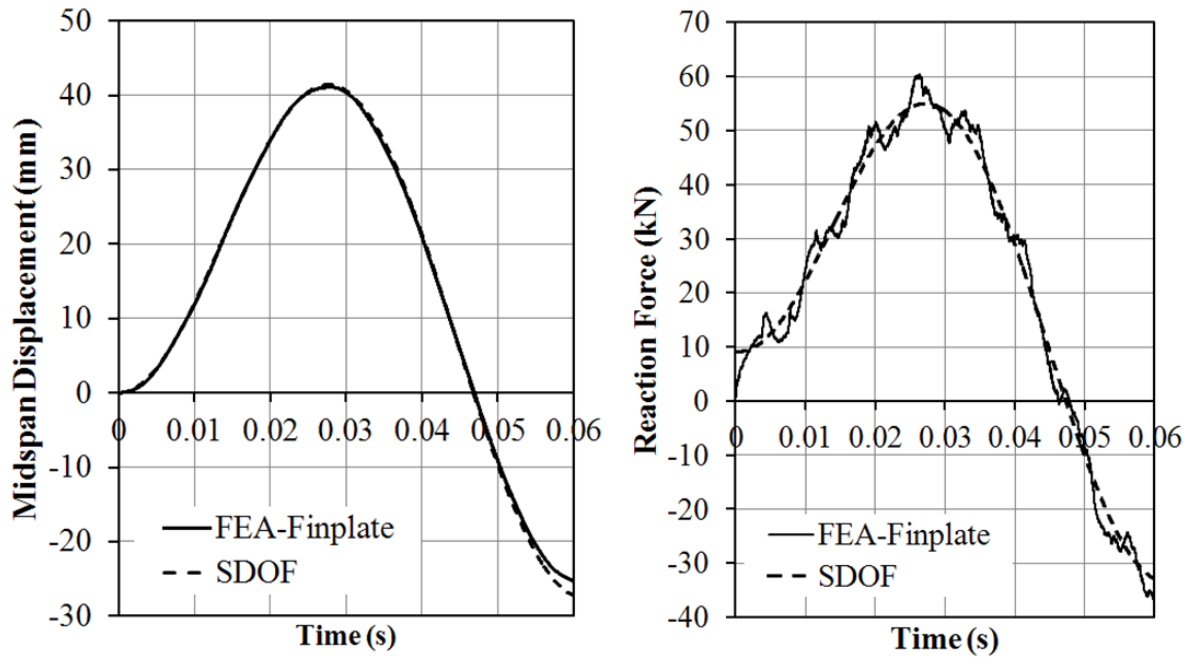
Figure 6-3: Fin-plate comparison for td/tn=0.9740 (a) Displacement (b) Dynamic reaction force

The duration of the applied load affects how much these alternative modes are excited. Comparing Figure 6-3b and Figure 6-4b for the fin-plate model demonstrates the effect these alternative modes can have. Where the loading duration is close to the natural period, the reaction force is dominated by the first mode hence where t_d/t_n is close to 1 a close correlation is observed between SDOF and FEA methods (Figure 6-3b). In comparison where the loading duration is 1/10 of the natural period the higher modes have a larger effect on the peak reaction force (Figure 6-4b) which the SDOF method cannot account for.
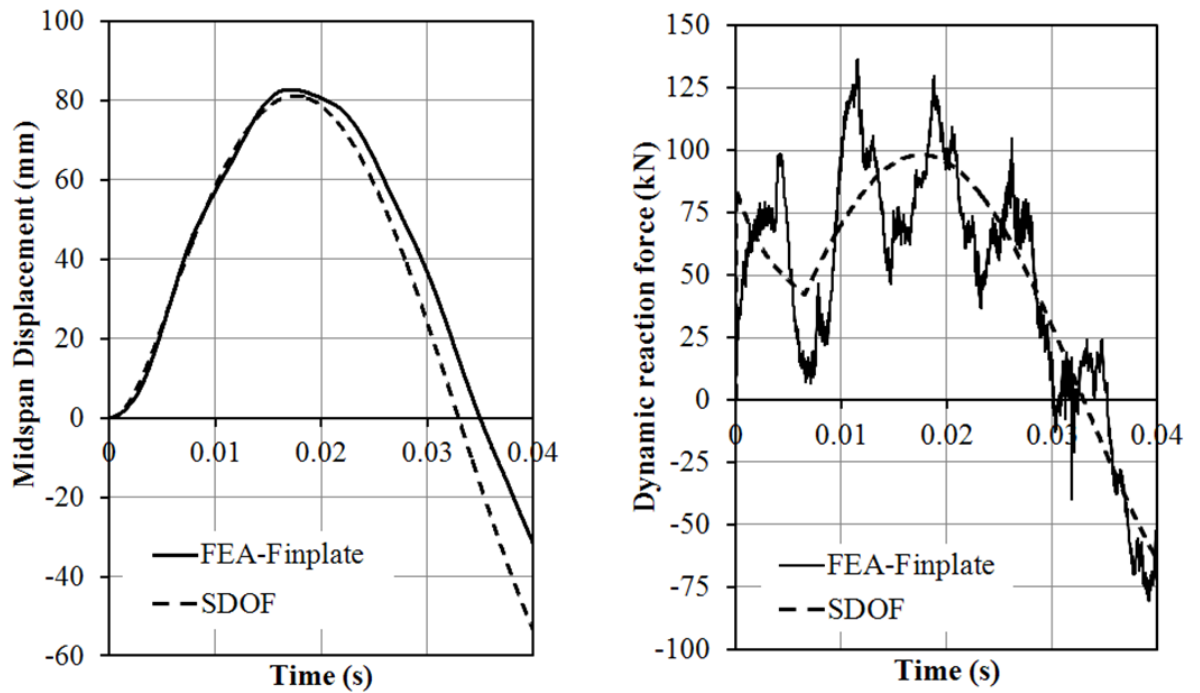
Figure 6-4: Fin-plate comparison for for td/tn=0.1055 (a) Displacement (b) Dynamic reaction force

Comparing the fin-plate and flexible end-plate results indicates there is a significant difference in overall performance. Although both connection types are classified as "simple" the flexible end-plate is inherently stiffer at low rotations and thus provides greater rotational resistance and reduces the peak midspan displacement. The fin-plate connection is able to rotate about the central bolt hole and thus initially resistance is provided only by friction, whereas for similar rotations in the flexible end-plate connection the end-plate must be deformed.
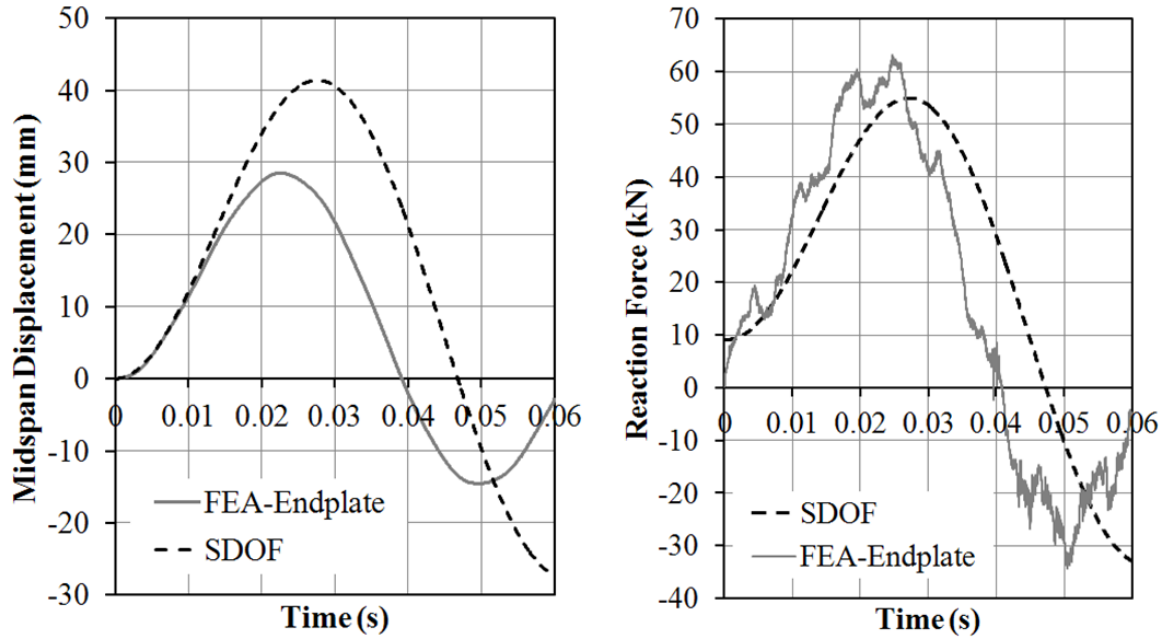
Figure 6-5: 10mm End-plate comparison for td/tn=0.9740 (a) Displacement (b) Dynamic reaction force

By making the beam stiffer, the flexible end-plate connections have reduced the natural period of the system and thus the peak displacement is achieved earlier in the loading cycle. In all cases this led to an increased dynamic reaction force.
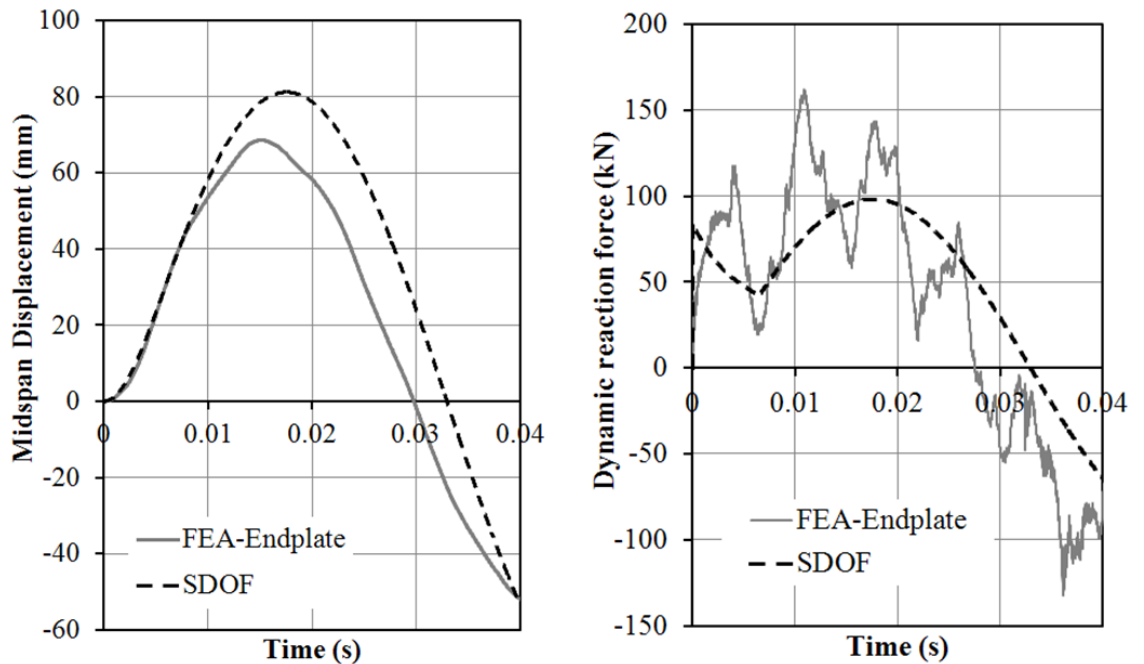
Figure 6-6: 10mm End-plate comparison for td/tn=0.1055 (a) Displacement (b) Dynamic reaction force

The results for both types of connection were normalised against the results from the SDOF analysis and are presented in Figure 6-7.
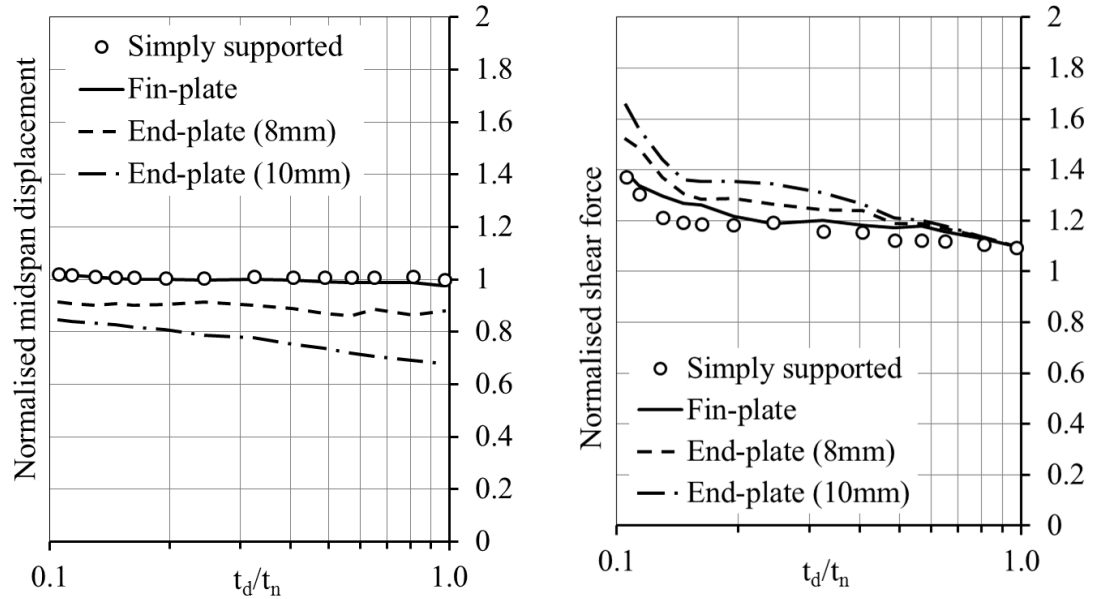
Figure 6-7: Normalised results against SDOF method

In conclusion SDOF methods closely matched the results for the beam model with fin-plate connections for midspan displacement in all loading cases. However the inability to account for alternative modes of vibration means that a significant underestimate of the dynamic reaction force is made for lower values of t_d/t_n. The use of end-plate connections results in a stiffer system and thus the midspan displacement is reduced. The stiffer connections reduce the natural period of the beam and thus increase the ratio of t_d/t_n; effectively making the loading less impulsive and resulting in a higher shear load. These results show the importance of including the real connection behaviour and the effect different connections can have on frame performance. By assuming simple support conditions the dynamic reaction forces could be underestimated by up to 20%.

6.2.2 Alternate load path analysis – component method vs. rotational springs

Two strategies are used to investigate the behaviour of steel frames and are presented in this section and section 6.2.3. This, the first, uses a point load at the central support condition and then instantaneously removes the support. The second, in 6.2.3, uses a displacement controlled analysis of the central support at a constant velocity.

Many design strategies to improve the resistance of structures involve the removal of one of more structural elements. In particular, instantaneous column loss has been identified as a realistic upper bound damage scenario to represent the loading redistribution during progressive collapse [Izzuddin (2010)]. The analysis of these scenarios can be achieved using full three-dimensional finite element analysis but this is often cumbersome and time

consuming. Alternatively reduced complexity finite element models can be used where the beams and columns are modelled using beam elements and the connections using rotation springs or hinges. However, these are limited by the availability of moment-rotation connection behaviour and the inability to account for axial loads or dynamic effects. The use of component-based methods is seen as a way to explicitly account for real connection performance in the analysis of progressive collapse without dramatically increasing the complexity. In this method, the beam and columns are modelled using beam elements and the connections modelled using the component-based methods developed previously.

An analysis of a steel sub-frame subject to column loss (Figure 6-8a) was conducted using fin-plate connections as tested in Chapter 3. The beams were 7m long 356x171x45 UB sections made of S275 steel. The component-based connection model was the same as that developed earlier and included an additional shear element at each bolt row to maintain global equilibrium. This spring is assumed to be rigid at present as defined by Block et al. (2007) but could be developed further in future to include slip and shear failure of the bolts. This model explicitly accounted for the dynamic effects and failure was based upon individual component behaviour.

The rotational spring method was implemented using the static moment-rotation behaviour. In addition, an axial spring was included to prevent overestimating the lateral restraint, whose behaviour was obtained by assuming the connection was subject to direct tension providing an ultimate tensile capacity of 402kN.
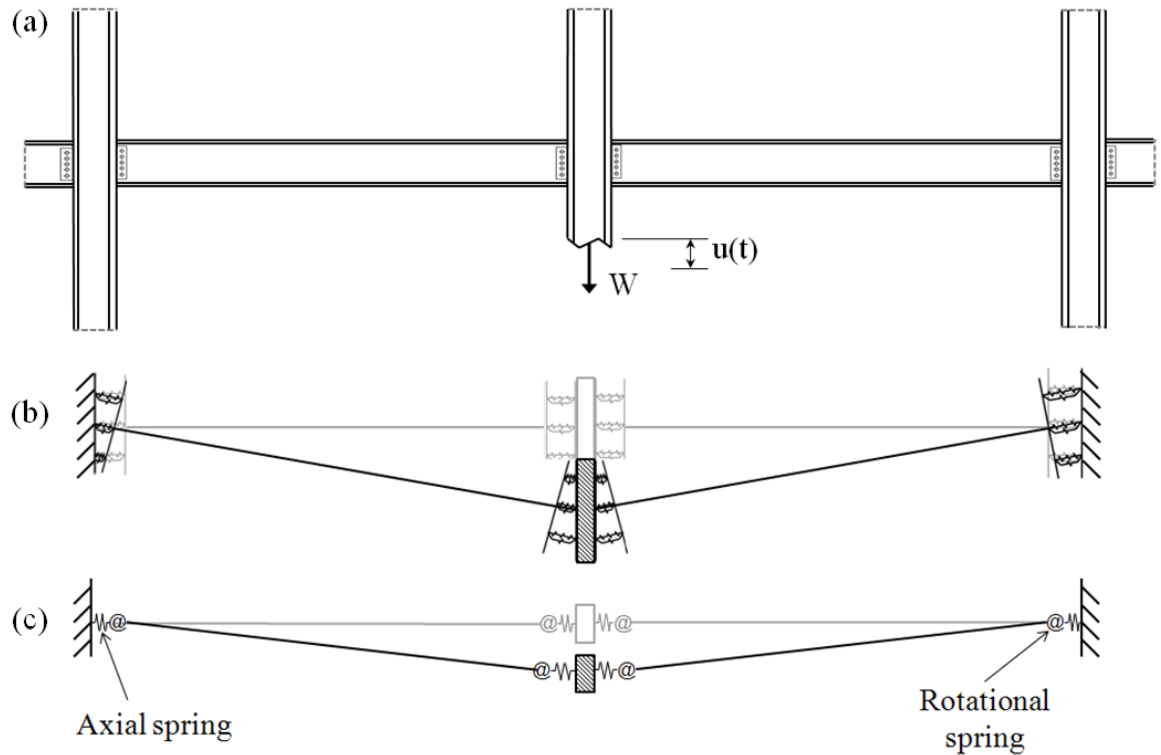
Figure 6-8: (a) Simple column loss scenario (b) component method (c) rotational spring method

A point load, *W*, was applied to the centre column and the restraint instantaneously removed. The resulting displacement time history for each method was assessed using ABAQUS/Explicit and the central displacement, *u(t)*, recorded. Where the frame demonstrated sufficient robustness, the load was increased and the problem re-analysed until an ultimate failure load was found. No gravity loads were incorporated in the analysis.

Results indicated that the component method model predicted a reduced ultimate failure load compared to using rotational springs (Figure 6-9a). The sum of all bolt row forces was used to calculate the total horizontal reaction; which indicated that failure occurred at an axial load of approximately 200kN, less than the ultimate tensile capacity.
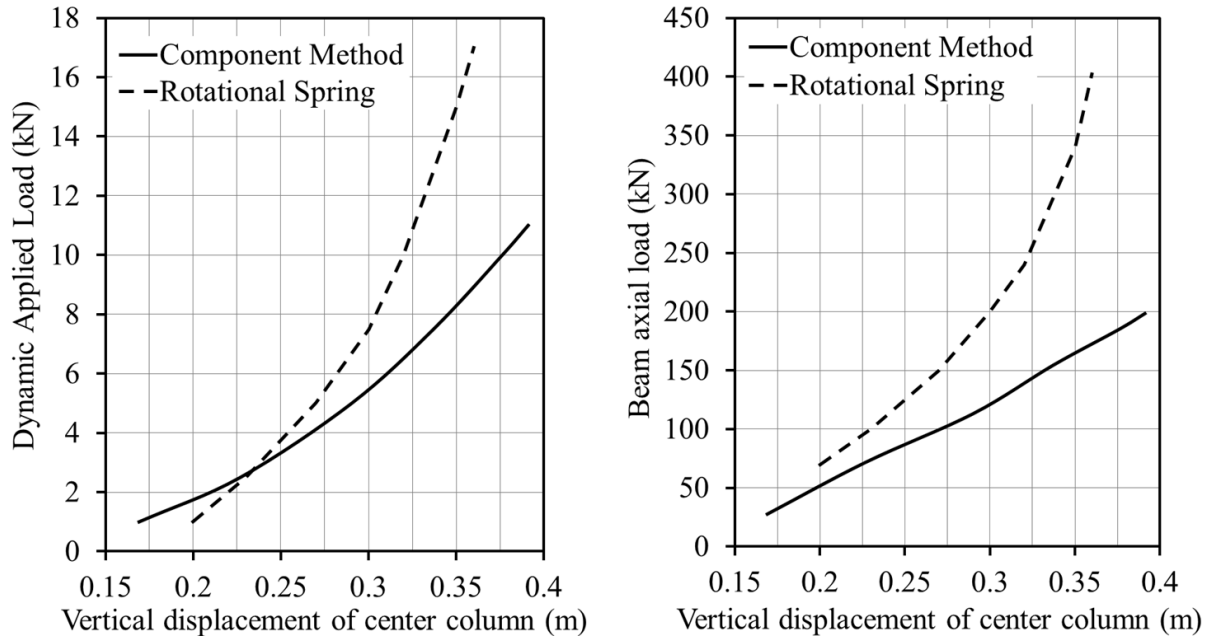
Figure 6-9: Results from frame analysis (a) Column displacement (b) Horizontal reaction

The rotational spring acts in isolation from the axial spring and therefore sufficient rotation capacity was always available at the connections meaning that axial load was the dominating failure mechanism rather than excessive rotation capacity. In comparison the component method model predicted failure at a lower rotation due to inclusion of horizontal beam forces. These horizontal forces in combination with the applied moment caused significantly higher loads to develop within the individual bolt rows at comparable rotations and thus lead to a difference in frame behaviour.

The connection response developed in the component-based model at failure is shown in Figure 6-10. Failure occurred approximately 0.125 seconds after the column was removed, considerably slower than the experimental connection tests conducted in Chapter 3. Since the rate dependent component models were able to model response successfully at the shorter load durations confidence in the predictions at these loading rates is high. This loading rate equated to a peak velocity of the upper bolt row of approximately 0.08m/s. The moment-rotation curve in Figure 6-10 indicates reduced failure moment and rotation compared to a connection subject to pure moment. This is a result of the beam axial loads causing an increased load in each bolt row at lower rotations. The rotational spring can only predict a single moment-rotation curve and thus cannot account for the effect of these axial loads.
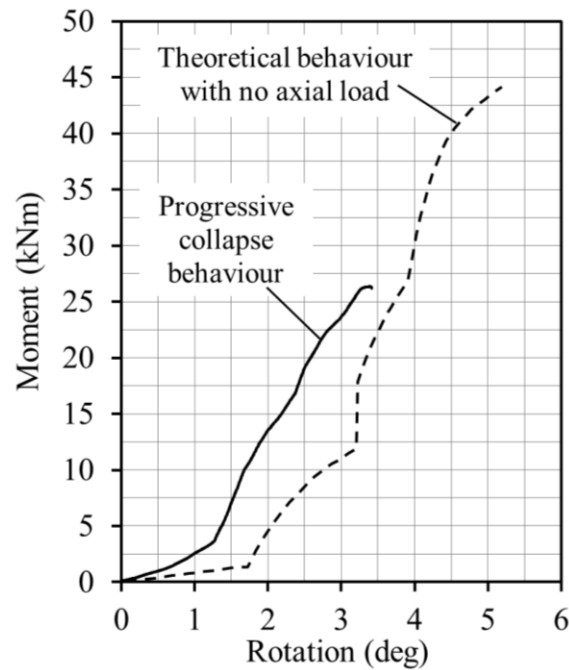
Figure 6-10: Fin-plate connection response using component-based model

These results indicate that the commonly applied "tying force" approach is unsuitable for column loss scenarios due to the disregard of connection behaviour at large or elevated rates of rotation. Large rotations induce prying action, which reduces the ultimate axial capacity of the connections. Elevated rates of rotation, such as during progressive collapse, have been observed to inflict strain-rate effects on the individual components and thus alter the connection response.

6.2.3 Alternate load path analysis – effect of connection type

This second progressive collapse assessment method displaces the central column at a constant velocity and compares the effect of connection type. The velocities used were chosen as bounding values of those experienced during progressive conditions. Whilst it is typically assumed the frame will fall at an acceleration equal to gravity, this does not account for the redistribution of the elastic strain energy as the beam returns to its undeflected shape and thus initial accelerations could be higher.

An alternate load path analysis was used to investigate the effect of connection type on response. Both fin-plate and 10mm flexible end-plate component connection models were incorporated into a finite element model using the same specification as those detailed in Chapter 5 and assembled in a similar manner. Section sizes were 356x171x45 UB with a span of 8.5m giving a double span length of 17m. These were modelled using R121 beam elements from the Abaqus element library. The columns, both peripheral and central, were

constructed from rigid elements. Fixed boundary conditions were applied to the peripheral columns. No gravity loads were included in the analysis.
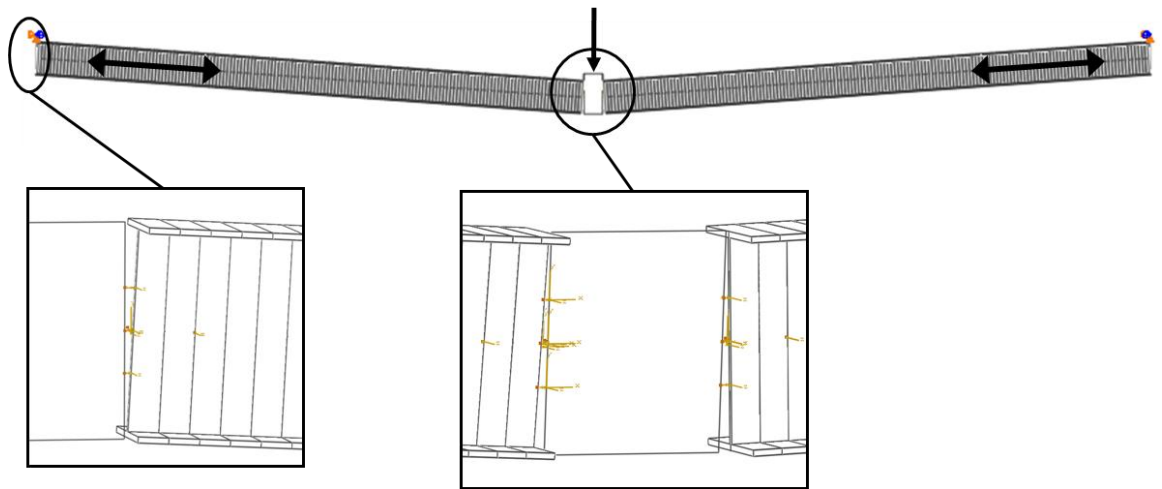
Figure 6-11: FE model showing connection details

Defining the deformation demands of a frame subject to column loss is difficult. A simple method is to assume the frame accelerates under gravity. However the presence of loads along the length of the beams causes deformation and elastic strain energy to be stored, which is released when the central support is removed. In addition, the connections at the central support are required to transfer the rotation from a sagging moment to a hogging moment and therefore could experience significantly high rotations in a very short time span. A displacement controlled analysis is therefore proposed where the central column is displaced at a constant velocity (V_c) and the resulting time-history behaviour of the system analysed. This method allows assessment of the influence of dynamic effects for a range of deformation velocities independent of the acceleration of the real frame behaviour. Preliminary studies indicated that failure would occur at a central displacement of approximately 450mm. If the frame did accelerate under gravity, assuming no restraint, the central column velocity at failure would be 2.96m/s. The frame will therefore be tested for a range of column velocities up to 3m/s to give an indication of dynamic performance.

The following data were recorded:

- Central column displacement
- Vertical reaction force at the central displacement node
- Beam axial force
- Component displacements and forces
- Connection rotation

Initially the central column was displaced at a velocity of 1mm/s to give an indication of the static behaviour. Observation of the load-displacement behaviour (Figure 6-12) indicates significant deflections and rotations prior to failure. The fin-plate and end-plate frames failed at a central vertical displacement of 402 and 498mm respectively and a fundamental difference in the frame response for the two different connection types was observed.
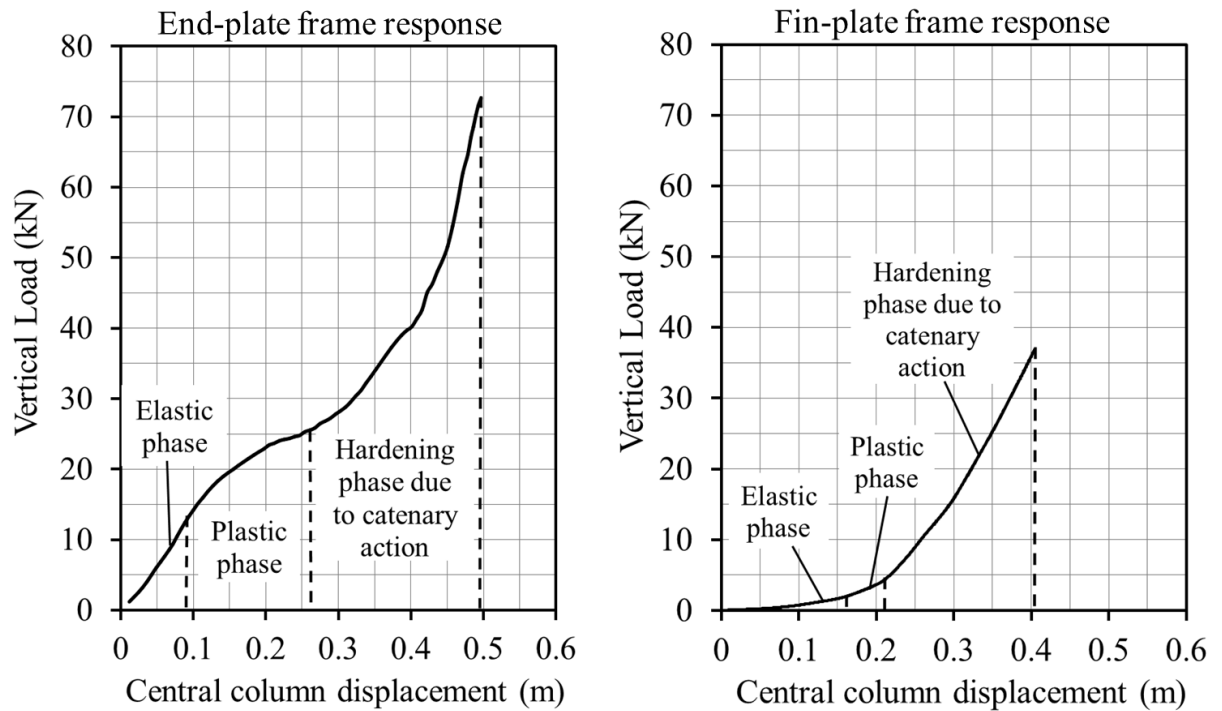
Figure 6-12: Static load-displacement response (a) End-plate frame (b) Fin-plate frame

Initially, the fin-plate connection rotates with very little resistance gradually stiffening with increased displacement. This behaviour is almost entirely due to catenary action as indicated in Figure 6-13b, where tensile beam axial forces are generated almost immediately. In contrast the end-plate connection remained in the elastic range up to a displacement of approximately 90mm. In this early stage of the loading, the response is at least partly flexural with negative axial beam forces indicating a small amount of compressive membrane action (Figure 6-13a). With increased load, the behaviour becomes dominated by catenary action. At the point of failure the beam axial tension in the fin-plate and flexible end-plate supported frames was 212kN and 341kN respectively. This corresponds with the connection test data from Chapter 3 where the flexible end-plate connections were shown to provide a greater restraint stiffness and ductility in comparison to the fin-plate connections.
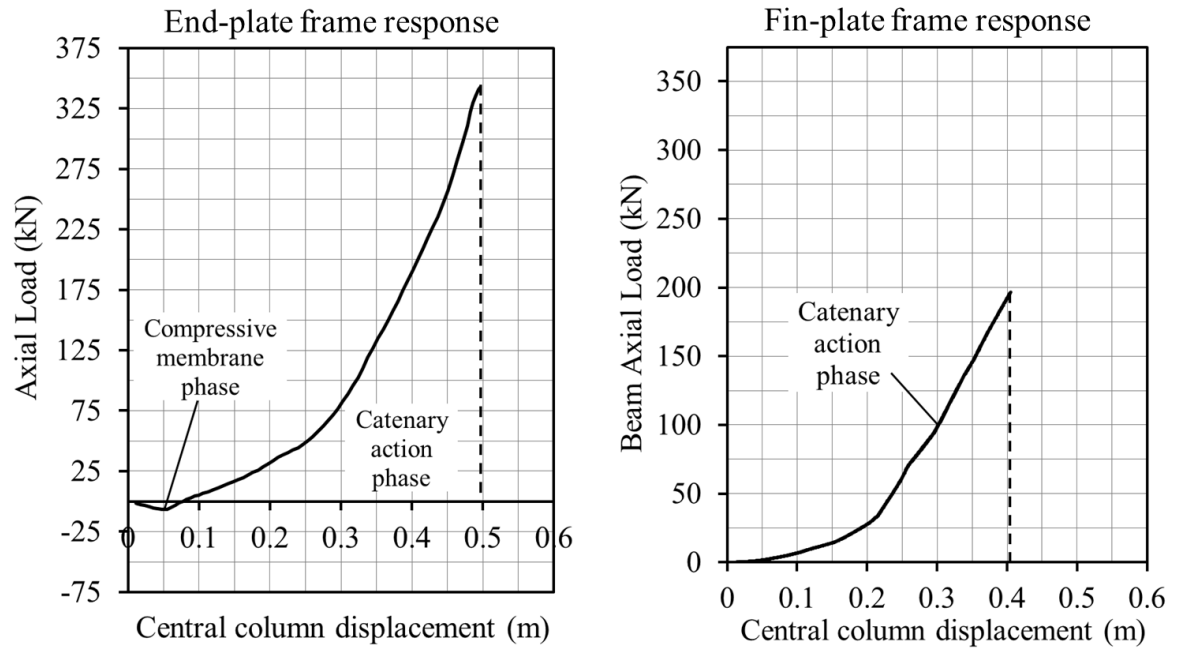
Figure 6-13: Static axial load-displacement response

The dynamic behaviour of the frames was then investigated by varying the velocity of the central column. Compared to the static behaviour, the fin-plate supported frame showed a reduced failure displacement of 16mm and a dynamic axial load enhancement of 25kN at the highest velocity tested (Figure 6-14). Similar behaviour was observed for the flexible end-plate frame (Figure 6-15) where the reduced failure displacement and load enhancement were 11mm and 79kN respectively. The general trend is that the faster the central column is displaced, the higher the load capacity of the connections and thus the frame itself.
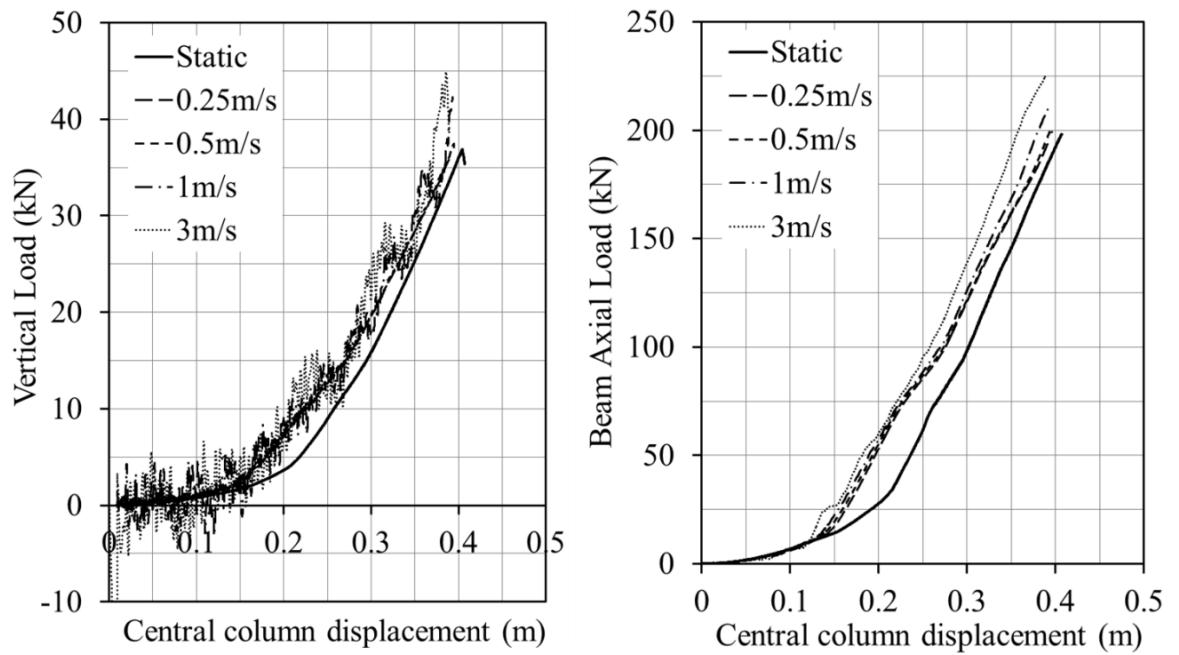
Figure 6-14: Results of frame analysis using fin-plate connections
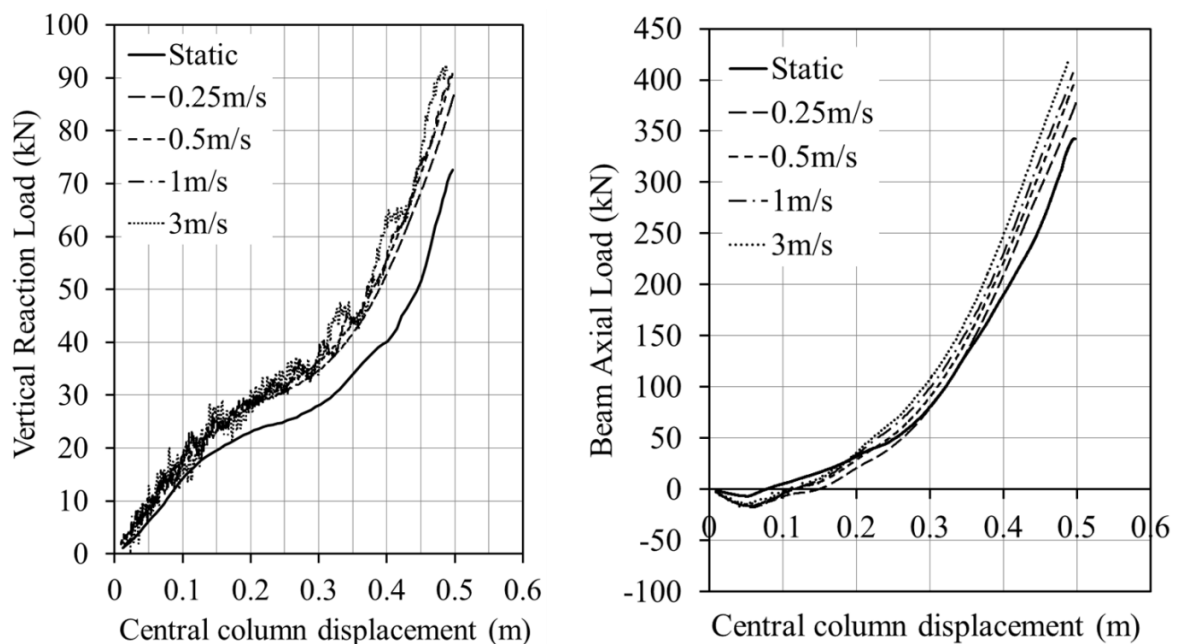
Figure 6-15: Results of frame analysis using 10mm end-plate connections

By increasing the central column velocity, the connections are forced to rotate faster and thus the components must extend at an elevated rate. However, the situation is complicated by the presence of beam axial forces which act against the movement and effectively restrain the connections. For the geometry tested, these axial forces caused failure to occur before prying action could take place.
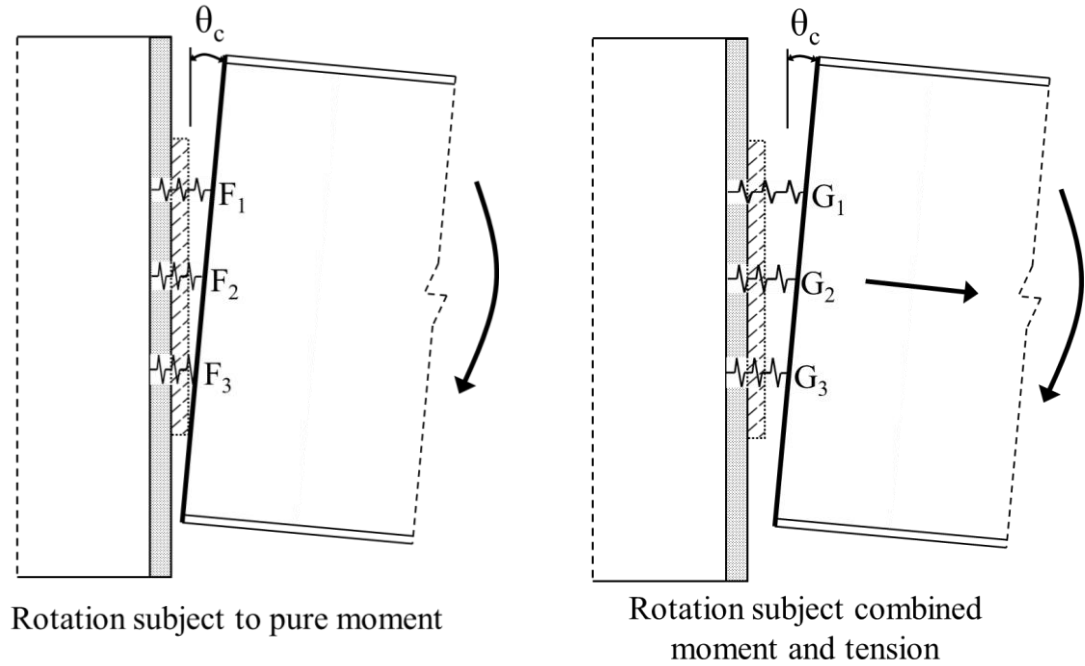
Figure 6-16: Effect of beam axial load on connection rotation and component loads

This effect is shown in Figure 6-16 for two connections at the same rotation. The connection on the left is subjected to a pure bending moment whilst the one on the right has an additional axial tension force. In this case the effect of the axial force is to pull the connection away from the supporting column and therefore the bolt row forces (G_{1-3}) are greater than those for the connection subject to pure moment (F_{1-3}). Thus failure will occur at a lower rotation.

The values for dynamic axial load enhancement correspond to increases of 12.5% and 20% for the fin-plate and end-plate. This is explained by plotting the displaced column velocity (V_c) against the peak component extension rate (Figure 6-17a). The end-plate connection exhibits a higher component extension rate at all values of V_c due to the fact that it is forced to rotate about the base of the end-plate and thus has a larger distance from the pivot location than the same bolt row in the fin-plate connection. The higher extension rate corresponds to a higher DIF on the component properties accounting for the larger difference in axial load capacity of the end-plate model.
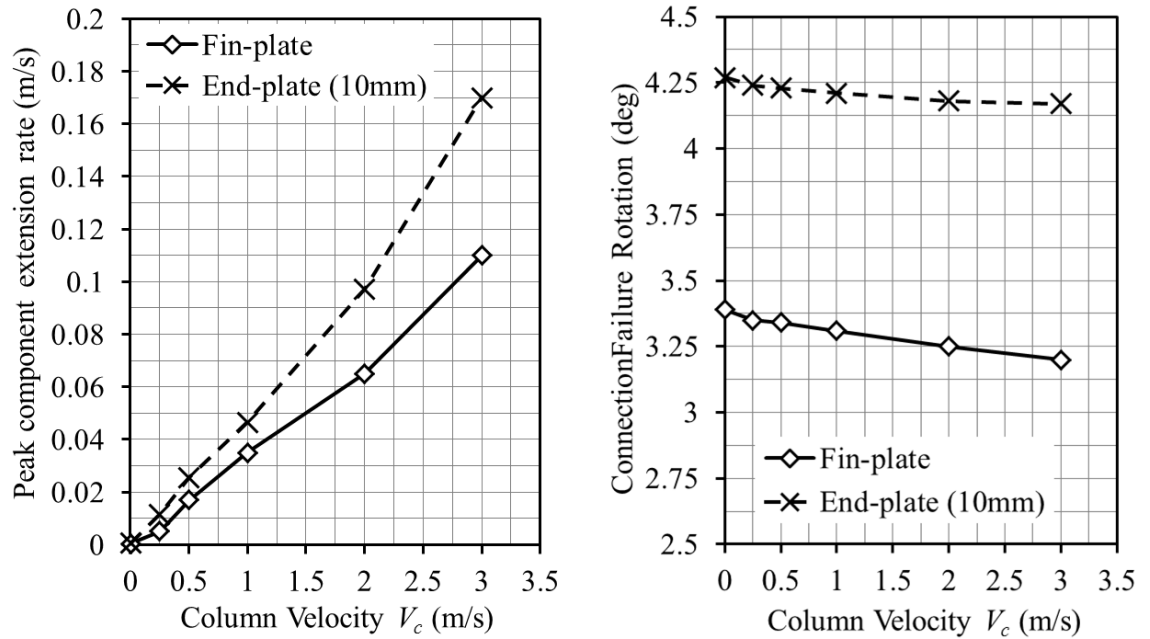
Figure 6-17: Effect of deformation velocity (a) Component extension rate (b) Failure rotation

The robustness of the frame is improved by using end-plate connections in place of fin-plate connections. The additional load capacity makes a large difference when the connection has to resist both moment and axial loads. For both connection types, the axial load caused failure at a lower rotation than witnessed in the experimental tests emphasizing the importance of using a connection model which can account for this combined loading.

6.2.4   Multi-storey office block subject to column loss

An alternate load path analysis for a typical medium rise office block subject to column loss is presented. An earlier investigation into catenary action by Byfield and Paramasivam (2007) for steel-framed structures was used as a basis for this study with similar structural detailing to allow comparisons to be drawn. The material properties and full loading conditions were based upon a multi storey office structure with 4m floor to floor height, 125mm composite concrete slab and steel frame construction. The idealised frame plan is shown in Figure 6-18 using 533x210x82 primary beams with 457x191x67 secondary beams at 3m spacings.
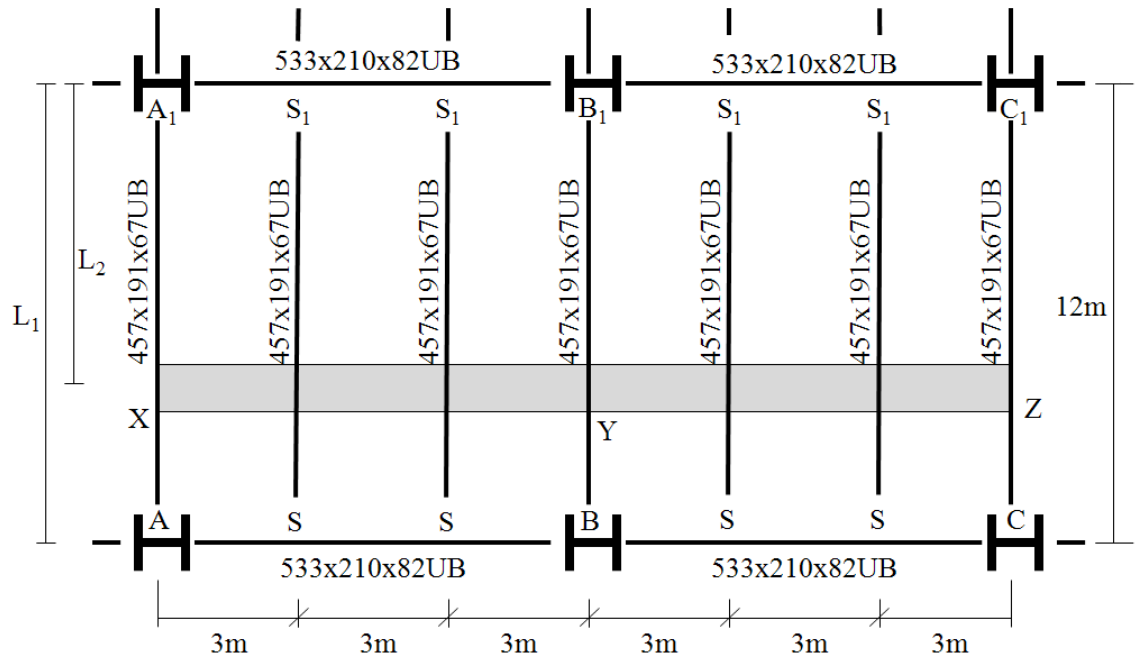
Figure 6-18: Idealised frame plan

In the original investigation assumptions about the connection behaviour were made including reduction of tying capacity from prying action, connection rotational capacity and dynamic amplification of the loading. Use of the component method negates the need for these assumptions as the connection model is able to account for them. However assumptions do need to be made about the slab behaviour in compression and tension in order to fully utilise all available strength.
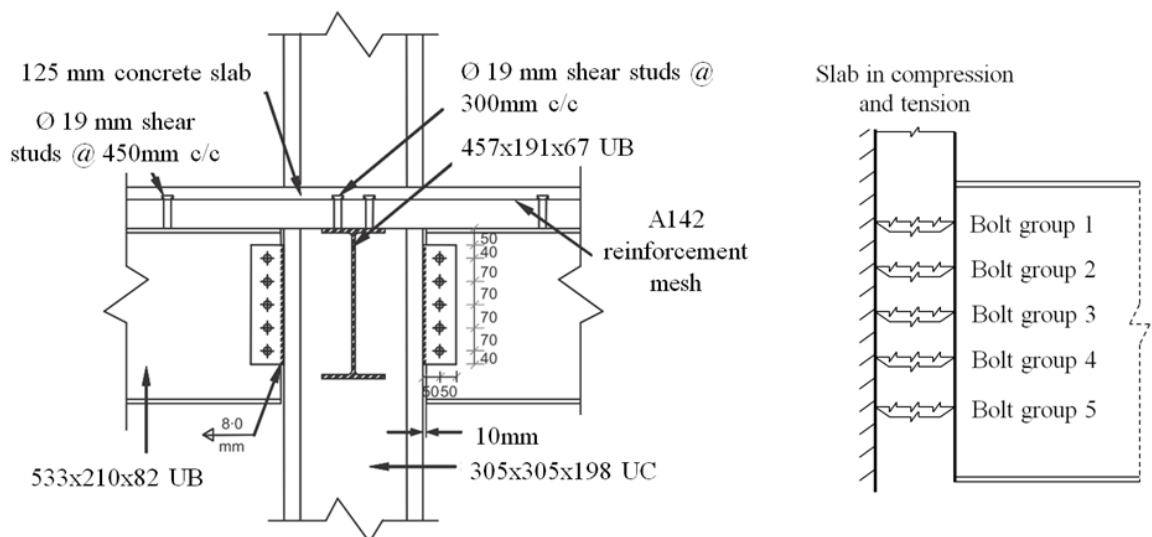
Figure 6-19 (a) Connection detail (b) Equivalent component model without shear springs

It is assumed that the slab tensile strength is obtained from the reinforcement mesh and metal decking.

155

The tensile capacity of the decking is 42 kNm from:

$$T_{deck} = N d_s t_d p_{b,d}$$ (5.77)

Where:

N is the number of shear studs used to connect an edge of profiled sheet on beam normal to sag per metre

d_s is the diameter of the shear studs

t_d is the thickness of the profiled decking

$p_{b,d}$ is the bearing strength of the profiled decking

The tensile capacity of the reinforcement mesh was calculated using:

$$T_{mesh} = A_{mesh} f_{y,mesh}$$ (5.78)

Giving a maximum mesh tensile strength of 65 kN/m and a combined slab tensile strength of 107 kN/m. Allowing for restraint from the concrete it is assumed that this tensile capacity is achieved over an initial length of 50mm with elastic behaviour calculated from the Young's modulus. At yield, perfectly plastic behaviour is assumed up to an elongation of 20% at which point failure occurs. The slab is assumed to be infinitely stiff in compression.

The slab behaviour is assembled with the connection component properties to give the final component model presented in Figure 6-19b.

W_1 is the reaction from beam SS_1 calculated by multiplying the accidental limit state load by half the area. W_2 is calculated according to the method presented by Byfield and Paramasivam (2007) where a 1m section across the double span is considered in order to take into account the reduction in load caused by catenary action within the slab. The reduction in load (P_{up}) is a factor of the upwards load from T_{slab} which is dependent on the end slope of the slab which varies from 0 at ABC to $\varTheta$ at ABC_1. The full tensile load

capacity is assumed over the width of the slab and q is the uniformly distributed load acting directly on beam ABC.

$$P_{up} = 2T_{slab} sin\left(\theta \frac{L_2}{L_1}\right) \tag{5.79}$$

The full combined tensile strength of the slab was mobilised giving $W_1 = 134.3$ and $W_2 = 83.2$. The load reduction from catenary action of the slab is assumed to act up to a maximum slab end rotation of 3 degrees.

(a) Problem schematic
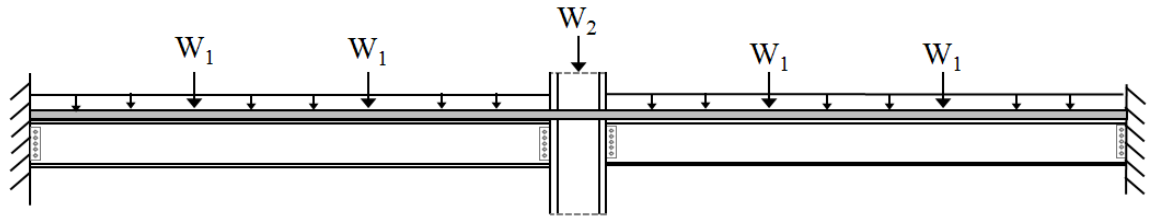
(b) Component-based method
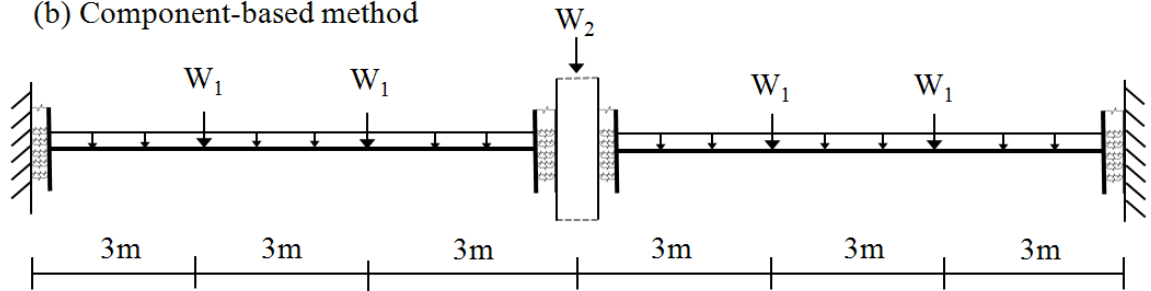
Figure 6-20: Double span loading conditions

The stiffness of the slab was included by assuming it behaves as a composite section and no failure of shear studs occurs along its length. The analysis predicts failure of the slab at the supports followed by progressive collapse of the connections and floor system. This agrees with the original assessment by Byfield and Paramasivam (2007).
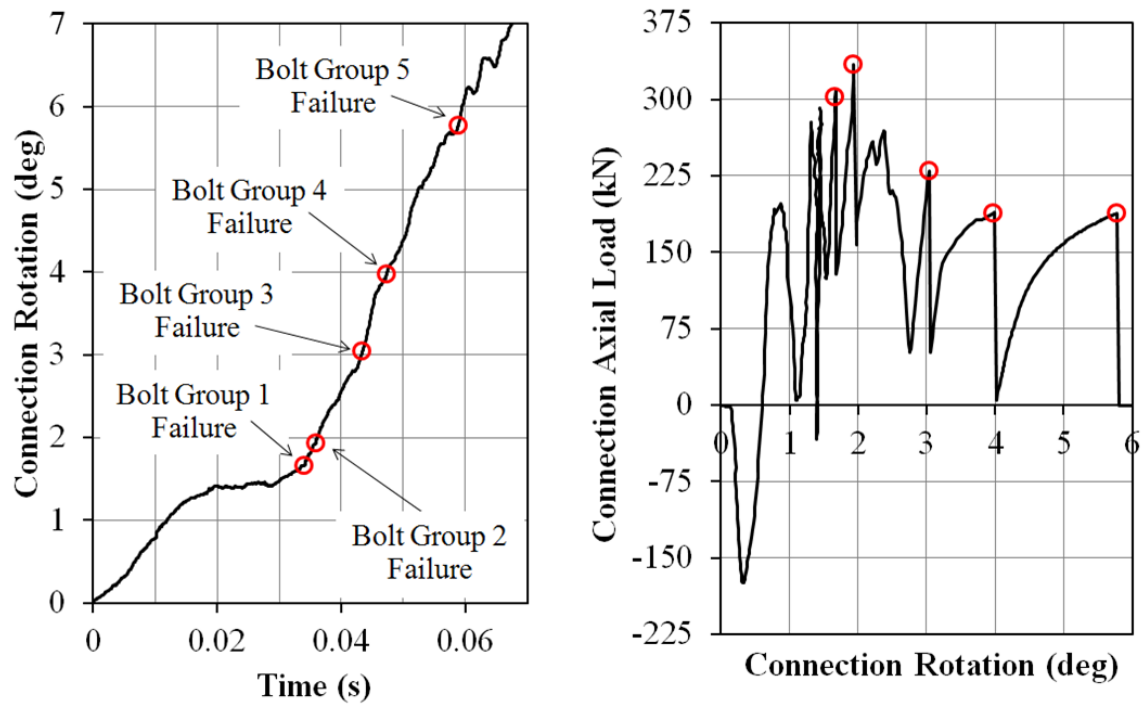
Figure 6-21: Left hand support (a) Connection rotation (b) Total axial load at connection

Results from the analysis indicate that as soon as the central supporting column is removed the slab is put into tension and the connection is forced to rotate with bolt groups 1 and 2 put into tension and 4 and 5 into compression indicating rotation approximately at the central bolt group. The upper bolt fails at a rotation of 1.65 degrees as a result of the large lever arm caused by the relatively deep beam section. The sum of all the bolt loads was used to calculate the total axial load and is presented in Figure 6-21b which indicates that at low rotations there is a negative axial load indicating compressive membrane action in the concrete slab. Between 20 and 30ms the connection stiffens as bolt groups 1 and 2 approach their ultimate capacity. Failure of bolt group 1 occurs at approximately 35ms followed almost immediately by bolt group 2 by which time the peak axial load experienced by the connection is recorded. This loss of connection stiffness causes the floor to accelerate which can be seen in Figure 6-21a as an increased rate in the connection rotation at 37ms. The large rotation forces the beam lower flange to contact the column inducing prying action and causing the successive failure of the remaining bolt groups and reducing the connection axial load to zero.

6.3   Summary and conclusion

The component method has proven a useful tool for modelling the dynamic behaviour of connections when compared against results from experimental work. The method of

adapting present models allows the wealth of knowledge in this field to be fully utilised and expanded upon.

The ability of finite element packages to include rigid and axial connector sections allows incorporation of these component-based models into frame analysis for a variety of scenarios and numerous benefits have been demonstrated. Principally, the flexibility of the method to account for loading conditions which arise from load redistribution between individual structural elements makes it particularly suited to progressive collapse analysis. Additionally, when compared to using simple rotational springs, the planar nature of the method allows p-delta effects to be considered and allows for compressive or tensile action within the connections.

Component-based methods compared favourably with alternatives as they are easily integrated into non-linear dynamic analysis and can account for all loading, geometrical and physical conditions experienced at the joints. In addition they are straightforward to modify, allowing variations of structural configuration to be investigated with ease, whilst keeping computational analysis time to a minimum.

7 CONCLUSIONS AND FURTHER RECOMMENDATIONS

7.1 Introduction

Steel structures are often protected against progressive collapse by prescriptive design measures such as minimum tying forces. These guidelines have been developed to improve the robustness of structures and allow redistribution of the loading following local failure; however the structural elements are designed in isolation and therefore the interaction between beams, columns, and floor slabs is not taken into account.

To overcome this limitation the use of analysis tools, such as the finite element method, have become common to allow prediction of the global frame behaviour. By modelling all structural elements to the smallest detail including individual bolts, nuts, washers and shear studs the complete behaviour can be predicted. However this level of detail uses a large amount of resources and is not particularly suitable for design due to the level of complexity and restricted ability to alter the model. Therefore simplifying assumptions are often made particularly at the most complex region of the model, the connections. The simplest is to assume that either all of the moment at the end of a beam is transferred to the supporting column (rigid connection) or none of it is (simple connection). Alternatively a rotational spring can be employed using a predetermined moment-rotation curve to allow the inclusion of semi-rigid behaviour.

The behaviour of the connections during collapse is therefore assumed to be the same as under ultimate limit state conditions i.e. pinned connections are assumed to remain pinned throughout the collapse conditions. However, this assumption does not always hold true as pinned connections have been shown to provide a certain level of connection restraint under certain loading scenarios and can therefore affect the overall frame behaviour. The loading conditions and resulting connection behaviour before, during and after extreme events must be understood as these are essential in ensuring continuity within the frame and providing alternate load paths [Ellingwood and Dusenberry (2005)]. This lack of knowledge led to the formation of this work, with the aim of improving the understanding of connection performance in extreme loading conditions.

7.2   Summary of findings

The following conclusions were drawn as a result of this work:

- "Simple" steel connections can exhibit considerable stiffness and moment resistance

- The behaviour of steel connections is influenced by rate of rotation and axial load

- Component-based methods incorporating dynamic material properties can be used to provide a reasonable representation of connection behaviour at normal and elevated loading rates

- Connection restraint and ductility supply can affect the overall response of a structure and must be included in analysis of scenarios where the ultimate limit state is achieved

- Generic robustness provisions, such as tying forces, cannot guarantee integrity following extreme events without consideration of ductility supply at the connections

7.3   Experimental testing

The process of redistributing loads during a progressive collapse is a dynamic event; however a lack of knowledge exists with regard to connection behaviour at elevated rates of rotation. Therefore a test rig was designed and constructed for the purpose of investigating this behaviour. Of particular interest were the effects of rate of rotation and the contact between the beam lower flange and the column face. Both direct tension and applied moment-rotation tests were conducted on three "simple" connection types; flexible end-plate, fin-plate or shear tab and web cleat at equivalent static and dynamic loading rates.

The test arrangement consisted of pneumatically driven loading rams which forced a column section to rotate about a fixed beam and thus deform the test connection. The instrumentation consisted of laser displacement gauges, accelerometers, calibrated load cells and a three dimensional image correlation system. Two laser displacement gauges were installed at either end of the column to measure the rotation and were also used to

verify the readings from the accelerometers. Load cells were used to record the load applied perpendicular to the face of the column from which the applied moment was calculated.

The first series of tests evaluated the performance of fin-plate connections. This was chosen because in theory the behaviour should most closely resemble a 'simple' connection as at low rotations the moment is resisted only by friction. For all moment-rotation tests the failure mechanism was bolt shear starting at the upper bolt row, contradicting the design guidelines which suggest the beam web as the critical check. Three stages of response were recorded. The first is the initial bolt slip where, because the 20mm bolts were installed in the centre of their 22mm clearance holes, friction is the only restrictive force. Once these bolts are displaced 2mm the moment required to rotate the connection increases due to the bolts bearing against the beam web and fin-plate. The final stage of the response is the result of prying action when contact occurs between the beam flange and column face, forcing the point of rotation to move further from the bolt rows and thus increasing the rotational stiffness. Comparison of the moment-rotation curves indicates that the behaviour is dependent upon the loading rate. In the first stage of response the dynamic tests showed a considerable stiffness increase but this is thought to be due to the high ratio of axial load to applied moment resulting in the entire column moving away from the beam section and thus not rotating exactly about the central bolt. The second stage of the response indicates a variation in stiffness and also in yield moment. The final stage demonstrates similar stiffness for both static and dynamic tests however the ultimate moment is increased whilst the failure rotation is reduced. The static direct tension tests of fin-plate connections indicated that they are capable of sustaining a load of at least 1.5 that of the design axial load capacity. The results from the moment-rotation tests suggest that this axial load capacity is significantly reduced (by up to 50%) when the connection is subject to combined moment and axial load.

The second series of tests considered flexible end-plate connections. A total of 17 moment-rotation tests were conducted at varying load rates for both 8mm and 10mm thick end-plate specimens. For all 8mm end-plate connections the modes of failure were similar in that a crack developed along the line of the fillet weld which ultimately propagated through the plate. The static moment-rotation curve indicates 4 stages of response. The first is the initial stiffness until the end-plate yields. This is followed by a reduced plastic stiffness

until contact between the beam flange and column occurs. The third stage occurs as the point of rotation is transferred from the corner of the end-plate to the bottom of the beam section resulting in an increase in stiffness. This does not appear to be an instantaneous event but transpires over 1 degree of rotation. The final stage is after the moment is transferred and further plastic deformation takes place until failure. The dynamic tests provided similar moment-rotation curves albeit at a higher equivalent moment. The initial yield moment was increased by up to 1.5 times the static value with similar increases seen in the ultimate moment capacity. The failure rotation was not significantly influenced by the rate of loading.

Similar stages of response were witnessed for the 10mm thick end-plate connections; however a variety of failure modes were observed. These included tearing of the beam web, bolt failure and fracture of the end-plate. The initial yield moment was increased compared with the 8mm end-plate connection and the third stage of response occurred at a larger rotation due to the added thickness of the end-plate. The static rotation capacity was also increased because the weakest component (the end-plate) was strengthened and therefore the strength reserve of the other regions could be utilised. With regard to the dynamic behaviour, the rotation capacity was reduced from 9 degrees to just over 6 at the highest rate of loading which is a greater effect than that of the 8mm end-plate. This suggests that whilst a thicker end-plate provides greater ductility and capacity, it also makes the connection more susceptible to dynamic loading. The 8mm connections showed continued ductility in the fourth stage of response whilst the 10mm connections appeared to fail very shortly after contact occurred, particularly in the dynamic tests. It is thought that this may be due to the impact and sudden increase in load causing the material to behave more brittle. Results from 3 direct tension tests of 8mm end-plate connections indicated that the connections could achieve a load 1.6 times that of the design tying capacity. Compared to these, the moment-rotation tests showed a considerable reduction in axial load capacity.

The final test series of 9 samples, investigated the performance of double angle web cleat connections. This followed the pattern of the previous series by using the standard detailing of 10mm cleats as well as testing more flexible 8mm cleats. All tests demonstrated a similar failure mode where the beam web failed in block shear and was torn out by the bolts in agreement with the design guidelines. In comparison to a fin-plate

connection the bolts in a web cleat connection are loaded in double shear, hence have twice the shear capacity which caused the weaker beam web to be the critical failure mode. The initial stiffness was low because, like the fin-plate connection, there is only friction to resist the moment until the bolts begin to bear against their clearance holes. Following contact between the beam flange and column the stiffness increases but due to the ductility of the web cleats this is not as pronounced as the flexible end-plate connections. There was little difference in static behaviour of the two web cleat thicknesses although the thinner cleat appeared to produce a slightly more ductile connection.

The dynamic behaviour was of interest. The 8mm angle appeared to perform similarly at all loading rates albeit at a slightly higher moment under elevated loading rates. In contrast the 10mm cleated connection failed at substantially reduced rotations when loaded dynamically. This was in part due to the thicker web cleat which creates an inherently stiffer connection. This results in less deformation of the web cleat at similar levels of rotation leading to higher bearing deformation of the beam web. Observations of the 10mm web cleats after failure support this and show the total displacement, or opening of the angle, is significantly less than that experienced in the 8mm cleats.

7.4   Connection representation

The results from the experimental investigations indicated that loading the connections dynamically caused a change in the overall moment-rotation behaviour and that this effect varied according to the connection typology and detailing. The main features of this behaviour are an increased yield load and reduced failure rotation.   In addition large connection rotations can cause prying action where the lower beam flange contacts the column face resulting in an increased stiffness.

Component-based connection modelling was identified as a suitable method for which the complete connection behaviour could be accounted for. A connection model is made by first dividing the connection into its deformable parts or components and predicting their individual force-displacement relationships. These individual behaviours are then reassembled into a geometrically similar model. Assuming the individual component behaviour is available all connection variations can be represented without having to perform expensive connection testing. Compared to using rotational springs, the method can account for all loading conditions including combined axial load and moment. Benefits

over using full three dimensional finite element modelling, are that component-based methods require less technical knowledge and allow variations in structural configuration to be achieved more easily. The individual behaviour can be found from numerical analysis or experimental testing and can be calculated as a function of further variables.

Originally developed to allow prediction of connection moment-rotation behaviour in wind-moment frame design, component-based methods have also proven capable of predicting degraded performance in the field of structural fire engineering where large deformations and axial loads are often encountered. Temperature dependent material properties are applied to individual components to predict the reduction in strength. In a similar manner this work considered the effect of dynamic behaviour by applying dynamic increase factors to the components. This allowed prediction of the yield and ultimate stress of steel at different strain rates and was applied to individual component behaviour using simple assumptions.

Under static conditions, component-based connection models can be solved using equilibrium and the force in each component calculated. The dynamic nature of the testing, and progressive collapse in general, requires inertial forces to also be accounted for. The best way to achieve this, in respect of time and resources available, was to use finite element methods. The finite element program ABAQUS was selected for this study.

7.5 Dynamic component-based fin-plate connection model

A component-based model has been developed to predict the behaviour of fin-plate connections at elevated loading rates. The model can follow the full connection response based upon the individual deformable regions. Three stages of response were considered and compared against the results from the experimental investigations.

Deformation of the bolts, beam web and fin-plate was assumed to represent the connection response including the friction between the components. The individual force-displacement relationship was calculated based upon mechanical models developed to predict response under static conditions. The influence of dynamic effects was taken into account by applying dynamic increase factors to the yield and ultimate strength of the steel from Malvar and Crawford (1998). Comparison with the experimental results for the static test indicated a good correlation for the initial and yield response and a slight overestimation in the post yield behaviour.

The recorded loading from each dynamic experimental test was used as input for the component-based model which allowed a comparison of the complete physical behaviour of the system as well as the connection response. Observation of the rotation-time history of the column showed that the model was capable of accurately predicting the connection response and that with increasing load rate the amplified connection stiffness compared reasonably well with the experimental data. The model predicted bolt shear as the failure mode in agreement with all experimental tests however the failure moment was overestimated in all samples.

It is concluded that the component-based model provides a realistic prediction of the connection response at elevated loading rates and is able to account for the main features witnessed in the experimental tests.

7.6 Dynamic component-based flexible end-plate connection model

Using the same principles, a second component-based model was developed for flexible end-plate connections. This was chosen due to it being an inherently stiffer connection and providing greater moment resistance at low rotations. It also differs from a fin-plate connection in that the initial center of rotation is about a fixed point; the lower edge of the end-plate.

The components included in the connection model were the end-plate, the bolts and the column flange whose individual responses were defined using simple mechanical models originally developed for static conditions. Dynamic effects were included using a similar technique to the fin-plate model. Comparison with the experimental data showed that the model can predict the connection response for both 8mm and 10mm end-plate thicknesses at both static and dynamic load rates.

The initial stiffness of the connection and yield moment were accurately predicted for both end-plate thicknesses under static conditions and the resulting increase in yield moment due to the dynamic load was also captured with good accuracy. The plastic response showed a good trend as did the increased stiffness at the point where contact occurred between the lower beam flange and column. The experimental data indicated that the failure rotation was approximately 1 degree higher than predicted for both 8mm and 10mm end-plate thicknesses.

These results show that component-based methods can be used to provide a reasonable prediction of the overall connection response under dynamic conditions for a range of connection types. A comparison of the fin-plate and flexible end-plate behaviour shows that whilst both of these connections are often assumed to exhibit 'simple' behaviour they can in fact provide substantial moment at higher rotations which could invalidate design assumptions. Using component-based methods within finite element software allows the complete range of connection response to be easily included assuming that knowledge of the individual component behaviour exists.

7.7 Influence of dynamic connection characteristics on frame behaviour

A series of parametric studies were conducted on sub frame assemblies to investigate the effect of dynamic connection behaviour on frame performance. Beam elements representing beams and columns were joined using the component-based models developed for both fin-plate and flexible end-plate connections and the results compared against more common methods of analysis. The connection models have proved capable of predicting the connection performance at the load combinations and rates experienced in the experimental tests and therefore are assumed to provide a reasonable approximation in these frame models.

The first scenario investigated was that of an isolated structural beam subject to theoretical blast loading for a range of t_d/t_n values. The typical response was calculated using a single-degree-of-freedom (SDOF) method where, due to both connection types being classed as 'simple' connections, a simply supported one-way spanning element was assumed. It was observed that using the fin-plate connection model produced displacements comparable with that of the simply supported assumption however the use of the flexible end-plate model resulted in a considerable reduction in the mid-span displacement for all recorded loading values and meant the response lay somewhere between simple and rigid behaviour.

The dynamic shear loads experienced at the supports were also recorded and compared against the SDOF system. Previous work [Paramasivam (2008)] has highlighted the limitation of SDOF methods to predict shear loads due to the effect of additional modes of vibration and this was observed. In general the end-plate connected beam developed higher shear loads than the comparable fin-plate connection. This behaviour is explained because the stiffer connection reduces the natural period of the structural system and therefore

effectively increases the value of t_d/t_n. The time taken to reach the maximum connection rotation was comparable to that seen in experimental investigations.

The second sub-frame arrangement considered that of a double spanning beam scenario typically assumed to occur following loss of a lower floor column. Although there is no set method to analyse such an event, the use of component-based connection models were compared against the use of a rotational spring with predefined moment-rotation behaviour using non-linear dynamic finite element analysis. The observed behaviour indicated that use of component-based connection models predicted a lower failure load compared with using rotational springs as a result of the ability to include the effect of combined axial load and moment. Analysis of the frame with different connection types showed the effect end restraint can have on the performance. Stiffer connections result in reduced midspan displacements but can lead to higher moments causing premature failure. Equally weaker connections allow catenaries to form earlier but the higher rotations can cause reduction of the axial capacity. The two-dimensional nature of the component-based model allows second order (P-delta) effects to be considered as shown by a negative horizontal reaction force at low loads indicating compressive membrane or arching action.

Up to this point the component-based method has been applied to theoretical sub-frames consisting only of steel structural elements and their connections. The final scenario considered the loading demands on a real structure. This was based on a previous investigation into the performance of a multi-storey steel structure, using fin-plate connections, subjected to a middle bay column loss. The section sizes were larger than those considered previously and therefore the actual connection performance could not be verified experimentally before using the component-based model. In addition the restraint provided by the floor slab was included using an additional spring component whose behaviour was calculated based upon the tensile strength of the concrete and reinforcement. The original investigation predicted the frame response based upon assumptions of the tying capacity of the connections including the effect of prying action. The analysis conducted using component-based connection models showed that the connections demonstrated insufficient ductility to survive the event of column loss in agreement with the findings of the original investigation. However initial failure was predicted at a rotation of only 2 degrees as opposed to the theoretical rotation capacity of 4 degrees used originally. This reduced failure rotation is attributable to the fact that fin-plate

connections were used; which have been shown to provide very little ductility. In addition the beam section was deeper than that tested in the experimental series

These results suggest the connection type can have considerable influence on the overall structural performance. What are normally considered 'simple' connections have been shown to develop considerable moment and therefore this behaviour needs to be included in analysis of structures where the ultimate capacity is of importance. In addition, the effect of high rotation rate can reduce the rotation capacity of connections and cause them to fail prematurely. Component-based connection models have proven to be a useful tool in allowing this behaviour to be included in analysis of structures.

7.8　Recommendations for further work

Future work into the behaviour of steel connections during extreme events needs to consider the effect of rotation rate and the various load combinations experienced during such scenarios. Instrumentation of controlled demolitions could be a valuable source of data providing likely loads and general response. Connection testing of instrumented sub-frame arrangements would also allow consideration of the effect of structural continuity and axial loads from catenary action. However this is costly and therefore isolated connection tests are more likely. Testing a range of rigid connections at elevated loading rates would show whether they followed the trends witnessed in the previous experimental investigation where stiffer connections appear to demonstrate reduced ductility. However, the loads required to make these connections fail would be substantially higher and a different testing procedure would be required.

Component-based methods have proven useful for the prediction of connection behaviour under extreme loading conditions. Whilst simplified assumptions have been made to predict the performance of each component numerically further understanding of this behaviour is required. Ideally experimental testing of each component at a variety of loading rates should be conducted in order to verify the predicted behaviour and increase the knowledge in this field.

Analysis of connection response using finite element methods has become increasingly popular in recent years. Assuming accurate material models are available, including dynamic enhancement, then these could be used in association with full scale testing to provide an improved understanding of the connection behaviour and the influence of various parameters. These would also be of use in verifying component-based connection models, allowing full connection performance to be included in frame analysis for a wide variety of connection types.

8   References

Aggarwal, A.K. and Coates, R.C. (1986). "*Moment-rotation characteristics of bolted beam-column connections.*" Journal of Constructional Steel Research **6**(4): 303-318.

AISC (1993). *Load and resistance factor design specification for structural steel buildings*. Chicago, American Institute of Steel Construction.

Al-Jabri, K.S. (1999). *The Behaviour of Steel and Composite Beam-to-Column Connections in Fire*. Department of Civil and Structural Engineering, University of Sheffield. **PhD Thesis**.

Al-Jabri, K.S., Burgess, I.W. and Plank, R.J. (2005). "*Spring-stiffness model for flexible end-plate bare-steel joints in fire.*" Journal of Constructional Steel Research **61**(12): 1672-1691.

Al-Jabri, K.S., Lennon, T., Burgess, I.W. and Plank, R.J. (1998). "*Behaviour of steel and composite beam-column connections in fire.*" Journal of Constructional Steel Research **46**(1-3): 308-309.

Alexander, E.M. (1977). "*Analysis and design of threaded assemblies.*" SAE Technical Paper 770420 **10.4271**(770420).

ASCE/SEI (2010). *Minimum design loads for buildings and other structures (7-10)*. Reston, Virginia, American Society of Civil Engineers and Structural Engineering Institute.

Astaneh-Asl, A., Liu, J. and McMullin, K.M. (2002). "*Behavior and design of single plate shear connections.*" Journal of Constructional Steel Research **58**(5-8): 1121-1141.

ASTM (2011). *Standard test methods for determining the mechanical properties of externally and inetrnally threaded fasteners, washers, direct tension indicators and rivets*. (ASTM F606-11), American Society for Testing and Materials.

Baker Engineering and Risk Consultants Inc (2002). *WBiggs v.4.4 : Elastic-Plastic Single Degree of Freedom Equivalent System Using the Biggs Method*. San Antonio, Texas, Baker Engineeering and Risk Consultants Inc.

Baker, J.E., Cox, P.A., Westine, P.S., Kulesz, J.J. and Strehlow, R.A. (1983). *Explosion hazards and evaluation*. Amsterdam, Oxford and New York, Elsevier Scientific Publishing Company.

Baker, J.F., Williams, E.D. and Lax, D. (1948). *The design of framed buildings against high-explosive bombs*. The Civil Engineer in War - W.E.P: Volume 3. London, Institution of Civil Engineers**:** p. 80-112.

Bayo, E., Cabrero, J.M. and Gil, B. (2006). "*An effective component-based method to model semi-rigid connections for the global analysis of steel and composite structures.*" Engineering Structures **28**(1): 97-108.

BCSA (2005). *Steel details (Publication No 41/05)*, The British Constructional Steelwork Association.

BCSA/SCI (1995). *Joints in steel construction: Moment Connections*. SCI Publication P207, The British Constructional Steelwork Association/The Steel Construction Institute.

BCSA/SCI (2002). *Joints in steel construction: Simple Connections*. SCI Publication P212, The British Constructional Steelwork Association/The Steel Construction Institute.

Becker, T., Splitthof, K., Siebert, T. and Kletting, P. (2006). *Error estimations of 3d digital image correlation measurements*. http://www.dantecdynamics.com. Germany, Dantec Systems.

Beg, D., Zupancic, E. and Vayas, I. (2004). "*On the rotation capacity of moment connections*." Journal of Constructional Steel Research **60**(3-5): 601-620.

Bernuzzi, C., Zandonini, R., and Zanon, P. (1995). "*Experimental analysis and modelling of semi-rigid steel joints under cyclic reversal loading*." Journal of Constructional Steel Research **38**(2): 95-123.

Biggs, J.M. (1964). *An introduction to structural dynamics*. New York, McGraw-Hill Book Company.

Block, F., Burgess, I., Davison, B. and Plank, R. (2004). *A component approach to modelling steelwork connections in fire: Behaviour of column webs in compression*. Proceedings of the 2004 Structures Congress - Building on the Past: Securing the Future, Nashville, Tennessee, American Society of Civil Engineers.

Block, F.M., Burgess, I.W., Davison, J.B. and Plank, R.J. (2007). "*The development of a component-based connection element for endplate connections in fire*." Fire Safety Journal **42**(6-7): 498-506.

Broderick, B.M. and Thomson, A.W. (2002). "*The response of flush end-plate joints under earthquake loading*." Journal of Constructional Steel Research **58**(9): 1161-1175.

BS EN 1990 (2002). *Basis of structural design*. BS EN 1990:2002.

BS EN 1991-1-7 (2006). *Eurocode1 - Actions on structures: Part 1-7: General actions - Accidental actions*. BS EN 1991-1-7:2006, , European Committee For Standardization (CEN).

BS EN 1993-1-1 (2005). *Eurocode 3 - Design of steel structures Part 1.1: General rules and rules for buildings*. BS EN1993-1-1:2005, European Committee For Standardization (CEN).

BS EN 1993-1-2 (2005). *Eurocode 3 - Design of steel structures Part 1.2: General rules. Structural fire design*. BS EN 1993-1-2, European Committee For Standardization (CEN).

BS EN 1993-1-8 (2005). *Eurocode 3 - Design of Steel Structures Part 1.8: Annex J Design of Joints*. BS EN 1993-1-8, European Committee For Standardization (CEN).

Building Regulations (2004). *The Building Regulations 2000, Part A3 (Amendment No.3) Disproportionate Collapse*. London, Office of the Deputy Prime Minister**:** 47.

Burgess, I. (2007). *Connection Modelling in Fire*. 4th Cost C26 Working Group 1, Prague, Department of Civil and Structural Engineering - University of Sheffield.

Byfield, M.P. and Paramasivam, S. (2007). "*Catenary action in steel-framed buildings*." Structures and Buildings **160**(SB5).

Cabrero, J.M. and Bayo, E. (2007). "*The semi-rigid behaviour of three-dimensional steel beam-to-column steel joints subjected to proportional loading. Part II: Theoretical model and validation*." Journal of Constructional Steel Research **63**(9): 1254-1267.

Chopra, A. (2000). *Dynamics of Structures: Theory and applications to earthquake engineering*. New York, Prentice-Hall.

Considine, J.M., Glesner, R. and Zhu, J.Y. (2005). *Use of digital image correlation to study the local deformation field of paper and paperboard*. 13th Fundamental research symposium. Cambridge.

Cook, R.D., Malkus, D.S. and Plesha, M.E. (1989). *Concepts and applications of finite element analysis*. New York, John Wiley and Sons.

Cormie, D., Mays, G. and Smith, P. (2009). *Blast effects on buildings*. London, UK, Thomas Telford.

Cowper, G.R. and Symonds, P.S. (1957). *Strain-hardening and strain-rate effects in the impact loading of cantilever beams*, Report to Brown University.

Daniunas, A. and Urbonas, K. (2008). "*Analysis of the steel frames with the semi-rigid beam-to-beam and beam-to-column knee joints under bending and axial forces*." Engineering Structures **30**(11): 3114-3118.

DoD (2008). *UFC 3-340-02: Structures to resist the effects of accidental explosions*. Unified Facilities Criteria, United States Department of Defense.

Ellingwood, B., Marjanishvili, S., Mlakar, P., Sasani, M. and Williamson, E. (2009). *Disproportionate collapse research needs*. Structures 2009: Don't mess with structural engineers, Austin, Texas, American Society of Civil Engineers.

Ellingwood, B.R., and Dusenberry, B. O. (2005). "*Building design for abnormal loads and progressive collapse*." Computer-aided civil and infrastructure engineering.

Ellingwood, B.R. and Dusenberry, D.O. (2005). "*Building Design for Abnormal Loads and Progressive Collapse*." Computer-aided civil and infrastructure engineering **20**(3): 194-205.

Faella, C., Piluso, V. and Rizzano, G. (2000). *Structural Steel Semirigid Connections*. New York, CRC Press.

FEMA (1995). *The Oklahoma City Bombing – Improving Building Performance Through Multi-hazard Mitigation: FEMA 277*. Washington DC, Federal Emergency Management Agency.

FEMA (1997). *NEHRP Guidelines for the Seismic Rehabilitation of Buildings: FEMA 273*. Washington DC, Federal Emergency Management Agency. **FEMA 273**.

FEMA (2000). *State of the art report on connection performance FEMA-355D*, Federal Emergency Management Agency.

FEMA (2002). *World Trade Center Building Performance Study: Data collection, preliminary observations and recommendations (FEMA 403)*, Federal Emergency Management Agency.

Foley, C.M. and Vinnakota, S. (1995). "*Toward design office moment-rotation curves for end-plate beam-to-column connections*." Journal of Constructional Steel Research **35**(2): 217-253.

Fransplass, H., Langseth, M. and Hopperstad, O.S. (2011). "*Tensile behaviour of threaded steel fasteners at elevated rates of strain*." International Journal of Mechanical Sciences **10.1016**(2011.07.006).

Fu, F. (2009). "*Progressive collapse analysis of high-rise building with 3-D finite element modeling method*." Journal of Constructional Steel Research **65**(6): 1269-1278.

Goodier, J.N. (1940). "*The distribution of load in the threads of screws*." Trans. American Society of Mechanical Engineers (ASME) **62**: A10-A16.

Goverdhan, A.V. (1983). *A collection of experimental moment-rotation curves and evaluation of prediction equations for semi-rigid connections*. Department of Civil Engineering. Nashville, TN, Vanderbilt University. **Masters Thesis**.

GSA (2003). *Progressive Collapse Analysis and Design Guidelines for New Federal Office Buildings and Major Modernization Projects*. Washington DC, United States General Services Administration.

Guravich, S.J. and Dawe, J.L. (2006). "*Simple beam connections in combined shear and tension*." Canadian Journal of Civil Engineering **33**(4): 357-372.

Heidarpour, A. and Bradford, M.A. (2008). "*Behaviour of a T-stub assembly in steel beam-to-column connections at elevated temperatures*." Engineering Structures **30**(10): 2893-2899.

Hensman, J.S. and Nethercot, D.A. (2001). "*Numerical study of unbraced composite frames: generation of data to validate use of the wind moment method of design*." Journal of Constructional Steel Research **57**(7): 791-809.

Hibbitt, Karlson and Sorenson (2007). *Getting started with Abaqus/Standard*. Michigan, Hibbitt, Karlson and Sorenson Inc.

Hooper, J.D., Lubke, C.D. and Moehle, J.P. (2008). "*Seismic design of reinforced concrete special moment frames*." NIST GCR 8-917-1

ICE (1948). *The Civil Engineer in War: A symposium of papers on war-time engineering problems, Volume 1 - Airfields, roads, railways and bridges*. London, The Institution of Civil Engineers.

ICE (1948). *The Civil Engineer in War: A symposium of papers on war-time engineering problems, Volume 2 - Docks and harbours*. London, The Institution of Civil Engineers.

ICE (1948). *The Civil Engineer in War: A symposium of papers on war-time engineering problems, Volume 3 - Properties of materials, structures, hydraulics, tunnelling and surveying*. London, The Institution of Civil Engineers.

IStructE (1995). *The structural engineer's response to explosion damage*. London, The Institution of Structural Engineers.

Izzuddin, B.A. (2010). "*Robustness by design - Simplified progressive collapse assessment of building structures*." Stahlbau **79**: 556-564.

Izzuddin, B.A., Vlassis, A.G., Elghazouli, A.Y. and Nethercot, D.A. (2007). "*Assessment of progressive collapse in multi-storey buildings*." Proceedings of the Institution of Civil Engineers: Structures and Buildings **160**(4 B): 197-205.

Izzuddin, B.A., Vlassis, A.G., Elghazouli, A.Y. and Nethercot, D.A. (2008). "*Progressive collapse of multi-storey buildings due to sudden column loss -- Part I: Simplified assessment framework*." Engineering Structures **30**(5): 1308-1318.

Jaramillo, T.J. (1950). "*Deflections and moments due to a concentrated load on a cantilever plate of infinite length*." Journal of Applied Mechanics **17**(1): 67-72.

Jaspart, J.P. and Weynand, K. (1995-2000). *The Connection Program: Software to design joints in steel building frames*. Liege, RWTH Aachen, ECCS by Hoofddorp.

Jones, S.W., Kirby, P.A. and Nethercot, D.A. (1983). "*Analysis of frames with semi-rigid connections - A state of the art report*." Journal of Constructional Steel Research **3**(2): 2-13.

Khandelwal, K., El-Tawil, S. (2007). "*Collapse behavior of steel special moment resisting frame connections*." Journal of Structural Engineering **133**(5): 646-655.

Kim, J.S., Huh, H. and Kwon, T.S. (2009). *Characterization of dynamic tensile and shear strength of safety bolts in light collision safety devices of a train*. in Materials Characterisation IV: Computational Methods and Experiments (ISBN: 978-1-84564-189-4), Wit Press Publishing.

Kishi, N. and Chen, W.F. (1986). *Database of Steel Beam-to-Column Connections*. Structural Report No. CE-STR-86-26. West Lafayette, Indiana, School of Civil Engineering, Purdue University.

Leston-Jones, L.C. (1997). *The influence of semi-rigid connections on the performance of steel framed structures in fire*. Department of Civil and Structural Engineering, University of Sheffield. **PhD Thesis**.

Liew, J.Y.R. (2008). "*Survivability of steel frame structures subject to blast and fire*." Journal of Constructional Steel Research **64**(7-8): 854-866.

Liu, J. and Astaneh-Asl, A. (2004). "*Moment--Rotation Parameters for Composite Shear Tab Connections*." Journal of Structural Engineering **130**(9): 1371-1380.

Liu, Y., Xu, L. and Grierson, D.E. (2010). "*Influence of semi-rigid connections and local joint damage on progressive collapse of steel frameworks*." Computer-aided civil and infrastructure engineering **25**(Compendex): 184-204.

Malvar, L.J. and Crawford, J.E. (1998). *Dynamic increase factors for steel reinforcing bars*. Twenty-eighth Department of Defence Explosives Safety Board (DDESB) Seminar. Orlando, Florida.

Marchand, K. and Alfawakhiri, F. (2004). *Blast and progressive collapse*. Facts for steel building (Volume 2), American Institute of Steel Construction.

Marchand, K.A.a.A., F. (2004). *Blast and progressive collapse*. United States of America, AISC.

Marjanishvili, S.M. (2004). "*Progressive analysis procedure for progressive collapse*." Journal of Performance of Constructed Facilities **18**(2): 79-85.

Mlakar, P.F., Corley, W. G., Sozen, M. A., Thornton, C. H. (1998). "*The Oklahoma City Bombing: Analysis of Blast Damage to the Murrah Building*." Journal of Performance of Constructed Facilities **12**(3): 113-119.

Moore, D.B. (1988). *The design of end-plate connections*. Conference on modern developments in frame and slab structures, Building Research Establishment, UK.

Moore, J.F.A. (1983). "*The incidence of accidental loadings in buildings 1971-1981*." UK Building Research Establishment **Current Paper 2/83**.

Mouritz, A.P. (1994). "*Failure mechanisms of mild steel bolts under different tensile loading rates*." International Journal of Impact Engineering **15**(3): 311-324.

Munoz-Garcia, E., Davison, B. and Tyas, A. (2005). *Structural Integrity of Steel Connections Subjected to Rapid Rates of Loading*. Metropolis & Beyond: 2005 Structures Congress and the Forensic Engineering Symposium, New York, ASCE.

Nabil Bassim, M. and Panic, N. (1999). "*High strain rate effects on the strain of alloy steels*." Journal of Materials Processing Technology **92-93**: 481-485.

Naito, C.J. and Wheaton, K.P. (2006). "*Blast assessment of load-bearing reinforced concrete shear walls*." Practice periodical on structural design and construction **11**(2): 112-121.

Nethercot, D.A. (1985). *Utilisation of experimentally obtained connection data in assessing the performance of steel frames*. Connection Flexibility and Steel Frames, New York, USA, ASCE.

Nethercot, D.A., Davison, J.B. and Kirby, P.A. (1988). "*Connection flexibility and beam design in non-sway frames*." Engineering Journal **25**(3): 99-108.

NFM. (2011). "*Overview of M5 optical distance sensors*." New Features Measurements Retrieved 23rd March 2011, from http://www.nfminc.com/html/em5.htm.

NIST (2005). *Final report on the collapse of the World trade Center Towers: NIST NCSTAR 1*. USA, National Institute of Standards and Technology.

Odeshi, A.G., Al-ameeri, S. and Bassim, M.N. (2005). "*Effect of high strain rate on plastic deformation of a low alloy steel subjected to ballistic impact*." Journal of Materials Processing Technology **162-163**: 385-391.

Owens, G. and Cheal, B. (1989). *Structural steelwork connections*. London, Butterworth and Co. Ltd.

Owens, G.W. and Moore, D.B. (1992). "*The robustness of simple connections*." The Structural Engineer **70**(3).

Paramasivam, S. (2008). *Protective design of r.c and steel framed buildings against disproportionate collapse*. Department of Civil Engineering and the Environment, University of Southampton. **PhD Thesis**.

Pierron, F., Sutton, M.A. and Tiwari, V. (2010). "*Ultra high speed DIC and virtual fields method analysis of a three point bending impact test on an aluminium bar*." Experimental Mechanics **10.1007**(s11340-010-9402-y).

Pucinotti, R. (2001). "*Top-and-seat and web angle connections: prediction via mechanical model*." Journal of Constructional Steel Research **57**(6): 663-696.

Rassati, G.A., Leon, R.T. and Noe, S. (2004). "*Component Modeling of Partially Restrained Composite Joints under Cyclic and Dynamic Loading*." Journal of Structural Engineering **130**(2): 343-351.

Rebelo, N., Nagtegaal, J.C., Taylor, L.M. and Passmann, R. (1992). *Industrial application of implicit and explicit finite element methods to forming processes*. American Society of Mechanical Engineers, Computer Engineering Division, CED, Anaheim, CA, USA, Publ by ASME.

Rex, C.O. and Easterling, W. (2003). "*Behavior and modeling of a bolt bearing on a single plate*." Journal of Structural Engineering **129**(Compendex): 792-800.

Richard, R.M., Hsia, W.-K. and Chmielowiec, M. (1987). *Moment rotation curves for double framing angles*, New York, NY, USA, ASCE.

Ruth, P., Marchand, K.A. and Williamson, E.B. (2006). "*Static equivalency in progressive collapse alternate path analysis: Reducing conservatism while retaining structural integrity*." Journal of Performance of Constructed Facilities **20**(4): 349-364.

Sabuwala, L.a.K. (2005). "*Finite element analysis of steel beam to column connections subjected to blast loads*." International Journal of Impact Engineering.

Sadek, F., Main, J.A., Lew, H.S. and Bao, Y. (2011). "*Testing and analysis of steel and concrete beam-column assemblies under a column removal scenario*." Journal of Structural Engineering **137**(9): 881-892.

Sarraj, M. (2007). *The behaviour of steel fin plate connections in fire*. Department of Civil and Sructural Engineering, University of Sheffield, UK. **PhD thesis**.

Sasani, M. and Sagiroglu, S. (2008). "*Progressive collapse resistance of hotel San Diego*." Journal of Structural Engineering **134**(3): 478-489.

Selamet, S. and Garlock, M.E. (2009). *Modified connection details for single plate steel connections under fire*, Austin, TX, United states, American Society of Civil Engineers.

Siebert, T.H. and Becker, K. (2005). "*High speed digital image correlation technique*." SAE Special Publication Papers **SP2033**(2006-01-0528).

Simões da Silva, L., Coelho, A.G. and Lucena Neto, E. (2000). "*Equivalent post-buckling models for the flexural behaviour of steel connections*." Computers & Structures **77**(6): 615-624.

Simões da Silva, L. and Girão Coelho, A.M. (2001). "*A ductility model for steel connections*." Journal of Constructional Steel Research **57**(1): 45-70.

Simulia (2007). *Abaqus/CAE User's Manual. Version 6.7*. USA, Dassault Systems.

Simulia (2009). *Abaqus Analysis Users Manual - Volume 4: Elements. Version 6.9*. USA, Dassault Systems.

Sopwith, D.G. (1947). "*The distribution of load in screw threads*." Proceedings of the Institution of Mechanical Engineers (IMechE) 1847-1982 **159**: 373-383.

Spyrou, S. (2002). *Development of a component-based model of steel beam-to-column joints at elevated temperatures*. Department of Civil and Structural Engineering, University of Sheffield. **PhD Thesis**.

Spyrou, S., Davidson, B., Burgess, I. and Plank, R. (2004). "*Experimental and analytical studies of steel joint components at elevated temperatures*." Fire and Materials **28**: 83-94.

Spyrou, S., Davison, J.B., Burgess, I.W. and Plank, R.J. (2004). "*Experimental and analytical investigation of the "tension zone" components within a steel joint at elevated temperatures*." Journal of Constructional Steel Research **60**(6): 867-896.

Sun, J.S., Lee, K.H. and Lee, H.P. (2000). "*Comparison of implicit and explicit finite element methods for dynamic problems*." Journal of Materials Processing Technology **105**(1-2): 110-118.

Thomas, W.N. (1946). *The effects of impulsive forces on materials and structural members*. The Civil Engineer in War - W.E.P: Volume 3. London, Institution of Civil Engineers**:** p. 65-79.

TM5-1300 (1990). *Structures to resist the effects of accidental explosions: Technical Manual 5-1300*, United States Army Corps of Engineers.

Tsai, M.-H. and Lin, B.-H. (2009). "*Dynamic amplification factor for progressive collapse resistance analysis of an RC building*." The Structural Design of Tall and Special Buildings **18**(5): 539-557.

Tschemmernegg, F. (1987). *On the nonlinear behaviour of joints in steel frames*. Connections in Steel Structures. R. Bjorhovde. London, Elsevier Applied Science.

Tyas, A., Warren, J., Davison, B., Stoddart, E., Tait, S. and Huang, Y. (2011). "*A methodology for combined rotation-extension testing of simple steel beam to column joints at high rates of loading*." Engineering Mechanics **DOI: 10.1007/s11340-011-9562-4**.

US DoD (2009). "*Unified Facilities Criteria: Design of buildings to resist progressive collapse*." UFC 4-023-03(United States Department of Defense).

Vlassis, A.G., Izzuddin, B.A., Elghazouli, A.Y. and Nethercot, D.A. (2008). "*Progressive collapse of multi-storey buildings due to sudden column loss--Part II: Application*." Engineering Structures **30**(5): 1424-1438.

Wales, M.W. and Rossow, E.C. (1983). "*Coupled moment-axial force behavior in bolted joints*." Journal of Structural Engineering **109**(5): 1250-1266.

Way, A.G.J. (2011). *Structural robustness of steel framed buildings*. SCI Publication 391.

Yu, H., Burgess, I., Davison, B. and Plank, R. (2007). *Experimental investigation of the robustness of fin plate connections in fire*. 5th International Conferemce on Advance in Steel Structures. Singapore**:** pp 722-727.

Yu, H., Burgess, I.W., Davison, J.B. and Plank, R.J. (2009). "*Experimental investigation of the behaviour of fin plate connections in fire*." Journal of Constructional Steel Research **65**(3): 723-736.